

Description and molecular analysis of *Tylencholaimus helanensis* sp. n. from China (Dorylaimida, Tylencholaimidea)

Wen-Jia Wu^{1,2}, Lu Yu^{1,2}, Hui Xie¹, Chun-Ling Xu¹, Jiao Yu¹, Dong-Wei Wang¹

1 Lab of Plant Nematology/Research Center of Nematodes of Plant Quarantine, Department of Plant Pathology /Guangdong Province Key Laboratory of Microbial Signals and Disease Control, College of Agriculture, South China Agricultural University, Guangzhou, Guangdong 510642, China **2** Key Laboratory of Vegetation Restoration and Management of Degraded Ecosystems, South China Botanical Garden, Chinese Academy of Sciences, Guangzhou, Guangdong 510160, China **3** Grassland supervision and management of Alxa, Bayanhaote, Alxa Left Banner, Alxa League, Inner Mongolia 750399, China

Corresponding author: Hui Xie (xiehui@scau.edu.cn)

Academic editor: Steven Nadler | Received 7 June 2018 | Accepted 30 August 2018 | Published 23 October 2018

<http://zoobank.org/EAC239FE-7062-48ED-BD88-F3155421D773>

Citation: Wu W-J, Yu L, Xie H, Xu C-L, Yu J, Wang D-W (2018) Description and molecular analysis of *Tylencholaimus helanensis* sp. n. from China (Dorylaimida, Tylencholaimidea) ZooKeys 792: 1–14. <https://doi.org/10.3897/zookeys.792.27255>

Abstract

A new species, *Tylencholaimus helanensis* sp. n., extracted from the rhizosphere soil of unidentified grasses from Helan Mountain, Inner Mongolia, China was identified. The new species is characterized by having a body length of 0.93–1.07 mm with the lip region approximately one-quarter of the body diameter at the posterior end of the neck region wide; female didelphic-amphidelphic; pars proximalis vaginae violin-shaped. Males were not found. SEM observations of the new species were made and a phylogenetic analysis of both the 18S rDNA and the D2-D3 region of 28S rDNA is presented.

Keywords

China, morphology, new species, phylogenetic analysis, taxonomy, *Tylencholaimus*

Introduction

The genus *Tylencholaimus* de Man, 1876 is common in most soils all over the world and contains more than 50 valid species. It is mainly characterized by having small body, cap-shaped lip region, weak odontostyle and knobbed odontophore. The types of female genital system and tail of the genus are various (amphidelphic, monoprodelphic, or mono-opisthodelphic for female genital system, hemispherical to elongate-conical for tail) (Andrássy 2009). Peña-Santiago and Coomans (1994a, b, c, d; 1996a, b, c) revised the genus and its species, discussed the intrageneric variability and taxonomic value of some important morphological features such as the lip region, odontostyle, odontophore, pharynx, female genital system, tail and so on, and provided a key to the species. Peña-Santiago (2008) analyzed and discussed 15 species of *Tylencholaimus* described from 1996 to 2008, confirmed nine species to be valid, revised five species to be junior synonyms of other known species, transferred *T. annulatus* Baqri & Bohra, 2001 to the genus *Cricodorylaimus*, and provided an updated list and a key to the species of *Tylencholaimus*. Ahad and Ahmad (2016) added two new species to *Tylencholaimus*, redescribed six known species, and revised the diagnostic compendium and key to the species on the basis of Peña-Santiago (2008). In China, *Tylencholaimus* is widely distributed in many types of habitats such as mixed forest, broad-leaved forest, coniferous forest, alpine meadow, grassland, farmland, tea plantations, and wetland and others (Tong et al. 2009; Sang et al. 2010; Zhang et al. 2010; Wang et al. 2011; Xue et al. 2013; Hua et al. 2014; Xing et al. 2014; Yu et al. 2015). However, all the descriptions at the species level of these populations from China are lacking.

With detailed examinations based on light microscopy, SEM observations and phylogenetic analysis of 18S rDNA and the D2–D3 region of 28S rDNA, one nematode population from Inner Mongolia, China, was identified to be a new member of *Tylencholaimus* and is described as *Tylencholaimus helanensis* sp. n.

Materials and methods

Morphology and morphometrics

Soil samples were collected from the rhizosphere soil of unidentified grasses from Helan Mountain, Alxa Left Banner, Alxa League, Inner Mongolia, China. Nematode populations were extracted from the soil samples by using the modified Baermann funnel method (Whitehead and Hemming 1965). Then specimens were killed at 62 °C for 3 min, fixed in 4% FG fixative, dehydrated by using the glycerol-ethanol method, and then mounted on permanent slides (Xie 2005). The best preserved specimens were observed, photographed, and measured as described previously (Wu et al. 2016). For SEM observations, nematodes were prepared as described by Abolafia and Peña-Santiago (2005) and observed with a FEI XL-30-ESEM electron microscope at 10KV.

DNA extraction, amplification, and sequencing

A single nematode was picked into 10 μL mixed solution (distilled water: 2 \times buffer for KOD FX = 1:1) and cut using a sterilized needle. 1 μL 20 $\mu\text{g}/\text{mL}$ proteinase K was added and then reacted at 65 $^{\circ}\text{C}$ for 1 h and 95 $^{\circ}\text{C}$ for 15 min to release the genomic DNA. PCR reactions were performed in a 10 μL reaction mixture containing 5 μL of 2 \times buffer for KOD FX, 0.3 μL of each primer (10 μM), 2 μL of dNTPs (200 μM), 1 μL of DNA, 1.2 μL of distilled water and 0.2 μL of KOD FX polymerase (1 U/ μL). Two overlapping fragments of the 18S rDNA were amplified using two primer sets, 988F (5'-CTCAAAGATTAAGCCATGC-3') and 1912R (5'-TTTACGGTCAGAACTAGGG-3') for the first fragment, and 1813F (5'-CTGCGTGAGAGGTGAAAT-3') and 2646R (5'-GCTACCTTGTTACGACTTTT-3') for the second one (Holterman et al. 2006; Nedelchev et al. 2014). For the D2-D3 region of the 28S rDNA amplifications, D2A (5'-ACAAGTACCGTGAGGGAAAGTTG-3') and D3B (5'-TCGGAAGGAACCAGCTACTA-3') (De Ley et al. 1999) were used. The PCR reactions were carried out as described previously (Wu et al. 2017). Electrophoresis was performed on 1% TAE agarose gels and observed under UV transillumination (AlphaImager[®] EP). Sequencing of PCR products was carried out by Sangon Biotech (Shanghai) Co. Ltd. The newly obtained sequences of the new species were deposited in GenBank (<http://www.ncbi.nlm.nih.gov/Genbank/>).

Phylogenetic analysis

The sequences of the new species were compared with sequences in GenBank using BLAST. The sequences of other dorylaimid species and the outgroup taxa were chosen according to previous studies (Holterman et al. 2008; Nedelchev et al. 2014; Álvarez-Ortega and Peña-Santiago 2016), the sequences of other *Tylencholaimus* spp. were also included. The sequence alignment was done by using the software MEGA v.6 and the conservative regions were selected by using the online Gblocks server (http://molevol.cmima.csic.es/castresana/GBLOCKS_server.html). Substitution saturation was tested by DAMBE and the model of base substitution was evaluated using MrModeltest v2.3. The best-fit models were selected by AIC (Akaike Information Criterion) in MrModeltest v2.3. Phylogenetic trees were constructed by using MrBayes v3.1.2 running the chain for 5,000,000 generations for the 18S rDNA and 1,000,000 generations for the D2-D3 region of the 28S rDNA, respectively, with a sample frequency of 100 generations and setting the 'burnin' at 2500. The topologies were used to generate a 50% majority rule consensus tree with posterior probabilities (PP) for appropriate clades. The software Figtree v.1.3.1 was used to visualize and edit the phylogenetic trees.

Results

Tylencholaimus helanensis sp. n.

<http://zoobank.org/F0BFD129-C8C7-442C-8A1F-A7C144310D0D>

Figs 1, 2

Material examined. Seven females from Qinghai Province; 38°40.311'N, 105°50.905'E; 22 August 2014; collected by Dong-Wei Wang, Wen-Jia Wu, Lu Yu, and Hui Xie. Female holotype (M51.B.a) and six female paratype specimens (slide numbers: M51.A.a, b, c, d, e and M51.B.b) are deposited in the Lab of Plant Nematology/Research Center of Nematodes of Plant Quarantine, South China Agricultural University, Guangzhou, Guangdong 510642, China.

Descriptions. Female. Body robust and cylindrical, tapering towards the anterior end. Habitus variable, almost straight or slightly twisted after fixation. Cuticle two layers, 1.0–2.0 μm thick in anterior region, 1.5–2.5 μm at mid-body, and 2.5–3.5 μm on tail; outer layer with fine transverse striations, the inner one loose and often shrunken after fixation. Lateral chord occupying about one-third of the body diameter at mid-body, lateral pores indistinct. Lip region cap-shaped, offset from the body by a constriction, 2.4–2.8 times as wide as high or 25% in average of the body diameter at posterior end of the neck region wide. Lips not amalgamated, the outer part of each lip not distinct from the inner one. Labial and cephalic papillae distinct but not interfering with the contour. Amphidial foveae cup-shaped, opening at the level of the constriction, apertures 0.4 times on average as wide as the lip region. Odontostyle straight with a distinct lumen, 8–9.5 μm long, 0.9–1.0 times as long as the lip region width, its aperture about one-third of its length. Odontophore rod-like with small basal knobs, 9–11 μm long, 1–1.3 times as long as the odontostyle. Guiding ring single. Nerve ring situated at 35–42% of the neck length. Anterior part of pharynx slender and expanded gradually, basal expansion occupying 39–43% of the total neck length. Pharyngeal gland nuclei locations (Andrássy 1998) are as follows: D = 60–66%, AS1 = 21–30%, AS2 = 36–44%, PS1 = 62–74%, PS2 = 67–79%. Cardia short, conoid to rounded. Genital system didelphic-amphidelphic. Ovary reflexed, the anterior one 67–86 μm and the posterior one 54–79 μm long. Each oviduct consists of a wider *pars dilatata* and a slender part, 0.9–1.3 times the uterus long; anterior oviduct 83–107 μm and the posterior one 61.5–92 μm long. Sphincter present at the junction of oviduct and uterus. Uterus simple and with a wide lumen, the anterior one 66–85 μm and the posterior one 58–72 μm long. Vulva transverse. Vagina showing ‘+’ shape in ventral view, extending 44.5–46% inwards the corresponding body width. The walls of *pars proximalis* vaginae recessed inward in the middle, making *pars proximalis* vaginae violin-shaped, 12–13 μm long and 13–15 μm wide, with poorly developed musculature surrounding only the part adjacent to *pars distalis* vaginae. *Pars refringens* lacking, *pars distalis* vaginae 7 μm long. No sperm observed in the genital system. Prerectum 2.4–4.2 times and rectum 0.9–1.2 times the body diameter at anus level. Tail hemispheroid with blunt rounded to flat terminus. One caudal papilla opening in tail terminus.

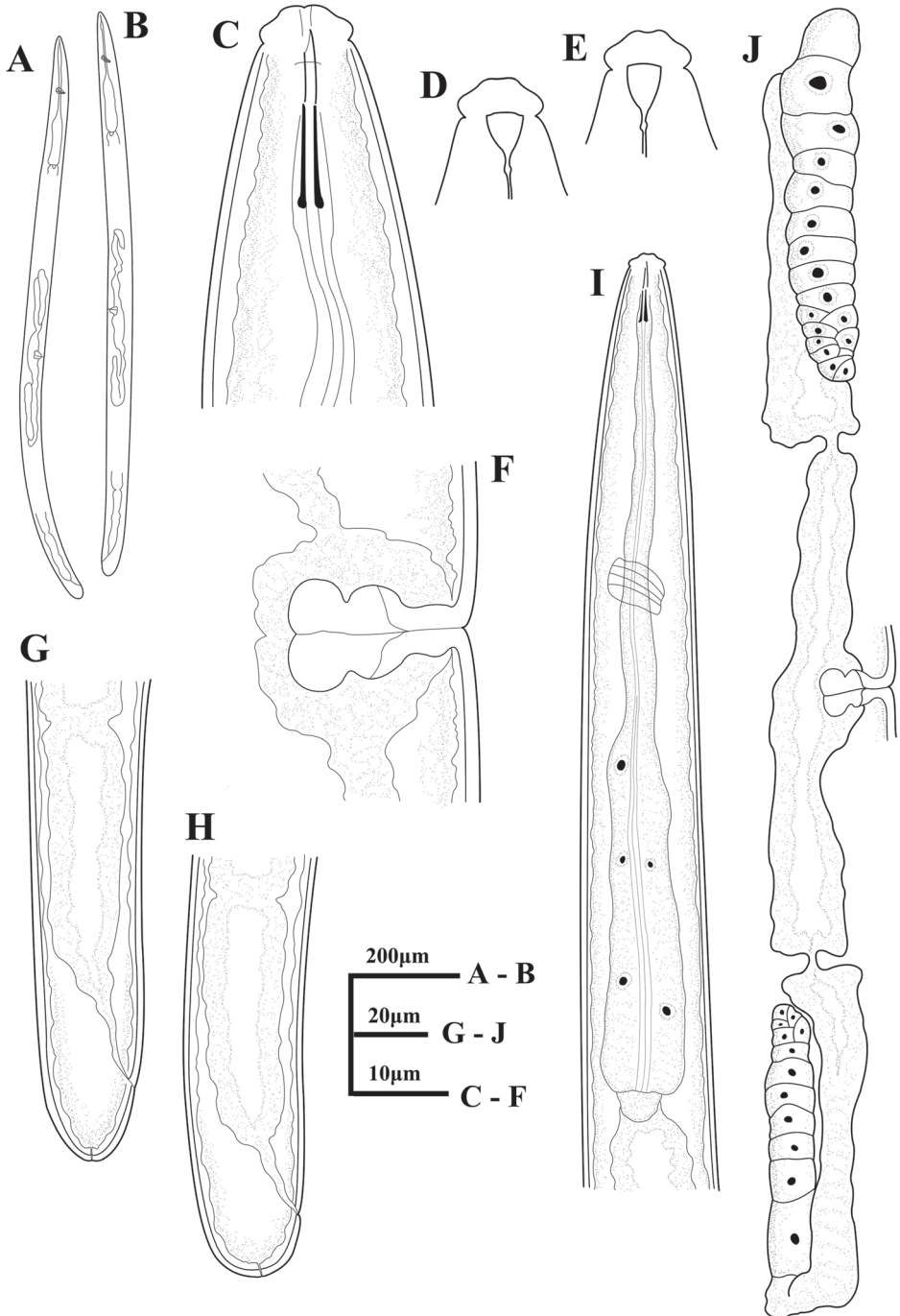


Figure 1. *Tylencholaimus helanensis* sp. n. Female: **A, B** entire body **C** anterior region showing odontostyle and odontophore **D, E** amphidial fovea **F** vulva in lateral view **G, H** posterior region **I** anterior region showing pharynx **J** genital system.

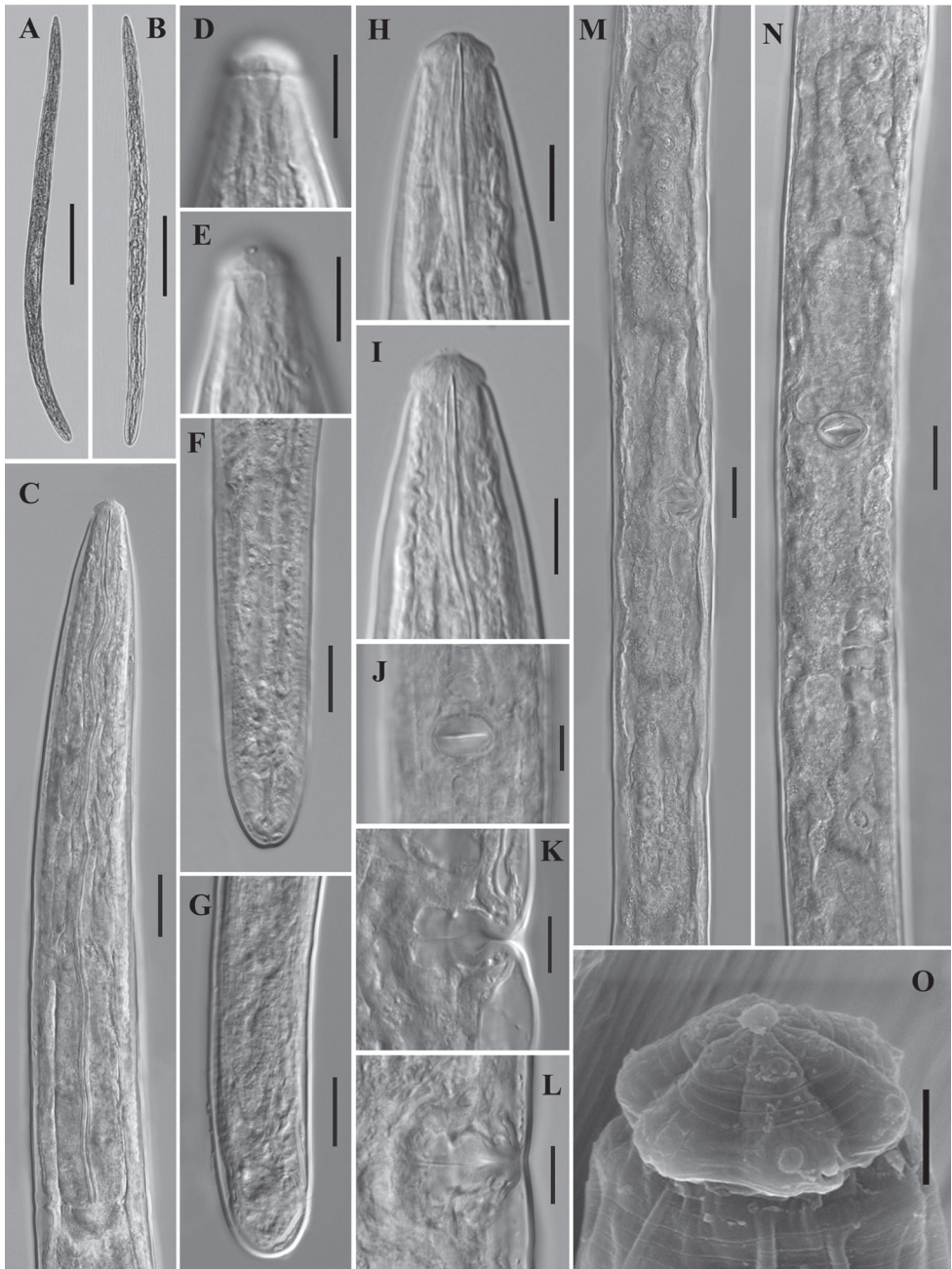


Figure 2. *Tylencholaimus helanensis* sp. n. Female: **A, B** entire body **C** anterior region showing pharynx **D, E** amphidial fovea **F, G** posterior region **H, I** anterior region showing odontostyle and odontophore **J** vulva in ventral view **K, L** vulva in lateral view **M, N** genital system **O** SEM of the lip region. Scale bars: 200 μm (**A, B**); 20 μm (**C, F, G, M, N**); 10 μm (**D, E, H-L**); 2 μm (**O**).

Table 1. Morphometrics of *Tylencholaimus belanensis* sp. n. and the females of its six close species. Measurements for *Tylencholaimus belanensis* sp. n. are in the form: mean \pm s.d. (range), for other six species are in the form of range, and all in μm (except for 'L' in mm).

Character	<i>Tylencholaimus belanensis</i> sp. n.		<i>T. teves</i> (1-4)*	<i>T. congestus</i> (4, 5)*	<i>T. cosmos</i> (6, 7)*	<i>T. crassus</i> (4, 5)*	<i>T. paracrassus</i> (4)*	<i>T. sinensis</i> (8)*
	Holotype	Paratypes						
n	1♀	6♀♀	>20♀♀	5♀♀	15♀♀	28♀♀	5♀♀	2♀♀
L	1.00	1.00 \pm 0.06 (0.93-1.07)	0.8-1.06	0.72-0.83	0.57-0.9	0.68-0.92	0.9-1.1	0.76-0.82
a	26.3	25.6 \pm 1.0 (24.8-27.5)	20-35.8	29.2-33	25.7-35	20-24	24-31	27-28.5
b	4.4	4.4 \pm 0.4 (3.7-4.9)	4.0-5.1	3.2-4.2	3.7-5	3.2-4.7	4.0-4.8	3.6-4.3
c	54.5	51.3 \pm 5.8 (46.2-60.7)	55.0-67.3	40-46	34.8-39.1	28-39	35-37	45-45.8
c'	0.6	0.7 \pm 0.1 (0.6-0.8)	0.7-1.0	1	1.0-1.3	1	1.1-1.9	0.8-0.85
V	55.1	55.3 \pm 1.2 (53.3-56.5)	51-66	60-62	57-63.4	52-57	52-58.5	57-57.5
G1	18.2	14.0 \pm 3.2 (8.6-17.3)	18.4-27.9	17.3	9-24	-	-	18.5-19.5
G2	14.2	14.3 \pm 1.8 (11.7-16.3)	13.9-21.5	17.0	10-17	-	-	16.5-18.5
Lip region diameter	10	10 \pm 0.2 (9.5-10)	8-9.5	8	7-8	10.5-12	11.5-13	8
Lip region height	4	4 \pm 0.2 (3.5-4.0)	4	3.5	2-3	5-5.5	-	3
Amphid aperture	4	4 \pm 0.2 (3.5-4)	3-4	4	2	-	-	4-5
Odontostyle length	9	9 \pm 0.4 (8-9.5)	5-6	7-8	7-8	8.5-9.0	10-11.5	7
Odonophore length	10	10 \pm 0.7 (9-11)	8-9	8-9	9-14	9-11	-	8
Guiding ring from anterior end	6	5.8 \pm 0.4 (5.5-6.5)	5-6	-	4-5.5	-	-	4-5
Nerve ring from anterior end	94	86 \pm 6.6 (78-93)	72-90	80	63-71	-	-	73-83
Pharyngeal length	230	222 \pm 8.5 (216-237)	202-244	193-220	146-207	211-222	213-249	191-208
Expanded part of pharynx	98	91.0 \pm 6.4 (87-102)	81-110	76	61-87	90	90-106	67-75
Cardia length	12	11 \pm 1.2 (9-12)	6-12	6	5-7	-	-	5-8
Body diameter at neck base	34	36 \pm 4.1 (31.5-41.5)	24-31.5	26	19-24	-	-	-
Body diameter at mid-body	38	39 \pm 2.7 (36-43)	26-34.5	28	19-26	-	-	-
Body diameter at anus	28	25 \pm 1.3 (24-27)	19-22	18	15-21	28	21-25	-
Anterior genital branch	182	142 \pm 38.2 (80-185)	172-265	141	58-95	-	-	142-164
Posterior genital branch	142	144 \pm 16.3 (117-161)	134-219	139	68-87	-	-	125-155
Vaginal depth	14.5	19.0 \pm 1.0 (18-20)	11-16.5	13	8-11	-	-	-
Vulva from anterior end	552	559 \pm 34.8 (513-607)	553-658	492	345-420	-	-	440-474
Preectum length	68.5	85 \pm 12.9 (71-100)	69-200	94	22-70	-	47-66	100-105
Rectum length	26	25 \pm 2.7 (22-28)	17-23	18	13-25	-	-	18-20
Tail length	18	19 \pm 1.5 (16.5-21)	14-19	18	16-22	28	30-38	17-18

* References: (1) Loof 1971; (2) Thorne 1974; (3) Vinciguerra 1986; (4) Peña-Santiago and Coomans 1994a; (5) Loof and Jairajpuri 1968; (6) Dhanam and Jairajpuri 1999; (7) Ahad and Ahmad 2016; (8) Li et al. 2008.

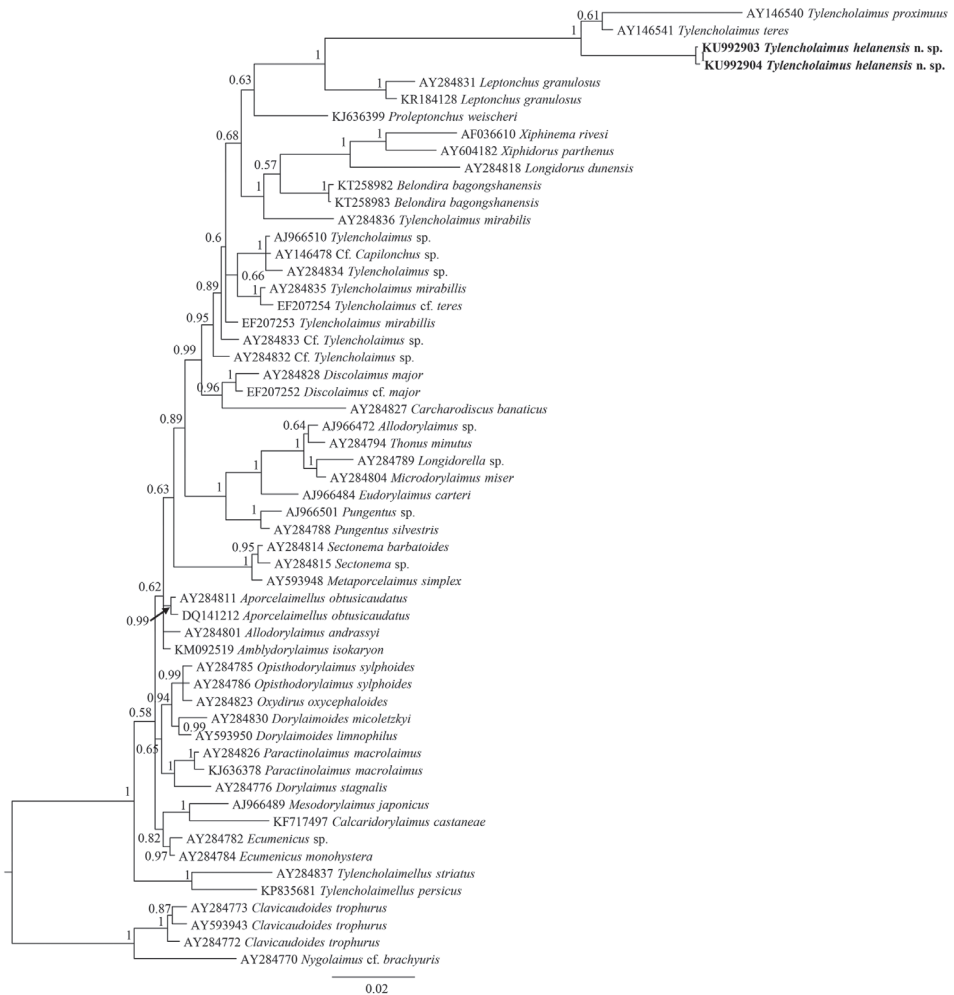


Figure 3. Phylogenetic relationships of *Tylencholaimus helanensis* sp. n. and other Dorylaimida species for 18S rDNA. Bayesian inference strict consensus tree is acquired under GTR+I+G model. Posterior probabilities higher than 50% are presented. Newly obtained sequences are given in bold.

Fore measurements see Table 1. The male was not found.

Sequence and phylogenetic analysis. The sequences of 18S rDNA and D2-D3 region of 28S rDNA of *Tylencholaimus helanensis* sp. n. were obtained. The inter-individual variabilities of the 18S rDNA sequences and the 28S rDNA sequences are one gap and two base pair differences, respectively. Two sequences for each of the genes were deposited in GenBank (accession numbers: KU992903 (1746 bp long) and KU992904 (1747 bp long) for 18S rDNA, KU992905 and KU992906 (both 840 bp long) for D2-D3 region of 28S rDNA). The BLAST search for the 18S rDNA showed the highest similarity (94% and 95%) to the sequence of an unidentified species of *Tylencholaimus* (AJ966510). For the D2-D3 region of 28S rDNA, both sequences

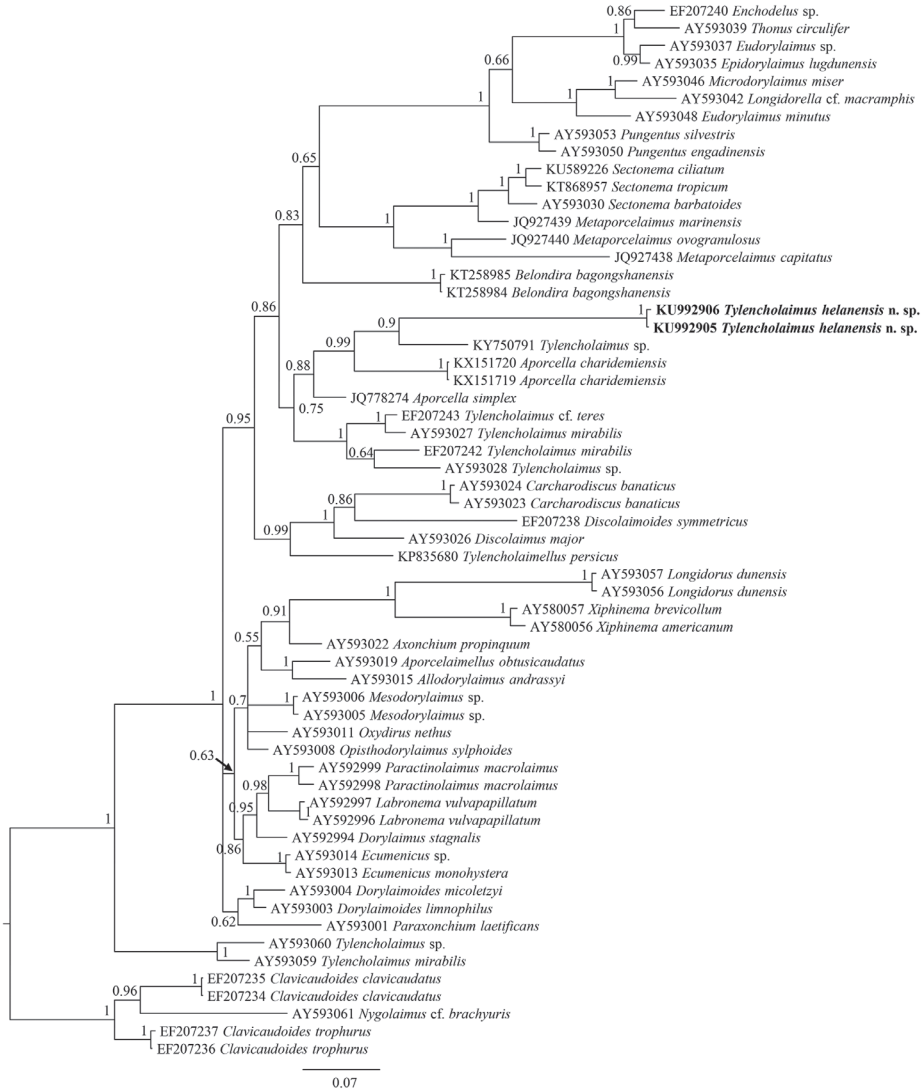


Figure 4. Phylogenetic relationships of *Tylencholaimus helanensis* sp. n. and other Dorylaimida species for the D2-D3 region of 28S rDNA. Bayesian inference strict consensus tree is acquired under GTR+I+G model. Posterior probabilities higher than 50% are presented. Newly obtained sequences presented in bold.

showed the highest similarity (79%) to the sequences of *Xiphinema brevicollum* Lordello & Da Costa, 1961 (AY580057). In the 18S rDNA phylogenetic reconstructions (Fig. 3), the new species is in a 100% supported clade with *T. teres* and *T. proximus*. And in the D2-D3 region of 28S rDNA phylogenetic reconstructions (Fig. 4), the new species is in a clade with an unidentified species of *Tylencholaimus* with 90% posterior probability.

Type habitat. Rhizosphere soil of unidentified grasses from Helan Mountain, Alxa Left Banner, Alxa League, Inner Mongolia, China.

Etymology. The new species is named after the mountain Helan, which is a famous mountain with a wealth of human history including rock paintings, architecture, vineyards, and a national park.

Diagnosis and relationships. *Tylencholaimus helanensis* sp. n. is characterized by having a body length of 0.93–1.07 mm; body tapering towards the anterior end; lip region offset from the body by a constriction and 25% in average of the body diameter at posterior end of the neck region wide; amphid aperture 0.4 times in average as wide as the lip region; odontostyle 8–9.5 μm long and 0.85–1.0 times as long as the lip region width; odontophore 1–1.3 times as long as the odontostyle; basal expansion of pharynx 39–43% of the total neck length; female genital system didelphic-amphidelphic; vulva transverse; prerectum 2.4–4.2 times and rectum 0.9–1.2 times the body diameter at anus long; tail hemispheroid with blunt rounded to flat terminus; males not found.

Tylencholaimus helanensis sp. n. is close to *T. congestus* Loof & Jairajpuri, 1968, *T. cosmos* (Dhanam & Jairajpuri, 1999) Peña-Santiago, 2008, *T. crassus* Loof & Jairajpuri, 1968, *T. paracrassus* Monteiro, 1970, *T. sinensis* Li, Baniyamuddin, Ahmad & Wu, 2008 and *T. teres* Thorne, 1939 in having a body length about 1 mm or less, female genital system didelphic-amphidelphic, odontostyle less than 10 μm and ‘V’ value less than 62 in average, but can be differentiated by having panduriform *pars proximalis vaginae*. In addition, the new species differs from *T. congestus* (Loof and Jairajpuri 1968; Peña-Santiago and Coomans 1994a) by having longer body (0.93–1.07 mm vs. 0.72–0.83 mm), lower ‘a’ value ($a = 24.8\text{--}27.5$ vs. 29–33), different lip region (lip region cap-shaped, lips not amalgamated and no inner liplets vs. lips apparently separated, inner part protruding and forming liplets), absence of large cells in the vaginal area (vs. presence) and oviducts 0.9–1.3 (vs. 3–4) times the uterus long. From *T. cosmos* (Dhanam and Jairajpuri 1999; Ahad and Ahmad 2016), the new species differs by having longer pharynx and basal expansion (216–237 μm vs. 146–207 μm ; 87–102 μm vs. 61–87 μm , respectively), and sphincter present at the junction of oviduct and uterus (vs. uterus and oviduct without distinct sphincter differentiation). From *T. crassus* (Loof and Jairajpuri 1968; Peña-Santiago and Coomans 1994a) by longer body (0.93–1.07 mm vs. 0.68–0.92 mm), smaller lip region (9.5–10 μm vs. 10.5–12 μm wide; 3.5–4.0 μm vs. 5–5.5 μm high), absence of postrectal blind sac (vs. presence) and tail hemispheroid with blunt rounded to flat terminus (vs. convex conoid with rounded tip). From *T. paracrassus* (Peña-Santiago and Coomans 1994a), the new species can be differentiated by having narrower lip region (9.5–10 μm vs. 11.5–13 μm wide), shorter odontostyle (8–9.5 μm vs. 10–11.5 μm), longer prerectum (71–100 μm vs. 47–66 μm), tail hemispheroid with blunt rounded to flat terminus (vs. convex conoid with rounded tip) and males absent (vs. present). It differs from *T. sinensis* (Li et al. 2008) by lip region one-fourth (vs. one-third) of the body diameter at posterior end of neck region, longer odontostyle and odontophore (8–9.5 μm vs. 7 μm ; 9–11 μm vs. 8 μm , respectively), longer pharynx and basal expansion (216–237 μm vs. 191–208 μm ; 87–102 μm vs. 67–75 μm and occupying 39–43% vs. 35–36% of the total neck length, respectively), much longer oviducts (anterior one 83–107 μm

vs. 53–63 μm and the posterior one 61.5–92 μm vs. 45–50 μm long), prerectum 2.4–4.2 (vs. about 5) times the body diameter at anus long, longer rectum (22–28 μm vs. 18–20 μm). From *T. teres* (Loof 1971; Thorne 1974; Vinciguerra 1986; Peña-Santiago and Coomans 1994a), it differs by the females having lip region one-fourth in average (vs. one-third) of the body diameter at posterior end of the neck region, odontostyle longer (8–9.5 μm vs. 5–6 μm), one caudal opening in tail terminus (vs. one pair of subterminal pores), the anterior and posterior genital branch equally developed (vs. the anterior branch more developed than the posterior one), no sperm observed in the genital tract and males not known (vs. sperm present along the entire genital tract and males as frequent as females).

Discussion

In addition to the above characteristics used to differentiate the new species from its conspecifics, the pars proximalis vaginae of the new species should be noticed. Among the known didelphic species of *Tylencholaimus*, a cylindrical, spindle, convex, or pyriform pars proximalis vaginae has been described or illustrated. The violin-shaped structure in *Tylencholaimus helanensis* sp. n. is described here for the first time. This enriches the diversity of the pars proximalis vaginae and makes this characteristic more valuable for identification. In fact it is so distinctive that in the 18S rDNA and 28S rDNA Bayesian trees, *Tylencholaimus helanensis* sp. n. forms a monophyletic clade with 100% support. In the 18S rDNA tree, *Tylencholaimus helanensis* sp. n. is sister to a clade including *T. teres* and *T. proximus*. As mentioned previously, *Tylencholaimus helanensis* sp. n. is close to *T. teres* in morphology, but differs from the latter by several morphological characteristics such as a wider amphid aperture, a shorter prerectum, longer odontostyle and tail, and the fragments of their 18S rDNA sequences in common showed ten nucleotide differences. The new species does not otherwise show close relationships to *T. teres* in the 28S rDNA Bayesian trees, while the other close relative inferred from the 18S rDNA Bayesian tree, *T. proximus*, has a prodelphic genital system that is different to the didelphic-amphidelphic genital system of *Tylencholaimus helanensis* sp. n., and thus can be easily differentiated from the new species morphologically.

The sequences of *Tylencholaimus* species were not all grouped together in one clade in both the 18S rDNA and 28S rDNA Bayesian trees, suggesting that *Tylencholaimus* is not monophyletic. The deeper evolutionary relationships among *Tylencholaimus* currently cannot be further clarified due to because the few molecular data available for *Tylencholaimus*, especially 28S rDNA sequences, available on GenBank. For example, the relationship of the new species and *T. proximus* inferred from the 18S rDNA Bayesian tree was close, but this relationship cannot be confirmed because the 28S rDNA sequence of *T. proximus* is unavailable. Thus, the detailed relationships of *Tylencholaimus* species cannot be further resolved until more molecular data of *Tylencholaimus* are obtained.

Acknowledgements

This work was supported by a Special Project of Scientific and Technological Basis of the Ministry of Science and Technology of the People's Republic of China to Hui Xie (Grant no. 2006FY120100).

References

- Andrássy I (1998) Once more: the oesophageal gland nuclei in the dorylaimoid nematodes. *Opuscula Zoologica Budapest* 31: 165–171.
- Andrássy I (2009) Free-living nematodes of Hungary (Nematoda errantia). III. *Pedozoologica Hungarica* 5. Hungarian Natural History Museum and Systematic Research Group of the Hungarian Academy of Sciences, Budapest, Hungary, 608 pp.
- Abolafia J, Peña-Santiago R (2005) Nematodes of the order Rhabditida from Andalucía Oriental, Spain. *Pseudacrobeles elongatus* (de Man, 1880) comb. n. *Nematology* 7: 917–926. <https://doi.org/10.1163/156854105776186415>
- Ahad S, Ahmad W (2016) Description of two new and six known species of the genus *Tylencholaimus* de Man, 1876 (Nematoda: Dorylaimida) with a diagnostic compendium and key to species. *Zootaxa* 4107(4): 451–490. <https://doi.org/10.11646/zootaxa.4107.4.1>
- Álvarez-Ortega S, Peña-Santiago R (2016) *Aporcella charidemiensis* sp. n. (Dorylaimida: Aporcelaimidae) from the southern Iberian Peninsula, with comments on the phylogeny of the genus. *Nematology* 18(7): 811–821. <https://doi.org/10.1163/15685411-00002995>
- De Ley P, Loof PAA, Coomans A (1993) Terrestrial nematodes from the Galápagos Archipelago II: Redescription of *Aporcelaimellus obtusicaudatus* (Bastian, 1865) Altherr, 1968, with review of similar species and a nomenclature for the vagina in Dorylaimida (Nematoda). *Bulletin de l'Institut Royal des Sciences naturelles de Belgique, Biologie* 63: 13–34. <https://doi.org/10.1111/j.1471-8286.2007.01963.x>
- Dhanam M, Jairajpuri MS (1999) New leptonchid nematodes: One new genus and eleven new species from Malnad Tracts of Karnataka, India. *International Journal of Nematology* 9: 1–18.
- Holterman M, Wurff AVD, Elsen SVD, Megen HV, Bongers T, Holovachov O, Bakker J, Helder J (2006) Phylum-wide analysis of SSU rDNA reveals deep phylogenetic relationships among nematodes and accelerated evolution toward crown clades. *Molecular Biology and Evolution* 23: 1792–1800. <https://doi.org/10.1093/molbev/msl044>
- Holterman M, Rybarczyk K, Van den Elsen S, Van Megen H, Mooyman P, Peña-Santiago R, Bongers T, Bakker J, Helder J (2008) A ribosomal DNA-based framework for the detection and quantification of stress-sensitive nematode families in terrestrial habitats. *Molecular Ecology Resources* 8: 23–34.
- Hua C, Wu PF, He XJ, Zhu B (2014) Effects of different amounts of straw returning treatments on soil nematode community in purple soil. *Biodiversity Science* 22: 392–400. <https://doi.org/10.3724/SPJ.1003.2014.13217>

- Loof PAA, Jairajpuri MS (1968) Taxonomic studies on the genus *Tylencholaimus* De Man, 1876 (Dorylaimoidea) with a key to the species. *Nematologica* 14: 317–350. <https://doi.org/10.1163/187529268X00011>
- Loof PAA (1971) Freelifving and plant parasitic nematodes from Spitzbergen, collected by Mr. H. van Rossen. *Mededelingen Landbouwhogeschool Wageningen* 71: 1–86.
- Li YJ, Baniyamuddin M, Ahmad W, Wu JH (2008) Four new and four known species of *Tylencholaimoidea* (Dorylaimida: Nematoda) from China. *Journal of Natural History* 42: 1991–2010. <https://doi.org/10.1080/00222930802254722>
- Nedelchev S, Elshishka M, Lazarova S, Radoslavov G, Hristov P, Peneva V (2014) *Calcaridorylaimus castaneae* sp. n. (Nematoda, Dorylaimidae) from Bulgaria with an identification key to the species of the genus. *ZooKeys* 410: 41–61. <https://doi.org/10.3897/zookeys.410.6955>
- Peña-Santiago R, Coomans A (1994a) Revision of the genus *Tylencholaimus* de Man, 1876. Didelphic species. *Nematologica* 40: 32–68. <https://doi.org/10.1163/003525994X00049>
- Peña-Santiago R, Coomans A (1994b) Revision of the genus *Tylencholaimus* de Man, 1876. Prodelphic species: Part I. *Nematologica* 40: 175–185.
- Peña-Santiago R, Coomans A (1994c) Revision of the genus *Tylencholaimus* de Man, 1876. Prodelphic species: Part II. *Nematologica* 40: 186–213. <https://doi.org/10.1163/003525994X00139>
- Peña-Santiago R, Coomans A (1994d) Revision of the genus *Tylencholaimus* de Man, 1876. Prodelphic species: Part III. *Nematologica* 40: 348–368. <https://doi.org/10.1163/003525994X00256>
- Peña-Santiago R, Coomans A (1996a) Revision of the genus *Tylencholaimus* de Man, 1876. Prodelphic species: Part IV. *Nematologica* 42: 282–310. <https://doi.org/10.1163/004425996X00038>
- Peña-Santiago R, Coomans A (1996b) Revision of the genus *Tylencholaimus* de Man, 1876. Remaining species. *Nematologica* 42: 417–439. <https://doi.org/10.1163/004525996X00037>
- Peña-Santiago R, Coomans A (1996c) Revision of the genus *Tylencholaimus* de Man, 1876. General discussion and key to the species. *Nematologica* 42: 440–454. <https://doi.org/10.1163/004525996X00046>
- Peña-Santiago R (2008) The genus *Tylencholaimus* de Man, 1876 (Dorylaimida: Tylencholaimidae), revisited twelve years after. *Journal of Nematode Morphology and Systematics* 11: 119–128.
- Sang Y, Jia C, Ruan WB, Ma CC, Gao YB (2010) Effect of fencing on plant and nematode communities in the grassland in mid and eastern Inner Mongolia, China. *Ecology and Environmental Sciences* 19: 2332–2338.
- Thorne G (1974) Nematodes of the Northern Great Plains. Part II. Dorylaimoidea in part (Nemata, Adenophorea). *Technical Bulletin Agricultural Experimental Station South Dakota State University, Brookings* 41: 1–120.
- Tong FC, Xiao YH, Wang QL (2009) Nematode community composition and diversity associated with different vegetations in Changbai Mountain in spring. *Ecology and Environmental Sciences* 18: 653–657.

- Vinciguerra MT (1986) New and known species of *Tylencholaimus* de Man, 1876 (Dorylaimida, Nematoda) from Italian beech forests with a key to the species. *Nematologia Mediterranea* 14: 107–116.
- Whitehead AG, Hemming JR (1965) A comparison of some quantitative methods of extracting small vermiform nematodes from soil. *Annals of Applied Biology* 55: 25–38. <https://doi.org/10.1111/j.1744-7348.1965.tb07864.x>
- Wang XF, Su YZ, Liu WJ, Yang R, Yang X (2011) Characteristics of soil nematode communities under the canopy of *Tamarix* spp. in different habitats. *Arid Zone Research* 28: 1057–1063.
- Wu WJ, Yan L, Xu CL, Wang K, Jin SY, Xie H (2016) Morphology and morphometrics of *Heterodorus qinghaiensis* n. sp. (Dorylaimida, Nordiidae) from soil samples in China. *Journal of Helminthology* 90: 385–391. <https://doi.org/10.1017/S0022149X15000358>
- Wu WJ, Huang X, Xie H, Wang K, Xu CL (2017) Morphometrics and molecular analysis of the free-living nematode, *Belondira bagongshanensis* n. sp. (Dorylaimida, Belonidiridae), from China. *Journal of Helminthology* 91: 7–13. <https://doi.org/10.1017/S0022149X15001091>
- Xie H (2005) *Taxonomy of plant nematodes*, 2nd edn. Higher Education Press, Beijing, China, 435 pp.
- Xue HY, Hu F, Luo DQ (2013) Effects of alpine meadow plant communities on soil nematode functional structure in Northern Tibet, China. *Acta Ecologica Sinica* 33: 1482–1494. <https://doi.org/10.5846/stxb201204170549>
- Xing SW, Zhu H, Zhuang DH, Fan HM, Luo GH, Qiu ST (2014) Characteristics of soil nematode community in Fenghuang Dancong tea plantations. *Chinese Journal of Ecology* 33: 666–673.
- Yu CJ, Sun JN, Fu KH, Dou K, Cen JM, Chen J (2015) Isolation and molecular identification of nematodes of main nematodes in rhizosphere soils and seedlings associated with corn dwarf. *Journal of Plant Protection* 42: 892–898.
- Zhang WD, Shang YF, Wang XF (2010) The response of soil nematode community to vegetation restoration in Shimenshan in Dalian. *Acta Ecologica Sinica* 30: 0878–0886.

New records of bees of the genus *Sphecodes* Latreille in the Palaearctic part of China (Hymenoptera, Halictidae)

Yulia V. Astafurova¹, Maxim Yu. Proshchalykin², Ze-qing Niu³, Chao-dong Zhu^{3,4}

1 Zoological Institute, Russian Academy of Sciences, Universitetskaya Nab., 1, Saint Petersburg 199034, Russia
2 Federal Scientific Centre for East Asian Terrestrial Biodiversity, Far Eastern Branch of Russian Academy of Sciences, Vladivostok 690022, Russia **3** Key Laboratory of Zoological Systematics and Evolution, Institute of Zoology, Chinese Academy of Sciences, 1 Beichen West Road, Chaoyang District, Beijing, 100101, PR China
4 College of Life Sciences, University of Chinese Academy of Sciences, No.19(A) Yuquan Road, Shijingshan District, Beijing, 100049, PR China

Corresponding author: Maxim Yu. Proshchalykin (proshchalikin@biosoil.ru)

Academic editor: M. S Engel | Received 28 June 2018 | Accepted 15 August 2018 | Published 23 October 2018

<http://zoobank.org/B6B988C5-521B-4854-B9B0-1F9713779323>

Citation: Astafurova YV, Proshchalykin MY, Niu Z-q, Zhu C-d (2018) New records of bees of the genus *Sphecodes* Latreille in the Palaearctic part of China (Hymenoptera, Halictidae). ZooKeys 792: 15–44. <https://doi.org/10.3897/zookeys.792.28042>

Abstract

The available information about the cleptoparasitic bees of the genus *Sphecodes* in the Palaearctic part of China is summarized. Twenty-four species are currently known from this area including 16 newly recorded. Based on type specimens, new synonymies have been proposed for *Sphecodes cristatus* Hagens, 1882 = *S. alfkeni* Meyer, 1922, **syn. n.**; *S. longulus* Hagens, 1882 = *S. subfasciatus* Blüthgen, 1934, **syn. n.**; *S. nippon* Meyer, 1922 = *S. kansuensis* Blüthgen, 1934, **syn. n.**; *Sphecodes pieli* Cockerell, 1931 = *S. orientalis* Astafurova & Proshchalykin, 2014, **syn. n.** Lectotypes are designated for *Sphecodes alfkeni* Meyer, 1922 and *S. pellucidus niveipennis* Meyer, 1925. Illustrated keys to males and females of all species known from Palaearctic China and an updated checklist of the 33 Chinese species of *Sphecodes* are provided.

Keywords

Anthophila, Apiformes, cleptoparasites, fauna, new synonymy, taxonomy

Introduction

The present paper is part of a series of works dealing with the bees of the cleptoparasitic genus *Sphecodes* Latreille, 1804 from the Palaearctic region (Astafurova and Proshchalykin 2014, 2015a, b, 2016a, b, 2017a, b, Astafurova et al. 2014, 2015, 2018). Consequently, we focus on species in northern China and do not deal with the southern, Oriental species of China.

The question of where the zoogeographical boundary exists between the Oriental and the Palaearctic regions in China has been discussed by many researchers working on various groups of animals (Emeljanov 1974, Hoffman 2001, Fellowes 2006, Chen et al. 2008, Heiser and Schmitt 2013, He et al. 2017). In this paper, the views of Pesenko (2007) and Astafurova (2013) are followed for halictid bees, which posit that the approximate border between Palaearctic and Oriental Regions in China lies between 30°–35° northern latitude.

Sphecodes formosanus Cockerell was the first species of the genus described from China (Taiwan) (Cockerell 1911). Since then, a total of ten species and three subspecies have been described (Meyer, four species and two subspecies; Cockerell, four species; Blüthgen, two species and one subspecies), seven of which are still valid (see section on taxonomy for details). Sixteen *Sphecodes* species have been recorded from China so far (Meyer 1920, 1922, 1925, Blüthgen 1924, 1927, 1934, Cockerell 1911, 1922, 1931, Strand and Yasumatsu 1938, Ascher and Pickering 2018). Among them, only seven species were known from the Palaearctic.

Based on a comprehensive study of specimens in various collections, we catalogue 24 species of the genus *Sphecodes*, with 16 species recorded from China for the first time. New synonymies are proposed for four specific names: *Sphecodes cristatus* Hagens, 1882 = *S. alfkeni* Meyer, 1922, syn. n.; *S. longulus* Hagens, 1882 = *S. subfasciatus* Blüthgen, 1934, syn. n.; *S. nippon* Meyer, 1922 = *S. kansuensis* Blüthgen, 1934, syn. n.; *Sphecodes pieli* Cockerell, 1931 = *S. orientalis* Astafurova & Proshchalykin, 2014, syn. n. Illustrated keys to the species known from the Palaearctic part of China are presented to facilitate further studies.

Materials and methods

The results presented in this paper are based on 453 specimens collected in the Palaearctic part of China and currently housed in the Institute of Zoology, Chinese Academy of Sciences (Beijing, China, IZCAS); the Zoological Institute, Russian Academy of Sciences (St. Petersburg, Russia, ZISP); and the private collection of Maximilian Schwarz (Ansfelden, Austria, PCMS). The following acronyms are used for the collections where type specimens are deposited:

MNHB Museum für Naturkunde der Humboldt Universität zu Berlin, Germany.

NHRS Naturhistoriska riksmuseet, Stockholm, Sweden.

USNM National Museum of Natural History, Smithsonian Institution, Washington, DC, USA.

KUF Kyushu University, Fukuoka, Japan.

The taxonomy and distribution of species generally follow that of Warncke (1992), Bogusch and Straka (2012), and Astafurova and Proshchalykin (2017b). A detailed current synonymy of the species has been given by Astafurova and Proshchalykin (2017b). Morphological terminology follows that of Michener (2007) and Engel (2001). The ventral surface of some flagellomeres bear a distinctive patch of sensilla trichodea A (sensu Årgent and Svensson 1982), which we refer to as “tyloids;” they are easily observable under light microscopy. The abbreviations F, T, and S are used for flagellomere, metasomal tergum, and metasomal sternum, respectively. The density of integumental punctures is described using the following formula: puncture diameter (in μm) / ratio of distance between punctures to average puncture diameter, e.g., 15–20 μm / 0.5–1.5. Integumental sculpturing, aside from distinctive surface punctation, is described as follows: reticulate: superficially net-like or made up of a network of raised lines; rugose: irregular, non-parallel, wrinkled raised lines (rugae); tessellate: regular network of shallow grooves with flat interspaces.

Specimens were studied with a Leica M205A stereomicroscope and photographs were taken with a combination of a stereomicroscope (Olympus SZX10) and a digital camera (Canon EOS70D). Final images represent a composite of several photographs taken at different focal planes and combined using the program Helicon Focus 6. All images were post-processed for contrast and brightness using Adobe® Photoshop®.

The species are presented alphabetically and those that could not be inspected in this paper are quoted from published sources. We use the following abbreviations for collectors: **JH** – Jiri Halada, **PK** – Petr Kozlov; **VR** – Vsevolod Roborovsky. New distributional records are noted with an asterisk (*).

Unfortunately, we have not examined the type of *S. manchurianus*, because it was not found in Kyushu University (Japan). We also have not found specimens corresponding to the original description of Strand and Yasumatsu (1938) in our material.

Taxonomy

Key to the *Sphecodes* species of the Palaearctic part of China

Additional species are included in this key because they are widespread in the Palaearctic and may also occur in China. These include *S. maruyamanus* Tsuneki, 1983, *S. murotai* Tsuneki, 1983, *S. tanoi* Tsuneki, 1983 (known from Japan and Russian Far East), *S. miniatus* Hagens, 1882, *S. puncticeps* Thomson, 1870, and *S. reticulatus* Thomson, 1870. *Sphecodes manchurianus* Strand & Yasumatsu, 1938, known only from the holotype, is not included.

Males

- 1 Costal margin of hind wing with 7–14 hamuli. Base of gonocoxite dorsally without impression. Usually large species: total body length 5.0–12.0 mm **2**
- Costal margin of hind wing with 5–6 hamuli. Base of gonocoxite dorsally with or without impression. Large or small species: total body length 3.5–11.0 mm **11**
- 2 Head rounded, about as long as wide. Hind wing with basal (*M*) vein strongly curved. T1 finely and sparsely (sometimes indistinctly) punctate. Gonostylus dorsally with small rectangular process directed to penis valve (Fig. 15). Body length 7.0–10.0 mm ***S. monilicornis* (Kirby)**
- Head transverse, wider than long. Hind wing with basal (*M*) vein weakly curved. T1 distinctly coarsely and densely punctate. Gonostylus another shape **3**
- 3 Mesoscutum densely punctate, with confluent punctures (areolate) **4**
- Mesoscutum sparsely punctate, medially with punctures separated by at least a puncture diameter **5**
- 4 Head more transverse, 1.2 times as wide as long. Vertex long, distance from top of head to upper margin of lateral ocellus about 2.5–3.0 lateral ocellar diameters as seen in dorsal view. Tyloids on flagellomeres (at least from F4 onward) semicircular across basal 1/5–1/3 and linear across remaining flagellomeres as seen in lateral view. Mesoscutellum sparsely punctate, medially with punctures separated by more than a puncture diameter and often with impunctate areas. T1 completely red. Gonostylus larger, not narrowed apically (Fig. 1). Body length 9.0–12.0 mm ***S. albilabris* (Fabricius)**
- Head less transverse, 1.1 times as wide as long. Vertex shorter, distance from top of head to upper margin of lateral ocellus about two lateral ocellar diameters as seen in dorsal view. Tyloids on flagellomeres semicircular across basal 1/6–1/4, linear portion along remaining flagellomeres not developed. Mesoscutellum densely punctate, with confluent punctures. T1 black or brownish at least on basal 1/3 Gonostylus smaller, distinctly narrowed apically (Fig. 23). Body length 7.0–12.0 mm ***S. scabricollis* Wesmael**
- 5 Vertex with a longitudinal carina. Gonostylus smaller, not overlapped apically, as in Figs 4, 21 **6**
- Vertex without a longitudinal carina. Gonostylus larger, another shape, overlapped apically **8**
- 6 Tyloids on flagellomeres (at least from F4 onward) are semicircular across basal 1/3–1/2. T1 with marginal zone very finely and indistinctly punctate. Body length 7.0–10.0 mm ***S. cristatus* Hagens**
- Tyloids on flagellomeres weakly developed, very narrow, semicircular across basal 1/7–1/5 of flagellomere. T1 with marginal zone coarsely and distinctly punctate **7**

- 7 Head more transverse, 1.2 times as wide as long. Mesoscutum more coarsely punctate (30–75 μm). T2 with marginal zone impunctate. Larger: total body length 7.0–11.0 mm ***S. olivieri* Lepeletier de Saint-Fargeau**
- Head less transverse, 1.10–1.15 times as wide as long. Mesoscutum more finely punctate (25–40 μm). T2 with marginal zone distinctly punctate. Smaller: total body length 5.0–7.0 mm..... ***S. pectoralis* Morawitz**
- 8 Vertex long, distance from top of head to upper margin of lateral ocellus about three lateral ocellar diameters as seen in dorsal view. Tyloids on flagellomeres cover at least 1/3 part of flagellomere Gonostylus with long apical process (Fig. 9)..... **9**
- Vertex shorter, distance from top of head to upper margin of lateral ocellus about two lateral ocellar diameters as seen in dorsal view. Tyloids on flagellomeres not covering more than 1/4 part of flagellomere. Gonostylus another shape at tip, as in Fig. 2 **10**
- 9 Tyloids on flagellomeres well developed, covering large part of flagellomere (as seen in lateral view, Fig. 57). Body length 7.0–14.0 mm ***S. gibbus* (Linnaeus)**
- Tyloids on flagellomeres weakly developed, covering about 1/3 of flagellomere (as seen in lateral view, Fig. 58). Body length 7.0–11.0 mm ***S. nippon* Meyer**
- 10 T4 with marginal zone finely tessellate, without punctures (Fig. 46). Body length 7.0–10.0 mm ***S. reticulatus* Thomson**
- T4 with marginal zone distinctly punctate, smooth between punctures (rarely indistinctly tessellate) (Fig. 45). Body length 7.0–12.0 mm..... ***S. alternatus* Smith**
- 11 Base of gonocoxite dorsally without impression **12**
- Base of gonocoxite dorsally with impression **19**
- 12 T1 densely punctate. Gonostylus elongate (Fig. 18). Body length 5.0–5.5 mm.. ***S. nurekensis* Warncke**
- T1 impunctate or with a few fine punctures. Gonostylus another shape **13**
- 13 Vertex coarsely and densely punctate, ocello-ocular area with confluent punctures, separated by at most a half puncture diameter **14**
- Vertex finely and sparser punctate, ocello-ocular area with punctures, separated by at least a puncture diameter **17**
- 14 Vertex with longitudinal carina (in *S. kozlovi* usually weakly developed) (Figs 38, 39) **15**
- Vertex without longitudinal carina..... **16**
- 15 Vertex with well visible longitudinal carina. Felt-like areas on last flagellomeres cover at least 1/2 underside of flagellomere, F2 as long as wide (Fig. 53). T1 impunctate or with a few fine punctures. Membranous portion of gonostylus smaller, as in Fig. 19. Body length 6.0–9.0 mm..... ***S. pieli* Cockerell**
- Vertex with weakly visible longitudinal carina. Felt-like areas on last flagellomeres cover about 1/3 underside of flagellomere, F2 slightly longer than wide (Fig. 54). T1 sparsely, but coarsely punctate. Membranous portion of

- gonostylus large, as in Fig. 12. Body length 8.0–10.0 mm
 **S. kozlovi Astafurova & Proshchalykin**
- 16 Tyloids on last flagellomeres (at least from F4 onward) usually cover more than 1/2 of ventral flagellar surfaces, often up to 4/5 Membranous portion of gonostylus larger, as in *S. kozlovi* (Fig. 12). Body length 7.0–11.0 mm
 **S. pellucidus Smith**
- Tyloids on last flagellomeres (at least from F4 onward) usually cover about 1/2 of ventral flagellar surfaces, rarely up to 3/4. Membranous portion of gonostylus smaller (Fig. 6). Body length 6.0–9.0 mm **S. ephippius (Linné)**
- 17 Ocello-ocular area densely punctate, with punctures separated by about one puncture diameter. Gonostylus joining apex and partly inner surface of gonocoxite (Fig. 22). Body length 5.0–7.5 mm **S. puncticeps Thomson**
- Ocello-ocular area sparsely punctate, with punctures separated by 1–3 puncture diameters. Gonostylus joining only apex of gonocoxite (Fig. 8) **18**
- 18 F2 shorter, 1.4–1.6 times as long as wide. Tyloids on the flagellomeres extend across 1/4–1/2 of ventral flagellar surfaces. Body length 3.5–6.0 mm
 **S. longulus Hagens**
- F2 longer, 1.7–1.8 times as long as wide. Tyloids on the flagellomeres extend across 1/2–3/4 of ventral flagellar surfaces. Body length 4.0–5.0 mm
 **S. turanicus Astafurova & Proshchalykin**
- 19 T1 densely punctate. Face with appressed white pubescence below and above the antennal toruli **20**
- T1 impunctate or with sparse punctures (in *S. miniatus* sometimes relatively densely punctate). Face with appressed white pubescence only below the antennal toruli **22**
- 20 Tyloids variable, covering 1/2–4/5 flagellar ventral surfaces. Membranous portion of gonostylus small, triangular (Fig. 17)
 **S. schwarzi Astafurova & Proshchalykin**
- Tyloids covering from 3/4 to entire ventral flagellar surfaces. Membranous portion of gonostylus large, close to rectangular (Figs 10, 20) **21**
- 21 Antenna longer, F2 1.4 times as long as wide (Fig. 55). Membranous portion of gonostylus almost straight on inner edge (Fig. 20). Body length 5.0–7.5 mm **S. pinguiculus Pérez**
- Antenna shorter, F2 1.2 times as long as wide (Fig. 56). Membranous portion of gonostylus weakly S-curved on inner edge (Fig. 10). Body length 5.0–7.5 mm **S. intermedius Blüthgen**
- 22 Pronotum, between dorsal and lateral surfaces, rounded, not angulate (Fig. 36) **23**
- Pronotum, between dorsal and lateral surfaces, with sharp angle (Fig. 35) **26**

- 23 Tyloids on flagellomeres covering less than 1/3 of ventral flagellar surfaces. Membranous portion of gonostylus larger, trapezoidal (Fig. 5). Body length 6.0–9.0 mm.....***S. ferruginatus* Hagens**
- Tyloids on flagellomeres (at least from F4 onward) covering about 1/2–3/4 or entire of ventral flagellar surfaces. Membranous portion of gonostylus smaller, oval or almost square (Figs 13, 16, 24)**24**
- 24 Clypeus with fine, simple and sparsely plumose setae, sculpturing clearly visible (Fig. 33). Membranous portion of gonostylus square (Fig. 13). Body length 6.0–7.0 mm ***S. maruyamanus* Tsuneki**
- Clypeus with densely plumose setae, partly obscuring sculpturing (Fig. 34). Membranous portion of gonostylus close to oval**25**
- 25 Antenna short, middle flagellomeres as long as or slightly longer than wide. Tyloids on flagellomeres covering entire of ventral flagellar surfaces. Membranous portion of gonostylus longer, reach penis valve (Fig. 16). Body length 5.5–6.5 mm.....***S. murotai* Tsuneki**
- Antenna long, flagellomeres (from F3 onward) 1.2–1.3 times as long as wide. Tyloids on flagellomeres (at least from F4 onward) covering about 1/2–3/4 of ventral flagellar surfaces. Membranous portion of gonostylus shorter, not reach penis valve (Fig. 24). Body length 6.0–7.0 mm.....***S. tanoi* Tsuneki**
- 26 F2 short, 0.9–1.0 times as long as F3. Tyloids on flagellomeres (at least from F4 onward) usually cover entire ventral flagellar surfaces. Gonostylus with trapezoidal membranous portion (Fig. 7). Body length 5.0–6.5 mm.....
.....***S. geoffrellus* (Kirby)**
- F2 longer, 1.1–1.2 as long as F3. Tyloids on flagellomeres shorter, covering at most 4/5 the ventral flagellar surfaces (in *S. miniatus* tyloids on last flagellomeres rare cover entire ventral flagellar surfaces).....**27**
- 27 Tyloids on flagellomeres covering more than 3/4 flagellar ventral surfaces. Gonostylus with large, trapezoidal membranous portion (Fig. 14). Body length 4.0–6.0 mm ***S. miniatus* Hagens**
- Felt-like areas on flagellomeres cover less 1/3 underside of flagellomere. Gonostylus with oval membranous portion or without one**28**
- 28 Head less transverse, 1.05 times as wide as long. Mesoscutum sparsely punctate, medially with punctures mostly separated by 1–3 puncture diameters. T1–T3 usually red, rarely terga entirely black. Gonostylus with oval membranous portion (Fig. 3). Body length 5.0–7.0 mm ***S. crassus* Thomson**
- Head more transverse, at least 1.15 times as wide as long. Mesoscutum very densely punctate, with confluent punctures (areolate). Terga usually wholly black, rare T1 dark red. Gonostylus without membranous portion (Fig. 11). Body length 7.5–8.5 mm.....***S. laticaudatus* Tsuneki**

Females

- 1 Hind wing with basal (*M*) vein weakly curved; costal margin with 7–14 hamuli. Usually large species: total body length 6.0–15.0 mm..... **2**
- Hind wing with basal (*M*) vein strongly curved; costal margin with 5–6 hamuli. Large or small species: total body length 5.5–11.0 mm..... **10**
- 2 Vertex less elevated (distance from top of head to upper margin of lateral ocellus less two lateral ocellar diameters as seen in frontal view), with longitudinal sharp carina (Fig. 37) **3**
- Vertex more elevated (distance from top of head to upper margin of lateral ocellus more two lateral ocellar diameters as seen in frontal view), acarinate, but sometimes with weak (indistinct) longitudinal ridge **5**
- 3 Face and gena with sparse, semi-erect, gray pubescence not obscuring integument. T1 with finer punctures (3–10 μm). Body length 6.0–8.0 mm ***S. cristatus* Hagens**
- Face and gena with dense, appressed, snow-white pubescence obscuring integument. T1 with coarser punctures (10–30 μm) **4**
- 4 Mesoscutum coarsely punctate (25–75 μm). T2 with marginal zone impunctate. Larger: body length 8.0–11.0 mm ***S. olivieri* Lepeletier de Saint Fargeau**
- Mesoscutum relatively finely punctate (25–40 μm). T2 with marginal zone distinctly punctate. Smaller: body length 6.5–8.5 mm ***S. pectoralis* Morawitz**
- 5 Gena flat. Preoccipital lateral carina developed (Fig. 40). Body length 9.0–12.0 mm ***S. scabricollis* Wesmael**
- Gena swollen. Preoccipital carina not developed **6**
- 6 Vertex shorter, distance from top of head to upper margin of lateral ocellus about 2 lateral ocellar diameters as seen in dorsal view (Fig. 42). T4 with marginal zone punctate and smooth between punctures or finely tessellate without punctures **7**
- Vertex longer, distance from top of head to upper margin of lateral ocellus equal to 2.5–3.0 lateral ocellar diameters as seen in dorsal view (Fig. 41). T4 with marginal zone impunctate, smooth (rarely indistinctly tessellate) **8**
- 7 T4 with marginal zone impunctate, finely tessellate (Fig. 46); T1 finely punctate (10–15 μm). Mesoscutum usually densely punctate, medially with punctures separated by not more than 1–3 puncture diameters, sometimes sparser. Body length 7.0–10.0 mm ***S. reticulatus* Thomson**
- T4 with marginal zone distinctly punctate, smooth between punctures (rarely indistinctly tessellate) (Fig. 45); T1 coarsely punctate (15–25 μm). Mesoscutum usually sparsely punctate, medially with punctures separated by mostly 2–4 puncture diameters. Body length 8.0–11.0 mm ***S. alternatus* Smith**
- 8 Mesoscutum densely punctate, with punctures separated by less than a puncture diameter (Fig. 47). Body length 9.0–12.0 mm ***S. albilabris* (Fabricius)**
- Mesoscutum sparsely punctate, medially with punctures separated by at least 2 puncture diameters (Fig. 50) **9**

- 9 Head rounded-rectangular on upper margin, square-shaped as seen in frontal view (Fig. 32); vertex sparsely punctate, punctures mostly separated by more than a puncture diameter. Pygidial plate equal or slightly narrower than metabasitarsus. T1 usually indistinctly punctate, with a few very fine punctures. Body length 7.0–10.0 mm..... ***S. monilicornis* (Kirby)**
- Head uniformly rounded on upper margin, oval as seen in frontal view (Fig. 28); vertex densely punctate, punctures mostly separated by less than a puncture diameter. Pygidial plate 0.5–0.6 times as wide as metabasitarsus. T1 distinctly punctate, with fine and coarser punctures. Body length 7.0–15.0 mm..... ***S. gibbus* (Linnaeus) and *S. nippon* Meyer***
- 10 Mandible simple (without an inner tooth)..... **11**
- Mandible bidentate..... **13**
- 11 Head narrower, at most 1.15 times as wide as long (Fig. 26). Body length 4.0–6.0 mm..... ***S. longulus* Hagens**
- Head broader, 1.2–1.3 times as wide as long..... **12**
- 12 Face, gena and mesepisternum with gray, sparse, semi-erect pubescence, not obscuring integument. Metasoma coarsely punctate (10–15 μm). Pygidial plate as wide as metabasitarsus. Body length 5.0–8.0 mm.....
..... ***S. puncticeps* Thomson**
- Face, gena and mesepisternum with dense, snow-white, appressed, pubescence obscuring integument (Fig. 31). Metasoma finely punctate (3–5 μm). Pygidial plate 1.2 times as wide as metabasitarsus
..... ***S. turanicus* Astafurova & Proshchalykin**
- 13 Pygidial plate at least 1.2 times wider than metabasitarsus, usually dull. Mesoscutum densely punctate, punctures usually separated by less than two puncture diameters. Total body length 7.0–11.0 mm..... **14**
- Pygidial plate equal to or narrower than metabasitarsus, shiny. Mesoscutum usually sparsely punctate, disc medially with punctures separated by more than two puncture diameters. Total body length 4.0–9.0 mm..... **18**
- 14 Vertex with longitudinal carina (Figs 38, 39) **15**
- Vertex without longitudinal carina..... **16**
- 15 Vertex with obvious longitudinal carina (Fig. 38). Setae on scape shorter than width of scape. Pygidial plate 1.2–1.4 times wider than metabasitarsus. Body length 7.0–9.0 mm..... ***S. pieli* Cockerell**
- Vertex with weakly visible longitudinal carina (Fig. 39). Setae on scape distinctly longer than width of scape (not obviously in old females). Pygidial plate 1.4–1.5 times wider than metabasitarsus. Body length 8.0–9.0 mm.....
..... ***S. kozlovi* Astafurova & Proshchalykin**
- 16 Pygidial plate 1.6–1.7 times as wide as metabasitarsus. Gena wider, 0.8 times as wide as eye in lateral view. Mesoscutum densely punctate, with punctures

* Females of this vicarious species are very difficult to distinguish morphologically; however, *S. nippon* is distributed in China to Gansu on the West, whereas *S. gibbus* is distributed in China to Xinjiang on the East.

- separated by at most a puncture diameter (Fig. 51). Body length 7.5–10.0 mm.....**S. laticaudatus Tsuneki**
- Pygidial plate 1.2–1.5 times as wide as metabasitarsus. Gena narrower, 0.7 times as wide as eye in lateral view. Mesoscutum sparsely punctate, medially with punctures usually separated by 1–2 puncture diameters (Fig. 52)..... **17**
- 17 Head more transverse, 1.30–1.35 times as wide as long; vertex, behind ocelli, not elevated in frontal view. Setae on scape distinctly longer than width of scape. Pygidial plate 1.3–1.5 times as wide as metabasitarsus..... **S. pellucidus Smith**
- Head less transverse, 1.20–1.25 times wider than long; vertex, behind ocelli, weakly elevated. Setae on scape shorter than width of scape. Pygidial plate 1.2–1.4 times as wide as metabasitarsus
-**S. ehippius (Linné) and S. grabami Cockerell***
- 18 Clypeus densely punctate, punctures separated by less than one puncture diameter. Pronotum, between dorsal and lateral surfaces, rounded, not angulate (Fig. 36)..... **19**
- Clypeus sparsely punctate, punctures separated by at least one puncture diameter. Pronotum, between dorsal and lateral surfaces, with sharp angle (Fig. 35)..... **22**
- 19 Hind femur narrow, regularly pointed toward distal end, its length more than 3.5 times its maximum width. Body length 6.0–7.5 mm
- **S. maruyamanus Tsuneki**
- Hind femur widened in proximal half, its length at most 3 times its maximum width..... **20**
- 20 Vertex, behind ocelli, weakly elevated in frontal view (Fig. 25). Body length 6.0–9.0 mm.....**S. ferruginatus Hagens**
- Vertex not elevated in frontal view (Fig. 30)..... **21**
- 21 Thorax ventrally with sculpture finer than on sides (Fig. 44). Pygidial plate slightly narrower than metabasitarsus. Body length 6–7 mm
-**S. tanoi Tsuneki**
- Thorax ventrally with sculpture as coarse as that on sides (Fig. 43). Pygidial plate as wide as metabasitarsus. Body length 5.5–6.5 mm.....
-**S. murotai Tsuneki**
- 22 Vertex longer, distance from top of head to upper margin of lateral ocellus equal to about 3–3.5 times lateral ocellar diameters as seen in dorsal view. Upper half of gena with appressed, dense pubescence obscuring integument..... **23**
- Vertex shorter, distance from top of head to upper margin of lateral ocellus equal to about two lateral ocellar diameters as seen in dorsal view. Gena with erect, sparse pubescence **24**

** Females of these species are very difficult to distinguish morphologically; however, *S. ehippius* is distributed in North-West China (Xinjiang), whereas *S. grabami* is recorded from Central, South and East China; the male of *S. grabami* is unknown.

- 23 Mesoscutum and mesoscutellum very sparsely punctate, with tiny punctures separated by 1–7 diameters (Fig. 48). Body length 5.0–7.0 mm
.....*S. pinguiculus* Pérez
- Mesoscutum and mesoscutellum more densely punctate, with coarse punctures separated by 1–3 puncture diameters (Fig. 49). Body length 6.5–8.5 mm.....
..... *S. intermedius* Blüthgen
- 24 F3 transverse, 0.6–0.7 times as long as wide, as long as F1. Pygidial plate 0.9–1.0 as wide as metabasitarsus.....**25**
- F3 square, as long as wide, longer than F1 Pygidial plate 0.6–0.8 as wide as metabasitarsus.....**26**
- 25 Paraocular area with dense, strongly plumose setae below the antennal toruli (Fig. 29). Body length 4.5–5.5 mm
..... *S. schwarzi* Astafurova & Proshchalykin
- Face with sparse, simple and weakly plumose setae (Fig. 27). Body length 4.0–6.0 mm.....
..... *S. miniatus* Hagens
- 26 Head more transverse, 1.25 times as wide as long. Labrum trapezoidal, 0.7 times as long as wide. Hind femur strongly enlarged on proximal half, maximum width 0.4 times its length. Body length 5.0–8.0 mm
.....*S. crassus* Thomson
- Head less transverse, 1.1 times as wide as long. Labrum semicircular, 0.5 times as long as width. Hind femur weakly enlarged on proximal half, maximum width 0.35 times its length. Body length 4.5–6.5 mm.....
.....*S. geoffrellus* (Kirby)

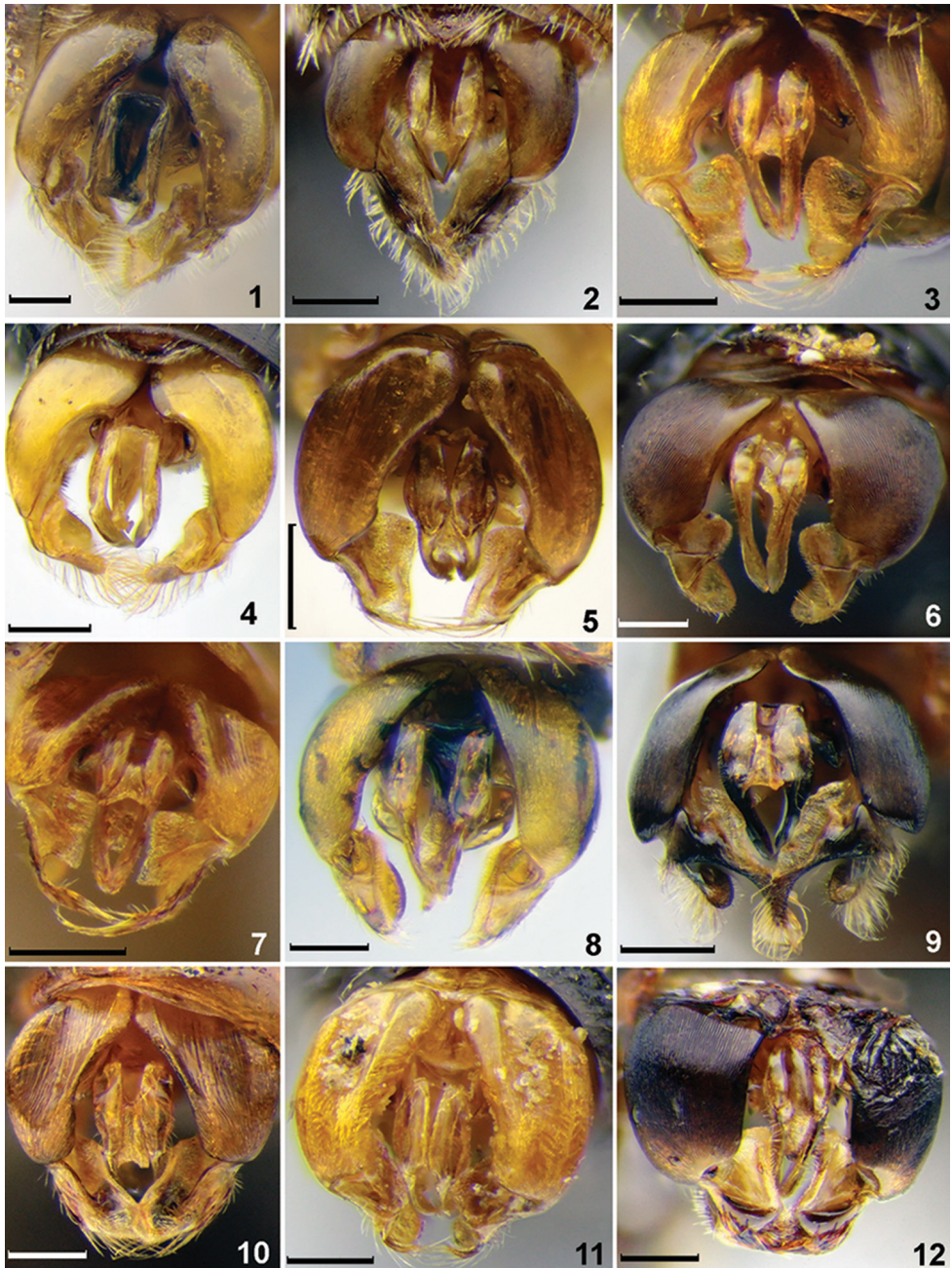
List of species

Sphcodes albilabris (Fabricius, 1793)

Figs 1, 47

Material examined. CHINA: *Liaoning*, 1 ♀, 50 km N Mukden [Shenyang] [42°12'N, 123°23'E], 20.VII.1952, leg. Rubtsov (ZISP); *Inner Mongolia*, 1 ♂, Xilinhot [43°54'N, 116°00'E], 27.VII.1971, leg. Y.-W. Zhang (IZCAS); *Hebei*, 1 ♀, Kreis Yongnian [36°25'N, 114°14'E], 1995, leg. S.-Q. Li (IZCAS); 1 ♀, Yangjiaping [39°58'N, 115°24'E], 3.VIII.1937, leg. O. Piel (IZCAS); 1 ♀, Yu Xian, Xiheyang [39°57'N, 114°00'E], 800 m, 29.VII.1964, leg. B.-Q. Li (IZCAS); *Beijing*, 1 ♀, Xiyuan [39°55'N, 116°24'E], 50 m, 23.VII.1962, leg. C.-G. Wang (IZCAS); *Shanxi*, 1 ♀, Xiexian, Zhongtiao Shan Mts. [34°48'N, 111°36'E], 22–24.V.1996, leg. JH (PCMS); *Gansu*, 1 ♂, Lanzhou [36°00'N, 103°25'E], 1500 m, 9.IX.1957, leg. Y.-R. Zhang (IZCAS).

Distribution. *China (Liaoning, Inner Mongolia, Hebei, Beijing, Shanxi, Gansu), Central Asia, Russia, Europe (north to Finland and Sweden), Turkey, Syria, Caucasus, North Africa, Israel, India.



Figures 1–12. Genitalia, males, dorsal view. **1** *Sphecodes albilabris* (Fabricius) **2** *S. alternatus* Smith **3** *S. crassus* Thomson **4** *S. cristatus* Hagens **5** *S. ferruginatus* Hagens **6** *S. ephippius* (Linné) **7** *S. geoffrellus* (Kirby) **8** *S. longulus* Hagens **9** *S. gibbus* (Linnaeus) **10** *S. intermedius* Blüthgen **11** *S. laticaudatus* Tsuneki **12** *S. kozlovi* Astafurova & Proshchalykin. Scale bars: 0.25 mm.

***Sphecodes alternatus* Smith, 1853**

Figs 2, 46

Material examined. CHINA: *Gansu*, 2 ♂♂, oasis Sachjou [Dunhuang] [40°09'N, 94°40'E], Gashun Gobi desert, 1–3.VIII.1895, VR, PK (ZISP); *Xinjiang*, 1 ♂, Yin-
ing, Boro Hqro Mts [44°06'N, 81°00'E], 27.VII.1991, Snizek (PCMS); 1 ♀, 37 ♂♂,
Bugas near Khami [43°14'N, 93°50'E], 20.VIII–8.IX.1895, VR, PK (ZISP).

Distribution. *China (Gansu, Xinjiang), Central Asia, Europe, Russia (south of European part and east to Khakassia Republic), Turkey, Iran, North Africa.

***Sphecodes crassus* Thomson, 1870**

Figure 3

Material examined. CHINA: *Inner Mongolia*, 2 ♀♀, Suburgan-gol, Alashan [Helan Shan] Mt., Gobi, 29–30.VI.1908, PK (ZISP); 6 ♀♀, Tszosto, Alashan [Helan Shan] Mt., Gobi, 13–14.V.1908, PK (ZISP); *Shanxi*, 1 ♀, Xiexian, Zhongtiao Shan Mts [34°48'N, 111°36'E], 22–24.V.1996, leg. JH (PCMS); 2 ♀♀, 13 km S Yichuan [35°54'N, 110°36'E], 19.V.1996, leg. JH (PCMS).

Distribution. *China (Inner Mongolia, Shanxi), Central Asia, Mongolia, Russia, Europe (north to 64°), Caucasus, Turkey, Iran, Japan, North Africa.

***Sphecodes cristatus* Hagens, 1882**

Figure 4

Sphecodes alfkeni Meyer, 1922: 172, ♀ (lectotype: ♀, **designated here**, China, Tientsin [Tianjin], [leg.] Weber, MNHB, examined). – Syn. n.

Material examined. CHINA: *Heilongjiang*, 1 ♀, Harbin [45°46'N, 126°39'E], 8.X.1952 (IZCAS); 1 ♀, idem, 27.VII.1952 (IZCAS); 1 ♀, idem, 19.VII.1953 (IZCAS); 1 ♀, idem, 25.VII.1955 (IZCAS); 1 ♂, idem, 8.X.1952 (IZCAS); 1 ♂, idem, 16.VII.1952 (IZCAS); *Jilin*, 1 ♀, Gongzhuling [43°79'N, 124°69'E], 9.VI.1962, leg. T.-L. Cheng (IZCAS); *Liaoning*, 1 ♂, 50 km N Mukden [Shenyang], 20.VII.1952, Rubtsov (ZISP); 1 ♀, Guicheng [43°40'N, 126°15'E], 30.VII.1962, leg. T.-L. Cheng (IZCAS); *Inner Mongolia*, 4 ♂♂, 2 ♀♀, Dingyuanying [Bayan Hot], Alashan [Helan Shan] Mt., 22.V., 26.V., 17–26.IX.1908, PK (ZISP); 1 ♂, Tszosto, Alashan [Helan Shan] Mt., Gobi, 13–14.V.1908, PK (ZISP); 1 ♂, Ulanqab Men, Tomortei [41°48'N, 113°06'E], 31.VIII.1971 (IZCAS); 2 ♂♂, Hailar Shi [49°12'N, 119°42'E], 3.VIII.2006, leg. H.-Y. Zhang (IZCAS), 2 ♂♂, idem, 2.VIII.2006, leg. Y.-J. Li (IZCAS), 1 ♂, idem, 8.VIII.2006, leg. P. Wang (IZCAS); 2 ♂♂, Ordos, Dundatu [37°43'N, 108°10'E], 24.VII.2006, leg. Y.-J. Li (IZCAS); 2 ♀♀, 1 ♂, idem, 25.VII.2006, leg. P. Wang (IZCAS), 5 ♀♀, 3 ♂♂, idem, 25.VII.2006, leg. H.-Y. Zhang (IZCAS); 3 ♀♀, idem, 25.VII.2006, leg. M. Luo (IZCAS); 1 ♀, 1 ♂, Hohhot Shi,

Heling Xian, Mengniu Zheng [40°49'N, 111°39'E], 15.VII.2006, leg. Y.-J. Li (IZCAS); 1 ♂, Hulun Buir Meng, Manzhouli Shi [49°12'N, 119°45'E], 5.VIII.2006, leg. Y.-J. Li (IZCAS); 1 ♀, Uxin Qi, Batugou [38°38'N, 108°53'E], 28.VII.2006, leg. M. Luo (IZCAS); *Hebei*, 1 ♀, Yangyuan Xian, Liufang [40°11'N, 114°28'E], 950 m, 12.IV.2002, leg. Z.-Q. Niu (IZCAS); *Tianjin*, 1 ♀, Balitai [38°57'N, 117°19'E], 13.X.1953, leg. Z.-R. Yu (IZCAS). *Beijing*, 1 ♀, 1 ♂, Xiangshan [39°54'N, 116°12'E], 100 m, 19.IX.1962, leg. Y.-S. Shi (IZCAS); 3 ♂♂, Beijing [39°55'N, 116°24'E], 28.VIII.1973, leg. S.-F. Wang (IZCAS); 1 ♀, Wofosi [40°03'N, 115°10'E], 100 m, 10.V.1962, leg. S.-Y. Wang (IZCAS); 1 ♂, idem, 18.IX.1981, leg. Q. Zhou (IZCAS); 1 ♀, Zizhuyuan [39°57'N, 116°19'E], 24.IV.1962, leg. S.-M. Ge (IZCAS); *Shanxi*, 1 ♀, Qingjian env. [36°54'N, 110°36'E], 15.V.1996, leg. JH (PCMS); 1 ♀, Monan [34°42'N, 111°42'E], 26–28.V.1996, leg. JH (PCMS); 1 ♀, Suide, [37°18'N, 110°42'E], 13–14.V.1996, leg. JH (PCMS); *Shandong*, 1 ♀, Jinan [36°48'N, 117°01'E], 24.VI.1937 (IZCAS); *Shaanxi*, 1 ♀, Gangui [36°48'N, 110°18'E], 35 km NE Yanan, 17–18.V.1996, leg. JH (PCMS); *Ningxia*, 1 ♂, Ningxia [Yinchuan], Ordos, Gobi, 1–4.VI.1908, PK (ZISP); 6 ♂♂, Yanchi Xian, Sidunzi [37°28'N, 107°09'E], 1455 m, 22.VI.2016, leg. Z.-Q. Niu, D. Zhang (IZCAS); *Xinjiang*, 1 ♀, Jimsar Xian [44°00'N 89°03'E], 14.V.1955, leg. S.-J. Ma, K.-L. Xia, Y.-L. Cheng (IZCAS); 1 ♀, Jeminay Xian, S229, 14 km [47°14'N, 85°19'E], 1080 m, 28.VIII.2002, leg. Z.-Q. Niu (IZCAS); 1 ♀, Tian Shan [43°10'N, 86°00'E], 28.VIII.1957, leg. G. Wang (IZCAS); 1 ♀, Manas Xian, Shihezi [44°07'N, 86°00'E], 550 m, 6.VI.1957, leg. C.-P. Hong (IZCAS); 1 ♀, idem, 590 m, 27.VIII.1957, leg. S.-Y. Wang (IZCAS); 1 ♀, Yining Xian [44°00'N, 81°21'E], 4.VIII.1957, leg. W.-Y. Yang (IZCAS).

Published records. Blüthgen 1927: 42, as *Sphecodes alfkeni* Meyer (Tianjin); Ascher and Pickering 2018 (Beijing).

Distribution. China (*Heilongjiang, *Jilin, *Liaoning, *Inner Mongolia, *Hebei, Tianjin, Beijing, *Shanxi, *Shandong, *Shaanxi, *Ningxia, *Xinjiang), Europe (north to Sweden), Korea, Russia, Caucasus, Turkey, Central Asia, Mongolia.

Sphecodes ephippius (Linné, 1767)

Figure 6

Material examined. CHINA: *Xinjiang*, 1 ♂, Yaerkate [42°52'N, 92°50'E], 3.VIII.1956, leg. W.-Y. Yang (IZCAS).

Distribution. *China (Xinjiang), Russia (east to Irkutsk Prov.), Mongolia, Central Asia, Caucasus, Turkey, Europe (north to 62°).

Sphecodes ferruginatus Hagens, 1882

Figs 5, 25, 36

Material examined. CHINA: *Beijing*, 2 ♀♀, 3 ♀♀, Bada Ling, Sanbu [40°22'N, 115°58'E], 500 m, 18, 27.IV.2002, leg. Z.-Q. Niu (IZCAS); 1 ♀, Miaofengshan

[40°01'N, 115°59'E], 24.V.1957, leg. M.-H. Wang (IZCAS); 1 ♀, Wofosi [40°03'N, 115°10'E], 15.V.1961, leg. S.-M. Ge (IZCAS); *Shanxi*, 1 ♀, Xiexian [34°48'N, 111°36'E], Zhongtiao Shan Mts., 22–24.V.1996, leg. JH (PCMS).

Distribution. *China (Beijing, Shanxi), Central Asia, Russia, Europe (north to 66°), Caucasus, Turkey, Japan.

Sphecodes geoffrellus (Kirby 1802)

Figure 7

Material examined. CHINA: *Heilongjiang*, 1 ♂, Da Hinggan Ling [51°42'N, 126°36'E], 23.VII.1980 (IZCAS); *Shaanxi*, 11 ♀♀, Gangui [36°48'N, 110°18'E], 35 km NE Yanan, 17–18.V.1996, leg. JH (PCMS); 1 ♀, 13 km S Yichuan [35°54'N, 110°36'E], 19.V.1996, leg. JH (PCMS).

Distribution. *China (Heilongjiang, Shanxi), Central Asia, Europe (north to 66°), Russia (east to Far East), Turkey, Near East, Mongolia, Japan.

Sphecodes gibbus (Linnaeus, 1758)

Figs 9, 41, 57

Sphecodes gibbus var. *turkestanicus* Meyer, 1920: 113 (holotype: 1 ♀, Uzbekistan: Golodnaja Steppe [Gulistan], MNHB). Synonymized by Blüthgen 1923: 510.

Material examined. CHINA: *Xinjiang*, 1 ♀, 13 ♂♂, Bugas near Khami [43°14'N, 93°50'E], 20.VIII–8.IX.1895, leg. VR, PK (ZISP); 1 ♂, Qitai Xian [44°31'N, 90°06'E], 10.VII.1975 (IZCAS); 1 ♀, Kashi [39°14'N, 75°32'E], 133 m, 10.VII.1959, leg. C.-Q. Li (IZCAS); 1 ♂, idem, 10.VII.1959, leg. A-F. Tian (IZCAS).

Published records. Meyer, 1920: Yarkand (Xinjiang), as *Sphecodes gibbus* var. *turkestanicus* Meyer, 1920.

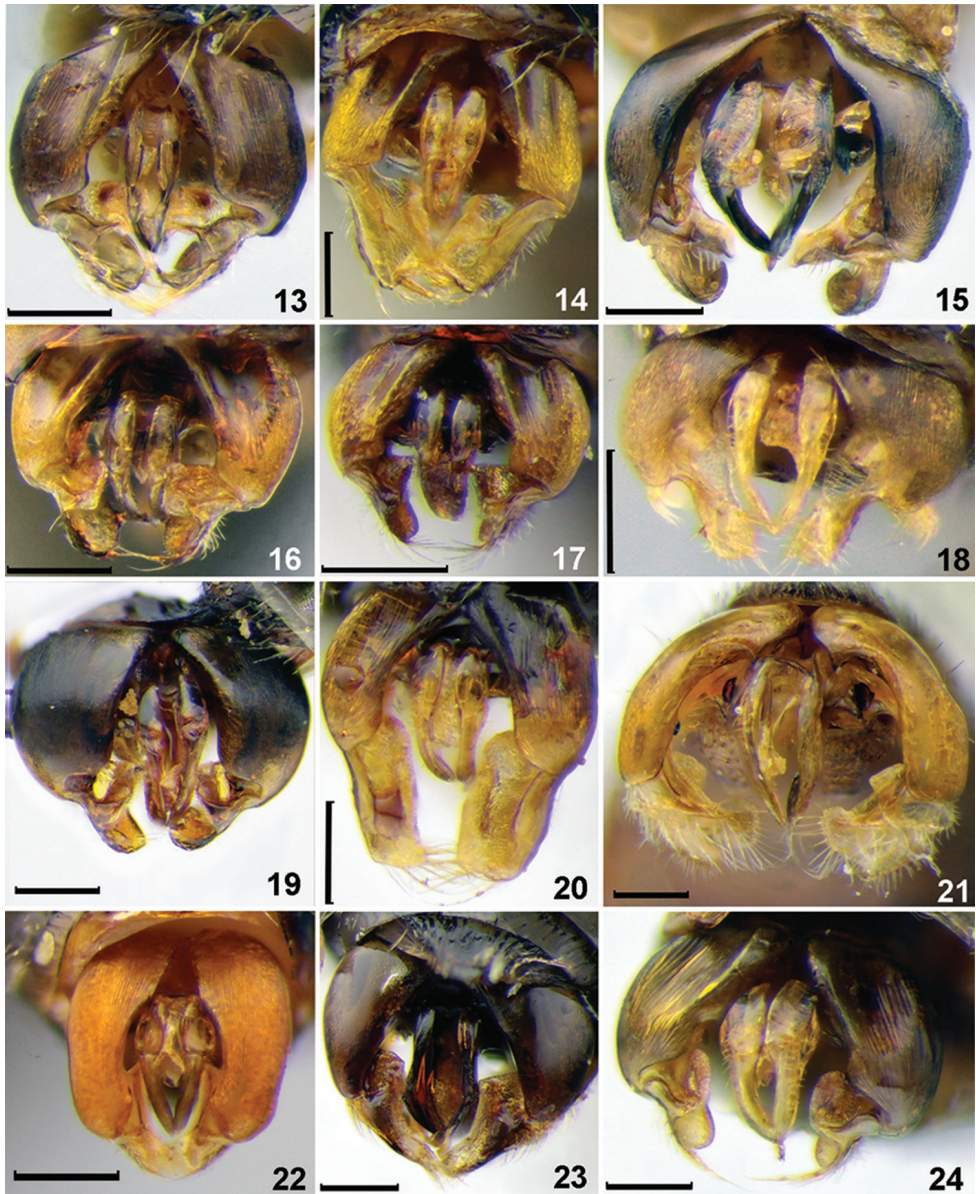
Distribution. China (Xinjiang), Central Asia, Russia (east to Yakutia), Pakistan, Mongolia, Europe (north to 63°), Turkey, Israel, North Africa, India.

Sphecodes grahami Cockerell, 1922

Figure 52

Sphecodes grahami Cockerell, 1922: 12 (holotype: ♀, China, Sichuan: Suifu, Graham coll.; USNM);

Material examined. CHINA: *Shanxi*, 1 ♀, Xiexian [34°48'N, 111°36'E], Zhongtiao Shan Mts., 22–24.V.1996, leg. JH (PCMS); *Shaanxi*, 2 ♀♀, Gangui [36°48'N, 110°18'E], 35 km NE Yanan, 17–18.V.1996, leg. JH (PCMS).



Figures 13–24. Genitalia, males, dorsal view. **13** *Sphecodes maruyamanus* Tsuneki **14** *S. miniatus* Hagens **15** *S. monilicornis* (Kirby) **16** *S. murotai* Tsuneki **17** *S. schwarzi* Astafurova & Proshchalykin **18** *S. nurekensis* Warncke **19** *S. pieli* Cockerell **20** *S. pinguiculus* Pérez **21** *S. olivieri* Lepeletier de Saint Fargeau **22** *S. puncticeps* Thomson **23** *S. scabricollis* Wesmael **24** *S. tanoi* Tsuneki. Scale bars: 0.25 mm.

Published records. Cockerell 1922: 12 (Shanghai); Ascher and Pickering 2018 (Jilin, Hebei, Anhui, Jiangsu, Shanghai, Zhejiang, Yunnan, Xizang, Guandong).

Distribution. China (Jilin, Hebei, *Shanxi, *Shaanxi, Anhui, Jiangsu, Shanghai, Shanghai, Zhejiang, Sichuan, Yunnan, Xizang, Guandong).

Remark. The female of this species is challenging to distinguish from West-Palae-arctic *S. ephippius* (Linné, 1767).

***Sphcodes intermedius* Blüthgen, 1923**

Figs 10, 49, 56

Material examined. CHINA: *Gansu*, 1 ♂, Shibendu, oasis Sachjou [Dunhuang] [40°09'N, 94°40'E], Gashun Gobi desert, 9–12.VIII.1895, leg. VR, PK (ZISP).

Distribution. *China (Gansu), Central Asia, Europe, Russia (European part, Ural), North Africa, Caucasus, Turkey.

***Sphcodes kozlovi* Astafurova & Proshchalykin, 2015**

Figs 12, 39, 54

Material examined. CHINA: *Inner Mongolia*, 3 ♀♀, Tszosto, Alashan [Helan Shan] Mt., Gobi, 10–18.V.1908, leg. PK (ZISP); 7 ♀♀, Dingyuanying [Bayan Hot], Alashan [Helan Shan] Mt., 10, 18–19.VI.1908, 15–16. IV.1909, leg. PK (ZISP); *Shanxi*, 1 ♀, Monan [34°42'N, 111°42'E], 26–28.V.1996, leg. JH (PCMS); *Ningxia*, 2 ♀♀, Yanchi [37°24'N, 107°36'E], 11.V.1996, leg. JH (PCMS).

Distribution. *China (Inner Mongolia, Shanxi, Ningxia), Mongolia (Dornod Aimag, Khentii Aimag).

***Sphcodes laticaudatus* Tsuneki, 1983**

Figs 11, 51

Material examined. CHINA: *Hebei*, 1 ♂, Xinglong Xian, Wuling Shan [40°26'N, 117°31'E], 28.VIII.1973 (IZCAS).

Distribution. *China (Hebei), Russia (Far East), Japan.

***Sphcodes longulus* Hagens, 1882**

Figs 8, 26

Sphcodes subfasciatus Blüthgen, 1934: 22, ♀ (holotype: ♀, China, S. Kansu, 19.VI.1930, leg. Hummel, NHRS, examined). – Syn. n.

Material examined. CHINA: *Inner Mongolia*, 1 ♀, Goytzo valley, Alashan, Gobi, 5.IV.1908, leg. PK (ZISP); *Hebei*, 1 ♀, Changli Xian [39°38'N, 119°05'E], 28.IV.1962, leg. T.-L. Cheng (IZCAS); 1 ♀, Xiaowutai Shan [38°36'N, 115°39'E], 1200 m, 22.VIII.1964, leg. Y.-H. Han (IZCAS); *Shaanxi*, 1 ♀, Gangui [36°48'N,



Figures 25–30. Head, females, frontal view. **25** *Sphecodes ferruginatus* Hagens **26** *S. longulus* Hagens **27** *S. miniatus* Hagens **28** *S. nippon* Meyer **29** *S. schwarzi* Astafurova & Proshchalykin **30** *S. tanoi* Tsuneki. Scale bars: 0.5 mm.

110°18E'], 35 km NE Yanan, 17–18.V.1996, leg. JH (PCMS); *Gansu*, 1 ♀, Lanzhou [36°00'N, 103°25'E], 27.IV.1955, leg. S.-J. Ma, K.-L. Xia, Y.-L. Cheng (IZ-CAS); *Xinjiang*, 1 ♂, Tacheng Xian [46°25'N, 82°32'E], 470 m, 10.IX.1960, leg.

S.-Y. Wang (IZCAS); 1 ♂, Bostanterak [39°07'N, 95°03'E], 9.VII.1959, leg. S.-Y. Wang (IZCAS).

Distribution. China (*Inner Mongolia, *Hebei, *Shaanxi, Gansu, *Xinjiang), Central Asia, Russia, Europe (north to Finland, Sweden, Denmark, England), Turkey, Syria, Japan.

Sphecodes manchurianus Strand & Yasumatsu, 1938

Sphecodes manchurianus Strand & Yasumatsu, 1938: 80 (holotype: ♂, China : “Fengtien (Mukden), South Manchoukuo, 5.VIII.1930, T. Nozawa leg.”; KUF, lost).

Material examined. No material examined.

Distribution. China (Liaoning).

Remark. Known only from the holotype.

Sphecodes monilicornis (Kirby, 1802)

Figs 15, 32

Material examined. CHINA: *Heilongjiang*, 1 ♂, Morin Dawa [47°21'N, 128°03'E], 24.VII.1976 (IZCAS); 1 ♂, Harbin [45°46'N, 126°39'E], 6.VII.1947 (IZCAS); 1 ♀, idem, 27.VII.1952 (IZCAS); 2 ♂♂, idem, 25.VII.1953 (IZCAS); 7 ♂♂, idem, 4.VII.1955 (IZCAS); 1 ♂, idem, 8.VII.1955 (IZCAS); 1 ♀, 3 ♂♂, idem, 10.VII.1955 (IZCAS); 1 ♀, 5 ♂♂, idem, 19.VII.1955 (IZCAS); 5 ♂♂, idem, 10.VII.1955 (IZCAS); 1 ♂, idem, 11.VII.1955 (IZCAS); 3 ♂♂, idem, 23.VII.1953 (IZCAS); 1 ♂, idem, 9.VIII.1955 (IZCAS).

Distribution. *China (Heilongjiang), Central Asia, Mongolia, Russia, North Pakistan, Europe (north to 64°), Caucasus, Turkey, North Africa.

Sphecodes nippon Meyer, 1922

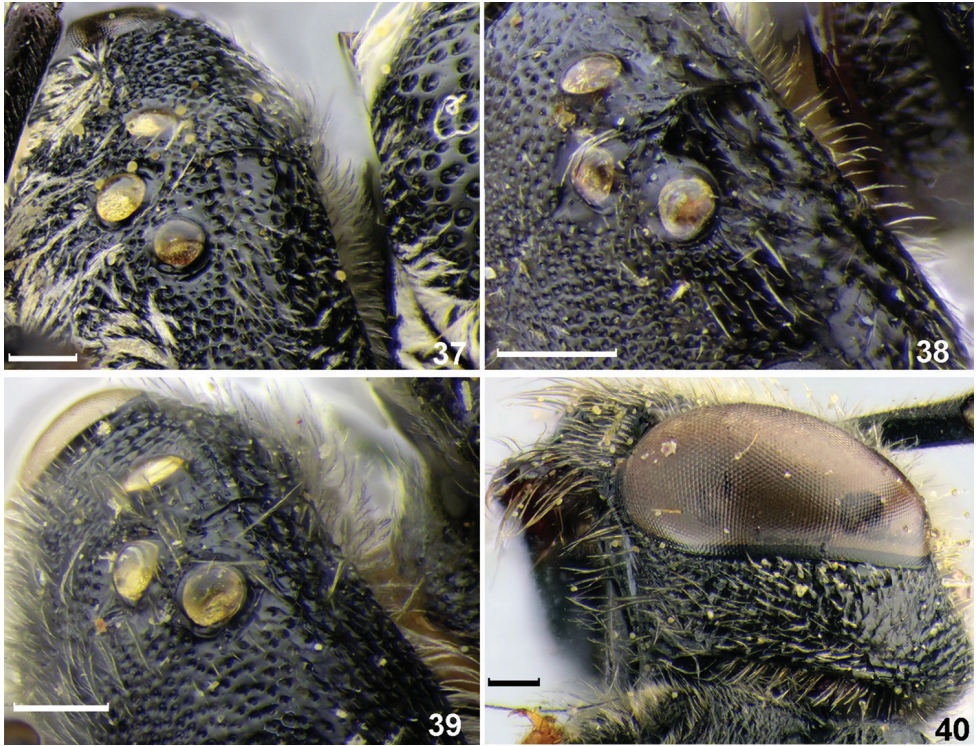
Figs 28, 50, 58

Sphecodes kansuensis Blüthgen, 1934: 21, fig. 11, ♂ (holotype: ♂, China, S. Kansu [Gansu] 19.VI.1930, leg. Hummel, NHRS, examined). – Syn. n.

Material examined. CHINA: *Heilongjiang*, 1 ♂, Harbin [45°46'N, 126°39'E], 24.IX.1950; 1 ♂, idem, 16.VII.1952; 1 ♂, idem, 25.VII.1952; 1 ♂, idem, 23.VII.1953; 1 ♂, idem, 11.VII.1954; 1 ♂, idem, 4.VII.1955; 4 ♂♂, idem, 8.VII.1955; 2 ♂♂, idem, 25.VII.1955 (IZCAS); 2 ♂♂, Mao'ershan [47°21'N, 128°03'E], 29.VII.1951 (IZCAS); 1 ♂, Hengdaohezi [45°57'N, 129°57'E], 28.VII.1951 (IZCAS); *Inner Mongolia*, 1 ♂, 3 ♀♀, Dingyuanying [Bayan Hot], Alashan [Helan Shan] Mt., 16–17.V., 3–6.VI., 11–16.IX.1908, PK (ZISP); *Hebei*, 1 ♂, Yangjiaping [39°58'N,

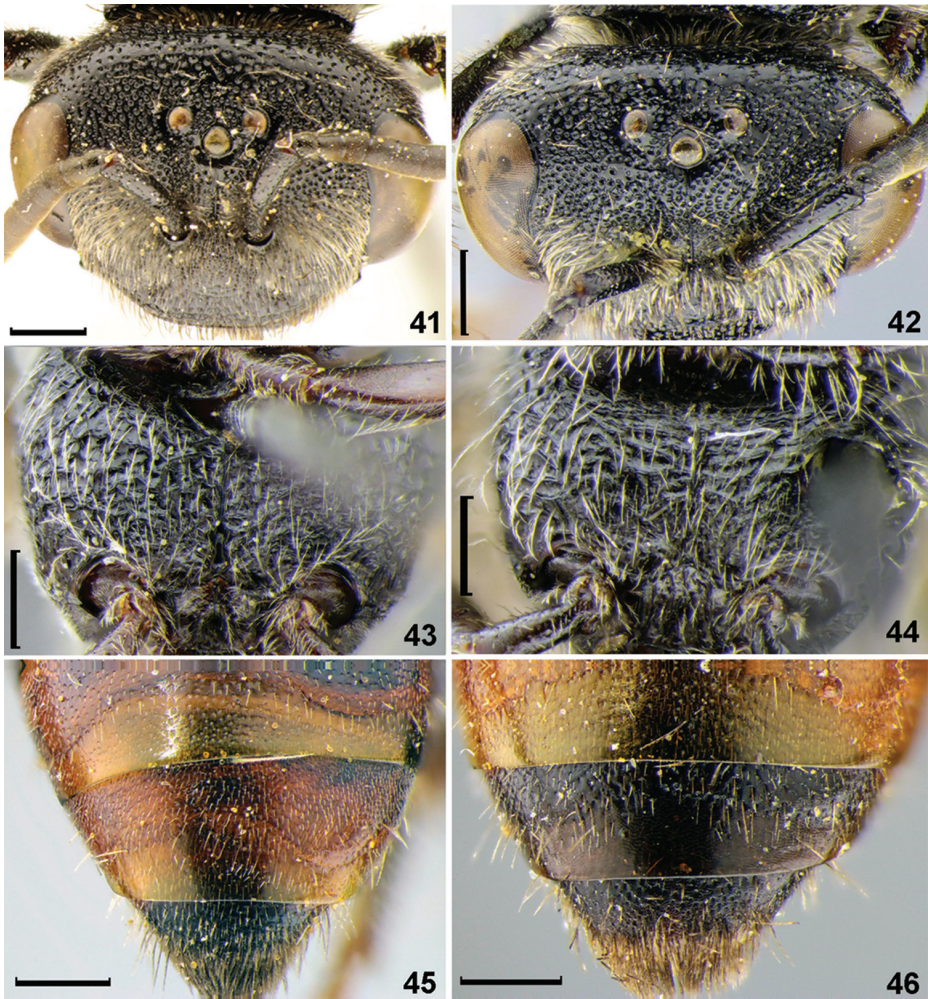


Figures 31–36. Diagnostic characters of *Sphecoides* species. **31, 32, 35, 36** Females **33, 34** Males **31–34** head, frontal view **35, 36** pronotum, lateral, view **31** *Sphecoides turanicus* Astafurova & Proshchalykin **32** *S. monilicornis* (Kirby) **33** *S. maruyamanus* Tsuneki **34** *S. murotai* Tsuneki **35** *S. pellucidus* Smith **36** *S. ferruginatus* Hagens. Scale bars: 0.5 mm.



Figures 37–40. Diagnostic characters of *Sphecodes* species, females. **37–39** vertex, dorso-lateral view **40** preoccipital carina and gena, dorso-lateral view **37** *Sphecodes olivieri* Lepeletier de Saint Fargeau **38** *S. pieli* Cockerell **39** *S. kozlovi* Astafurova & Proshchalykin **40** *S. scabricollis* Wesmael. Scale bars: 0.25 mm.

115°24'E], 17.VII.1937; 1 ♂, idem, 20.VII.1937; 1 ♀, idem, 6.VII.1937; 1 ♀, idem, 8.VII.1937, leg. O. Piel (IZCAS); 1 ♂, Xiaowutai Shan [38°36'N, 115°39'E], 1200 m, 25.VIII.1964; 1 ♂, idem, 11.VII.1964; 1 ♂, idem, 12.VII.1964, leg. Y.-H. Han (IZCAS); 1 ♂, Xinglong Xian, Wuling Shan [40°26'N, 117°31'E], 28.VIII.1973 (IZCAS); *Tianjin*, 1 ♀, Balitai [38°57'N, 117°19'E], 24.IV.1953, leg. Z.-Y. Xu (IZCAS); *Beijing*, 1 ♂, 40 km N Beijing [40°09'N, 116°14'E], 28.IX.1952, Rubtsov (ZISP); 1 ♀, Bada Ling [40°22'N, 115°58'E], 700 m, 2.VII.1974, leg. Y.-S. Shi (IZCAS); 1 ♀, Bada Ling, Sanbu [40°22'N, 115°58'E], 500 m, 27.IV.2002, leg. Z.-Q. Niu (IZCAS); 1 ♀, Xidazhuangke village, Songshan [40°31'N, 115°47'E], 910 m, 15.V.2007, leg. H.-R. Huang (IZCAS); 1 ♀, Miaofengshan [40°01'N, 115°59'E], 2.VIII.1957; 1 ♂, idem, 18.VII.1957, leg. M.-H. Wang (IZCAS); *Shaanxi*, 9 ♀♀, Gangui [36°48'N, 110°18'E], 35 km NE Yanan, 17–18.V.1996, leg. JH (PCMS); *Gansu*, 5 ♂♂, oasis Sachjou [Dunhuang] [40°09'N, 94°40'E], Gashun Gobi desert, 28–30.VII.1895, leg. VR, PK; 1 ♀, Lanzhou, 25.VII.1908, leg. PK (ZISP).



Figures 41–46. Diagnostic characters of *Sphecodes* species, females. **41, 42** head, dorsal view **43, 44** thorax, ventral view **45, 46** T4–T5, dorsal view **41** *S. gibbus* (Linnaeus) **42, 45** *S. reticulatus* Thomson **43** *S. murotai* Tsuneki **44** *S. tanoi* Tsuneki **46** *S. alternatus* Smith. Scale bars: 0.5 mm.

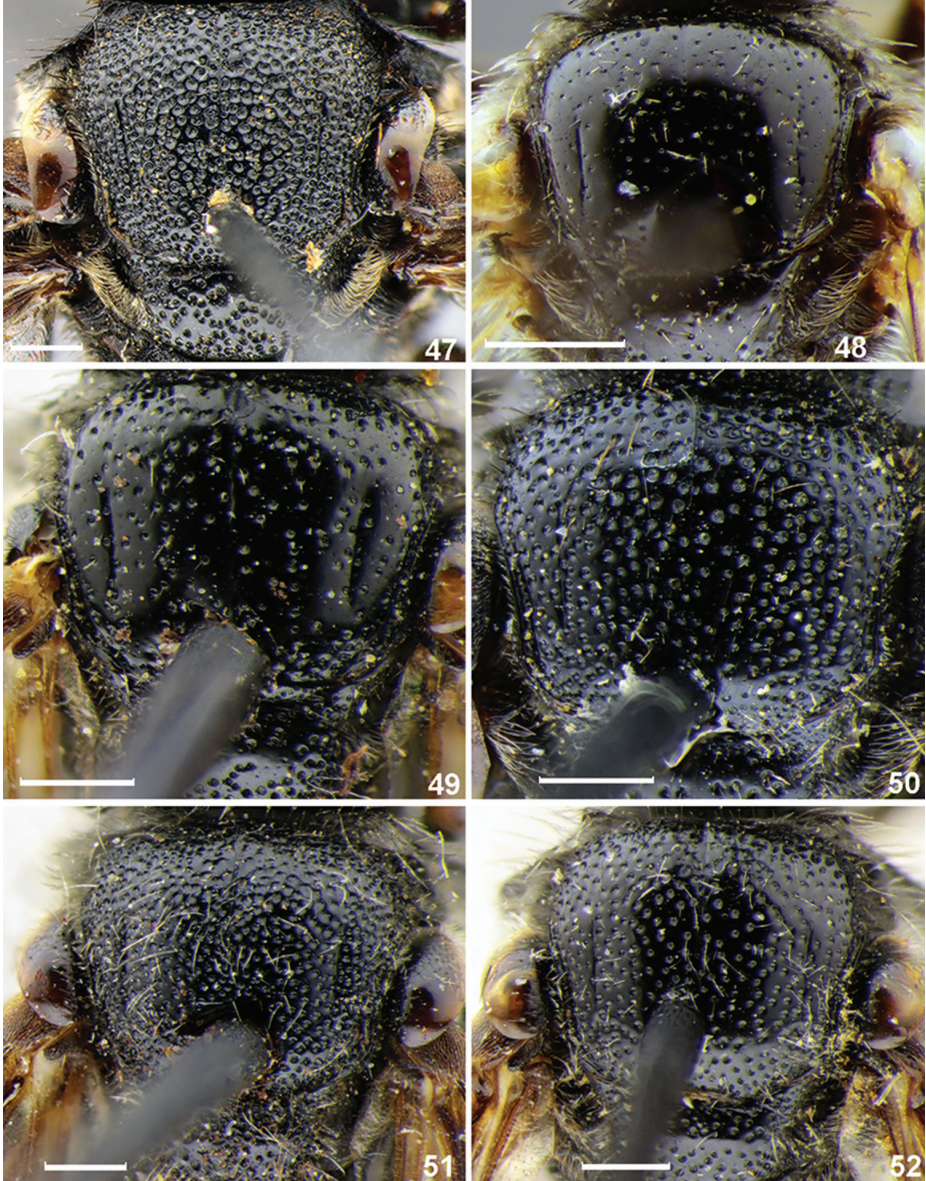
Distribution. China (*Heilongjiang, *Inner Mongolia, *Hebei, *Tianjin, *Beijing, *Shaanxi, Gansu), Russia (East Siberia, Far East), Mongolia, Japan.

Sphecodes nurekensis Warncke, 1992

Figure 18

Material examined. CHINA: *Xinjiang*, 1 ♂, Bugas near Khami [N43°14' E93°50'], 20.VIII.1895, leg. VR, PK (ZISP); 1 ♂, Ürümqi [43°28'N, 87°32'E], 980 m, 2.IX.1959, leg. S.-Y. Wang (IZCAS).

Distribution. *China (Xinjiang), Tajikistan.



Figures 47–52. Scutum, females, dorsal view. **47** *S. albilabris* (Fabricius) **48** *S. pinguiculus* Pérez **49** *S. intermedius* Blüthgen **50** *S. nippon* Meyer **51** *S. laticaudatus* Tsuneki **52** *S. grahami* Cockerell. Scale bars: 0.5 mm.

***Sphecodes olivieri* Lepeletier de Saint-Fargeau, 1825**

Figs 21, 37

Material examined. CHINA: *Gansu*, 1 ♀, 2 ♂♂, oasis Sachjou [Dunhuang] [40°09'N, 94°40'E], Gashun Gobi desert, 24.VII, 1–3.VIII.1895, leg. VR, PK (ZISP); 1 ♂, Zhangye [38°32'N, 100°14'E], 1450 m, 29.VII.1957, leg. Y.-R. Zhang (IZCAS); *Xinjiang*, 117 ♂♂, Bugas near Khami [43°14'N, 93°50'E], 20.VIII-8.IX.1895, leg.

VR, PK (ZISP); 3 ♀♀, Manas Xian [44°10'N, 86°07'E], 400 m, 9.VI.1953, leg. C.-P. Hong (IZCAS); 1 ♀, idem, 9.VI.1953, leg. W.-Y. Yang (IZCAS); 1 ♂, Manas Xian, Shihezi [44°07'N, 86°00'E], 500 m, 27.VIII.1959, leg. C.-Q. Li (IZCAS); 1 ♂, Burqin Xian [47°25'N, 86°32'E], 480 m, 25.VIII.1960, leg. S.-Y. Wang (IZCAS); 1 ♂, Turpan Xian [42°32'N, 89°07'E], 30.VI.1958 (IZCAS).

Distribution. *China (Gansu, Xinjiang), Central Asia, South Europe, Russia (south of European part), Caucasus, Turkey, Iran, Pakistan, India, Israel, United Arab Emirates, Qatar, North Africa.

Sphecodes pectoralis Morawitz, 1876

Material examined. CHINA: *Gansu*, 1 ♀, 1 ♂, oasis Sachjou [Dunhuang] [40°09'N, 94°40'E], Gashun Gobi desert, 28.VII–4.VIII.1895, leg. VR, PK (ZISP); *Xinjiang*: 4 ♀♀, 140 ♂, Bugas near Khami [43°14'N, 93°50'E], 20.VIII–8.IX.1895, leg. VR, PK (ZISP).

Distribution. *China (Gansu, Xinjiang), Central Asia.

Sphecodes pellucidus Smith, 1845

Figure 35

Sphecodes pellucidus var. *hybridus* Blüthgen, 1924: 516, ♀ (syntypes: ♀♀, China: Sichuan, NHRS). Synonymized by Warncke 1992: 20.

Sphecodes pellucidus var. *niveipennis* Meyer, 1925: 7, ♂ (lectotype: ♂, **designated here**, Chin. Turkestan, Uss-Lusch. Jarkand [China, Xinjiang, Yarkand] 1600 m, 4–6.8.90, Conrandt S. / *pellucidus* v. *niveipennis* Dr. R Meyer det.; MNHB, examined). Synonymized by Warncke 1992: 20.

Material examined. CHINA: *Gansu*, 1 ♀, Lanzhou, 11–25.III.1901, leg. PK (ZISP); 3 ♂♂, Dankhe River, S to Sachzhou [Dunhuang], Gashunskoe Gobi [39°55'N, 94°20'E], 24.VII.1895, leg. VR, PK (ZISP).

Distribution. China (*Gansu, Xinjiang, Sichuan), Central Asia, Russia, Mongolia, Europe (north to 66°), Caucasus, Turkey, North Africa.

Sphecodes pieli Cockerell, 1931

Figs 19, 38, 53

Sphecodes pieli Cockerell, 1931: 13, ♂ (holotype: ♂, China, Shanghai, Zo-Se, June 16, 1930 (Piel No 34), USNM).

Sphecodes orientalis Astafurova & Proshchalykin, 2014: 517–518, ♀, ♂ (holotype: ♂, Russia, Primorskiy Terr.: 15 km SW Slavyanka, 31.VIII.1995, S. Belokobylskij, ZISP, examined). – Syn. n.

Material examined. CHINA: *Hebei*, 1 ♀, Xiaowutai Shan [38°36'N, 115°39'E], 1200 m, 19.VI.1964, leg. Y.-H. Han (IZCAS); *Beijing*, 1 ♀, Bada Ling, Sanbu [40°22'N, 115°58'E], 500 m, 27.IV.2002 (IZCAS); 2 ♀♀, idem, 28.IV.2002, leg. Z.-Q. Niu (IZCAS); 1 ♀, Xidazhuangke village, Songshan [40°31'N, 115°47'E], 910 m, 15.V.2007, leg. H.-R. Huang (IZCAS); 1 ♀, Mentougou, Xiaolongmen, Liyuanling [39°58'N, 115°28'E], 1140–1250 m, 19.V.2002, leg. Z.-Q. Niu (IZCAS); *Shaanxi*, 1 ♀, Gangui, 35 km NE Yanan [36°48'N, 110°18'E], 17–18.V.1996, leg. JH (PCMS); 1 ♀, 13 km S Yichuan [35°59'N, 110°36'E], 19.V.1996, leg. JH (PCMS); 1 ♀, Jingangling, 50 km W Linfen, [36°12'N, 111°42'E], 29–30.V.1996, leg. JH (PCMS); *Sichuan*, 1 ♀, Nanping, Ta Zang [33°15'N, 104°15'E], 2200 m, 15–18.VI.1990, JH (PCMS).

Published records. Ascher and Pickering, 2018 (Zhejiang, Jiangsu).

Distribution. China (*Hebei, *Beijing, *Shaanxi, Jiangsu, Shanghai, Zhejiang, *Sichuan), Russia (Far East).

Sphecodes pinguiculus Pérez, 1903

Figs 20, 48, 55

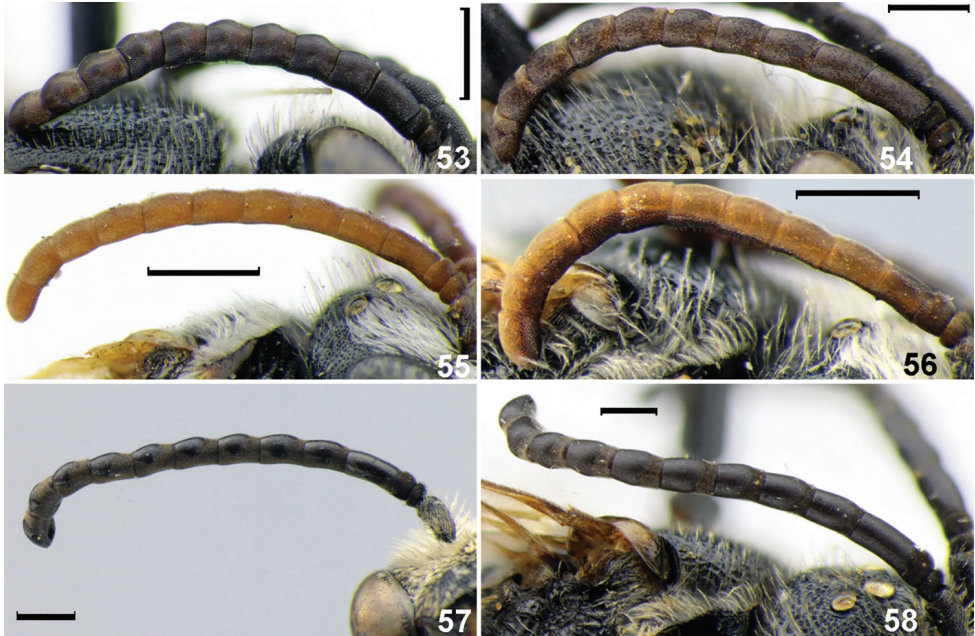
Material examined. CHINA: *Inner Mongolia*, 1 ♀, Dingyuanying [Bayan Hot], Alashan [Helan Shan] Mt., 22–24.VI.1908, PK (ZISP); *Gansu*, 1 ♀, oasis Sachjou [Dunhuang] [40°09'N, 94°40'E], Gashun Gobi desert, 4.VIII.1895, leg. VR, PK (ZISP).

Distribution. *China (Inner Mongolia, Gansu), Central Asia, Mongolia, Russia, South Europe, Caucasus, Turkey, Iran, Israel, United Arab Emirates, North Africa, Cape Verde Islands.

Sphecodes scabricollis Wesmael, 1835

Figs 23, 40

Material examined. CHINA: *Heilongjiang*, 2 ♀♀, Harbin [45°46'N, 126°39'E], 11.VII.1954 (IZCAS); 1 ♀, idem, 8.VII.1955 (IZCAS); 1 ♀, idem, 19.VII.1955 (IZCAS); 1 ♀, idem, 20.VII.1955 (IZCAS); 2 ♀♀, idem, 25.VII.1955 (IZCAS); 1 ♂, idem, 8.VII.1955 (IZCAS); 2 ♂♂, idem, 25.VII.1955 (IZCAS); 1 ♂, idem, 11.IX.1955 (IZCAS); *Liaoning*, 1 ♂, Guicheng [43°40'N, 126°15'E], 10.VII.1962, leg. T.-L. Cheng (IZCAS); *Beijing*, 1 ♂, Changping district, Liucun town, Wangjiayuan village [40°12'N, 116°00'E], 5.IX.2011, leg. F. Yuan (IZCAS); 16 ♂♂, Wofosi [40°03'N, 115°10'E], 18.IX.1981, leg. Y.-R. Wu (IZCAS); 2 ♂♂, idem, 10.IX.1981, leg. Q. Zhou (IZCAS); 2 ♀♀, idem, 10.IX.1981, leg. W.-Z. Ma (IZCAS); 1 ♀, Bada Ling [40°22'N, 115°58'E], 3.IX.1981, leg. P.-Y. Yu (IZCAS); 1 ♂, idem, 28.VIII.1974 (IZCAS); 1 ♂, 13.VIII.1981 (IZCAS); 1 ♂, 20.VIII.1988, leg. Y.-S. Shi (IZCAS); 1 ♂, idem, 30.VIII.1977, leg. S.-F. Wang (IZCAS); 1 ♂, idem, 25.VIII.1981, leg. Q. Zhou (IZCAS); 1 ♀, idem, 7.IX.1982, leg. Z.-C. Jin (IZCAS); 1 ♂, Xiangshan



Figures 53–58. Antennae, males. **53** *Sphecodes pieli* Cockerell **54** *S. kozlovi* Astafurova & Proshchalykin **55** *S. pinguiculus* Pérez **56** *S. intermedius* Blüthgen **57** *S. gibbus* (Linnaeus) **58** *S. nippon* Meyer. Scale bars: 0.5 mm.

[39°54'N, 116°12'E], 22.IX.1983, leg. J.-G. Fan (IZCAS); 4 ♀♀, Qinglongqiao [39°54'N, 116°21'E], 5.IX.1988, leg. H.-L. Xu (IZCAS); 1 ♂, idem, 12.V.1981, leg. Y.-R. Wu (IZCAS); 4 ♀♀, 1 ♂, Beijing [39°55'N, 116°24'E], 28.VIII.1973, leg. Y.-R. Wu (IZCAS); 3 ♂♂, idem, 28.VIII.1973, leg. S.-F. Wang (IZCAS); *Shaanxi*, 2 ♀♀, Qihling Mts., 6 km E Xunyangba [33°32'N, 108°33'E], 1000–1300 m, 23.V–13.VI.1998, leg. Marshal (PCMS); *Qinghai*, 1 ♂, Sinin-khe River valley [36°30'N, 101°40'E], 29.VII.1908, leg. PK (ZISP); *Zhejiang*, 1 ♂, Lian Country, West Tianmu Mt. [30°20'N, 119°25'E], 1000 m, 16.IX.2000, S. Belokobylskij (ZISP).

Distribution. *China (Heilongjiang, Liaoning, Beijing, Shaanxi, Qinghai, Zhejiang), Kazakhstan (East Kazakhstan), Russia, Europe (north to S England and Latvia), Caucasus, Turkey, Iran, South Korea, Japan, India.

Sphecodes turanicus Astafurova & Proshchalykin, 2017

Figure 31

Material examined. CHINA: *Gansu*, 1 ♀, 2 ♂♂, oasis Sachjou [Dunhuang] [40°09'N, 94°40'E], Gashun Gobi desert, 1–9.VIII.1895, leg. VR, PK (ZISP).

Distribution. *China (Gansu), Central Asia.

Table 1. Checklist of the *Sphecodes* species of China including distribution by provinces.

	Species	Province	Published data	Type of areal
1	<i>S. albilabris</i> (Fabricius, 1793)	Gansu, Liaoning, Inner Mongolia, Shanxi	first record	P
2	<i>S. alternatus</i> Smith, 1853	Xinjiang, Gansu	first record	P
3	<i>S. chinensis</i> Meyer, 1922	China (exactly locality is unknown)	Meyer 1922	?
4	<i>S. crasus</i> Thomson, 1870	Inner Mongolia, Shanxi	first record	P
5	<i>S. cristatus</i> Hagens, 1882	Xinjiang, Inner Mongolia, Ningxia, Liaoning, Hebei, Shandong, Shanxi, Shanxi, Heilongjiang, Jilin, Beijing, Tianjin	Meyer 1922, Blüthgen 1927, Ascher and Pickering 2018, current data	P
6	<i>S. ephippius</i> (Linné, 1767)	Xinjiang	first record	P
7	<i>S. ferruginatus</i> Hagens, 1882	Shanxi, Beijing	first record	P
8	<i>S. formosanus</i> Cockerell, 1911	Taiwan	Cockerell 1911	O
9	<i>S. galeritus</i> Meyer, 1927	Guandong	Meyer 1927	O
10	<i>S. gibbus</i> (Linnaeus, 1758)	Xinjiang	Meyer 1920, current data	P
11	<i>S. geoffrellus</i> (Kirby, 1802)	Shanxi, Inner Mongolia	first record	P
12	<i>S. grabami</i> Cockerell, 1922	Sichuan, Shanghai; Hebei, Shaanxi, Shanxi, Jilin, Jiangsu, Anhui, Zhejiang, Xizang, Guandong, Yunnan	Cockerell 1922, 1931, Ascher and Pickering 2018, current data	PO
13	<i>S. howardi</i> Cockerell, 1922	Guandong	Cockerell 1922, Blüthgen 1924	O
14	<i>S. intermedius</i> Blüthgen, 1923	Gansu	first record	P
15	<i>S. kershawi</i> Perkins, 1921	Guandong	Meyer 1927	O
16	<i>S. kozlovi</i> Astafurova & Proshchalykin, 2015	Inner Mongolia, Ningxia, Shanxi	first record	P
17	<i>S. laticaudatus</i> Tsuneki, 1983	Hebei	first record	P
18	<i>S. laticeps</i> Meyer, 1920	Taiwan	Meyer 1920	O
19	<i>S. longulus</i> Hagens, 1882	Gansu, Shanxi, Hebei, Inner Mongolia	Blüthgen 1934, current data	P
20	<i>S. manchurianus</i> Strand & Yasumatsu, 1938	Liaoning	Strand and Yasumatsu 1938	P
21	<i>S. monilicornis</i> (Kirby, 1802)	Heilongjiang	first record	P
22	<i>S. nippon</i> Meyer, 1922	Gansu, Inner Mongolia, Shaanxi, Heilongjiang, Beijing, Gansu	Blüthgen 1934, current data	P
23	<i>S. nurekensis</i> Warncke, 1992	Xinjiang	first record	P
24	<i>S. olivieri</i> Lepeletier de Saint-Fargeau, 1825	Xinjiang, Gansu	first record	P
25	<i>S. pieli</i> Cockerell, 1931	Sichuan, Shanghai, Shanxi, Hebei, Beijing, Zhejiang, Jiangsu	Cockerell 1931, Ascher and Pickering 2018, current data	PO
26	<i>S. pinguiculus</i> Pérez, 1903	Gansu, Inner Mongolia	first record	P
27	<i>S. pectoralis</i> Morawitz, 1876	Xinjiang, Gansu	first record	P
28	<i>S. pellucidus</i> Smith, 1845	Xinjiang, Sichuan, Gansu	Blüthgen 1924, Meyer 1922, 1925, current data	P
29	<i>S. sauteri</i> Meyer, 1925	Taiwan	Meyer 1925	O
30	<i>S. scabricollis</i> Wesmael, 1835	Qinghai, Zhejiang, Shaanxi, Heilongjiang, Beijing	first record	P
31	<i>S. takaensis</i> Blüthgen, 1927	Taiwan	Blüthgen 1927	O
32	<i>S. tertius</i> Blüthgen, 1927	Guandong	Ascher and Pickering 2018	O
33	<i>S. turanicus</i> Astafurova & Proshchalykin, 2017	Gansu	first record	P

P – Palearctic species; O – Oriental species; PO – Palearctic and Oriental species

Discussion

In total, 33 species of *Sphecodes* are recorded from China (Table 1). Twenty-two of these species are Palaearctic and two species have a Palaearctic-Oriental range. For comparison, 37 species are known from Russia, 20 species of these from the Russian Far East (Astafurova and Proshchalykin 2014, 2017b) and 36 from Central Asia (Astafurova and Proshchalykin 2017a, Astafurova et al. 2018). In contrast, the Oriental fauna of the genus is poorly studied: only nine species are recorded from Oriental China, most of which are only known from type series, suggesting that further revision is necessary.

The majority of the Palaearctic Chinese *Sphecodes* is composed of 14 widespread Trans-Palaearctic or Euro-Asian species. Of them, eight species are distributed from Europe to the Russian Far East, Japan and the eastern provinces of China (*S. albilabris*, *S. crassus*, *S. cristatus*, *S. ferruginatus*, *S. geoffrellus*, *S. longulus*, *S. monilicornis*, and *S. scabricollis*). One species, *S. pellucidus*, occurs in the Russian Far East, but is rare in the East Palaearctic and has not yet been found in eastern China. Five species are distributed from Europe to Siberia and are, as expected, recorded in north-west China (*S. alternatus*, *S. gibbus*, *S. ehippius*, *S. pinguiculus*, *S. intermedius*).

The other eight Palaearctic species have smaller distributional ranges. *Sphecodes olivieri* is found in semi-desert and desert habitats of the Western Palaearctic, including Xinjiang and Gansu within China. Three species, *S. nurekensis*, *S. pectoralis* and *S. turanicus*, are desert and steppe Irano-Turanian species distributed in Central Asia which also occur in Xinjiang and Gansu. Four species, *S. kozlovi*, *S. laticaudatus*, *S. manchurianus*, and *S. nippon* are East Palaearctic species, not found farther west than 90°E.

None of the above Palaearctic species are recorded below 30°N. However, two species, *S. grahami* and *S. pieli*, have an inter-realm range and are distributed in the East Palaearctic well as Oriental China. More study is necessary to revise the Oriental *Sphecodes*.

Acknowledgments

We are grateful to Maximilian Schwarz and Fritz Gusenleitner (OÖLM) for help during our visit to Austria. We thank Hege Vårdal (NHRS), Michael Ohl and Viola Richter (MNHB) for providing *Sphecodes* type specimens. Michael Orr helped to edit the English text during his busy field trips. We also wish to thank Peter Bogusch and Julio Genaro, who reviewed the manuscript and helped to improve this article. This investigation was supported by the Russian Funds for Basic Research (grant numbers 16–04–00197 and 17–04–00259) and the state research project (AAAA-A17–117030310210–3). Ze-Qin Niu is supported by the National Science Foundation of China (31772487). Chao-Dong ZHU acknowledges the supports of the National Science Fund for Distinguished Young Scholars (Grant number 31625024) and Singapore-China Joint Research Grant (41761144068) to work on bee systematics.

References

- Årgent L, Svensson B (1982) Flagellar sensilla on *Sphecodes* bees (Hymenoptera, Halictidae). *Zoologica Scripta* 11: 45–54. <https://doi.org/10.1111/j.1463-6409.1982.tb00517.x>
- Ascher JS, Pickering J (2018) Discover Life bee species guide and world checklist (Hymenoptera: Apoidea: Anthophila). http://www.discoverlife.org/mp/20q?guide=Apoidea_species [Accessed 25 May 2018]
- Astafurova YuV (2013) Geographic distribution of halictid bees of the subfamilies Rophitinae and Nomiinae (Hymenoptera, Halictidae) in the Palaearctic. *Entomological Review* 93(4): 437–451. <https://doi.org/10.1134/S0013873813040052>
- Astafurova YuV, Proshchalykin MYu (2014) The bees of the genus *Sphecodes* Latreille 1804 of the Russian Far East, with key to species (Hymenoptera: Apoidea: Halictidae). *Zootaxa* 3887(5): 501–528. <http://dx.doi.org/10.11646/zootaxa.3887.5.1>
- Astafurova YuV, Proshchalykin MYu (2015a) Bees of the genus *Sphecodes* Latreille 1804 of Siberia, with a key to species (Hymenoptera: Apoidea: Halictidae). *Zootaxa* 4052(1): 65–95. <http://dx.doi.org/10.11646/zootaxa.4052.1.3>
- Astafurova YuV, Proshchalykin MYu (2015b) New and little known bees of the genus *Sphecodes* Latreille (Hymenoptera: Halictidae) from Mongolia. *Far Eastern Entomologist* 289: 1–9.
- Astafurova YuV, Proshchalykin MYu (2016a) To the knowledge of the genus *Sphecodes* Latreille (Hymenoptera: Halictidae) of Caucasus. *Euroasian Entomological Journal* 5(Suppl. 1): 15–9.
- Astafurova YuV, Proshchalykin MYu (2016b) The bees of the genus *Sphecodes* Latreille (Hymenoptera: Halictidae) of the European part of Russia. *Far Eastern Entomologist* 321: 1–21.
- Astafurova YuV, Proshchalykin MYu (2017a) To the knowledge of the *Sphecodes hyalinatus* species-group (Hymenoptera, Halictidae). *Entomological Review* 97(5): 664–671. <https://doi.org/10.1134/S0013873817050104>
- Astafurova YuV, Proshchalykin MYu (2017b) The genus *Sphecodes* Latreille 1804 (Hymenoptera: Apoidea: Halictidae) in Central Asia. *Zootaxa* 4324(2): 249–284. <https://doi.org/10.11646/zootaxa.4324.2.3>
- Astafurova YuV, Proshchalykin MYu, Schwarz M (2015) New data on the genus *Sphecodes* Latreille (Hymenoptera: Halictidae) from Mongolia. *Far Eastern Entomologist* 302: 1–9.
- Astafurova YuV, Proshchalykin MYu, Schwarz M (2018) New and little known bees of the genus *Sphecodes* Latreille, 1804 (Hymenoptera: Apoidea: Halictidae) from Central Asia. *Zootaxa* 4441(1): 76–88. <https://doi.org/10.11646/zootaxa.4441.1.4>
- Astafurova YuV, Proshchalykin MYu, Shlyakhtenok AS (2014) Contribution to the knowledge of bee fauna of the genus *Sphecodes* Latreille (Hymenoptera: Halictidae) of the Republic of Belarus. *Far Eastern Entomologist* 280: 1–8.
- Blüthgen P (1923) Beiträge zur Systematik der Bienengattung *Sphecodes* Latr. *Deutsche Entomologische Zeitschrift* 5: 441–513.
- Blüthgen P (1924) Beiträge zur Systematik der Bienengattung *Sphecodes* Latr. II. *Deutsche Entomologische Zeitschrift* 6: 457–516.
- Blüthgen P (1927) Beiträge zur Systematik der Bienengattung *Sphecodes* Latr. III. *Zoologische Jahrbücher. Abteilung für Systematik, Ökologie und Geographie der Tiere* 53(1/3): 23–112.

- Blüthgen P (1934) Schwedisch-chinesische wissenschaftliche Expedition nach den nordwestlichen Provinzen Chinas unter Leitung von Dr. Sven Hedin und Prof. Sü Ping-chang: Insekten, gesammelt vom schwedischen Arzt der Expedition Dr. David Hummel 1927–1930. 27 Hymenoptera. 5. *Halictus*- und *Sphecodes*-Arten (Hym.; Apidae; Halictini). Arkiv för Zoologi 27(1, 13): 1–23.
- Bogusch P, Straka J (2012) Review and identification of the cuckoo bees of central Europe (Hymenoptera: Halictidae: *Sphecodes*). Zootaxa 3311: 1–41.
- Chen L, Song Y, Xu S (2008) The boundary of Palaearctic and Oriental realms in western China. Progress in Natural Science 18: 833–841. <https://doi.org/10.1016/j.pnsc.2008.02.004>
- Cockerell TDA (1911) Descriptions and records of bees – XXXIV. Annals and Magazine of Natural History 7(39): 225–237. <https://doi.org/10.1080/00222931108692933>
- Cockerell TDA (1922) Bees in the collection of the United States National Museum. 4. Proceedings of the United States National Museum 60(2413): 1–20. <https://doi.org/10.5479/si.00963801.60-2413.1>
- Cockerell TDA (1931) Bees collected by the Reverend O. Piel in China. American Museum Novitates 466: 1–16.
- Emeljanov AF (1974) Proposals on Classification and Nomenclature of Ranges. Entomologicheskoe Obozrenie 53(3): 497–521. [In Russian]
- Engel MS (2001) A monograph of the Baltic amber bees and evolution of the Apoidea (Hymenoptera). Bulletin of the American Museum of Natural History 259: 1–192. [https://doi.org/10.1206/0003-0090\(2001\)259<0001:AMOTBA>2.0.CO;2](https://doi.org/10.1206/0003-0090(2001)259<0001:AMOTBA>2.0.CO;2)
- Fellowes JR (2006) Ant (Hymenoptera: Formicidae) genera in southern China: observations on the Oriental-Palaearctic boundary. Myrmecologische Nachrichten 8: 239–249.
- He J, Kreft H, Gao E, Wang Z, Jiang H (2017) Patterns and drivers of zoogeographical regions of terrestrial vertebrates in China. Journal of Biogeography 44: 1172–1184. <https://doi.org/10.1111/jbi.12892>
- Heiser M, Schmitt T (2013) Tracking the boundary between the Palaearctic and the Oriental region: new insights from dragonflies and damselflies (Odonata). Journal of Biogeography 40: 2047–2058. <https://doi.org/10.1111/jbi.12133>
- Hoffmann RS (2001) The Southern boundary of the Palaearctic realm in China and adjacent countries. Acta Zoologica Sinica 47(2): 121–131.
- Meyer R (1920) Apidae Sphecodinae. Archiv für Naturgeschichte. Abteilung A 85(1/2): 79–160; 161–244.
- Meyer R (1922) Nachtrag 1 zur Bienengattung *Sphecodes* Latr. Archiv für Naturgeschichte. Abteilung A 88(8): 165–174.
- Meyer R (1925) Zur Bienengattung *Sphecodes*. Archiv für Naturgeschichte. Abteilung A 90(12): 1–12.
- Michener CD (2007) The Bees of the World (2nd edn). Johns Hopkins University Press, Baltimore, 953 pp.
- Pesenko YuA (2007) Family Halictidae. In: Lelej AS (Ed.) Key to the insects of Russian Far East. Volume 4. Part 5. Dalnauka, Vladivostok, 745–878. [In Russian]
- Strand E, Yasumatsu K (1938) Two new species of the genus *Sphecodes* Latreille from the Far East (Hymenoptera: Apoidea). Mushi 11(1): 78–82.
- Warncke K (1992) Die westpaläarktischen Arten der Bienengattung *Sphecodes* Latr. Bericht der Naturforschende Gesellschaft Augsburg 52: 9–64.

Survey research on the habitation and biological information of *Callipogon relictus* Semenov in Gwangneung forest, Korea and Ussurisky nature reserve, Russia (Coleoptera, Cerambycidae, Prioninae)

Seung-Gyu Lee¹, Cheolhak Kim², Alexander V. Kuprin³, Jung-Hoon Kang⁴,
Bong-Woo Lee⁵, Seung Hwan Oh¹, Jongok Lim¹

1 Korea National Arboretum, Pocheon 11186, South Korea **2** Osang K-insect Biological Resource Research Center, Yesan 32426, South Korea **3** Federal Scientific Center of the East Asia Terrestrial Biodiversity, Far East Branch of the Russian Academy of Sciences, Vladivostok, 690022, Russia **4** National Research Institute of Cultural Heritage, Daejeon 34122, South Korea **5** Korea Forest Service, Daejeon 35208, South Korea

Corresponding author: Jongok Lim (jjongok79@gmail.com)

Academic editor: F. Vitali | Received 18 May 2018 | Accepted 21 August 2018 | Published 23 October 2018

<http://zoobank.org/F661DE51-8993-49D0-893A-5A9E841746BE>

Citation: Lee S-G, Kim C, Kuprin AV, Kang J-H, Lee B-W, Oh SH, Lim J (2018) Survey research on the habitation and biological information of *Callipogon relictus* Semenov in Gwangneung forest, Korea and Ussurisky nature reserve, Russia (Coleoptera, Cerambycidae, Prioninae). ZooKeys 792: 45–68. <https://doi.org/10.3897/zookeys.792.26771>

Abstract

An investigation on the habitation of *Callipogon relictus* Semenov, 1899 in Gwangneung forest was carried out, where the Korea National Arboretum is located. In an investigation spanning the last eleven years (2007–2017), 22 emergence holes, nine pupal chambers, six adults, and two larvae of *C. relictus* were identified. In this study, biological information about habitation of *C. relictus* is provided by comparing and combining the results of this investigation with a survey conducted in Ussurisky Nature Reserve, Russia, in 2015. The distribution is also reviewed to include the Korean Peninsula and a new location of South Korea is added to the distribution for *C. relictus*.

Keywords

Coleoptera, *Callipogon relictus*, critically endangered species, Gwangneung forest, habitation, Korea natural monument

Introduction

The genus *Callipogon* Audinet-Serville, 1832, includes nine species in five subgenera worldwide, one of which, *C. (Eoxenus) relictus* Semenov, 1898, is found in East Asia, while the other eight species are mainly distributed in Central and South America, including Mexico, Guatemala, and Colombia (Lameere 1904; Monne 2017). The presence of *C. relictus* in East Asia may provide evidence that the old world and the new world were connected when the Bering land bridge was above sea level (Kuprin and Bezborodov 2012).

Callipogon relictus, which is known to be one of the largest Coleoptera species in the Palearctic region, was first recorded in Vladivostok, far eastern Russia, and is also found in some parts of China, Mongolia and central and northern parts of the Korean Peninsula (Byun et al. 2007; Li et al. 2013; Yi et al. 2018).

In the first report from the Korean Peninsula, *Callipogon relictus* was misidentified by Saito (1932) as *Macrotoma fisheri* Waterhouse, 1884 (Figure 1) with no precise collection record. Later, Cho (1934) collected specimens from Mt. Bukhansan in Seoul, the capital of South Korea, and additionally summarized the host plants and the distribution in 1955. Murayama (1936) first recorded the appearance of larvae collected from Gwangneung forest in Pocheon-si, Gyeonggi province, and reported that *Carpinus laxiflora* (Siebold & Zucc.) Blume (Betulaceae) was its host plant. Thereafter, when a large number of specimens were collected from Chujeon-ri, Buksan-myeon, Chuncheon-si, Gangwon province, this region was designated as a natural monument No. 75 on 3 December 1962, a habitat of *C. relictus*. However, the habitat was destroyed during construction of the Soyanggang dam, and its natural monument status was annulled on 19 July, 1973.

Detailed and quantitative investigations of the Korean distribution and population size of *Callipogon relictus* have not been conducted, but the population density has been observed to be decreasing rapidly, and for conservation, the species was afforded legal protection, designated as a natural monument No. 218, on 20 November 1968, by the Korean Cultural Heritage Administration. It was designated a class I endangered species by the Ministry of Environment on 31 May 2012, and was declared to be “Critically Endangered” (CR) on 6 December 2013 (Cho and Lee 2013).

Callipogon relictus is being protected as a CR species based on its dwindling numbers both in Korea and in its type locality, Russia. However, due to the difficulty of obtaining specimens, there has been very little ecological research on the species.

Several Korean researchers have conducted investigations of habitation, taxonomical studies on, and research into the measures of conservation of *Callipogon relictus*. In particular, Kim et al. (1976) surveyed the state of habitation in Yangju-gun, Gyeonggi province (currently Gwangneung forest, Pocheon-si) and Gangneung-si, Gangwon province (currently Sogeumgang, Gangneung-si), and recorded the occurrence frequency, distribution, and host plants of adults, and the appearance of larvae. Hong and Kim (1991) discussed the distribution, morphological variation in adult and biological information based on 28 Korean specimens. Byun et al. (2007) surveyed

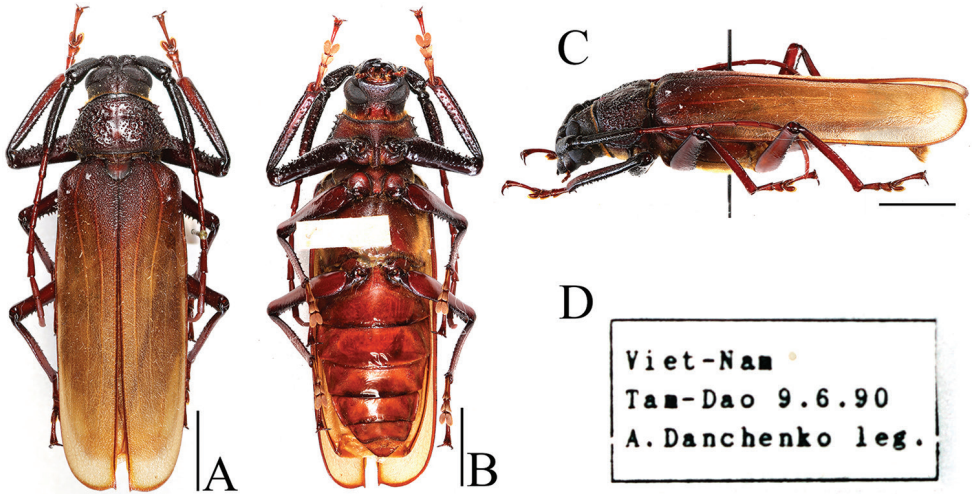


Figure 1. *Macrotoma (Bander) fischeri*, male: **A** dorsal aspect **B** ventral aspect **C** lateral aspect **D** label data. Scale bars: 10 mm.

habitation of *C. relictus* in Gwangneung forest between 1999 and 2006 and discussed various on-site conservation measures. An (2010) reviewed the Korean literature and proposed measures for the systematic conservation and management of *C. relictus*. Lim et al. (2013) performed a molecular study of a large larva found in Gwangneung forest in 2010 and on an adult of *C. relictus* collected in 1990. They identified that the specimens belonged to the same species, while also re-describing the morphology of the larva. Lim et al. (2017) used a female adult discovered in Gwangneung forest in 2014 and 2015 to conduct mitochondrial genome analysis. Recently, various research institutes in the East Asia, including the Korea National Arboretum, have taken an interest in *C. relictus*, and through international collaboration, are engaging in diverse research to establish conservation measures. However, there is a severe lack of basic biological data on *C. relictus*, making it very difficult to collect specimens, and, owing to the rapid decline in its population size, they are rarely observed lately.

In this study, we combined the results of investigations that we conducted between 2007 and 2017 in Gwangneung forest (currently, the only known habitat in Korea) and we compared the results with a habitation survey in the Ussurisky nature reserve in Russia, type locality and one of the largest habitat of this species. Finally, we provide biological information that can aid species conservation measures by reviewing all reported information of *C. relictus* previously discovered in Gwangneung forest and in the rest of Korea, as well as various researches in other countries.

Materials and methods

The major investigation area was the whole Gwangneung forest, spanning Namyangju-si and Pocheon-si in Gyeonggi province (Figure 2, red). In particular, the investigation



Figure 2. Locations of investigation sites (red symbol: Gwangneung forest, Korea; blue symbol Ussurisky nature reserve, Russia).

focused on the northeast part of Soribong, where *Callipogon relictus* have often been collected in the past.

Another investigation area was the Ussurisky nature reserve, Primorsky Krai, Russia (Figure 2, blue) with the cooperation of Dr. Alexander Kuprin (Far East Branch, Russian Academy of Sciences). We conducted an investigation focusing on two areas with a high density of *Callipogon relictus* habitation (43°37'58.5"N, 123°13'57.0"E, Alt. 78; 43°39'49.7"N, 132°30'1.73"E, Altitude 164 m). Survey research on the habitat in Gwangneung forest, Korea, was conducted over 11 years, from 2007 to 2017. Between 2007 and 2009, the research was conducted once a month from June to August, when adults had previously been found; between 2010 and 2016, surveys were conducted once a month from March to June, and at least twice a month from July to August. In 2017, surveys were conducted once a week from February to May and in September, and twice a week from June to August. At the Ussurisky nature reserve (Russia), one survey was conducted from 25–27 August 2015.

In order to survey research on the habitat in the immature stage, we first looked for the presence of adult emergence holes, focusing on dead trees, which have been reported to be host plants, and measured the size, height, direction of the holes and the diameter at breast height (DBH) of the tree. When emergence holes were found, they were opened to check for the presence of larvae and to measure the size of any feeding scars and pupal chambers.

In order to survey adults directly, during the day we conducted a visual survey using binoculars to look for the appearance of adults near the sap of the host plants (Figure 3A); at night, we used a light trap to try to lure adults (Figure 3B). When necessary, a heli-cam (helicopter camera) and a ladder truck were used to look for



Figure 3. Investigation methods: **A** visual survey (naked eye) **B** light trap **C** heli-cam **D** ladder truck **E** bait trap **F** pheromone trap.

emergence holes in high places and trap surveys were conducted using other types of trap, including bait trap with rotting fruit and sap fermented with honey, circular cage traps, and pheromone trap (Figure 3C–F).

Results

Occurrence frequency of adult

During the research period (2007–2017), we observed a total of six adults during four consecutive years: one male in 2014, one female in 2015, one male in 2016, and one male and two females in 2017 (Figure 4A–F, Tables 1–2).

The body length (from apex of mandible to apex of elytra) of the male found on 19 August 2014 was 88.0 mm (Figure 4A). At the time of finding, the right elytron was missing, and much of the left elytral pubescence was missing. The individual was in a state of exhaustion and died the next day.



Figure 4. Adults of *Callipogon relictus* discovered in Gwangneung forest: **A** male in 2014 **B** female in 2015 **C** male in 2016 **D** female in 2017 **E** female in 2017 **F** male in 2017.

The body length of the female found on 27 July 2015 was 78.0 mm (Figure 4B). At the time of its finding the pronotum was severely damaged, the left elytron was missing, and much of the right elytral pubescence was missing. The mesonotum was partially detached and the individual was gathered by numerous ants, dying within a few hours of discovery.

The body length of the male found on 10 August 2016 was 98.0 mm (Figure 4C). At the time of finding, there was a crack running longitudinally in its pronotum, much of the pubescence was missing, and some claws were also missing. The individual was in a state of exhaustion and died the next day.

The body length of the female found on 20 July 2017 was 78.0 mm (Figure 4D). At the time of finding, there were no particularly damaged parts; some of the pubescence

Table 1. Signs of habitation of *Callipogon (Eoxenus) relictus* discovered in Gwangneung forest in 2007–2016 (units: ex).

	2007	2008	2009	2010	2011	2012	2013	2014	2015	2016	2017	Total
Larva	–	–	–	1	–	–	–	–	–	1	–	2
Pupal chamber	–	–	–	2	2	2	1	–	–	1	–	8
Exuvium	–	–	–	–	–	1	–	–	–	1	–	2
Adult	–	–	–	–	–	–	–	1 ♂	1 ♀	1 ♂	1 ♂ 2 ♀	6
Emergence hole	–	–	–	3	2	3	2	2	–	1	–	13
Total	–	–	–	6	4	6	3	3	1	5	3	31

Table 2. Larvae of *Callipogon (Eoxenus) relictus* discovered in Gwangneung forest in 2007–2017.

Year	Month		Collecting site
	July	August	
2014	–	19 th (♂)	Korea National Arboretum
2015	27 th (♀)	–	Korea National Arboretum
2016	–	10 th (♂)	near Mt. Jukyeopsan
2017	20 th (♀)	11 th (♀), 14 th (♂)	Korea National Arboretum

was missing, but the insect was moving actively. After artificial egg collection, the individual died on 31 July 2017.

The body length of the female found on 11 August 2017 was 75.6 mm (Figure 4E). At the time of finding, its right tibiae and tarsi were missing, much of the pubescence was missing, and the ovipositor was prolapsed. The individual was in a state of exhaustion and died in under an hour.

The body length of the male found on 14 August 2017 was 60.0 mm, making it the smallest of all the males discovered to date (Figure 4F). At the time of discovery, the individual was already dead; the left elytron, some legs, and the whole abdomen were missing, and there were ants gathering on the inside of the pronotum.

Emergence holes

In the survey in Gwangneung forest, we found a total of 22 emergence holes on four species of dead tree (*Carpinus cordata* Blume, *C. laxiflora* (Siebold & Zucc.) Blume, *Quercus aliena* Blume, and *Q. mongolica* Fisch). The largest number of holes was found on *C. laxiflora* and as many as six holes were found on a single tree. The holes were observed at heights of 0.9–3.1 m, and six holes faced north and five holes faced northeast (Table 3). The shapes of the emergence holes were subcircular to elliptical, with most holes having a slanted elliptical shape; the mean width and height were 32.1 mm and 26.1 mm, respectively (Figure 5A–D, Table 4).

In Ussurisky nature reserve, we observed a total of 56 emergence holes, on *Ulmus davidiana* var. *japonica* (Rehder) Nakai only. The DBH of the dead trees with emergence holes was 56–130 cm, and there were as many as 18 holes on the only one

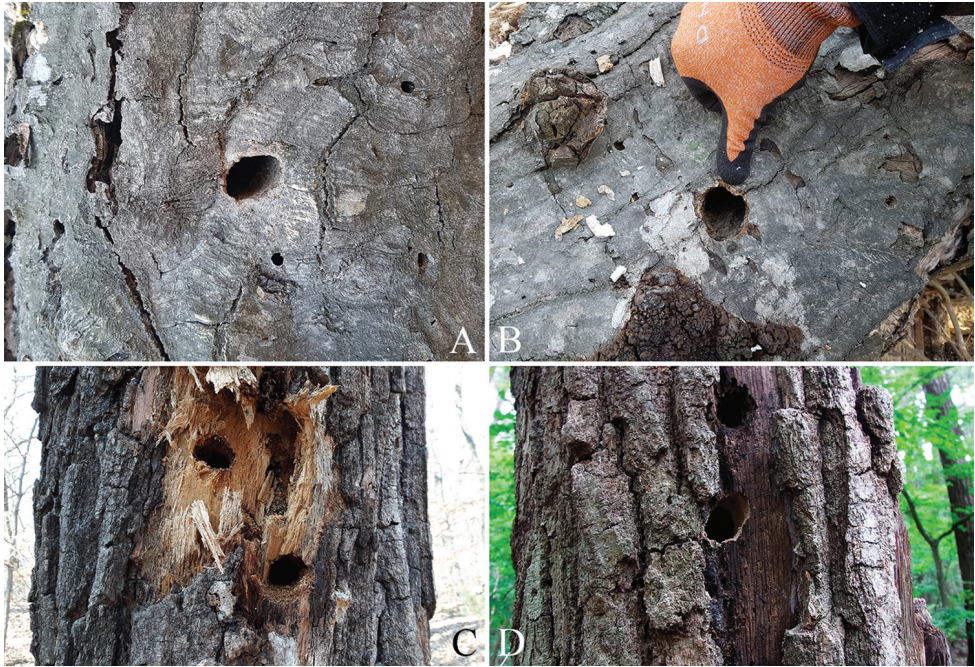


Figure 5. Emergence hole of *Callipogon relictus* in Gwangneung forest, Korea: **A–B** emergence hole on *Carpinus laxiflora* **C** emergence hole on *Quercus* sp. **D** emergence hole on *Quercus aliena*.

tree (that could be observed with naked eyes). The emergence holes were found at various heights in the range of 1.0–24.0 m (Table 3). The shapes of the holes were very similar to those found in Korea, albeit a little larger, with a mean width and height of 33.4 mm and 28.2 mm, respectively (Figure 6A–B, Table 4).

Larvae and feeding scars

Larval feeding scars of *C. relictus* were mostly observed on old (DBH: ≥ 35 cm), less vigorous *Carpinus* spp. and *Quercus* spp., and were observed more commonly on standing dead trees than on fallen trees. Most of the trees with feeding scars have fungal growth (Figure 7A, B) or fungal infection around or on the surface of the feeding scars (Figure 8A, B).

The feeding scar tunnels stretched from below the bark to deep within the trunk. In general, the tunnels had a gradually widening shape oriented vertically in relation to the ground, but the shapes were highly irregular. Some tunnels were horizontal to the ground, and sometimes vertical and horizontal tunnels intersected. Larval excreta varied according to the type and maturity of the host plant and according to the age of the larvae but they were typically slightly thicker than those of the other cerambycids and similar to those of *Dorcus hopei binodulosus* Waterhouse, 1874 (Coleoptera: Lucanidae) (Figure 9A–D).

Table 3. Characteristics of emergence holes of *Callipogon (Eoxenus) relictus* identified in Gwangneung forest and the Ussurisky Nature Reserve (*CC, *Carpinus condata*; CL, *C. laxiflora*; QA, *Quercus aliena*; QM, *Q. mongolica*; Qsp, *Quercus* sp.; UJ, *Ulmus davidiana* var. *japonica*; NO, North; NE, Northeast).

	Gwangneung forest (Korea)												Ussurisky Nature Reserve (Russia)						
	1	2	3	4	5	6	7	8	9	10	11	12	1	2	3	4	5	6	7
Host plant	CL	CL	CL	CL	CL	CL	CC	QM	QA	Qsp	CL	CL	UJ	UJ	UJ	UJ	UJ	UJ	UJ
Diameter of breast height (cm)	69	60	59	55	50	53	48	46	36	51	72	-	56	125	130	70	60	110	80
Number of emergence hole	2	2	2	1	1	2	1	1	1	2	1	6	1	5	18	13	6	1	12
Height of emergence hole (m)	0.9/1.2	1.6/3.1	2.2/2.6	2.2	2.4	2.1/3.1	1.8	1.9	2.1	1.2/1.3	3.1	-	1.8	1.8-2.3	1.0-24.0	1.0-4.0	2.0-12.0	1.5	2.0-10.0
Direction of emergence hole	NO	NO	NE	NO	NE	NO	NE	NO	NO	NE	NE	-	-	-	-	-	-	-	-

Table 4. Sizes of emergence holes of *Callipogon (Eoxenus) relictus* identified in Gwangneung forest and the Ussurisky Nature Reserve (units: mm).

	Gwangneung forest (Korea)		Ussurisky Nature Reserve (Russia)	
	Width	Height	Width	Height
1	35	32	26	18
2	32	28	34	25
3	36	28	37	29
4	27	24	34	27
5	28	27	26	20
6	30	22	36	32
7	31	24	32	28
8	31	25	31	24
9	35	24	31	25
10	35	29	35	30
11	36	28	37	34
12	32	25	40	26
13	31	22	33	26
14	31	27	36	30
15	-	-	35	33
16	-	-	45	34
17	-	-	22	41
18	-	-	32	26
Mean	32.1	26.1	33.4	28.2



Figure 6. Emergence hole of *Callipogon relictus* in Ussurisky nature reserve, Russia: **A–B** emergence hole on *Ulmus davidiana* var. *japonica*.

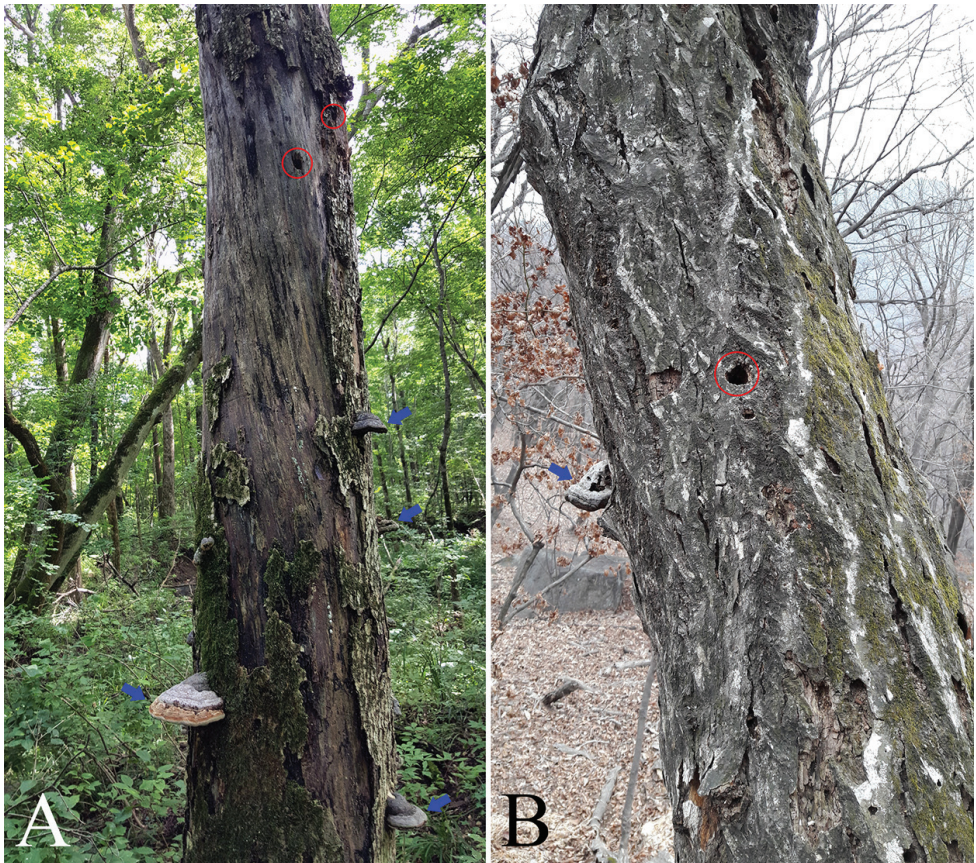


Figure 7. Emergence hole and fungus on host plant (red circle, emergence hole; blue arrow, fungus): **A** *Ulmus davidiana* var. *japonica* **B** *Carpinus cordata*.

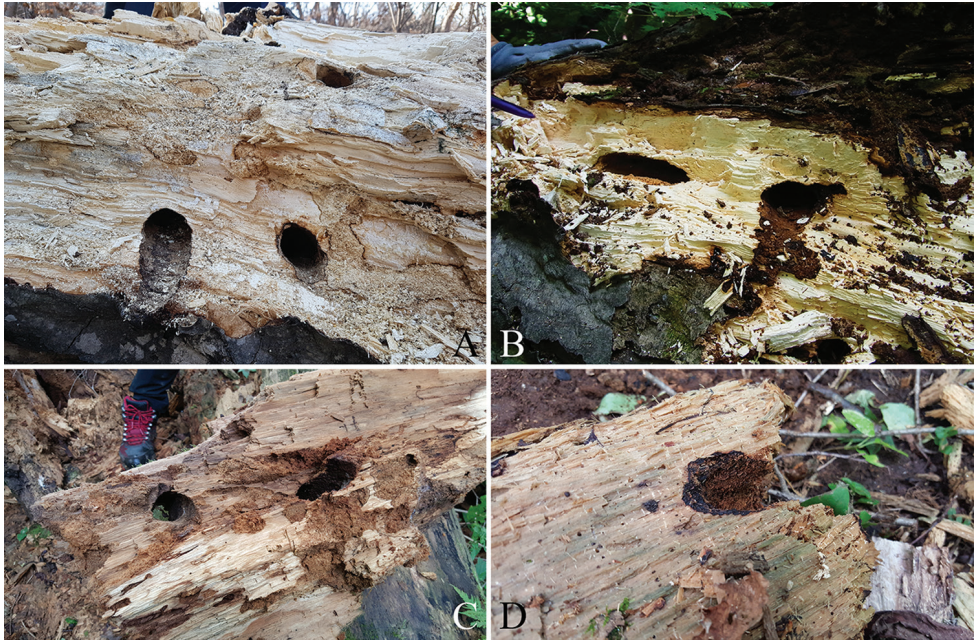


Figure 8. Larval gallery and pupal chamber of *Callipogon relictus* in Gwangneung forest.

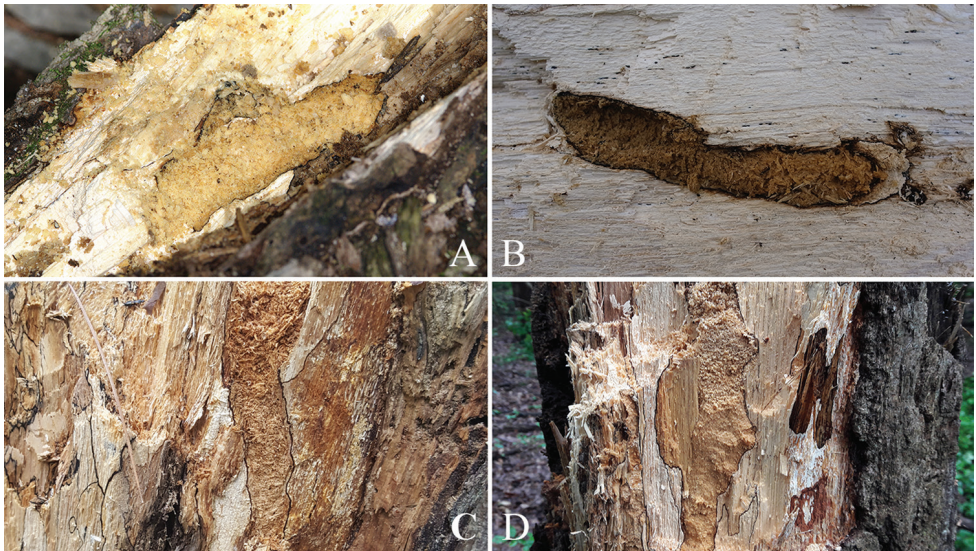


Figure 9. Larval excreta of *Callipogon relictus* in gallery: **A–B** larval excreta in *Carpinus laxiflora* **C–D** larval extra in *Quercus aliena*.

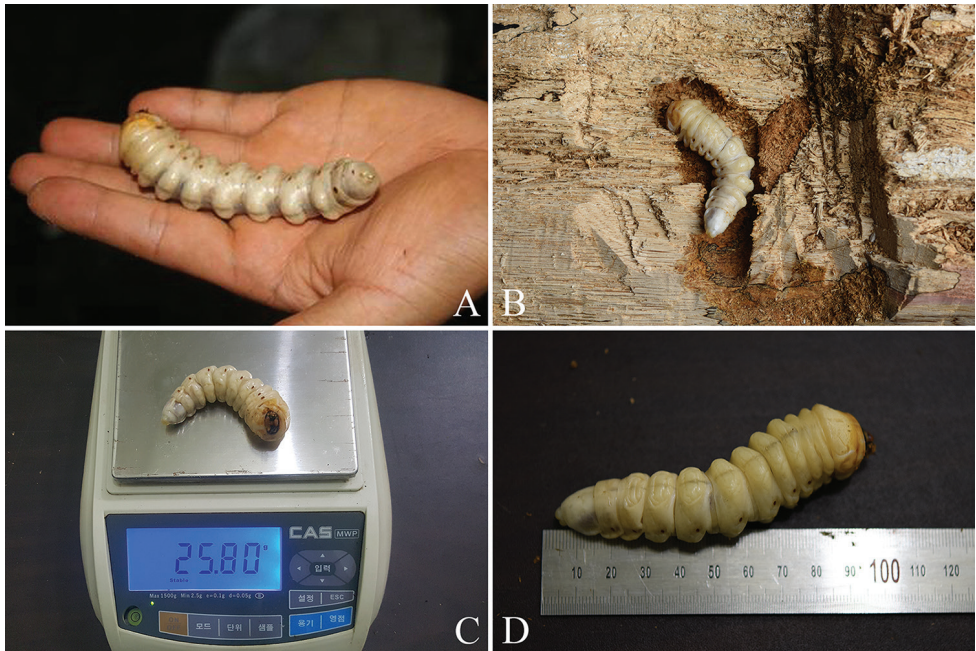


Figure 10. Larvae of *Callipogon relictus* discovered in Gwangneung forest: **A** larva in 2010 **B–D** larva in 2016.

Two larvae were found, one in 2010 and one in 2016. The larva collected in a *C. laxiflora* tree on 29 July, 2010 had a length of 11.6 cm, a head width of 1.14 cm, and was found dead, infected with a pathogenic organism (Figure 10A). The larva discovered in a *Q. aliena* tree on 1 August, 2016 was very healthy, with a length of 10.5 cm, a head width of 1.14 cm, and a weight of 25.8 g (Figure 10B–D).

Two larval exuviae were collected, one in 2012 and one in 2016. One pupal exuvia was found in a *C. laxiflora* tree on 26 July 2012 (Figure 11A) and one female pupal exuvia was found in the same *Q. aliena* of dead tree where the larva was discovered on 1 August, 2016 (Figure 11B). In addition, in 2017, the right mandible of a larva was found in a dead *C. laxiflora* tree.

Pupal chambers

During the study period (2007–2017), we found a total of nine pupal chambers of *C. relictus* in three species of dead trees in Gwangneung forest (*Carpinus cordata*, *C. laxiflora*, and *Q. aliena*). The highest number of pupal chambers was found in *C. laxiflora* trees and as many as three pupal chambers were found in one *C. laxiflora* tree. The DBH of dead trees containing pupal chambers was in the range 39–69 cm, with a mean DBH of 57.1 cm. The pupal chambers were either ellipses with a long horizontal axis, or long tunnel shapes. They were 13–20 cm in length, located 4.5–10.0 cm deep inside the bark, parallel to the ground and perpendicular to the tree trunk (Figure 12A, B, Table 5).

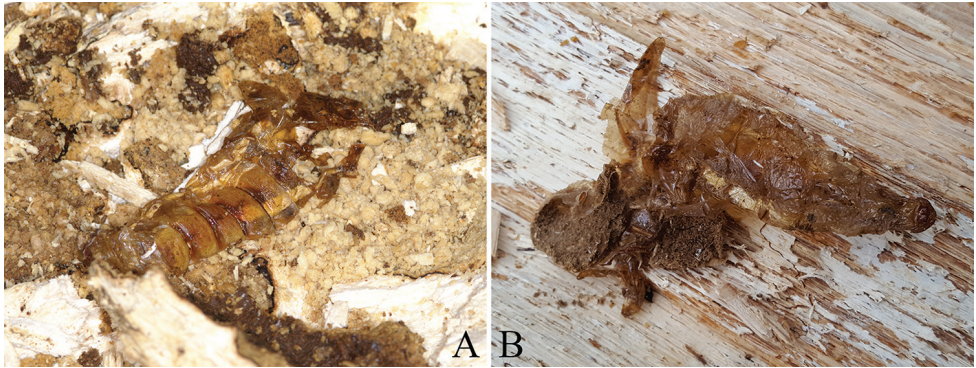


Figure 11. Pupal exuvium of *Callipogon relictus* in Gwangneung forest: **A** exuvium in *Carpinus laxiflora* in 2012 **B** exuvium in *Quercus aliena* in 2016.



Figure 12. Pupal chambers of *Callipogon relictus* in Gwangneung forest: **A** pupal chamber in *Carpinus laxiflora* **B** pupal chamber in *Quercus aliena*.

Table 5. Sizes of pupal chambers of *Callipogon (Eoxenus) relictus* identified in Gwangneung forest (Korea) (*CC, *Carpinus cordata*; CL, *C. laxiflora*; QA, *Q. aliena*) (units: cm).

	1	2	3	4	5	6	7	8	9	Mean
Length of chamber	18	20	20	15	17	18	18	14	13	17.5
Longest axis pupal chamber diameter	4.1	4.4	4.3	3.8	3.9	3.8	4.2	4.4	4.3	4.1
Shortest axis pupal chamber diameter	3.3	3.6	3.5	3.2	3.2	3.3	3.4	3.2	3.1	3.3
Host plant	CL	CC	QA	3 spp.						
Diameter at breast height	60	69	69	55	53	50	60	59	39	57.1
Depth under bark	7.0	9.0	8.0	7.0	8.0	5.0	10.0	6.0	4.5	7.2

Host plants and habitats

In the Gwangneung forest in Korea, direct identification of individuals and signs of habitation occurred in four species of tree: *Carpinus cordata*, *C. laxiflora*, *Quercus aliena*, and *Q. mongolica* (Figs 5A–D, 7B). In addition, we observed a number of feeding scars in other *Quercus* spp. that could not be precisely identified at the species level, due to the high extent of decay in these dead trees. Most of these trees were located in areas on the northern slope, close to the valley, where the terrain was not too steep.

The species in which we directly observed larvae were *C. laxiflora* and *Q. aliena*. The state of decay of *Q. aliena* was as follows: trunk left standing; approximately 80–90% bark remaining; bark tightness tight to loose; wood texture hard; shape of cross section round; branches absent (Figure 13A).

At the Ussurisky nature reserve in Russia, we identified various host plants such as *Fraxinus mandschurica*, *Quercus mongolica*, *Ulmus laciniata*, and *U. davidiana* var. *japonica* – but emergence holes of *C. relictus* and feeding marks were observed only in *U. davidiana* var. *japonica* (Figure 13B); overall, this region contains several tributaries and the mountain wetlands are well developed (Figure 13C).

Discussion

Distribution in the Northeast Asia

Callipogon relictus has so far been reported from four countries in East Asia: Russian Far East, China and Korean Peninsula (Kuprin and Bezborodov 2012; Bezborodov 2016; Yi et al. 2018).

In the Russian Far East, which is type locality of this species, its distribution was summarized by Kuprin and Bezborodov (2012). They reported that *C. relictus* were distributed across four federal subjects of Russia (Primorsky Krai, Khabarovsk Krai, the Jewish Autonomous Oblast, and Amura Oblast) and distinguished four local popula-

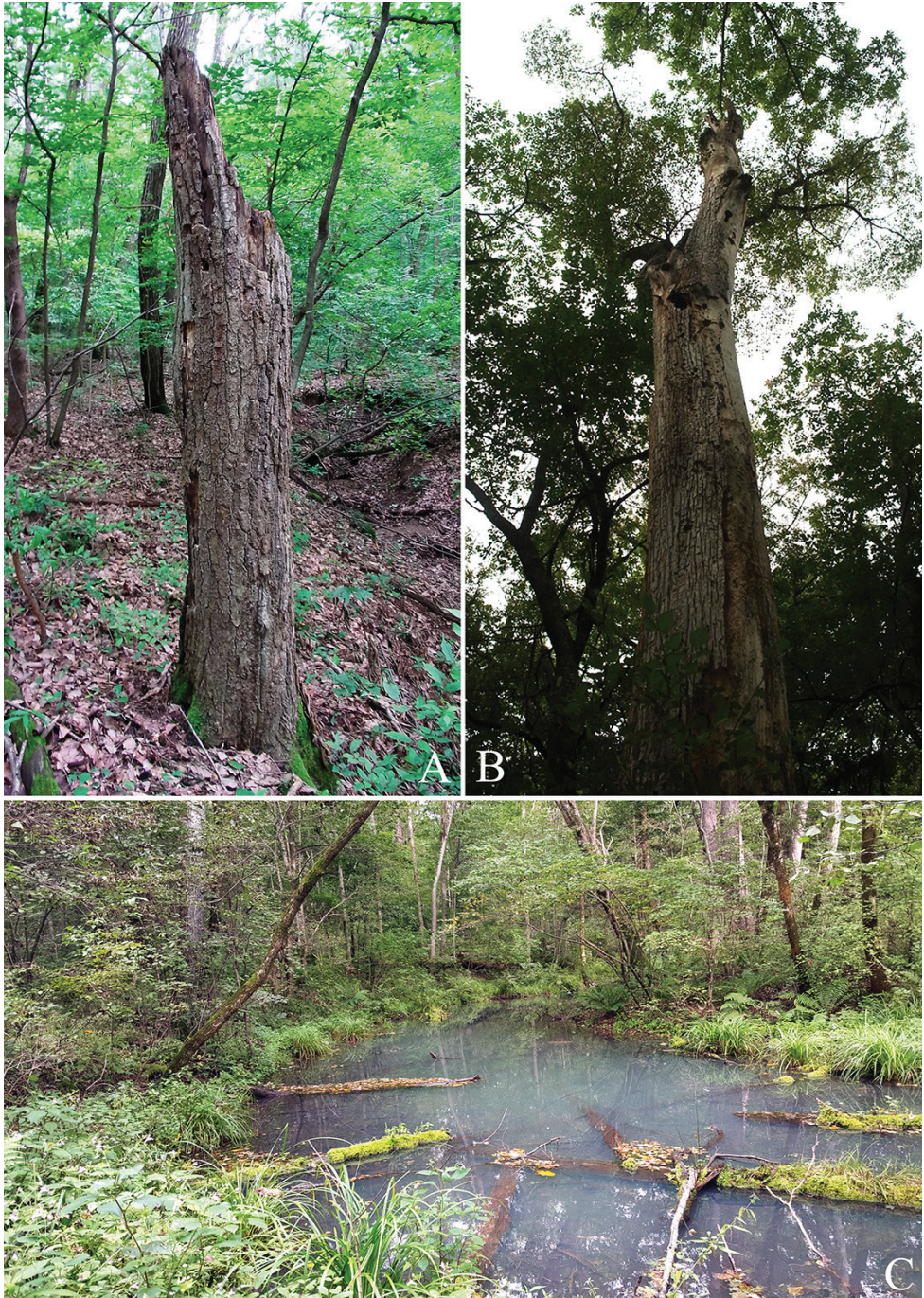


Figure 13. Host plants and habitat of *Callipogon relictus*: **A** *Quercus aliena* in Gwangneung forest **B** *Ulmus davidiana* var. *japonica* in Ussurisky nature reserve **C** forest in Ussurisky nature reserve.

tions: Ussuriiskaya, Khoro-Bikinskaya, Khingano-Bure-inskaya, and Selemdzhinskaya populations (Kuprin and Bezborodov 2012).

The distribution of *C. relictus* in China has been reported to span eight provinces: Tianjin, Gansu, Hebei, Heilongjiang, Inner Mongolia, Jilin, Liaoning, Shaanxi, and Shanxi (Li et al. 2014). Of these, the largest number of individuals has been recorded in the three provinces (Heilongjiang, Jilin, and Liaoning) that border North Korea and Primorsky Krai, the type locality in Russia (Bezborodov 2016).

Recently, Bezborodov (2016) and Yi et al. (2018) reassessed the distribution of *C. relictus* based on sampling data. Based on current reports, the eastern limit of the distribution of *C. relictus* is the Imeni Lazo district, Khabarovsk Krai, Russia, located at 135°E (Kuprin and Bezborodov 2012); the northern limit is the Selemdzhinsky district, Amur Oblast, Russia, located at 53°N; the southwestern limit is Houyugou city, Shaanxi, China, located at 35°N, 110°E (Hua 2002); the northeastern limit is Mt. Si-fang-shan in A-er-jin city, Inner Mongolia, China, located at 49°N, 123°E (Li et al. 2013); and the southeastern limit is Sogeumgang of Mt. Odaesan, Gangwon province, South Korea, located at 37°N, 128°E (Yi et al. 2018). So far, *C. relictus* has been observed in the range of latitudes 35°N to 53°N and longitudes 110°E to 135°E. It is possible that the known range will expand if more precise surveys are conducted in Northeast Asia.

Distribution in the Korean Peninsula

The first record of *Callipogon relictus* in South Korea was provided by Saito (1932), who misidentified the species as *Macrotoma fisheri*, after which Cho (1934) collected and reported *C. relictus* at Namjangdae in Mt. Bukhansan, Seoul.

Cho (1955) added a record of distribution in two regions in Gyeonggi province (Pocheon-gun and Paju-si) and four regions in Gangwon province (Chuncheon-si, Hwacheon-gun, Yanggu-gun, and Gangneung-si) in the north of South Korea. In addition, Cho (1961) reported the following specific locations from where specimens were collected: Chujeon-ri (Bukhan-myeon, Chuncheon-si), Georye-ri (Hanam-myeon, Yuchon-ri, Gandong-myeon, Hwacheon-gun), Eupnae-ri (Yanggu-myeon, Yanggu-gun) (Gangwon province), Bukhan-san (Seoul) and Gwangneung (Gyeonggi province) (Figure 14).

Kim (1978) reviewed specimens of *C. relictus* deposited in various Korean research institutions and found that, after the addition of records for Gangwon province (Cheongpyeong-ri, Bukhan-myeon, Chuncheon-si, Sogeumgang, Odae-san, and Gangneung-si), the only official collection records came from Gwangneung forest in Pocheon-si, Gyeonggi province (Byun et al. 2007: Table 2).

In this study, we found adults of *C. relictus* in the Gwangneung forest for four consecutive years from 2014 to 2017 (Table 1) and we also added a new location to the Korean distribution of the species in Yangyang-gun, Gangwon province, based on photographic evidence (Figure 15). This region is thought to be a suitable alternative conservation site (habitat), as it has not only a much wider habitat area than

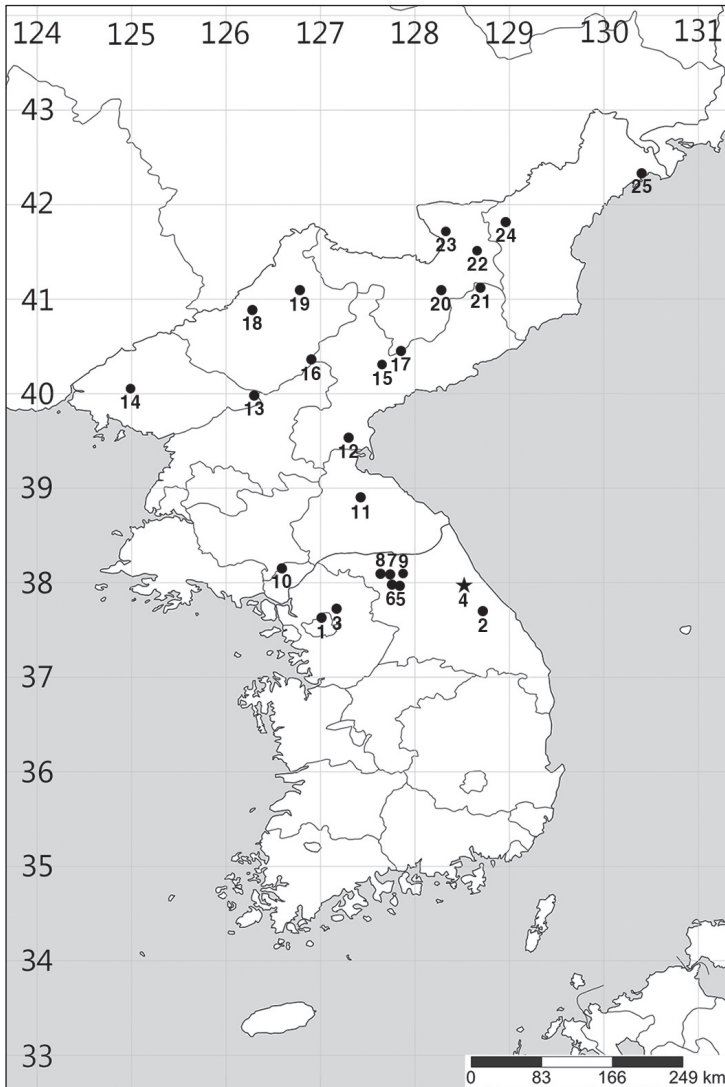


Figure 14. Distribution map of *Callipogon relictus* in the Korean Peninsula (An 2010; Bezbordodov 2016; Yi et al. 2018; *per. obs.*): **1** Gyeonggi Province, Seoul-si, Mt. Bukhansan, Namjangdae **2** Gangwon Province, Gangneung-si, Mt. Odaesan, Sogeungang **3** Gyeonggi Province, Pocheon-si, Gwangneung forest **4** Gangwon Province, Yangyang-gun, Seo-myeon (new record) **5** Gangwon Province, Chuncheon-si, Buksan-myeon, Chujeon-ri **6** Gangwon Province, Chuncheon-si, Buksan-myeon, Cheongpyeong-ri **7** Gangwon Province, Hwacheon-gun, Gandong-myeon, Yuchon-ri **8** Gangwon Province, Hwacheon-gun, Hanam-myeon, Georye-ri **9** Gangwon Province, Yanggu-gun, Yanggu-eup **10** Hwanghaebuk Province, upper region of the Imjingang River **11** Gangwon Province, Sepo-gun, Sambang-ri (Chugaryeong, Sambang-hyeop) **12** Hamgyeongnam Province, Geumya-gun **13** Pyeonganbuk Province, Mt. Myohyangsan **14** Pyeonganbuk Province, Mt. Cheonmasan **15** Hamgyeongnam Province, Sinheung-gun **16** Yanggang Province, Mt. Nangnimsan **17** Hamgyeongnam Province, Mt. Bulgaemiryeong **18** Jagang Province, Mt. Baekamsan **19** Jagang Province, Mt. Hwangsuryeong **20** Yanggang Province, Gapsan-gun **21** Hamgyeongnam Province, Mt. Duryubong **22** Jagang Province, Baekam-gun **23** Jagang Province, Mt. Bukpotaesan **24** Hamgyeongbuk Province, Yeonsa-gun **25** Hamgyeongbuk, Seonbong-gun.



Figure 15. Adult male of *Callipogon relictus* in Yangyang-gun of Gangwon province (photograph taken by Jeong-Ok Kim)

Gwangneung forest and little human interference, but also a large population of host plants. Habitation of Korean individuals has also been verified recently in this region.

In North Korea, *C. relictus* was first recorded by Nakane (1974) and up to now it has been reported to have a wide distribution in the following provinces: Gangwon province, Yanggang province, Jagang province, Pyeonganbuk province, Hamgyeongnam province, Hamgyeongbuk province, and Hwanghaebuk province (Bezborodov 2016; Yi et al. 2018). Of these, the largest numbers of individuals were reported in Yanggang province, Jagang province, Pyeonganbuk province and Hamgyeong province, which are adjacent to Russian Primorsky Krai and China northeastern regions (Jilin, Liaoning), with as many as 31 individuals being collected in a single survey (Mt. Bukpotaesan, Yanggang province) (Yi et al. 2018), suggesting a stable population inhabiting the area.

Survey research on habitation of *Callipogon relictus* in Gwangneung forest

Our study recognized that, except for the new record from Yangyang-gun (Gangwon province), Gwangneung forest is the only collecting site of *C. relictus*. Kim et al. (1976) performed 20 surveys between June and September when adults of *C. relictus* occur, but they did not observe the adults, indicating that the population density was already very low at that time.

During our study, through focused surveys on habitation, we directly found six adults, two larvae, and various other signs of *C. relictus* (22 emergence holes, nine pupal chambers, tunnels, and feeding scars) (Table 1), providing that the Korean population, although low in number, is still persisting in Gwangneung forest and is not extinct in the South Korea.

Conditions of adults

Of the six adults discovered in this study, except one individual, all five were either exhausted from severe damage and died within a day, or were already dead. Three of which individuals were missing an elytron (Figure 4A–B, F) and another was found with a crack in the pronotum (Figure 4C); these damages are considered to be the result of attacks by natural enemies (woodpeckers, squirrels, wild animal, etc.)

In previous studies, adults were observed in Gwangneung forest between June and September and particularly, high numbers were observed in August (Byun et al. 2007: Table 3). Similarly, in our study, we found two adults in July and four adults in August, meaning that the majority of adults were observed in August, consistent with the findings of other studies (Table 2). However, the individuals that we discovered in August were severely weakened, to the extent that they could not cling to a tree or were already dead. Given that they were also missing much of their pubescence, we expect that these individuals were also active as adults in July.

During this study, we discovered a total of six adults in Gwangneung forest but, apart from a male that flew over from a nearby factory, we found the other five adults in regions with a high density of *Quercus* spp. with flowing sap. Like other Prioninae species, *C. relictus* adult is known to be attracted by light at night (Lee 1987; Byun 2007). The male discovered at a factory in 2016 was also thought to have been attracted by bright light at nighttime, while the other five individuals were probably found during egg-laying or feeding activity.

We succeeded in collecting 16 eggs from a female found under a *Quercus* sp. tree through artificially induced oviposition; the hatched larvae are being reared to increase their population. Given that we consistently found a small number of adults over the last four years, although the population size is small, the population of *C. relictus* appears to remain more stable here than in the other parts of Korea.

Conditions of immature stages

The signs of habitation by immature stages of *C. relictus* (emergence holes, pupal chambers, tunnels, and feeding scars) were mostly found on *Carpinus* spp. and *Quercus* spp. of dead trees with DBH \geq 39 cm, in forest areas where *C. laxiflora* were dominant and there were a mixture of *Quercus* spp. Because fallen trees have a large surface

in contact with the ground, they decay rapidly and there is secondary invasion by wood boring insects (e.g. Lucanidae, Tenebrionidae). It was difficult to distinguish the signs of habitation of *C. relictus* from those of other species. In the natural state, the immature period is very long, over 4–5 years (Li et al. 2012), and so, rapidly decaying dead trees are predicted to be disadvantageous for survival.

The shapes of the emergence holes we found were mostly elliptical, but some were close to being circular (Figs 5A–D, 6A–B). Differences in the hole shape have been reported to be correlated with mandible length (Yi 2014), but this has still not been clearly elucidated. In this study, the majority of emergence holes were elliptical, consistent with that of other prognathous species in the subfamily Prioninae (e.g. *Prionus insularis* Motschulsky and *Aegosoma sinicum* White), suggesting that differences arise according to structure of head and mouthparts (prognathous, hypognathous, or retrognathic) rather than mandible length. The size of the holes was clearly larger than that of other large other Korean cerambycids (e.g. *Batocera lineolata* Chevrolat; *Neocerambyx raddei* Blessig & Solsky; *A. sinicum* White) and this is considered to be related to the body width (Korean averages: width 32.1 mm, length 26.0 mm; Russian averages: width 34.6 mm, length 28.2 mm). We found that the emergence holes have towards the north or northeast, and this is thought to be a strategy to minimize moisture loss due to excessive sunlight.

Pupal chambers were most commonly observed in *C. laxiflora*, with lengths in the range of 13–20 cm (Figure 12A, B). The length and size of the pupal chambers was correlated with the DBH of the host plant, where a larger DBH was associated with larger and longer pupal chambers (Table 5). This is because, in host plants with a larger DBH, there is more space available to make the pupal chamber as well as sufficient feeding resources for a favorable nutritional state, and therefore, the body can grow larger (Karino et al. 2004). We assume that the size of the pupal chamber increases in proportion with the size of the body.

The depth of the pupal chambers from the bark varied according to the level of decay and the hardness of the wood. In dead trees that were highly decayed and softer, pupal chambers were deeper; conversely, in dead trees that had harder wood, or that were less decayed, pupal chambers were shallower (Table 5). This suggests that the depth from the bark is adjusted to account for the properties of the wood, in order to facilitate emerge after exuviation.

Comparison of habitats (Gwangneung forest and Ussurisky nature reserve)

Gwangneung forest, South Korea, is located in the center of the Korean Peninsula (latitude 37°42'36"–37°47'41"N, longitude 127°8'20"–127°11'58"E), with a total area of 2,400 ha and an altitude of 40–620 m above sea level (Cho et al. 2007) (Figure 2A). The average annual rainfall is 1,433.8 mm and the average annual temperature

is 11.7 °C (Korea National Arboretum 2015). Gwangneung forest not only contains approximately 20% of the recorded plant species in South Korea (Korea National Arboretum 2004) but is also reported to contain 3,794 species of insect, representing 28% of all Korean insect species (Korea National Arboretum 2006).

Managed by the Korea National Arboretum, Gwangneung forest is composed of 54% natural forest and 42% artificial forest. The natural forest consists mostly of broadleaf trees centered on Soribong, including *Carpinus laxiflora*, *Quercus mongolica* and *Q. serrata*, while the artificial forest, mostly on low-lying ground, consists of a needleleaved plantation, *Abies holophylla*, *Pinus rigida*, and *Larix kaempferi*, and some planted broadleaved trees (Korea National Arboretum 2015).

In this study, adults of *C. relictus* were discovered in the natural stands in Gwangneung forest (Soribong, Mt. Jukyeop-san), while larvae and most signs of habitation were discovered from *Carpinus laxiflora* and *Quercus* spp. in north of Mt. Soribong. Host plants with signs of habitation were located on the northern slope, especially close to the valley, where the terrain was not steep. Because the northern slope receives less sunlight and has a lower rate of moisture evaporation, the temperature is cooler, the humidity is higher, and, being close to the valley, the host plants retain moisture better; this indicates that appropriate humidity in the surrounding environment is a very important factor for habitation of *C. relictus*.

Gwangneung forest is protected as a UNESCO biosphere reserve, but it is located very close to Seoul and is becoming increasingly isolated due to road construction and the development of the surrounding land as part of the expansion of the greater capital area. Habitat disruption caused by this human interference will have a significant negative effect on maintaining a stable *C. relictus* population.

The Ussurisky nature reserve in Russia, the type locality for *C. relictus*, is located at latitude 43°33'–43°47'N, longitude 132°15'–132°47'E, and has a total area of approximately 40,432 ha, with a width of 40 km and a length of 19.5 km; this is 17 times the area of Gwangneung forest (Figure 2B). The terrain is mostly flat and low-lying, with the tallest peak at an altitude of 600 m. The mean annual temperature is 2.7 °C and the mean annual rainfall is 750–800 mm (Institute of Biology and Soil Sciences 2003).

The survey area was a flat forest dominated by *Ulmus davidiana* var. *japonica*, which is a host plant for *C. relictus*. We observed large, old *U. davidiana* var. *japonica* trees that immature stages of *C. relictus* could inhabit, as well as trees producing sap, which is main food source for adults. The area contains many tributaries, and so, despite the relatively low rainfall, humidity is well maintained within the forest, which is thought to provide a suitable environment for *C. relictus* habitation (Fig 13C). Moreover, like Gwangneung forest, the nature reserve is designated as a nationally protected area, making it safe from indiscriminate felling and collection, and, because it has a broad area and is located far from urban areas, it is thought to be largely unaffected by disruption of the surrounding environment.

Host plants

There are seven known species of host plant for *Callipogon relictus* in Korea: *Carpinus cordata*, *C. laxiflora*, *Fraxinus mandschurica*, *F. rhynchophylla*, *Quercus aliena*, *Q. mongolica*, and *Ulmus davidiana* var. *japonica*. In our survey, we have found larvae and signs of habitation of *C. relictus* in Gwangneung forest in the following four species of tree: *Carpinus cordata*, *C. laxiflora*, *Quercus aliena*, and *Q. mongolica* (Figs 5A–D, 7B). These were most commonly discovered in *Carpinus laxiflora*, though we also observed a large number of feeding scars in *Quercus* spp. of dead trees that could not be accurately identified at the species level, due to the high extent of decay. If these dead trees could be identified, it is possible that new host plants could be reported.

In Russia, ten host plants of *C. relictus* have been known (including *Quercus mongolica*, *Ulmus laciniata*, *Ulmus davidiana* var. *japonica* and *Fraxinus mandschurica*), but although we identified various host plants in the survey in the Ussurisky nature reserve, *C. relictus* emergence holes and feeding scars were only found in *Ulmus davidiana* var. *japonica* (Figure 13B), suggesting that *C. relictus* prefer this species.

The host plants where individuals and signs of habitation of *C. relictus* were found were either dead trees that had low vigor or had died recently and were not in a state of advanced decay (Figure 13A, B). Meanwhile, given that fungi or mold infection were observed on host plants with signs of habitation (Figure 6A, B), we assume that habitation is closely related to fungi, and although there has been a study showing that fungus aid larval growth in indoor rearing (Lee et al. 2017), there has been no detailed research on the association with fungi in the natural environment.

Acknowledgements

We would like to thank Dr. Andrej K. Kotlyar (Russian Academy of Sciences, Ussuriysk) for cooperating in the field survey of habitation in Russian Ussurisky nature reserve. We thank Dr. Meiyang Lin (Chinese Academy of Sciences, Beijing) for providing valuable Chinese specimens of *Callipogon relictus* and verify collection information and Dr. Mikhail L. Danilevsky (Russian Academy of Sciences, Moscow) for helping us examine specimens of *Macrotoma fisheri*. We would also like to thank Mrs. Ok-Jeong Kim for providing *C. relictus* photographs and habitation information from Yangyang-gun. Finally, we would like to express out sincere gratitude to Prof. Bong-Kyu Byun, Mr. Jeong-Dal Son, Mrs. Shin-Young Park, Mr. Jong-Su Lim, and Mr. Ik-Je Choi, who have assisted with habitation surveys of *C. relictus* in Gwangneung forest for many years.

This study was conducted as a Korea National Arboretum research project (KNA1-2-28, 17-3) and a Korea Forest Service ‘Convergent Project for the Development of Technology for New Industrialization within the Forestry Industry (S111616L050100)’.

References

- An SL (2010) Notes on the status and conservation of *Callipogon relictus* Semenov in Korea. Annual Review in Cultural Heritage Studies 43(1): 260–279.
- Bezborodov VG (2016) Chorology and population structure of *Callipogon relictus* Semenov, 1899 (Coleoptera, Cerambycidae) in East Asia. Euroasian Entomological Journal 15(4): 393–398.
- Byun BK, Jo DG, Lee BW, Lee YM, Park SY, Weon GJ, Han HR (2007) Insect diversity of the Gwangneung forest. Korea National Arboretum, Pocheon, 257 pp.
- Byun BK, Kwon TS, Weon GJ, Jo DG, Lee BW, Lee YM, Choi HJ, Kim CH, Lee SH, Bae YS, An SL, Hong KJ, Park SY, Lim JO, Kwon DH (2007) Occurrence of *Callipogon relictus* Semenov (Coleoptera: Cerambycidae) in the Gwangneung forest, Korea with suggestions for the conservation. Korean Journal of Applied Entomology 46(1): 19–25. <https://doi.org/10.5656/KSAE.2007.46.1.019>
- Cho PS (1934) On the some longicorn beetles from Korea. Journal of the Chosen Natural History Society 17: 3.
- Cho PS (1955) Entomological observation of Korea. Bulletin of Liberal Arts, Korea University 1: 145–196.
- Cho PS (1961) Taxonomic study on the family Cerambycidae from Korea. Bulletin of Liberal Arts, Korea University, 174 pp.
- Cho YB, Lee SG (2013) *Callipogon relictus* Semenov-Tian-Shansky. In: Kim JI, Min WG, Park JY, Lee DH, Lee SG (Eds) Red data book of endangered insects in Korea II. Red data book 8. National Institute of Biological Resources, Incheon, 31–32.
- Cho YC, Shin HC, Kim SS, Lee CS (2007) Dynamics and Conservation of the Gwangneung National Forest in Central Korea: A National Model for Forest Restoration. Journal of Plant Biology 50(6): 615–625. <https://doi.org/10.1007/BF03030604>
- Hong SP, Kim YS (1991) Some notes and the other forms of *Callipogon relictus* Semenov in Korea. Journal of the Amateur Lepidopterists' Society of Korea 4: 44–45.
- Hua L (2002) List of Chinese Insects. Vol. 2. Zhongshan University Press, Guangzhou, 612 pp.
- Institute of biology and soil sciences, Far Eastern Branch, Russian Academy of Sciences (2003) Vertebrates of Ussurisky Zapovednik, Vladivostok, Dalnauka, 94 pp.
- Karino K, Seki N, Chiba M (2004) Larval nutritional environment determines adult size in Japanese horned beetles *Allomyrina dichotoma*. Ecological Research 19: 663–668. <https://doi.org/10.1111/j.1440-1703.2004.00681.x>
- Kim CW, Yoon IB, Nam SH (1976) On the habitats and habits of *Callipogon relictus* S. (Col. Cerambycidae). Nature Conservation 11: 5–16.
- Kim CW (1978) Distribution atlas of insects of Korea, series 2, Coleoptera. Korea University Press, Seoul, 189 pp.
- Kuprin AV, Bezborodov VG (2012) Areal of *Callipogon relictus* Semenov, 1899 (Coleoptera, Cerambycidae) in the Russian Far East. Biology Bulletin 39(4): 387–391. <https://doi.org/10.1134/S1062359012030090>
- Lameere A (1904) Révision des Prionides. Callipogonines. Annales de la Société entomologique belge 48: 7–78.

- Lee SM (1987) The longicorn beetles of Korean peninsula. National Science Museum, Seoul, 287 pp.
- Li J, Drumont A, Zhang X, Gao M, Zhou W (2012) The checklist of Northeast China's subfamily Prioninae and biological observations of *Callipogon (Eoxenus) relictus* Semenov-Tian-Shanskij, 1899 (Coleoptera, Cerambycidae, Prioninae). Les Cahiers Magellanes 9: 50–54.
- Li J, Drumont A, Zhang X, Lin L (2013) Note on the egg productivity of females of *Callipogon (Eoxenus) relictus* Semenov-Tian-Shanskij, 1899, and first record for Inner Mongolia Autonomous Region in China (Coleoptera, Cerambycidae, Prioninae). Les Cahiers Magellanes 12: 52–56.
- Li J, Drumont A, Mal N, Lin L, Zhang X, Gao M (2014) Checklist of the Prioninae of China with illustrations of genera and subgenera (Coleoptera, Cerambycidae). Les Cahiers Magellanes 16: 73–109.
- Lim J, Kim M, Kim IK, Jung S, Lim JS, Park SY, Kim KM, Kim C, Byun BK, Lee BW, Lee S (2013) Molecular identification and larval description of *Callipogon relictus* Semenov (Coleoptera: Cerambycidae), a natural monument of South Korea. Journal of Asia-Pacific Entomology 16: 223–227. <https://doi.org/10.1016/j.aspen.2013.01.006>
- Monne MA (2017) Catalogue of the Cerambycidae (Coleoptera) of the Neotropical Region. Part III. Subfamilies Lepturinae, Necydalinae, Parandrinae, Prioninae, Spondylidinae and Families Oxypeltidae, Vesperidae and Disteniidae. http://cerambyxcat.com/Parte3_Prioninae_Lepturinae_2018.pdf (accessed 22 August 2018).
- Murayama J (1936) On the larva and food plant of *Callipogon relictus* Semenov. Japanese Journal of Entomology 10: 280–290.
- Nakane T (1974) The beetles of Japan (new series), Cerambycidae. Nature and Insects 9(4): 2.
- Saito K (1932) On the longicorn beetles of Corea. Essays in celebration of the 25th Anniversary of the Agricultural and Forestry College Suigen, 439–478.
- Semenov A (1898) *Callipogon (Eoxenus) relictus* sp. n., Vertreter des neotropischen Genus der Cerambyciden in der russischen Fauna. Horae Societatis Entomologicae Ross 32: 562–580.
- Yi DA (2014) Breeding & restoration of Korean relic long-horned beetle *Callipogon relictus*. National Institute of Biological Resources, Incheon, 216 pp.
- Yi DA, Kuprin AV, Lee YH, Bae YJ (2017) Newly developed fungal diet for artificial rearing of the endangered long-horned beetle *Callipogon relictus* (Coleoptera: Cerambycidae). Entomological Research 47: 373–379. <https://doi.org/10.1111/1748-5967.12234>
- Yi DA, Kuprin A, Bae YJ (2018) Distribution of the longhorned beetle *Callipogon relictus* (Coleoptera: Cerambycidae) in Northeast Asia. Zootaxa 4369(1): 101–108. <https://doi.org/10.11646/zootaxa.4369.1.5>

A revision of *Lycinella* Gorham, 1884 with the description of six new species (Coleoptera, Lycidae, Calopterini)

Vinicius S. Ferreira¹, Michael A. Ivie¹

¹ Montana Entomology Collection, Marsh Labs, Room 50, Montana State University, Bozeman, MT 59717, USA

Corresponding author: *Vinicius S. Ferreira* (vinicius.sfb@gmail.com; mivie@montana.edu)

Academic editor: *H. Douglas* | Received 28 June 2018 | Accepted 26 September 2018 | Published 23 October 2018

<http://zoobank.org/A8CFA44B-27C4-463B-980C-4A0EE3E0108B>

Citation: Ferreira VS, Ivie MA (2018) A revision of *Lycinella* Gorham, 1884 with the description of six new species (Coleoptera, Lycidae, Calopterini). ZooKeys 792: 69–89. <https://doi.org/10.3897/zookeys.792.28034>

Abstract

The Neotropical genus *Lycinella* Gorham, 1884 is revised. *Lycinella opaca* Gorham, 1884 and *Lycinella parvula* Gorham, 1884 are redescribed and illustrated. Six new species are described for the genus: *Lycinella adamantis* sp. n., *L. bansonii* sp. n., *L. milleri* sp. n., *L. cidaoi* sp. n., *L. marshalli* sp. n. and *L. pugliesae* sp. n.. *Lycinella humeralis* Pic, 1933 is moved to *Ceratoprion humerale* (Pic, 1933), **comb. n.** A key to the species of *Lycinella*, illustrations and a distribution map is provided.

Keywords

Elateroidea, Leptolycini, Lycinae, Neotropical Region

Introduction

While searching for cantharoid beetles in Malaise traps samples generated by the Costa Rican Malaise Trap Network project, we found a remarkable number of tiny Lycidae specimens of a unique form. These Costa Rican specimens have eight pronotal stemmata (Figure 11), an apparently unpublished character discovered by Richard S. Miller

(1991) in *Leptolyctus* Leng & Mutchler, 1922 (Leptolyctini). However, they did not seem to belong to the Leptolyctini, based on current diagnoses (Ferreira and Ivie 2016, Ferreira et al. 2018).

In discussions with Miller, he pointed us to *Lycinella* Gorham, 1884, a poorly known genus of Calopterini with three named species from Central America (Bocáková 2003, 2005) that exhibit these unreported structures. Following this lead, we found the new specimens belong to *Lycinella*, and represent several new species. In this study we take the opportunity to rediagnose and redescribe the genus and the two original species described by Gorham (*Lycinella opaca* Gorham, 1884 and *Lycinella parvula* Gorham, 1884), describe six new species, and provide illustrations, distribution maps and a key to all the species. One last problem was the species *Lycinella humeralis* Pic, 1933, known in the literature only from a short description. Based on examination of the type, it is moved to *Ceratoprion* Gorham, 1884 (Leptolyctini).

Materials and methods

The specimens were examined under a Leica Wild M3C stereoscopic microscope with magnification up to 40×. Photos were taken using a JVC (DC Ky-F75U) digital camera mounted on a Leica MS5 stereoscope, a Visionary Digital Passport II imaging system, equipped with a Canon 6D DSLR (<http://www.duninc.com>), and a Canon T3i DSLR with a MP-E 65 mm lens and stacked using the software Zerene Stacker version 1.04. Enhancements to digital images were made in Adobe PhotoShop CC 2018. Drawings were prepared based on photographs using Adobe Illustrator CC 2018. The distribution map technique follows Ferreira (2016): the map was generated using the software Google Earth and Quantum GIS 2.18.9, using the maps available on the website <http://www.natureearthdata.com>, a free public database of maps.

Morphological terminology follows Crowson (1944), Bocák and Bocáková (1990), Miller (1991), Kazantsev (2003) and Lawrence et al. (2011). Of particular note is the term “stemma” (pl. stemmata) for a unique form of structure on Leptolyctini and related Calopterini, including *Lycinella*. These structures were first noted by Miller (1991), who was the first to use stemmata in this way. His usage has been subsequently followed by Ferreira and Ivie (2016) and Ferreira et al. (2018). Pronotal stemmata are tiny hemispherical white objects that occur on the pronotum, coxae and antenna of adult males (Figs 11, 12). The number and placement of these structures are diagnostic at the generic and species level. Their function and homology is unknown.

Male genitalia were dissected after the entire specimen was soaked in hot water. For disarticulation and clearing processes the specimens were left overnight in a warm solution of KOH after which they were dissected and left in cold KOH for approximately 2 hours, time enough for the musculature to detach from inner structures. Transcription of label data from specimens follows Ivie (1985): the end of each line on a label is indicated by a “;” (semicolon); the individual labels are separated by a “/” (slash).

The majority of specimens treated here were taken in the Costa Rican Malaise Trap Network project headed by Paul Hansen. Further data on this project and the localities and methods is available at Hansen (1992).

Material examined is deposited in the following collections (respective curators are indicated in parentheses):

- MAIC** Michael A Ivie collection, Bozeman, Montana, USA,
MNCR Museo Nacional de Costa Rica, San José, Costa Rica (the collection formerly known as INBio, Angel Solis),
MZPW Muzeum i Instytut Zoologii, Polskiej Akademii Nauk Warszawa, Poland (David Schimroszyk and Wioletta Tomaszewska),
NHMUK The Natural History Museum, London, United Kingdom (Maxwell VL Barclay and Michael Geiser),
USNM National Museum of Natural History, Washington D.C., USA (currently at the Montana Entomology Collection, Montana State University, Michael A Ivie).

Results

Examination of Pic's type showed that his *L. humeralis* belongs in the Leptolycini genus *Ceratoprion* Gorham, 1884. Therefore, we are moving it, in anticipation of a revision of the Leptolycini in progress by VF.

Ceratoprion humerale (Pic, 1933), comb. n.

Figure 10

Lycinella humeralis Pic, 1933: 109; Kleine 1933: 34; Blackwelder 1945: 348; Mroczkowski 1959: 35. Bocák and Bocáková 1990: 667.

Type material examined (1). Lectotype (hereby designated to preserve stability of nomenclature, in accordance with ICZN 1999, Art. 74.7): Costa Rica; F Nevermann; I.II.26/ Hamburgfarm; Reventazon; Ebene Limon/ Gebuseh [illegible]/ 33/ deje [illegible]/ *Lycinella*; sp. det. K.G. Blair/ *Lycinella*; humeralis; n.n./ Typus [in a red label]/ Inst. Zool. O.A.N. Warszawa; Cotypus; Nr. 544[in a red label]/ MIZ PAN; Warszawa; 12 1945 194/ *Lycinella humeralis* Pic, 1921; det V.S. Ferreira 2018 [MZPW].

Remarks. Pic (1933: 109) stated that *L. humeralis* is close to *L. parvula*, but clearly differing from the latter by the longer antennae, the last antennal flagellomere in part testaceous, by the humeral portion of the elytron largely testaceous and the legs partly testaceous. Pic's specimen lacks the diagnostic characters of *Lycinella* and possesses the characters of *Ceratoprion*: serrate antennae, reduced mandibles and strong reticulation in the elytra.

Genus *Lycinella* Gorham, 1884

Lycinella Gorham, 1884: 248; Bertkau 1886: 290; Bourgeois 1891: 344; Pic 1921: 21; Kleine 1933: 34; Blackwelder 1945: 348; Bocáková 2003: 212, 230; Bocáková 2005: 445; Bocák and Bocáková 2008: 713.

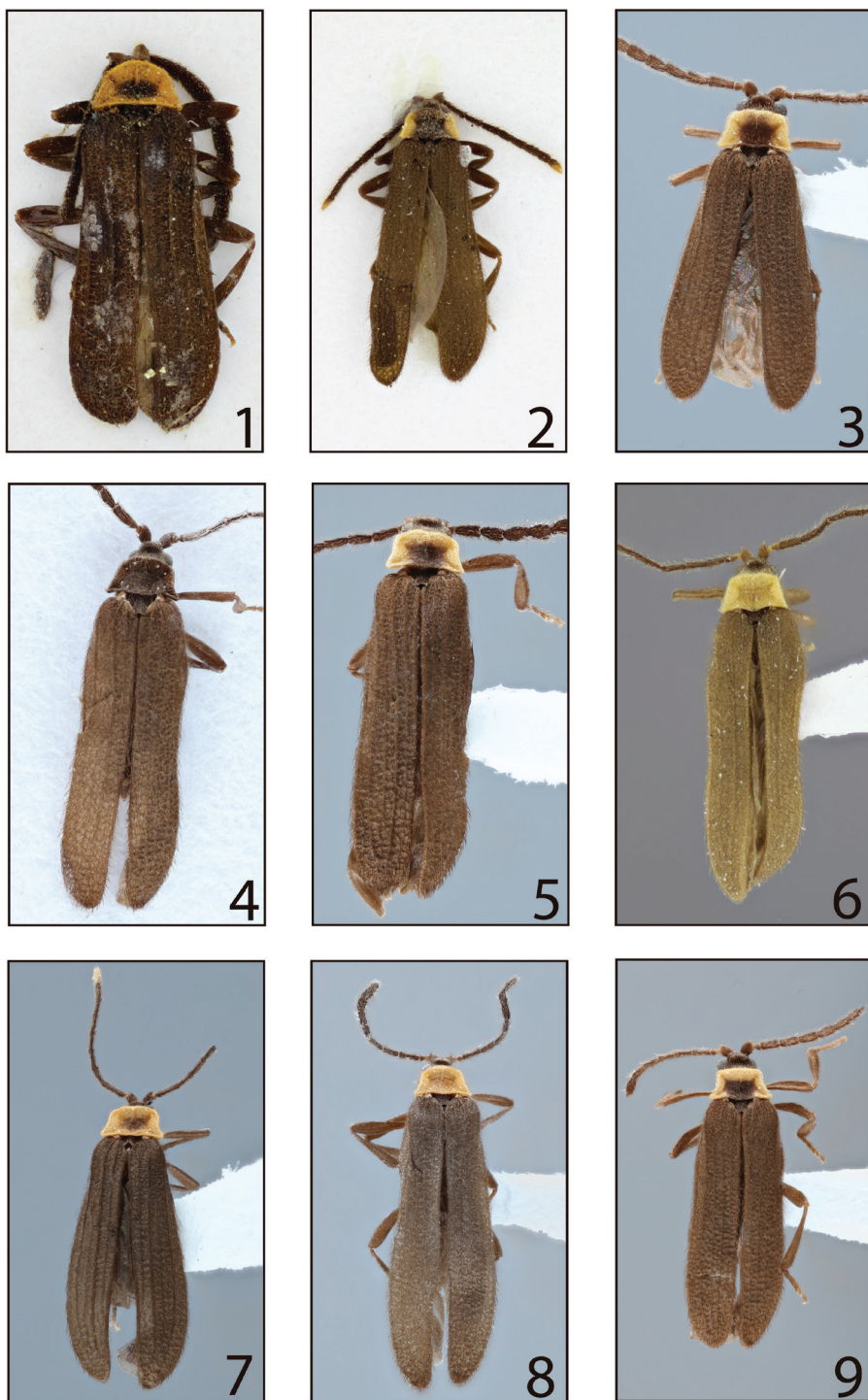
Type species. *Lycinella opaca* Gorham, 1884 (subsequent designation by Bourgeois 1891: 345)

Differential diagnosis. *Lycinella* can be easily identified among other Leptolycini and Calopterini by the subserrate antennae (Figs 13–20) with antennomere III longer than II but much shorter than IV, the relatively long and strongly hooked mandibles (Figure 22), the normal maxillary palps (Figure 23) and by the presence of eight discal stemmata on the pronotum (Figure 11) and stemmata on the pro- and mesocoxae (Figure 12).

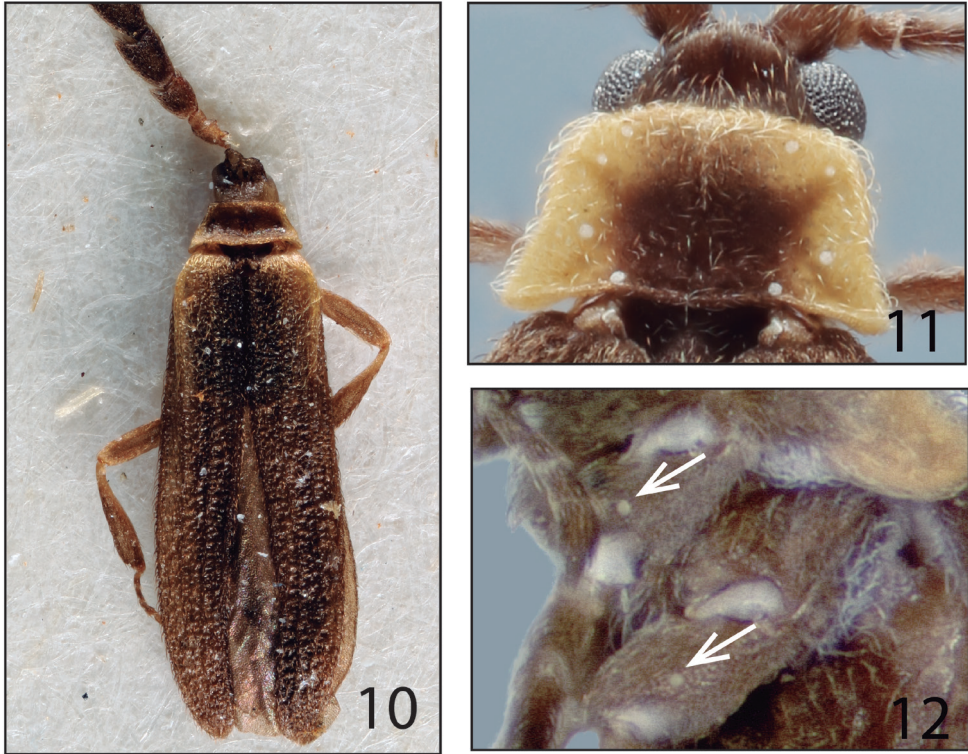
Description. General dorsal coloration dark brown to black, with pronotum black, yellow-brown or yellow in some species bearing dark macula in discal portion or with complete longitudinal medial region (Figs 1–9). Body densely setose, dorsal pubescence long and erect, remainder of body with fine yellow pubescence throughout (Figs 1–9).

Head as long as wide, widest behind eyes, posteriorly partially covered by pronotum, hypognathous. Eyes hemispherical, projecting anterolaterally when viewed dorsally; coarsely granulate. Mouthparts: Maxillary palp four-segmented, with last palpomere acuminate, densely setose (Figure 23). Labial palp 3-segmented, palpomeres I and II subequal in length, palpomere III elongate and cylindrical, acuminate, densely setose (Figure 23). Mandibles moderately enlarged to elongate, strongly hooked apically (Figure 22). Posterior margin of epistoma emarginate, labrum wider than long or longer than wide, setose (Fig. 21). Antennae inserted on gibbous prominence; subserrate to filiform; 11-segmented, with sparse short bristle-like setae on apices of antennomeres; reaching middle of elytra; scape conical to subconical, antennomere III approx. 1.5× longer than II, much shorter than IV; flagellomeres decreasing in length towards apex.

Prothorax: pronotum wider than long, trapezoidal; margins prominent; anterior angles round, posterior angles acute or moderately rounded; longitudinal carina in anterior portion of pronotum strongly to hardly visible, bifurcate posteriorly (Figs 1–9); eight pronotal stemmata located on edges of pronotum (Figs 1–9, 11). Hypomeron concave, hypomerall stemmata absent. Mesothorax: mesospiracles elongate, slightly protuberant (Figure 25). Prosternum V-shaped; posterior margin rounded to bifurcate and divergent; laterally reaching hypomeron (Figure 25). Mesoventrite trapezoidal, posteriorly reaching anterior margin of metaventrite, connected to mesanepisternum by additional segment, mesepimeron more densely pubescent than surrounding sclerites (Figure 25). Mesonotum (as represented by *L. parvula*) divided by scutellum into halves, posteriorly divergent (Figure 25); scutellum shortened, posteriorly bifurcate, of variable size (Figs 1–9; 26). Metathorax: metaventrite convex, posterolateral angles pronounced, acute; metadiscrimen complete; metanepisternum and metepimeron elongate (Figure



Figures 1–9. Dorsal habitus of *Lycinella*. 1 *L. opaca* Gorham, 1884 (lectotype) 2 *L. parvula* Gorham, 1884 (lectotype) 3 *L. parvula* 4 *L. adamantis* 5 *L. hansonii* 6 *L. milleri* 7 *L. cidaii* 8 *L. marshalli* 9 *L. pugliesae*.



Figures 10–12. 10) Dorsal habitus of *Lycinella humeralis*. 11) Pronotum and pronotal stemmata of *L. parvula* 12) Stemmata in pro- and mesocoxae of *L. pugliesae*.

25–26), metendosternite (as represented by *L. parvula*) elongate, membranous, with strongly visible ventral longitudinal flange, furcal arms divergent (Figure 26). Elytra subparallel, 6–11 × longer than pronotum; reticulate, with four elytral costae more or less developed on each elytron (Figs 1–9). Membranous wings (as represented by *L. parvula*) well developed (Figure 28). Legs: slender, elongate; protochanthin slender and exposed (Figure 27); trochanters tubular; femora and tibiae quite elongate, clavate, subequal in length (Figure 27); pro- and mesocoxae conical, moderately elongate, obliquely positioned, procoxae contiguous, some species with stemmata on each pro- and mesocoxae (Figure 12), metacoxae wider than long (Figure 25); tarsomeres 5-5-5, narrowed, tarsomere four not expanded laterally (Figure 27).

Abdomen of males with eight ventrites; male genitalia symmetrical; median lobe tapered apically to stout (Figs 29–36); parameres rounded apically (Figs 29–36); phallobase elongate to slightly shortened, with posterior margin rounded or irregular (Figs 29–36).

Females. Unknown.

Length (pronotum + elytra): 3.1–4.8 mm. Width (across humeri): 0.8–1.1 mm.

Distribution. *Lycinella* is known to occur in Panama, Guatemala, and Costa Rica (Figure 37).

Biology and immature. Females are unknown and presumably neotenic. Although information about the ecology and biology of *Lycinella* is unknown we can infer from the fact they were virtually all taken in Malaise traps that males of *Lycinella* species are flight active species.

Taxonomic placement of *Lycinella*. The initial tribal placement of *Lycinella* was difficult because it is among the genera that, like *Cephalolycus* Pic, 1926 and *Aporrhapis* Pascoe, 1887, shares features of both Calopterini and Leptolycini (see Miller 1991; Bocáková 2003, 2005; Ferreira and Ivie 2016; Ferreira et al. 2018). Bocák and Bocáková (1990) placed the genus in the Leptolycini, but based on examination of *Lycinella humeralis*, here moved to the Leptolycine genus *Ceratoprion*.

The subtribe Acroleptina (Calopterini), where *Lycinella* is currently placed, are suspected of having neotenus females (Barancikova et al. 2010), as do the known Leptolycini (Miller 1991, Kazantsev 2013, Ferreira and Ivie unpublished). Males of *Lycinella* conform to the general morphology of the groups with known or suspected neotenus females.

Ferreira and Ivie (2016) and Ferreira et al. (2018), discuss the morphological delimitation between males of Calopterini and Leptolycini, which is based on a weak tarsal character (Miller 1991, Ferreira and Ivie 2016), and placement of taxa such as *Cephalolycus*, *Aporrhapis* and Acroleptina (Ferreira and Ivie 2016, Kazantsev 2017) remains unclear. Although *Lycinella* has the narrow tarsomere IV normally present in Leptolycini, *Lycinella* lacks the reduced mouthparts found in all adult male Leptolycini. In the absence of molecular data or other evidence to the contrary, we place *Lycinella* in the Calopterini.

Key to the species of *Lycinella*

- | | | |
|---|--|-----------------------------------|
| 1 | Pronotum unicolor (Figs 4, 6, 8) | 2 |
| – | Pronotum bicolored (Figs 1–3, 5, 7, 9) | 4 |
| 2 | Pronotum black (Fig. 4) | <i>Lycinella adamantis</i> sp. n. |
| – | Pronotum orange or yellow (Figs 6, 8) | 3 |
| 3 | Pronotum orange (Fig. 8); phallobase with posterior margin evenly rounded, phallobase 2/3 the length of parameres (Fig. 33), labrum longer than wide | <i>Lycinella marshalli</i> sp. n. |
| – | Pronotum yellow (Fig. 6); phallobase with posterior margin irregular, phallobase 1/2 the length of parameres (Fig. 31), labrum wider than long | <i>Lycinella milleri</i> sp. n. |
| 4 | Elytral costae (costa I, II and III) prominent (Figs 1, 7) | 5 |
| – | Elytral costae weak at most, not prominent (Figs 2, 3, 5, 9) | 6 |

- 5 Antennomeres II and XI yellow; antenna without scaliform setae (Fig. 7); dark macula in pronotal disc region faint (Fig. 7); apex of median lobe round; apex of phallobase round (Fig. 32) *Lycinella cidaoi* sp. n.
- Antennomere II and XI black; antenna with scaliform setae (Fig. 1); dark macula on pronotal disc distinct (Fig. 1); apex of median lobe acuminate; apex of phallobase asymmetrical (Fig. 34)
..... *Lycinella opaca* Gorham, 1884
- 6 Stemmata present on pro- and mesocoxae (Fig. 12) 7
- Stemmata absent on pro- and mesocoxae *Lycinella hansonii* sp. n.
- 7 Median lobe uniformly wide, not tapered apically, phallobase 1.4× shorter than parameres (Fig. 35) *Lycinella parvula* Gorham, 1884
- Median lobe tapered apically, phallobase 1.5× shorter than parameres (Fig. 36) *Lycinella pugliesae* sp. n.

***Lycinella adamantis* Ferreira & Ivie, sp. n.**

<http://zoobank.org/717B8819-94BA-45AB-8E0A-05496762013B>

Figs 4, 13, 29, 37

Type material (1). Holotype: COSTA RICA: Cartago; 4Km NE Canon, Genesis II; 9.716°N, 83.916°W; JUNE 1995, 2350m; S & P Friedman. Malaise (USNM).

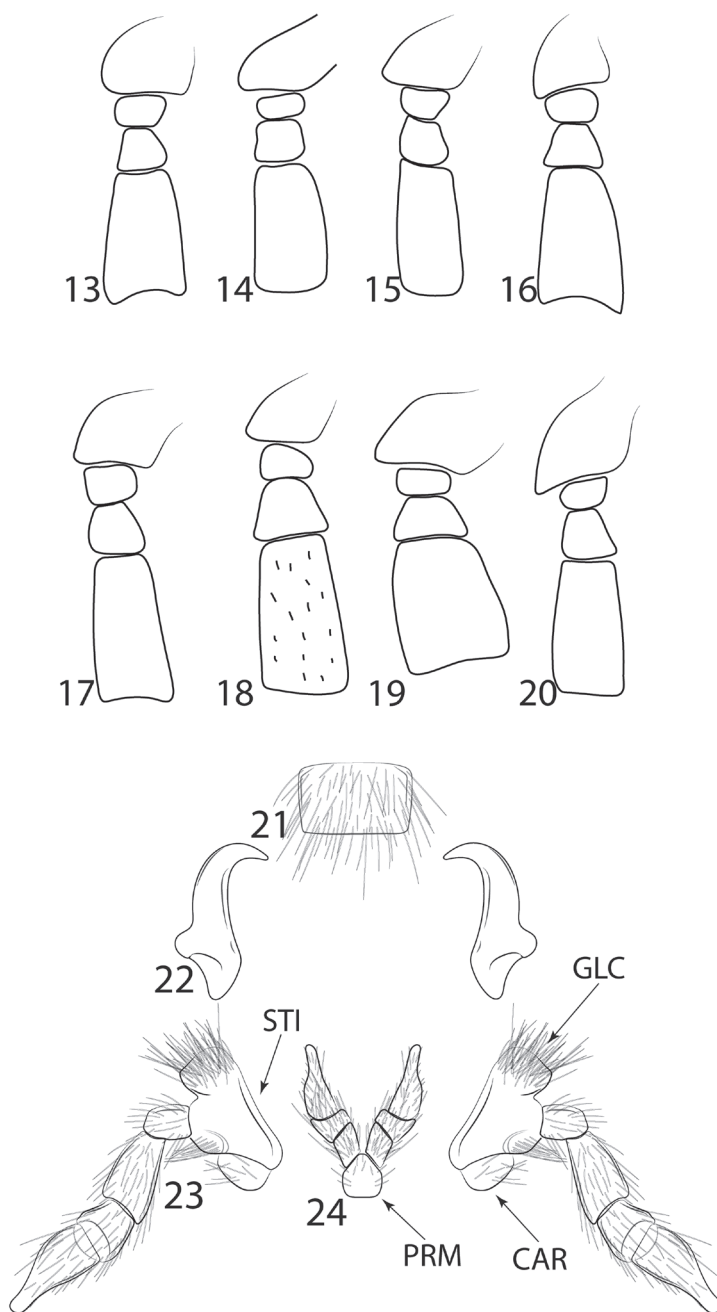
Etymology. The species name is in reference of the shiny pronotal stemmata that resemble small diamonds on the completely black pronotum.

Diagnosis. Both the completely black body (Figure 4) and the unique male genitalia with median lobe tapered apically (Figure 29) will distinguish *L. adamantis* from all other *Lycinella* species.

Description. General dorsal coloration black (Figure 4). Antennae subserrate; antennomeres IV–XI dorsoventrally flattened (Figure 13); scape subconical, antennomeres II and III short, subequal in length, approx. 1/4 length of I; antennomere IV elongate, approx. 1/3 longer than I; antennomeres V–X gradually decreasing in length; antennomere XI elongate. Mandibles elongate. Labrum wider than long. Maxillary palpomere I approx. 1/3 length of II, palpomere II cylindrical, palpomere III approx. half length of II, IV elongate, subequal in length to II, acuminate, densely setose. Labial palp 3-segmented, palpomeres I and II subequal in length, palpomere III elongate and cylindrical, acuminate, densely setose.

Pronotum trapezoidal, with posterolateral angles pronounced and acute, divergent, with weakly visible longitudinal carina in anterior portion of pronotum, bifurcate posteriorly forming an areola. Prosternum V-shaped; posterior margin rounded; laterally reaching hypomeron.

Elytra 9× longer than pronotum; costae II and IV visible, I and III weakly visible. Humeral region rounded in dorsal view. Legs slender, elongate (Figure 4). Pro- and mesocoxae with stemmata absent. Aedeagus with median lobe tapered apically,



Figures 13–24. 13–20. Antennae, antennomeres I–VI detail. 13 *L. adamantis* 14 *L. hansonii* 15 *L. milleri* 16 *L. cidaoi* 17 *L. marshalli* 18 *L. opaca* 19 *L. parvula* 20 *L. pugliesae* 21–24 *Lycinella opaca* mouthparts 21 Labrum 22 Mandibles 23 Maxillary palps 24 Labial palps. Scale bar 0.05 mm. Abbreviations: CAR: Cardo; GLC: Galea+Lacinia; PRM: Prementum; STI: Stipe.

1.4× longer than parameres; Parameres 0.6× longer than phallobase; phallobase emarginated posteriorly (Figure 29).

Length (pronotum+elytra): 4.5 mm. Width (across humeri): 1.0 mm.

Distribution. Costa Rica: Cartago (Figure 37).

***Lycinella cidaoi* Ferreira & Ivie, sp. n.**

<http://zoobank.org/74CEF391-7290-4D89-B7BD-AFEAB54182BC>

Figs 7, 16, 32, 37

Type material (1). Holotype: COSTA RICA: Alajuela; Est. Biol. Alberto Brenes; nr. San Ramon; 29 JUN 1999, 900m; MA Ivie. Malaise (USNM).

Etymology. The species was named after VSF's friend, Felipe Francisco Barbosa, a.k.a. Cidão, for his priceless advice and discussions on beetle taxonomy and systematics.

Diagnosis. The weak black discal macula that does not reach any margin is unique in this species, as most other species with bicolored pronota have the strong discal macula reaching the hind margin. The exception is *L. opaca*, which has a strongly demarcated discal macula. They are further distinguished by a black antennomere XI (white in *L. cidaoi*). The unique male genitalia have a stout median lobe which is 1.3× longer than parameres and a rounded apex (Figure 32).

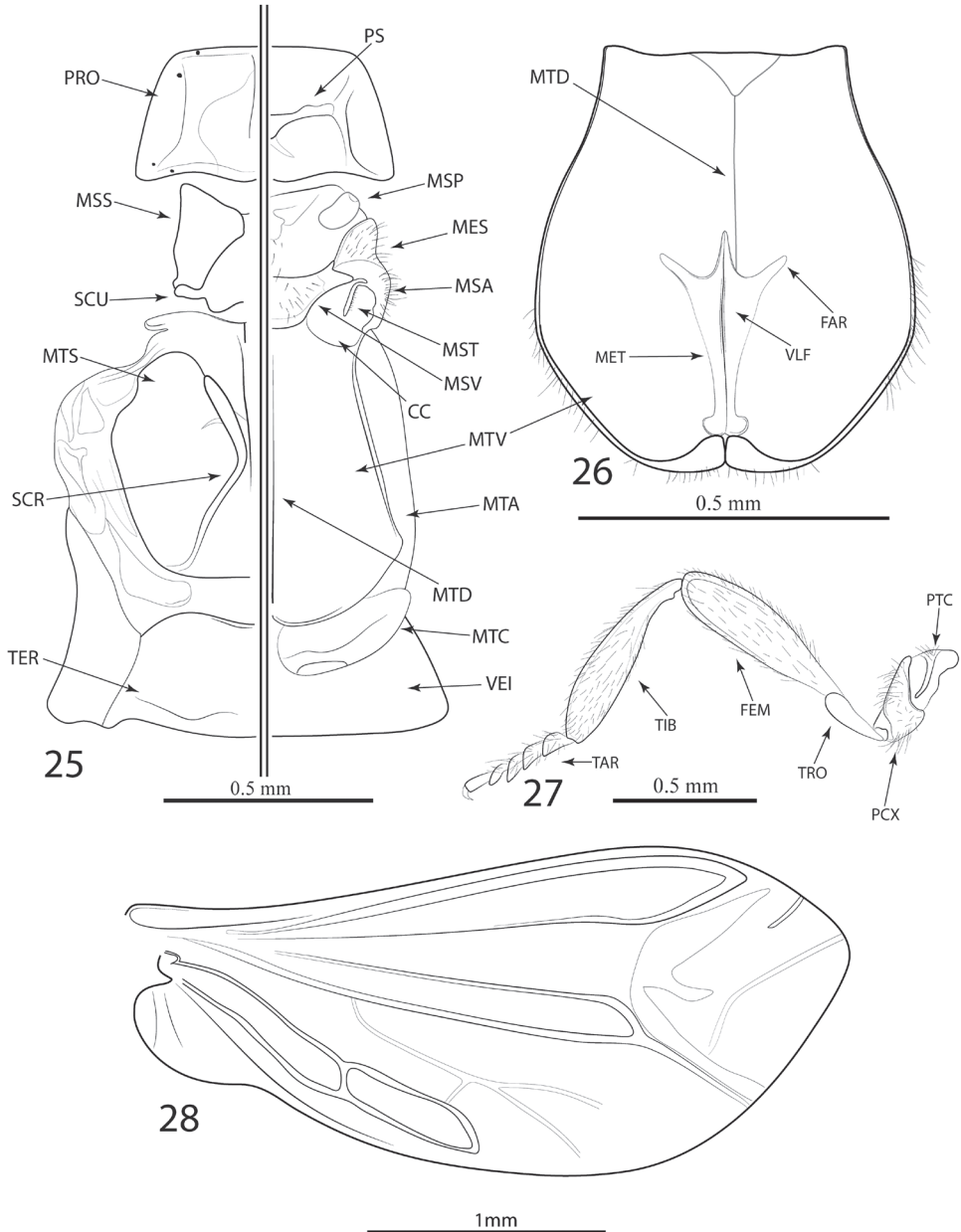
Description. General dorsal coloration dark brown, pronotum and antennomere XI yellow, pronotum bearing weak discal black macula (Figure 7). Antennae subserrate; antennomeres IV–IX dorsoventrally flattened (Figure 16); scape subconical, antennomeres II and III short, subequal in length, approx. 1/4 length of I; antennomere IV elongate, approx. 1/3 longer than I; antennomeres V–IX gradually decreasing in length. Mandibles elongate. Labrum wider than long. Maxillary palpomere I short, approx. 1/3 length of II, which is cylindrical, palpomere III approx. half length of II, IV elongate, subequal in length of II, acuminate, densely setose. Labial palp 3-segmented, palpomere I and II subequal in length, palpomere III elongate and cylindrical, acuminate, densely setose.

Pronotum trapezoidal, not constricted medially, with posterior margin straight, anterolateral angles rounded, with posterolateral angles and pronounced and acute, divergent, with weakly visible longitudinal carina in anterior portion of pronotum, bifurcate posteriorly forming an areola, hardly visible. Prosternum V-shaped; posterior margin rounded; laterally reaching hypomeron.

Elytra approx. 11× longer than pronotum, slightly expanded in 2/3 portion; costae I, II and IV strongly visible. Humeral region rounded, non-pronounced (Figure 7). Legs slender, elongate. Pro- and mesocoxae bearing stemmata. Aedeagus with median lobe stout, apex rounded, 1.3× longer than parameres; parameres 1.3× length of phallobase; phallobase elongate with posterior margin rounded (Figure 32).

Length (pronotum+elytra): 4.5 mm. Width (across humeri): 1.1 mm.

Distribution. Costa Rica: Alajuela, Biological Station Alberto Brenes (Figure 37).



Figures 25–28. *Lycinella parvula* morphology. **25** Thorax in ventral and dorsal view **26** Dorsal view of metaventrite and metendosternite **27** Proleg **28** Metathoracic wing. Abbreviations: CC: Coxal cavity; FAR: Furcal Arms; FEM: Femur; MES: Mesepimeron; MET: Metendosternite; MSA: Mesanepisternum; MSP: Mesoespiracle; MSS: Mesoscutum; MST: Mesotrochantin; MSV: Mesoventrite; MTA: Metanepisternum; MTD: Metadiscrimen; MTN: Metanotum; MTS: Metascutum; MTV: Metaventrite; PCX: Procoxae; PRO: Pronotum; PS: Prosternum; PTC: Protrochantin; SCR: Scutoprescutal ridge; SCU: Scutellum; TAR: Tarsi; TER: Tergite I; TIB: Tibia; TRO: Trochanter; VEI: Ventrite I; VLF: Ventral longitudinal flange.

***Lycinella hansonii* Ferreira & Ivie, sp. n.**

<http://zoobank.org/60C4DACA-8EC5-4FB9-878A-DA942192FFCE>

Figs 5, 14, 30, 37

Type material (1). Holotype: COSTA RICA: Cartago; La Cangreja 1950 m; 9.8°N, 83.58°W.; SEP–OCT 1992, Malaise; RA Calderon G. (USNM).

Etymology. The species was described after Paul Hanson, collector of most specimens of *Lycinella* used in this study.

Diagnosis. The unique genitalia of this species, characterized by the subquadrate apex of the short median lobe, which is 0.6× the length of the parameres, will distinguish this otherwise rather generalized species from all other *Lycinella* species. Among the species with a bicolored pronotum, only *L. opaca* also lacks stemmata on the pro- and mesocoxae. These two species are easily distinguished by the anteriorly rounded pronotum and strong elytral costae of *L. opaca* (Figure 1), in contrast to the angulate anterior angles and weakly costate elytra of *L. hansonii* (Figure 5).

Description. General dorsal coloration dark brown, pronotum yellow, bearing longitudinal black stripe not reaching anterior margin (Figure 5). Antennae subserrate; antennomeres IV–IX dorsoventrally flattened (Figure 14); scape subconical, antennomeres II and III short, subequal in length, approx. 1/4 length of I; antennomere IV elongate, approx. 1/3 longer than I; antennomeres V–IX gradually decreasing in length. Mandibles elongate. Labrum wider than long. Maxillary palpomere I short, approx. 1/3 length of II, which is cylindrical, palpomere III approx. half length of II, IV elongate, subequal in length of II, acuminate, densely setose. Labial palp 3-segmented, palpomere I and II subequal in length, palpomere III elongate and cylindrical, acuminate, densely setose.

Pronotum trapezoidal, slightly constricted medially, with posterior margin slightly curved, anterolateral angles rounded, with posterolateral angles pronounced and acute, divergent, with weakly visible longitudinal carina in anterior portion of pronotum, bifurcate posteriorly forming an areola. Prosternum V-shaped; posterior margin rounded; laterally reaching hypomeron.

Elytra approx. 11× longer than pronotum; costae I, II and IV moderately visible (Figure 5). Humeral region rounded, non-pronounced. Legs slender, elongate. Pro- and mesocoxae not bearing stemmata. Aedeagus with median lobe uniform, apex subquadrate, 1.7× longer than parameres; parameres subequal in length of phallobase; phallobase elongate, postero-lateral angles rounded, posterior margin straight (Figure 30).

Length (pronotum+elytra): 4.2 mm. Width (across humeri): 1.0 mm.

Distribution. Costa Rica: Cartago (Figure 37).

***Lycinella marshalli* Ferreira & Ivie, sp. n.**

<http://zoobank.org/81D0F2BC-0F2B-4A38-B53E-5B6111FCE58D>

Figs 8, 17, 33, 37

Type material (1). Holotype: CR: Puntarenas, San; Gerardo de Dota, Savegre; Lodge, Canto de las Aves; trail; 19–21 FEB 2008, SA Marshall; debut00319381 (MNCR).

Etymology. The species was named after Steve Marshall, who collected the specimen of this species for this study.

Diagnosis. The elongate labrum, which is longer than wide, is unique among all *Lycinella* species. The pronotum solid yellow-brown is shared only with *L. milleri*, which has a short labrum. The only known male genitalia are broken (Figure 33) and so cannot be fully diagnosed.

Description. General dorsal coloration dark brown, pronotum orange (Figure 8). Antennae subserrate; antennomeres IV–XI dorsoventrally flattened (Figure 17); scape subconical, antennomeres II and III short, subequal in length, approx. 1/4 length of I; antennomere IV elongate, approx. 1/3 longer than I; antennomeres V–X gradually decreasing in length; antennomere XI elongate. Mandibles elongate. Labrum wider than long. Maxillary palpomere I short, approx. 1/3 length of II, which is cylindrical, palpomere III approx. half length of II, IV elongate, subequal in length of II, acuminate, densely setose. Labial palp 3-segmented, palpomere I and II subequal in length, palpomere III elongate and cylindrical, acuminate, densely setose.

Pronotum trapezoidal, posterior margin straight, anterolateral angles rounded, with posterolateral angles pronounced and acute, divergent, with weakly visible longitudinal carina in anterior portion of pronotum, bifurcate posteriorly forming weakly visible areola. Prosternum V-shaped; posterior margin rounded; laterally reaching hypomeron.

Elytra approx. 10× longer than pronotum; costae weakly visible. Humeral region rounded (Figure 8). Legs slender, elongate. Pro- and mesocoxae without stemmata. Aedeagus with parameres 2× longer than phallobase; phallobase rounded posteriorly (Figure 33).

Length (pronotum+elytra): 4.8 mm. Width (across humeri): 1.0 mm.

Distribution. Costa Rica: San Gerardo de Dota (Figure 37).

***Lycinella milleri* Ferreira & Ivie, sp. n.**

<http://zoobank.org/42FA890B-A37A-4392-800C-63B5D56EB8EB>

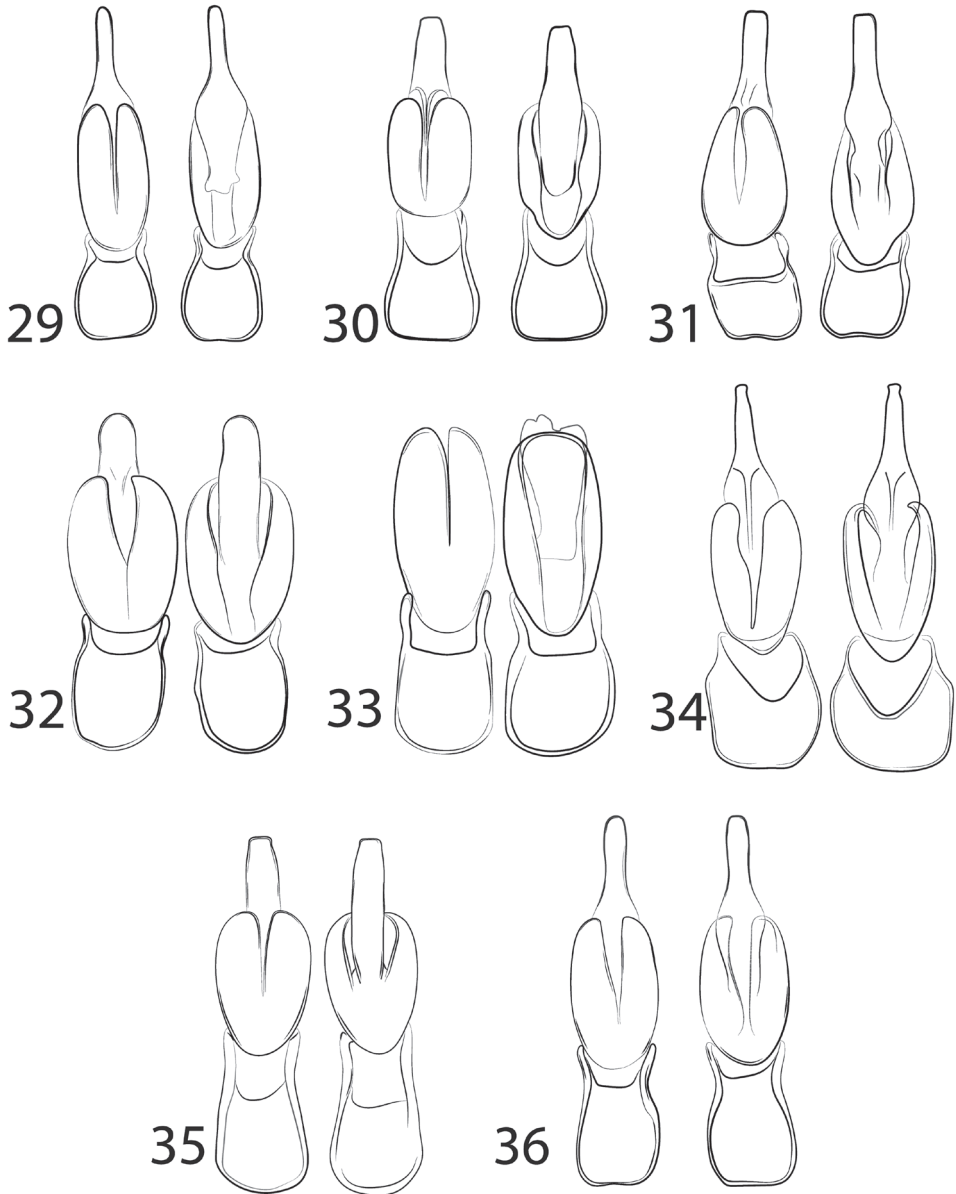
Figs 6, 15, 31, 37

Type material (1). Holotype: COSTA RICA: San Jose; 19 km S., 3 Km W. Empalme; 9.650°N, 83.866°W; DEC1992, 2600m; P Hanson Malaise (USNM).

Etymology. Noun, neuter. This species is named in honor of the great North American Lycidae systematist, Richard Stuart Miller.

Diagnosis. The unicolorous yellow-brown pronotum is shared with only *L. marshalli*, but the stronger elytral costae of *L. milleri* (Figure 6) and its wider-than-long labrum will distinguish it easily from *L. marshalli* (Figure 8). The male genitalia is also unique, with the emarginate posterior margin of the phallobase (Figure 31) shared only with *L. publiesae* (Figure 36), which has a bicolored pronotum and rounded apex of the median lobe.

Description. General dorsal coloration dark brown, pronotum orange (Figure 6). Antennae subserrate; antennomeres IV–XI dorsoventrally flattened (Figure 15); scape subconical, antennomeres II and III short, subequal in length, approx. 1/4 length of I; antennomere IV elongate, approx. 1/3 longer than I; antennomeres V–X gradually



Figures 29–36. Male genitalia of *Lycinella* spp. in dorsal and ventral view. **29** *L. adamantis* **30** *L. hansonii* **31** *L. milleri* **32** *L. cidaii* **33** *L. marshalli* **34** *L. opaca* **35** *L. parvula* **36** *L. pugliesae*.

decreasing in length; antennomere XI elongate. Mandibles elongate. Labrum elongate. Maxillary palpomere I short, approx. 1/3 length of II, which is cylindrical, palpomere III approx. half length of II, IV elongate, subequal in length of II, acuminate, densely setose. Labial palp 3-segmented, palpomere I and II subequal in length, palpomere III elongate and cylindrical, acuminate, densely setose.

Pronotum trapezoidal, anterolateral angles rounded, with posterolateral angles and pronounced and acute, divergent, with weakly visible longitudinal carina in anterior portion of pronotum, bifurcate posteriorly forming weakly visible areola. Prosternum V-shaped; posterior margin rounded; laterally reaching hypomeron.

Elytra approx. 10× longer than pronotum; costae strongly visible. Humeral region rounded (Figure 6). Legs slender, elongate. Pro- and mesocoxae without stemmata. Aedeagus with median lobe tapered apically, 1.5× longer than parameres; parameres 2.5× longer than phallobase; phallobase emarginated posteriorly (Figure 31).

Length (pronotum+elytra): 3.4 mm. Width (across humeri): 0.8 mm.

Distribution. Costa Rica: San José (Figure 37).

Lycinella opaca Gorham, 1884

Figs 1, 18, 34, 37

Lycinella opaca Gorham, 1884: 249 table XI, fig. 15; Bertkau 1886: 290; Bourgeois 1891: 345; Kleine 1933: 34 [in part, Panama record to *L. parvula*]; Blackwelder 1945: 348; Bocák and Bocáková 1990: 639; Bocáková 2003: 230 figs 19, 38, 49, 70, 71, 123–125.

Type material examined (2). Lectotype and paralectotype (hereby designated to preserve stability of nomenclature, in accordance with ICZN (1999) Art. 74.7). 1♂ Lectotype: *Lycinella; opaca*; Gorham/ B.C.A. Col. III. (2).; *Lycinella; opaca*, Gorham/ Type/ Syntype/ Type; sp. figured/ San Juan; Vera Paz.; Champion/ LECTOTYPE; *Lycinella opaca* Gorham, 1884; det V.S. Ferreira 2018 (NHMUK). 1♂ Paralectotype: San Juan; Vera Paz.; Champion/ Syntype/ B.C.A. Col. III. (2).; *Lycinella; opaca*, Gorham/ Compared with type/ PARALECTOTYPE; *Lycinella opaca* Gorham, 1884; det V.S. Ferreira 2018 (NHMUK).

Diagnosis. The stout antennae and rounded anterior margin of the pronotum are unique to this species (Figure 1). The strong pronotal macula that does not reach the base of the pronotum is also diagnostic. The scaliform setae on antennomeres IV–XI are likewise unique in the genus (Figure 18). The male genitalia (Figure 34) can be used to confirm the identification.

Redescription. General dorsal coloration dark brown, pronotum and antennomere XI yellow, pronotum bearing weak strong black macula (Figure 1). Antennae subserrate, bearing sparse scaliform setae on antennomeres IV–XI; antennomeres IV–IX dorsoventrally flattened (Figure 19); scape subconical, antennomeres II and III short, subequal in length, approx. 1/4 length of I; antennomere IV elongate, approx. 1/3 longer than I; antennomeres V–IX gradually decreasing in length. Mandibles elongate.

Pronotum trapezoidal, not constricted medially, with posterior margin slightly arcuate, anterolateral angles rounded, with posterolateral angles and pronounced and round, divergent, with weakly visible longitudinal carina in anterior portion of pronotum, bifurcate posteriorly forming an areola, hardly visible.

Elytra approx. 10× longer than pronotum, slightly expanded in 2/3 portion; costae I, II, and III strongly visible. Humeral region rounded, non-pronounced (Figure 1). Aedeagus with median lobe elongate, apex acuminate, twice longer than parameres; parameres half length of phallobase; phallobase elongate with posterior margin rounded (Figure 34).

Length (pronotum+elytra): 3.6 mm. Width (across humeri): 0.9 mm.

Distribution. Guatemala (Figure 37).

Lycinella parvula Gorham, 1884

Figs 2, 3, 11, 19, 25–28, 35, 37

Lycinella parvula Gorham, 1884: 249 table XI, fig. 16; Bertkau 1886: 290; Blackwelder 1945: 348; Bocáková 2003: 230.

Lycinella opaca not Gorham; Kleine 1933: 34 [Panama record], see Remarks below.

Type material examined (3). Lectotype and paralectotypes (designated to preserve stability of nomenclature, in accordance with ICZN (1999) Art. 74.7, hereby designated). 1♂ (Lectotype): B.C.A. Col. III. (2).; *Lycinella*; *parvula*, Gorham/*Lycinella*; *parvula*; Gorham/ Type/ Syntype/ Type; sp. figured/ Bugaba. 800–1500 ft.; Champion/ LECTOTYPE; *Lycinella*; *parvula* Gorham, 1884; det V.S. Ferreira 2018 (NHMUK). 2♂ (Paralectotypes): V. de Chiriqui; 25–4000 ft; Champion/ Syntype/ B.C.A. Col. III. (2).; *Lycinella*; *parvula*, Gorham /PARALECTOTYPE; *Lycinella marginata* Gorham, 1884; det V.S. Ferreira 2018(NHMUK). **Material examined in addition to type specimens (133):** 24: COSTA RICA: Puntarenas; 24Km W. Piedras Blancas; 8°46'N, 83°24'W, 200m; DEC1991, M. Salablanca N; Malaise trap, 1°forest (MAIC). 3: COSTA RICA: Puntarenas; 24Km W. Piedras Blancas; 8.766°N, 83.400°W; NOV1991, 200m, G. Dullce; P. Hanson. Malaise (MAIC). 2: COSTA RICA: Puntarenas; 24Km W. Piedras Blancas; 8.766°N, 83.400°W; 21 NOV1991, 200m, G. Dullce; P. Hanson. Malaise (MAIC). 6: COSTA RICA: Puntarenas; 24Km W. Piedras Blancas; 8.766°N, 83.400°W; MAR-APR 1993, 200m, G. Dullce; P. Hanson. Malaise (MAIC). 1: COSTA RICA: Puntarenas; 24Km W. Piedras Blancas; 8.766°N, 83.400°W; AUG-SEP 1993, 200m, G. Dullce; P. Hanson. Malaise (MAIC). 15: COSTA RICA: Puntarenas; 24Km W. Piedras Blancas; 8°46'N, 83°24'W, 200m; JUN1991, M. Salablanca N; Malaise trap, 1°forest (MAIC). 1: COSTA RICA: Puntarenas; 5Km W. Piedras Blancas; 8°46'N, 83°17'W, 100m; JUL1991.; Malaise trap (MAIC). 19: COSTA RICA: Puntarenas; 27Km S. Puerto Jimenez; Rio Piro; Nov 1990, 75m; P. Hanson. Malaise (MAIC). 3: COSTA RICA: Puntarenas 24Km S. Puerto Jimenez; Finca La Jilba; SEP1990, 75m [1 specimen 100m]); P. Hanson. Malaise (MAIC). 1: COSTA RICA: Puntarenas; 27Km S. Puerto Jimenez; Rio Piro; Nov 1993, 75m; P. Hanson. Malaise (MAIC). 1: COSTA RICA: Puntarenas; 27Km S. Puerto Jimenez; Finca La Jilba; JUL-SEP 1993, 100m; P. Hanson. Malaise (MAIC). 7: COSTA RICA: Pr. Pedernales; Penn. de Osa; Rancho Quemedo; 2Km N. on Camino

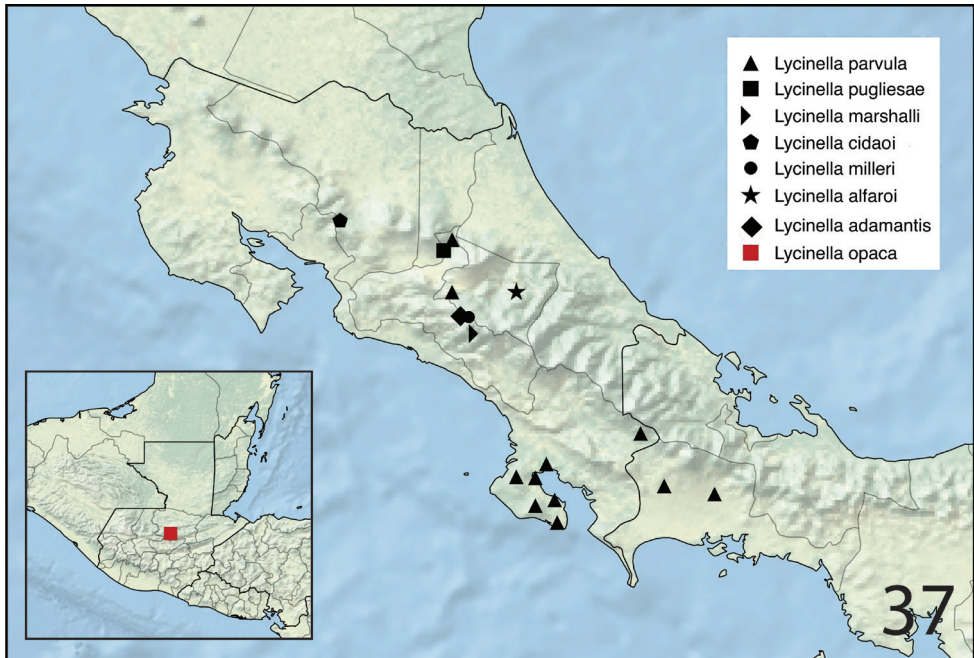


Figure 37. Distribution map of *Lycinella* species in Panama, Costa Rica, and Guatemala (inset map).

Drake; 275m, Nov 1990; Riyito colr. (MAIC). 3: COSTA RICA: Puntarenas; 24Km S. Puerto Jimenez; Finca La Jilba; JUL-SEP 1993 100m; P. Hanson. Malaise (MAIC). 3: COSTA RICA: Puntarenas; 3Km SW Rincon; 8.683°N, 83.438°W; June 1991, 10m; P. Hanson. Malaise (MAIC). 8: COSTA RICA: Puntarenas; 3Km SW. Rincon, Golfo Dulce; 8.683°N, 83.438°W; OCT-DEC1990, 10m; P.Hanson, Malaise (MAIC). 2: COSTA RICA: Puntarenas; Cerro Rincon, 200m, S. Hito; 8.516°N, 83.466°W; OCT1990, 745m, P.Hanson; & Godoy, Malaise (MAIC). 5: COSTA RICA: Puntarenas; 8KM S.Rio Rincon punte; 8.633°N, 83.466°W, 10m; APRIL 1992, Malaise trap; P. Hanson. (MAIC). 2: COSTA RICA: Pr. Puntarenas; 5Km NW Puerto Jimenez; 8°33'N, 82°21'W, 10m; APRIL 1992, Malaise trap.; P.E. Hanson colr. (MAIC). 3: COSTA RICA: Pr. Puntarenas; 3Km SW Rincon, 10m; 8°41'N, 83°29'W; AUG 1991. Malaise trap.; P.E. Hanson colr. (MAIC). 1: COSTA RICA: Puntarenas; Cerro Rincon, 745; 8.516°N 83.466°W; SEP 1990, P.Hanson; Malaise, virgin forest (MAIC). 1: COSTA RICA: Puntarenas; 5Km NW Puerto Jimenez; 8°683'N, 83.483°W; SEP 1991, 10m; P. Hanson, Malaise (MAIC). 2: COSTA RICA: Puntarenas; 23Km N. Puerto Jimenez; La Palma; JULY 1993, 10m; P.Hanson. Malaise (MAIC). 7: COSTA RICA: Puntarenas: Rancho Quemado; Rio Riyito; NOV 1990, 200m; P.Hanson, Malaise (MAIC). 1: COSTA RICA: San Jose; Zurqui de Moravia; 10°03'03"N, 84°00'22"W; MAY 1996 1600m; C. Flores. Malaise (MAIC). 1: COSTA RICA: Pr. Puntarenas; San Vito, Est. Biologica; Las Alturas, 1500m; 8°57'N, 82°50'W; JUNE 1992, Malaise trap; P.E. Hanson colr. (MAIC). 1: COSTA RICA: Puntarenas; San Vito, Est. Bio. Las; Alturas, 1500m; 8.950°N, 82.833°W; OCT1991;

P.Hanson, Malaise (MAIC). 1: COSTA RICA: Alajuela; Est. Biol. San Ramon; OCT-DEC 1995, 900m; P. Hansen. Malaise (MNCR). 1: COSTA RICA: Alajuela; Est. Biol. San Ramon; OCT-DEC 1995, 900m; P. Hansen. Malaise (MNCR). 1: COSTA RICA: Alajuela; Est. Biol. Alberto Brenes; nr. San Ramon; 29 JUN 1999, 900m; M. A. Ivie, Malaise (MNCR). 2: COSTA RICA: Alajuela; Est. Biol. Alberto Brenes; nr. San Ramon; JULY-AUGUST 1995, 900m; P. Hansen, Malaise (MAIC). 2: COSTA RICA: Alajuela; Est. Biol. Alberto Brenes; nr. San Ramon; AUGUST-SEPT 1995, 900m; P. Hansen, Malaise (MAIC). 1: COSTA RICA: Prov. Cartago; La Cangreja, 1950m; 9°48'N, 83°58'W; NOV 1991, Malaise trap; R.A. Calderón G. colr (MNCR). 1: COSTA RICA: Puntarenas; 24Km W. Piedras Blancas; 8°46'N, 84°24'W 200m; DEC1991, M. Salablanca N; Malaise trap, 1° Forest (MAIC). 1: Costa Rica: San Jose; P. N. Braulio Carrillo; 9.5Km E. tunnel, 1000m; 10.116°N, 83.966°W; JAN-FEB1990, P.Hanson; Malaise, Virgin Forest (MAIC).

Diagnosis. The bicolored pronotum with the discal macula reaching the posterior margin places this species with *L. hansonii* and *L. pugliesae*. It can be distinguished from *L. hansonii* by the presence of stemmata on the pro- and mesocoxae (also present in *L. pugliesae* and *L. cidaoi*). It is very similar to *L. pugliesae* but is more widespread and common than that high elevation species. The male genitalia must be consulted to be sure of the identification. In *L. parvula*, the median lobe is subparallel with a truncate apex and the parameres are broadly rounded (Figure 35). In *L. pugliesae* the median lobe is constricted just past the apex of the parameres and rounded at the apex (Figure 36) and the parameres are narrowly rounded.

Redescription. General dorsal coloration dark brown, pronotum and antennomeres XI yellow, pronotum bearing longitudinal black stripe (Figure 9). Antennae subserrate; antennomeres IV–XI dorsoventrally flattened (Figure 19); scape subconical, antennomeres II and III short, subequal in length, approx. 1/4 length of I; antennomere IV elongate, approx. 1/3 longer than I; antennomeres V–X gradually decreasing in length; antennomere XI elongate. Mandibles elongate. Labrum wider than long. Maxillary palpomere I short, approx. 1/3 length of II, which is cylindrical, palpomere III approx. half length of II, IV elongate, subequal in length of II, acuminate, densely setose. Labial palp 3-segmented, palpomere I and II subequal in length, palpomere III elongate and cylindrical, acuminate, densely setose. Pronotum trapezoidal, anterolateral angles rounded, with posterolateral angles and pronounced and acute, divergent, with weakly visible longitudinal carina in anterior portion of pronotum, bifurcate posteriorly forming weakly visible areola (Figure 11). Prosternum V-shaped; posterior margin rounded; laterally reaching hypomeron (Figure 25).

Elytra 7.5–10× longer than pronotum (Figs 2, 3); costae I, II, and III more visible. Humeral region rounded (Figs 2, 3). Legs slender, elongate (Fig. 27). Pro- and mesocoxae bearing stemmata. Aedeagus with median lobe uniform, slender, 1.4× longer than parameres; parameres 1.5× longer than phallobase; phallobase rounded posteriorly (Figure 36).

Length (pronotum + elytra): 3.2–3.5 mm. Width (across humeri): 0.8–1.0 mm.

Distribution. Costa Rica and Panama (Figure 37).

Type locality. Panama, Bugaba, Volcan de Chiriqui.

Remarks. *Lycinella parvula* was put in synonymy with *L. opaca* by Kleine (1933). *L. parvula* was reinstated as a valid species by Bocáková 2003.

***Lycinella pugliesae* Ferreira & Ivie, sp. n.**

<http://zoobank.org/A29ECA07-1D42-4BF4-AEA9-C5A4C7B4F492>

Figs 9, 12, 20, 36, 37

Type material (2). Holotype: COSTA RICA: Prov. San José; Zurquí de Moravia, 1600 m; 10°03'N, 84°01'W; APRIL 1996. cloud forest; JA Lizano, Malaise trap (USNM). Paratype: COSTA RICA: San José; Zurquí de Moravia; 10°03'03"N, 84°00'22"W; MAY 1996, 1600 m; C Flores, Malaise (MAIC).

Etymology. The species was described after VSF's former Zoology professor, Dr Adriana Pugliese Netto Lamas, which greatly influenced, inspired, and helped him in his early career as zoologist.

Diagnosis. *Lycinella pugliesae* is very similar to *L. parvula*, see the diagnosis for that species for further information.

Description. General dorsal coloration dark brown, pronotum yellow, bearing longitudinal black stripe not reaching anterior margin (Figure 9). Antennae subserrate; antennomeres IV–IX dorsoventrally flattened (Figure 20); scape subconical, antennomeres II and III short, subequal in length, approx. 1/4 length of I; antennomere IV elongate, approx. 1/3 longer than I; antennomeres V–IX gradually decreasing in length. Mandibles elongate. Labrum wider than long. Maxillary palpomere I short, approx. 1/3 length of II, which is cylindrical, palpomere III approx. half length of II, IV elongate, subequal in length of II, acuminate, densely setose. Labial palp 3-segmented, palpomere I and II subequal in length, palpomere III elongate and cylindrical, acuminate, densely setose.

Pronotum trapezoidal, slightly constricted medially, with posterior margin slightly curved, anterolateral angles rounded, with posterolateral angles and pronounced and acute, divergent, with weakly visible longitudinal carina in anterior portion of pronotum, bifurcate posteriorly forming an areola. Prosternum V-shaped; posterior margin rounded; laterally reaching hypomeron.

Elytra 10× longer than pronotum; costae on each elytron, costae I, II, and IV moderately visible. Humeral region rounded, non-pronounced (Figure 9). Legs slender, elongate. Pro- and mesocoxae bearing stemmata (Figure 14). Aedeagus with median lobe tapered apically, slender, apex rounded, 1.6× longer than parameres; parameres 1.5× longer than phallobase; phallobase elongate, posterior angles rounded (Figure 36).

Length (pronotum+elytra): 3.1 mm. Width (across humeri): 0.8 mm.

Distribution. Costa Rica: Prov. San José, Zurquí de Moravia (Figure 37).

Acknowledgments

Richard S. Miller's generous donation of his collection to the MTEC was critical to this project as well as Paul Hanson's donation of residues from his Malaise network run as part of the Hymenoptera of Costa Rica project. Miller also provided critical advice that allowed the proper identification of this material as *Lycinella*. Michael Geiser and Maxwell Barclay (NHMUK), David Schimroszyk and Wioletta Tomaszewska (MZPW) provided types that allowed this work to go forward. We thank Nathan P. Lord (Louisiana State University) by allowing the use of his photographic equipment. Oliver Keller and an anonymous reviewer made helpful suggestions that improved the paper. VSF is very grateful to *Conselho Nacional de Desenvolvimento Científico e Tecnológico* (CNPq) of Brazil for the scholarship (process 202559/2015-7) that allowed him to continue his study of the Lycidae. This is a contribution of the Montana Agricultural Experiment Station.

References

- Barancikova B, Nascimento EA, Bocáková M (2010) Review of the genus *Ceratopriomorphus* Pic, 1922 (Coleoptera: Lycidae). *Zootaxa* 2683: 61–65.
- Bertkau P (1886) Bericht über die wissenschaftlichen Leistungen im Gebiete der Entomologie während des Jahres 1885. *Archiv für Naturgeschichte* 52(2.2): 1–328.
- Blackwelder RE (1945) Checklist of the coleopterous insects of Mexico, Central America, the West Indies and South America. *Bulletin of the United States National Museum* 185(1–6): 1–925. <https://doi.org/10.5479/si.03629236.185.3>
- Bocák L, Bocáková M (1990) Revision of the suprageneric classification of the family Lycidae (Coleoptera). *Polskie Pismo Entomologiczne* 59: 623–676.
- Bocák L, Bocáková M (2008) Phylogeny and classification of the family Lycidae (Insecta: Coleoptera). *Annales Zoologici* 58: 695–720. <https://doi.org/10.3161/000345408X396639>
- Bocáková M (2003) Revision of the tribe Calopterini (Coleoptera, Lycidae). *Studies on Neotropical Fauna and Environment* 38: 207–234. <https://doi.org/10.1076/snfe.38.3.207.28169>
- Bocáková M (2005) Phylogeny and classification of the tribe Calopterini (Coleoptera, Lycidae). *Insect Systematics and Evolution* 35: 437–447. <https://doi.org/10.1163/187631204788912472>
- Bourgeois J (1891) Études sur la Distribution géographique des Malacodermes. I. Lycides. *Annales de la Société entomologique de France* LX: 337–364. [+ 1 map]
- Crowson RA (1944) Further studies on the metendosternite in Coleoptera. *Transactions of the Royal Entomological Society of London* 94: 273–310. <https://doi.org/10.1111/j.1365-2311.1944.tb01220.x>
- Ferreira VS (2016) A revision of the genus *Macrolygistopterus* Pic, 1929 (Coleoptera, Lycidae, Calochromini). *Zootaxa* 4105: 321–338. <https://doi.org/10.11646/zootaxa.4105.4.2>
- Ferreira VS, Barclay MVL, Ivie MA (2018) Redescription of *Aporrhypis* Pascoe, 1887 (Coleoptera: Lycidae), with a discussion of its tribal placement. *The Coleopterists Bulletin* 72: 371–375. <https://doi.org/10.1649/0010-065X-72.2.371>

- Ferreira VS, Ivie MA (2016) Redescription of *Cephalolycus major* Pic, 1926 (Coleoptera: Elateroidea: Lycidae) and a discussion on its taxonomic position. *The Coleopterists Bulletin* 70: 663–666. <https://doi.org/10.1649/0010-065X-70.3.663>
- Gorham HS (1884) Malacodermata. *Biologia Centrali-Americana* 2, III, supplement: 225–360.
- Hansen P (1992) Costa Rican Malaise Trap Network. http://www.phorid.net/malaise/malaise_index.html Last viewed 29 August 2018.
- ICZN [International Commission on Zoological Nomenclature] (1999) International code of zoological nomenclature. Fourth Edition. London: The International Trust for Zoological Nomenclature.
- Ivie MA (1985) Nomenclatural notes on West Indian Elaphidiini (Coleoptera: Cerambycidae). *Pan-Pacific Entomologist* 61: 303–314.
- Kazantsev SV (2003) Morphology of Lycidae with some considerations on evolution of the Coleoptera. *Elytron* 17: 49–226.
- Kazantsev SV (2013) New and little-known taxa of “neotenic” Lycidae (Coleoptera), with discussion of their phylogeny. *Russian Entomological Journal* 22: 9–31.
- Kazantsev SV (2017) New leptolycines from Ecuador and Peru (Coleoptera: Lycidae). *Russian Entomological Journal* 26: 127–146.
- Kleine R (1933) Lycidae Pars 128. In: Junk W, Schenkling S (Eds) *Coleopterorum Catalogueus auspiciis et auxilio*, Berlin, 145 pp.
- Lawrence JF, Slipinski A, Seago AE, Thayer MK, Newton AF, Marvaldi AE (2011) Phylogeny of the Coleoptera based on morphological characters of adults and larvae. *Annales Zoologici* 61: 1–217. <https://doi.org/10.3161/000345411X576725>
- Miller RS (1991) A revision of the Leptolycini (*Coleoptera: Lycidae*) with a discussion of pedomorphosis. PhD Thesis. Ohio, USA: The Ohio State University.
- Mroczkowski M (1959) List of type specimens in the collection of Institute of Zoology of the Polish Academy of Sciences in Warszawa. II. Lycidae (Coleoptera). *Annales Zoologici* XVIII, 2: 11–63.
- Pic M (1921) Contribution a l’etude des Lycides. *l’Echange, Revue Linneenne Hors texte* 409: 21–24.

Glareis hespericula sp. n. from the Cape Verde Islands (Coleoptera, Scarabaeoidea, Glaresidae)

David Král¹, Lucie Hružová¹

¹ Charles University, Faculty of Science, Department of Zoology, Viničná 7, CZ-128 43 Praha 2, Czech Republic

Corresponding author: David Král (kral@natur.cuni.cz)

Academic editor: *Andrey Frolov* | Received 8 August 2018 | Accepted 13 September 2018 | Published 23 October 2018

<http://zoobank.org/5F783110-2169-426D-AA87-F43A4BD13301>

Citation: Král D, Hružová L (2018) *Glareis hespericula* sp. n. from the Cape Verde Islands (Coleoptera, Scarabaeoidea, Glaresidae). ZooKeys 792: 91–97. <https://doi.org/10.3897/zookeys.792.28870>

Abstract

Glareis hespericula sp. n. from the Cape Verde Islands (Boa Vista Island) is described and its diagnostic characters are illustrated. The new species is compared with similar and probably closely related species *Glareis walzlae* Scholtz, 1983. The differential diagnosis is mainly based on the different shape of meso- and metatibiae.

Keywords

Afrotropical region, Coleoptera, Glaresidae, *Glareis*, new species, Republic of Cabo Verde, Scarabaeoidea

Introduction

The scarabaeoid family Glaresidae includes only the single genus *Glareis* Erichson, 1848 widespread in all zoogeographical regions except Australia and Antarctica. The genus comprises more than eight dozen of described species of small, uniformly looking beetles that usually prefer sandy, often arid habitats. Adults are active in the evening, often attracted by light sources. The immature stages and biology of this hidden living group are not yet known (e.g., Scholtz and Grebennikov 2016). In a phylogenetical analysis based on morphology, *Glareis* was placed as the sister taxon of the remaining Scarabaeoidea (Browne and Scholtz 1999). Fossil records of seven mesozoic glaresids

are classified in three genera (*Cretoglaresis* Nikolajev, 2007; *Glaresis* and *Lithoglaresis* Nikolajev, 2007) (Bai et al. 2014). Currently 82 extant species are assigned to the genus *Glaresis* (Král and Bezděk 2016; Gordon and Hanley 2014; Král and Batelka 2017; Král et al. 2017; Paulsen 2016; Zidek 2015).

The Afrotropical fauna of the family Glaresidae is inadequately known. Only 19 species have been formally described from this region (see e.g., Scholtz 1982, 1983; Zidek 2015) and the only two comprehensive works (Petrovitz 1968; Scholtz 1983) have been published in the last century.

Recently collected *Glaresis* material from the Boa Vista Island, Cape Verde Archipelago, revealed another, undescribed species whose formal description we present below.

Materials and methods

Specimens were examined with an Olympus SZ61 stereomicroscope, measurements were taken with an ocular grid. The habitus photographs were taken using a Canon MP-E 65mm/2.8 1–5× Macro lens attached to a Canon EOS 550D camera. Partially focused images of each specimen were combined using Zerene stacker software. Male genitalia images were taken with a Provis AX70 (Olympus) microscope with digital image processing capability using Micro Image (Olympus) software.

Specimens of the newly described species are provided with one printed red label: “*Glaresis* | *hespericula* sp. nov. | HOLOTYPUS ♂ [or] PARATYPUS ♀ | David Král & Lucie Hrůzová 2018”. Both type specimens are deposited in the National Museum Praha, Czech Republic.

Exact label data are cited for the type material examined. Lines within each label are separated by a single vertical bar “|”. Information in quotation marks indicates the original spelling. Our remarks and additional comments are placed in brackets.

For morphological terms used in the description we largely follow Gordon and Hanley (2014) and Král et al. (2017).

Taxonomy

Glaresis hespericula sp. n.

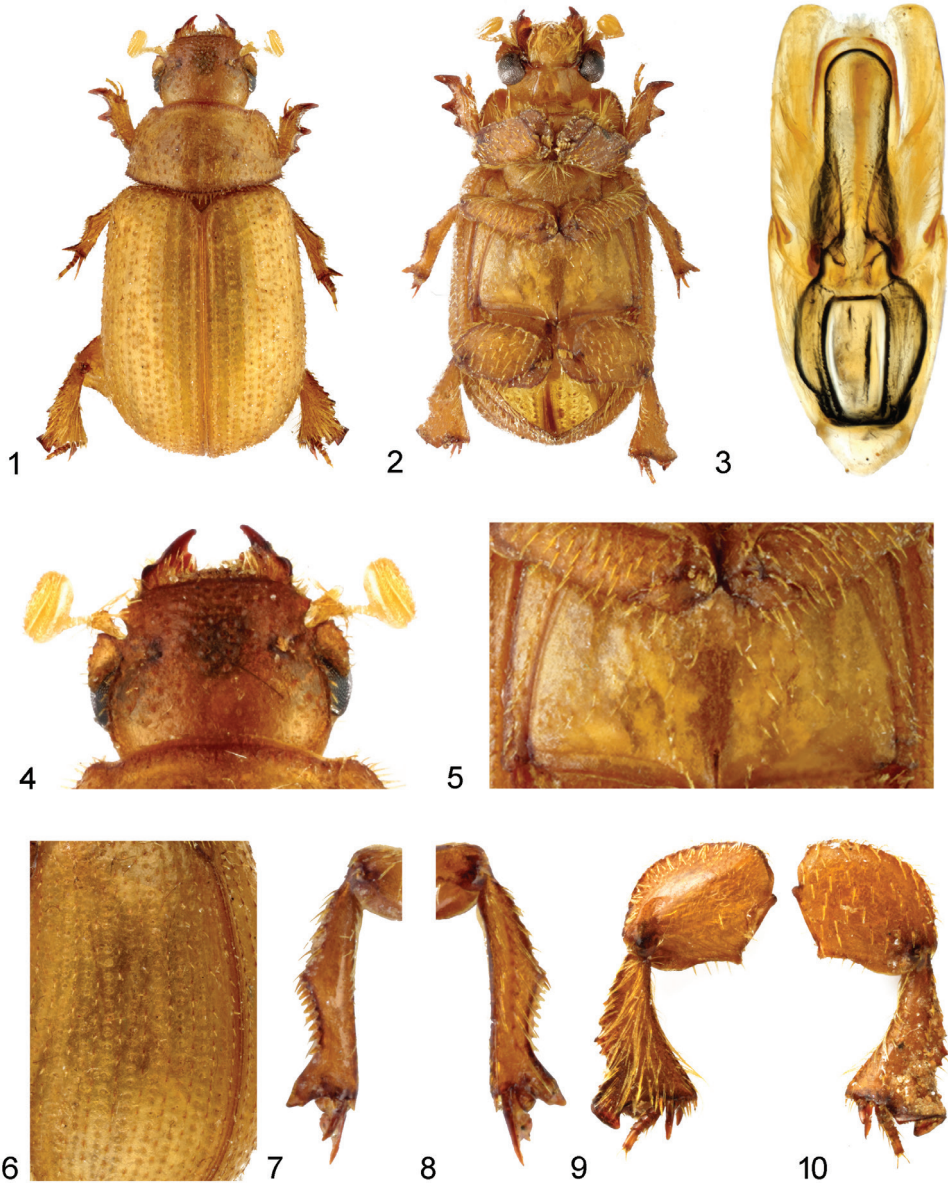
<http://zoobank.org/27201324-EB3E-4B2A-902E-C26F7DBC94A9>

Figures 1–10

Type locality. Cape Verde, Boa Vista Island, 10 km S of Sal Rei, near Praia de Chavez 16.12°N 22.91°W, [ca. 7 m a. s. l.].

Type material. Holotype (♂) and paratype (♀), “CAPE VERDE Boa Vista | Isl., 10 km S of Sal Rei, N | 16°12' W22°91'; near Praia | de Chavez, 28.-29.x.2015, | on light, V. Novák lgt.”

Description of male holotype. *Body* robust, strongly convex, weakly widened posteriad, brownish yellow coloured, weakly shining, macrosetation pale (Figs 1, 2).



Figures 1–10. *Glaresis hespericula* sp. n. **1** habitus, holotype, ♂, dorsal view **2** habitus, paratype, ♀, ventral view **3** aedeagus, dorsal view **4** head, dorsal view **5** meso-metaventral area, ventral view **6** detail of left elytron, dorsal view **7, 8** – left middle leg (**7** dorsal view, **8** ventral view) **9, 10** right hind leg (**9** dorsal view, **10** ventral view). Not to scale.

Head (Figs 1, 4) surface finely rugose, semialutaceous. Mandibles robust, with strong lateral prominence, external margins sinuate. Anterior margin of clypeus shallowly sinuate, distinctly upturned, smooth, lateral angles rounded; lateral margin shallowly sinuate; posterior angles acutely angular. Surface of frons and clypeus covered with sparsely,

irregularly spaced, shiny tubercles, some of them bearing stout, semi-erect macrosetae. Genae transversal, lateral margin rounded, smooth and bare. Epistomal grooves distinct. Occiput with irregularly spaced tubercles, tubercles somewhat smaller than on clypeus and frons. Each tubercle bearing very short, indistinguishable macroseta.

Pronotum (Figure. 1) transverse, moderately convex, pronotal grooves absent, medial longitudinal groove shallow; margins not bordered; anterolateral, lateral and basal margins serrate and with row of approximately clavate macrosetae, posterior corners rectangular; surface covered with densely almost regularly longitudinal carinae, each carina bearing thick, recumbent macroseta.

Scutellar plate small, almost triangular, alutaceous, smooth, and bare.

Elytra (Figs 1, 6) strongly convex, with ten striae and ten intervals; each stria with a row of coarse, simple punctures; intervals 1–7 and 10 remarkably costate, 8, 9 flat, all bearing a row of short, simple to weakly clavate, erect macrosetae.

Macropterous.

Pygidium weakly shining, scabrous.

Ventral surface (Figs 2, 5) alutaceous, abdominal ventrites covered with sparse fine macrosetae. Metaventral plate flat, bare and smooth, bearing row of stout macrosetae all around and with darkened translucent, longitudinal endocarina basally. Metaventral oblique grooves absent (Figure 5).

Legs. Posterior-superior margin of metafemora with blunt, broadly triangular teeth, anterior-superior margin of metafemora with a row of long macrosetae (Figs 9–10). Protibia distinctly tridentate (Figs 1, 2). Mesotibia (Figs 7, 8) long, nearly straight, with prominent median projection situated approximately in middle of length of mesotibia, distal part of outer edge broadly, shallowly emarginate, bearing nine short, stout spines; basal external tooth of mesotibia slightly emarginate basally. Metatibia (Figs 9, 10) broadly triangular, outer margin irregularly serrate, with faint median projection and faint median ridge, strongly macrosetaceous; row of four spine-bearing tubercles extending from base to apex medially; inner margin smooth, macrosetaceous; apex of metatibia with outer horseshoe shaped portion sub-equal than inner spur-bearing portion; inner margin of the horseshoe portion with a row of contiguous short macrosetae.

Male external genitalia (Figure 3). Aedeagus with parameres distinctly longer than phallobasis; parameres sclerotized in whole length, lateral margin regularly arcuate to almost regularly rounded tips; phallus sclerotised, sides straight, weakly divergent anteriorly.

Sexual dimorphism and variability. Female paratype differs from male by body indistinctly broader posteriorly (Figure 2) and by row of ten spines on outer edge of distal part of mesotibia.

Measurements. Total body length: 4.0–4.3 mm (holotype 4.2 mm; paratype 4.3 mm).

Differential diagnosis. The new species is similar to *Glareis walzlae* Scholtz, 1983, described from Sudan, mainly in having the following characters: absence of the pronotal grooves beside the medial longitudinal groove (Figure 1), absence of the metaventral oblique grooves (Figure 5), protibia with three prominent teeth (Figs 1,

2), and smooth anterior clypeal margin (Figs 1, 4); for more details see also Petrovitz (1968) and Scholtz (1983). From this species, *Glaresis hespericula* sp. n. clearly differs in the following characters:

- mesotibia with prominent median projection situated approximately in middle of length of mesotibia (Figs 1, 2, 7, 8) (mesotibia with small median projection situated before middle of length of metatibia in *G. walzlae* (Scholtz 1983: fig. 8));
- distal part of outer edge of mesotibia broadly, shallowly emarginate, with row of 9–10 spines (Figs 1, 2, 7, 8) (distal part of outer edge of mesotibia straight, with row of 7–9 spines (Scholtz 1983: fig. 8));
- metatibia with faint median projection on outer margin, with faint median ridge (Figs 1, 2, 9, 10) (metatibia with prominent median projection on outer margin, with distinct median ridge (Scholtz 1983: fig. 19)).

Collecting events. The material was collected on sand dunes using a light trap approximately between 7–9 p.m., the temperature was around 24 °C and two days before it rained very strongly.

Etymology. *Hespericula* means a small, yet juvenile hesperid; noun in apposition.

Distribution. So far known only from the Boa Vista Island, the Cape Verde Islands.

Discussion

Cape Verde Archipelago is classified together with other volcanic archipelagos (Azores, Madeira, Salvagens Islands and Canary Islands) and a thin strip of the Atlantic coast in southern Portugal, Morocco and the Western Sahara as the Macaronesian biogeographic subregion (e.g., Oromí 2004). Although Cape Verde harbours a high proportion of Afrotropical species, aside from its numerous endemic taxa, its insect fauna is poor both in endemic forms and in total number of species. Their fauna is considered unique and in some aspects deserves protection (e.g., Arechavaleta et al. 2005; Batelka and Straka 2011). Fauna of Coleoptera of the individual archipelagos and islands were treated as follows: Azores (Borges et al. 2005), Madeira and related islands (Borges et al. 2008), the Salvagens Islands (Erber and Wheeler 1987), the Canary Islands (Machado and Oromí 2000) and the Cape Verde Archipelago (Oromí et al. 2005). No Glaresidae have been reported from these islands and archipelagos so far. Hence, the newly described species represents the first record of the family Glaresidae from the volcanic islands west of Africa.

Acknowledgements

The present study was supported by the SVV grant no. 260 434/2018 (Lucie Hružová).

References

- Arechavaleta M, Zurita N, Marrero MC, Martín JL (2005) Lista preliminar de espécies silvestres de Cabo Verde. Fungos, Plantas e Animais Terrestres. Consejería de Medio Ambiente y Ordenación Territorial, Gobierno de Canarias, 155 pp.
- Bai M, Beutel RG, Liu WG, Li S, Zhang MN, Lu YY, Song KQ, Ren D, Yang XK (2014) Description of a new species of Glaresidae (Coleoptera: Scarabaeoidea) from the Jehol Biota of China with a geometric morphometric evaluation. *Arthropod Systematics & Phylogeny* 72: 223–236.
- Batelka J, Straka J (2011) *Ripiphorus caboverdianus* sp. nov. – the first ripiphorid record from the Macaronesian volcanic islands (Coleoptera: Ripiphoridae: Ripiphorinae). *Zootaxa* 2795: 51–62.
- Borges PAV, Abreu C, Aguiar AMF, Carvalho P, Jardim R, Melo I, Oliveira P, Sérgio C, Serano ARM, Vieira P (2008) A list of the terrestrial fungi, flora and fauna of Madeira and Selvagens archipelagos. Direcção Regional do Ambiente da Madeira and Universidade dos Açores, Funchal and Angra do Heroísmo, 440 pp.
- Borges PAV, Oromí P, Dinis F, Jarroca S (2005) Coleoptera. In: Borges PAV, Cunha R, Gabriel R, Martins AF, Silva L, Vieira V (Eds) A list of the terrestrial fauna (Mollusca and Arthropoda) and flora (Bryophyta, Pteridophyta and Spermatophyta) from Azores. Direcção Regional do Ambiente and Universidade dos Açores, Horta, Angra do Heroísmo and Ponta Delgada, 197–206.
- Browne J, Scholtz CH (1999) A phylogeny of the families of Scarabaeoidea (Coleoptera). *Systematic Entomology* 24: 51–84. <https://doi.org/10.1046/j.1365-3113.1999.00067.x>
- Erber D, Wheeler CP (1987) The Coleoptera of the Salvagem Islands, including a catalogue of the specimens in the Museu Municipal do Funchal. *Boletim do Museu Municipal do Funchal* 39: 156–187.
- Gordon RD, Hanley GA (2014) Systematic revision of American Glaresidae (Coleoptera: Scarabaeoidea). *Insecta Mundi* 333: 1–91.
- Král D, Batelka J (2017) Arthropod Fauna of the UAE: Order Coleoptera, superfamily Scarabaeoidea. *Arthropod Fauna of the UAE* 6: 78–168.
- Král D, Bezděk A (2016) Family Glaresidae. In: Löbl I, Löbl D (Eds) Catalogue of Palaearctic Coleoptera. Volume 3. Scarabaeoidea – Scirtoidea – Dasciloidea – Buprestoidea – Byrrhoidea. Revised and Updated Edition. E. J. Brill, Leiden–Boston, 58.
- Král D, Hružová L, Lu YY, Bai M (2017) First records of Glaresidae (Coleoptera) in China, with the description of a new species from Inner Mongolia and Shaanxi. *Zootaxa* 4306: 145–150. <https://doi.org/10.11646/zootaxa.4306.1.11>
- Machado A, Oromí P (2000) Elenco de los Coleópteros de las Islas Canarias (Catalogue of the Coleoptera of the Canary Islands). Instituto de Estudios Canarios, La Laguna, 308 pp.
- Oromí P (2004) Biospeleology in Macaronesia. *AMCS Bulletin 19 / SMES Boletín* 7: 98–104.
- Oromí P, Martín E, Zurita N, Cabrera A (2005) Coleoptera. In: Arechavaleta M, Zurita N, Marrero MC, Martín JL (Eds) Lista preliminar de espécies silvestres de Cabo Verde. Fungos, Plantas e Animais Terrestres. Consejería de Medio Ambiente y Ordenación Territorial, Gobierno de Canarias, 78–86.
- Paulsen MJ (2016) Two new species of South American Glaresidae (Coleoptera: Scarabaeoidea). *Zootaxa* 4154: 595–600. <https://doi.org/10.11646/zootaxa.4154.5.9>

- Petrovitz R (1968) Die Afrikanischen Arten der Gattung *Glaresis* Erichson nebst einer mit dieser nahe verwandten neuen Gattung. Entomologische Arbeiten aus dem Museum G. Frey 19: 257–271.
- Scholtz CH (1982) Catalogue of world Trogidae (Coleoptera, Scarabaeoidea). Entomology Memoir. Department of Agriculture and Fisheries Republic of South Africa 54: 1–27.
- Scholtz CH (1983) A review of the genus *Glaresis* Erichson (Coleoptera: Trogidae) of subsaharan Africa. Journal of the Entomological Society of Southern Africa 46: 209–225.
- Scholtz CH, Grebennikov VV (2016) 12. Scarabaeiformia Crowson, 1960. In: Beutel RG, Leshen RAB (Eds) Coleoptera, Beetles. Volume 1: Morphology and systematics (Archostemata, Adephaga, Myxophaga, Polyphaga partim). In: Kristensen NP, Beutel RG (Eds). Handbook of Zoology. A natural history of the phyla of the animal kingdom. Vol IV. Arthropoda: Insecta, Part 38, 2nd edn. Walter de Gruyter, Berlin, 367–425.
- Zidek J (2015) A review of the Glaresidae (Scarabaeoidea). *Animma.X* 6: 1–44.

Description of a new species of *Mediotipula* from Albania, with consideration of the eastern Mediterranean as a diversity hotspot (Diptera, Tipulidae)

Lujza Keresztes¹, Jesús Martínez Menéndez², Luis Martín², Edina Török^{1,3}, Levente-Péter Kolcsár³

1 Hungarian Department of Biology and Ecology, Centre of Systems Biology, Biodiversity and Bioresources, Faculty of Biology and Geology, University of Babeş-Bolyai Cluj-Napoca, Clinicilor 5-7, Romania **2** Department Zoología, Antropología Física & Genética, Faculty of Biology, University of Santiago de Compostela, R/Lope Gómez de Marzoa, s/n. Campus Vida. 15782 Santiago de Compostela, Spain **3** Romanian Academy Institute of Biology, Splaiul Independenței 296, 060031 București, Romania

Corresponding author: Lujza Keresztes (keresztes2012@gmail.com)

Academic editor: C. Borkent | Received 10 April 2018 | Accepted 15 September 2018 | Published 23 October 2018

<http://zoobank.org/D14BAFD2-3F55-46A0-8EC7-D796A7DA4E6F>

Citation: Keresztes L, Menéndez JM, Martín L, Török E, Kolcsár LP (2018) Description of a new species of *Mediotipula* from Albania, with consideration of the eastern Mediterranean as a diversity hotspot (Diptera, Tipulidae). ZooKeys 792: 99–115. <https://doi.org/10.3897/zookeys.792.25683>

Abstract

A new species of the *Tipula* subgenus *Mediotipula* is described from the south-eastern part of Albania, south-eastern Europe. Morphologically, the new species is most similar to *T. (M.) stigmatella* Schummel, 1833, but differs mainly with respect to males, having a distinctly shaped posterior margin of tergite 9–10, a widened outer gonostylus and a series of details of the inner gonostylus (anterior end of the anterior arm, shape of the posterior arm), as well as having more bulbous and rounded hypogynal valves in the females. Further morphological differences of the male terminalia between allopatric populations of *T. (M.) stigmatella* in the Carpathians and Balkans, south-eastern Europe, are discussed.

Keywords

Craneflies, *Mediotipula*, new species, morphological diversity, Mediterranean hotspots, the Balkans

Introduction

The Mediterranean region of Europe is one of the most species-rich biomes in the world with a high level of endemism shaped by tectonic shifts (Hewitt 2011, Oosterbroek and Arntzen 1992, Markova et al. 2010), Pleistocene climatic oscillations (Previšić et al. 2014), environmental heterogeneity (Triantis et al. 2005, Pinkert et al. 2017), and/or natural selection (Kraitsek et al. 2008, Rodriguez-Ramirez et al. 2017). Biodiversity hotspots from such areas as Iberia, the Apennines, the Balkans (south-eastern Europe), the Mediterranean islands, Northwest Africa, western Turkey and the Caucasus (at the border of Europe and Asia) all have a decisive role in the glacial survival of numerous endemic or range-restricted taxa (De Jong 1998). Furthermore, they also provided a continuous supply of European biodiversity during several postglacial periods (Zachos and Habel 2011).

The western Palearctic *Tipula* (*Mediotipula*) Pierre, 1924 is a small subgenus of only eleven species of moderately sized crane flies (Oosterbroek 2018). According to Savchenko (1966, 1979, 1983), Theowald (1978) and De Jong (1995), *Mediotipula* is the sister group of the subgenus *Savtshenkia* Alexander, 1965. However, all members of *Mediotipula* are unique among *Tipula*, by having a relatively small discoidal cell, while almost all the other *Tipula* have a relatively large discoidal cell (length-width ratio of approximately two or more). Other synapomorphies include the entirely fused, plate-like posterior apodemes of the sperm pump, in addition with a laterally compressed projection on the posterolateral corner of the gonocoxite in males (De Jong 1995). Additionally, females have the hypogynal valves fused for approximately one-half to two thirds of the length, in comparison with the totally separated (up to their bases) hypogynal valves in females of other *Tipula*. Sternite VIII of the females has a conspicuous sclerotisation of the ventral wall of the genital chamber near the openings of the gonopore, together with a usually less distinct and smaller posteroventral sclerite. Sternite IX is present as a slender and well-sclerotised structure, sometimes with a membranous medial part (De Jong 1995).

The majority of *Mediotipula* taxa have an isolated distribution in the western Palearctic area, showing high levels of endemism corresponding with the major biodiversity hotspots around the Mediterranean Sea while four species have a distribution area that is limited to the Iberian Peninsula (Oosterbroek 2018). The Balkans contain only three species with their ranges also covering Central Europe or the Caucasus. Only one species, *T. (M.) mikiana* Bergroth, 1888 has an exclusively extra-Mediterranean distribution, and only three species are range-restricted, one in Anatolia, (Asian Turkey) (*T. (M.) anatoliensis* Theowald, 1978), one in the Caucasus (*T. (M.) caucasiensis* Theowald, 1978) and one in Algeria (North Africa), (*T. (M.) fulvogrisea* Pierre, 1924) (Oosterbroek 2018).

Species of *Mediotipula* are distributed mostly in colline- to montane-subalpine ecosystems with a high level of humidity, often in very steep oak woods, and are rarely associated with open woods and hedges exposed to the sun (pers. obs., but see also Dufour 1986 and De Jong 1995). Larvae are considered to be bryobionts, and are

frequently collected under moist moss in/or along brooks, or banks of rivers and even under dry moss in the case of *T. (M.) stigmatella* (Savchenko 1966, Theowald 1967, Höchstätter 1963).

A comprehensive phylogenetic analyses of the species which belong to *Mediotipula* was published by De Jong (1995), who compared and analyzed 24 morphological characters of both sexes (with the exception of the female of *T. (M.) fulvogrisea*), using parsimony. According to his phylogeny, only the previous *T. (M.) brolemanni* group (sensu Theowald, 1978) proved to be monophyletic, and together with the species *T. (M.) siebkei* and *T. (M.) caucasiensis* constituted a well-defined group within the sub-genus *Mediotipula*.

In this paper we provide a morphological description of a new species and discuss its relationship with the similar *T. (M.) stigmatella*, based upon morphological features of the male and female terminalia. The morphological differences of male genital structures of different populations of *T. (M.) stigmatella* from the Carpathians and the Balkans are also discussed.

Materials and methods

Adults were collected using sweep nets and then stored in 96% ethanol or dry-pinned. Altogether, 54 male and four female individuals of *Mediotipula* belonging to four species were examined (see Table 1). All collection data are available in the TransDiptera Online Database (Kolcsár et al. 2018). Male and female genitalia were examined after being cleared in 10% KOH. Layer photos were taken using an Olympus SZ61 stereomicroscope equipped with a Canon 650D camera and LM Digital SLR Adapter; photos were combined using the Zerene Stacker software. Male and female genitalia terminology is in accordance with De Jong (1995). All specimens used in the present study were collected by the authors and deposited in the Diptera Collection of the Faculty of Biology and Geology, University Babes-Bolyai, Cluj Napoca, Romania (DCFBG) (Figure 1, Table 1).

Taxonomy

Description of the new species

Tipula (Mediotipula) gjipeensis Keresztes & Kolcsár, sp. n.

<http://zoobank.org/4CB2A315-1FF5-4DC4-84BF-202E44B9794F>

Figures 2, 3, 4A

Material examined. *Holotype*: 1 male. *Paratypes*: 20 males, 2 females, same locality as holotype.

Type locality. Albania; Vlora district, Illias, Gjipe Gorge, 267 m, 40.144172°N, 19.676905°E, 05.v. 2016, leg. L Keresztes & LP Kolcsár.

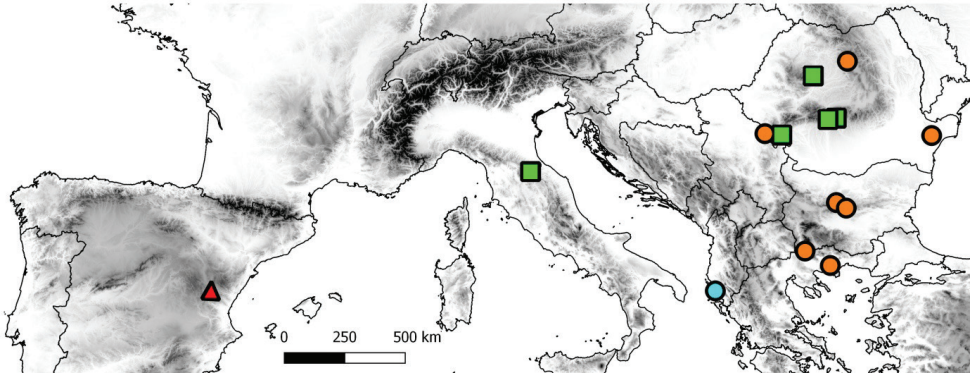


Figure 1. Sampling localities of different *Mediotipula* species investigated in this study. *Tipula (Mediotipula) cataloniensis* Theowald, 1978 (red triangle), *T. (M.) stigmatella* Schummel, 1833 (orange dots), *T. (M.) gjipeensis* sp. n. (blue dot), *T. (M.) siebkei* Zetterstedt, 1852 (green square).

Type specimens are deposited in the Diptera Collection of the Faculty of Biology and Geology (DCFGB), University Babeş-Bolyai, Cluj Napoca, Romania.

Diagnosis. Males: Tergite IX–X in males with the posterior margin having a medial spinous extension with a wide base and gradually narrowed tip. Lateral corner of the posterior margin of the tergite IX–X is mostly rounded. Outer gonostylus widened gradually to tip, ending oblique at dorsal margin. The anterior end of the anterior arm of the inner gonostylus has a long beak-like elongation. The posterior arm of the inner gonostylus has in its dorsal margin a concentration of strong stout setae directed anteriorly, and the anterior corner ending with a thorn-like process. On the middle of the posterior part of the inner gonostylus a small triangular posterolateral extension is present. Females have the base of the hypogynal valves bulbous and rounded.

Description. Medium sized species, Body length: holotype male 10 mm, paratype female 12 mm; wing length: holotype male 15 mm, paratype female 16 mm. Adult habitus: General colour yellowish brown. First two segments of antennae yellowish, third light brown, remainder brown. Nasus yellowish with stout black setae. Dorsal part of head, near antennae, with two whitish patches; rest of head grey-peach coloured with dark setae, except whitish yellow occipital area. Thorax -brownish grey, with four shiny brown stripes on dorsal surface. Scutellum yellowish. Wings transparent, *Mediotipula*-like, discoidal cell present. Coxae and trochanters yellowish; rest of leg segments brown. Abdomen yellowish, with dark brown patches to continuous bands on the posterior edge and lateral margin of tergites I–VII, tergite VIII entirely brown.

Male terminalia (Figures 2, 3). Tergite IX–X with medial part bearing a narrow medial longitudinal suture with reduced whitish area close to its posterior margin (Figure 2C) and a relatively small medial spiny extension with a wide base and gradually narrowed tip on its posterior margin (Figure 2C, E). Ventral surface of posterior margin of tergite IX–X flat, lacking ventrally produced extension (Figure 2E). Lateral corner of posterior margin of tergite IX–X rounded (Figure 2C). Posterior margin of sternite 8 V-shaped, with posterior margin ending straight (Figure 2D). Gonocoxite has a

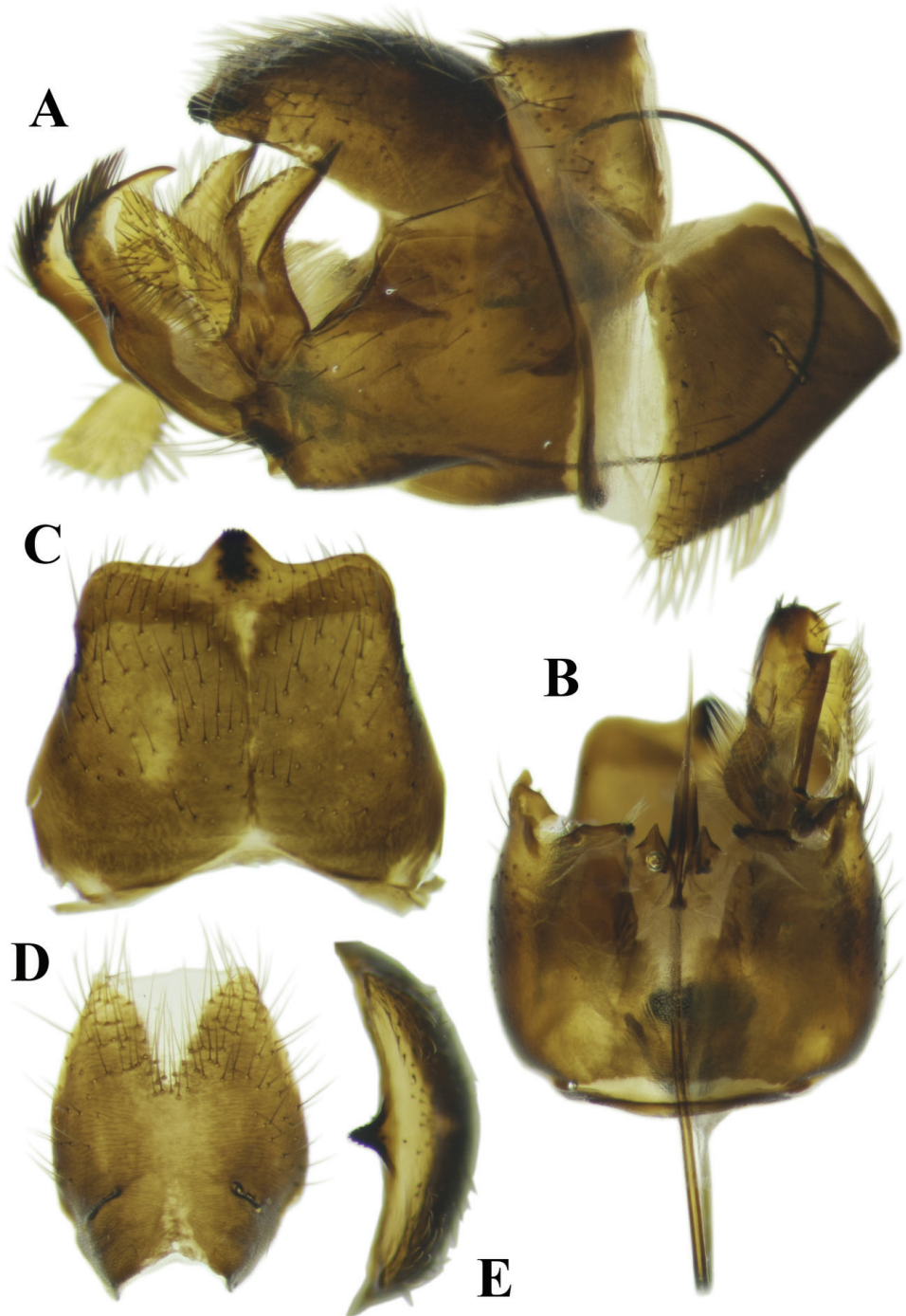


Figure 2. Photographs of the morphological structures of the male terminalia of the *Tipula (Mediotipula) gjipeensis* sp. n. **A** lateral view **B** distal view **C** tergite IX dorsal view **D** sternite VIII ventral view **E** tergite IX-X, distal view.

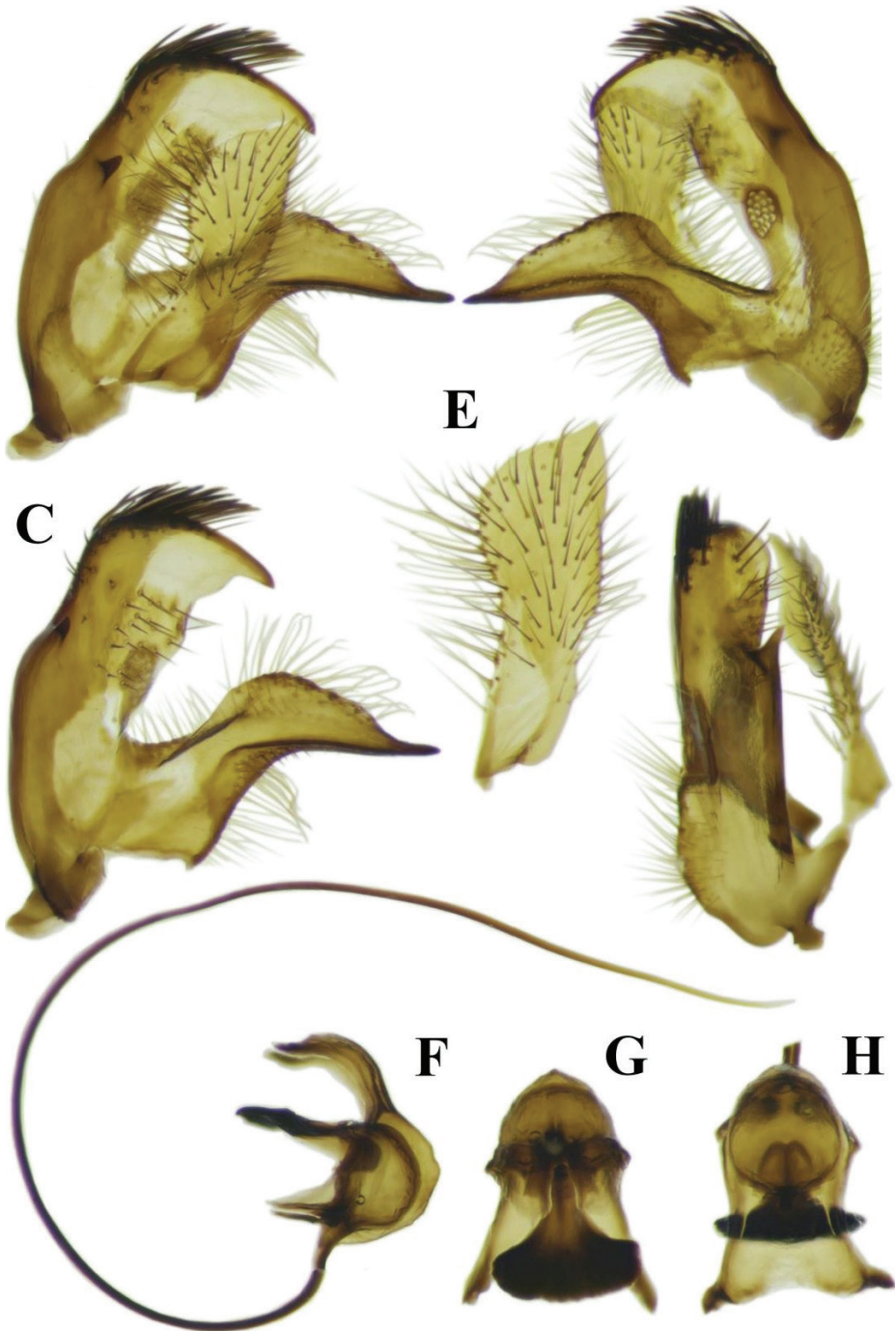


Figure 3. Photographs of the morphological structures of the male terminalia of the *Tipula (Mediotipula) gjipeensis* sp. n. **A** gonostyli outer-lateral view **B** gonostyli inner-lateral view **C** inner gonostylus outer-lateral view **D** gonostyli ventral view **E** inner gonostylus outer lateral view **F** aedeagus complex lateral view **G** sperm pump ventral view **H** sperm pump distal view.

Table 1. Material of the subgenus *Mediotipula* used in our study with localities (BG-Bulgaria, FYM-Macedonia, GR-Greece, IT-Italy, ES-Spain), geographic coordinates (given in decimal degrees), number of individuals found at each collection site, number of individuals used in the present study, date of the collection, and name of collector (leg.).

Species	Specimen	Location	Collection date	Latitude	Longitude	Collector(s)
<i>T. (M.) cataloniensis</i> Theowald, 1978	2♂	ES, Fuente del Cabrito, Camarena de la Sierra, Rio Camarena, 1122 m	02.vii.2016	40.16383N	-1.055242W	JM Gonzalez & J Martinez
<i>T. (M.) cataloniensis</i> Theowald, 1978	1♂	ES, Teruel, Camarena de la Sierra, Rio Camarena, 1216 m	02.vii.2016	40.15211N	-1.044561W	JM Gonzalez & J Martinez
<i>T. (M.) gjipeensis</i> sp. n.	21♂, 2♀	AL, Illias, Gjipe Gorge, 276 m	05.v.2016	40.144172N	19.676905E	L Keresztes & LP Kolcsár
<i>T. (M.) siebkei</i> Zetterstedt, 1852	3♂	RO, Brezoi, Cozia Mts., Stanisoara Monastery, 862 m	06.vi.2000	45.302015N	24.310468E	L Rákossy
<i>T. (M.) siebkei</i> Zetterstedt, 1852	4♂	RO, Cheia, Trascaului Mts., Cheile Turzii gorge, 444 m	11.vi.2005	46.544398N	23.701908E	L Keresztes
<i>T. (M.) siebkei</i> Zetterstedt, 1852	1♂	IT, Balze, Monte Fumaiolo, 1159 m	18.vii.2010	43.78068N	12.08317E	M Bálint
<i>T. (M.) siebkei</i> Zetterstedt, 1852	1♂, 1♀	RO, Pecinisca, Mehedinti Mts., Cheile Pecinisca gorge, 243 m	10.v.2013	44.850872N	22.406507E	LP Kolcsár
<i>T. (M.) siebkei</i> Zetterstedt, 1852	2♂	RO, Capatanenii Ungureni, Fogaras Mts., Vidraru Lake surroundings, 741 m	27.v.2014	45.338783N	24.643658E	LP Kolcsár.
<i>T. (M.) siebkei</i> Zetterstedt, 1852	1♂	IT, Balze, Monte Fumaiolo, 1159 m	18.vii.2010	43.78068N	12.08317E	M Bálint
<i>T. (M.) stigmatella</i> Schummel, 1833	1♂	RO, Slava Chercheza, Usmenia Monastery, 132 m	03.vi.2005	44.837727N	28.567579E	L Keresztes
<i>T. (M.) stigmatella</i> Schummel, 1833	2♂, 1♀	RO, Sasca Romana, Nera Mts., Cheile Nerei gorge, 159 m	09.v.2009	44.893238N	21.714745E	J Csepregi
<i>T. (M.) stigmatella</i> Schummel, 1833	1♂	BG, Kulata, Struma River gorge, 84 m	04.v.2011	41.380772N	23.36477E	LP Kolcsár
<i>T. (M.) stigmatella</i> Schummel, 1833	4♂	GR, Kavala, Batis camp area, 2 m	05.v.2011	40.934937N	24.402779E	LP Kolcsár
<i>T. (M.) stigmatella</i> Schummel, 1833	1♂	BG, Beli Osam, Stara Planina Mts., Vila Nana, 526 m	12.vi.2012	42.856119N	24.650439E	LP Kolcsár
<i>T. (M.) stigmatella</i> Schummel, 1833	7♂	BG, Tazha, Stara Planina Mts., Rusalka hut, 1096 m	13.vi.2012	42.688772N	25.055851E	LP Kolcsár
<i>T. (M.) stigmatella</i> Schummel, 1833	2♂,	RO, Lunca Bradului, Mures River gorge, 576 m	14.v.2013	46.956536N	25.103522E	LP Kolcsár
<i>T. (M.) stigmatella</i> Schummel, 1833	1♂	FYM, Jablanica Mts, Vevchani, springs, 922 m	29.iv.2018	41.239486N	20.585719E	L Keresztes

laterally compressed projection on the posterodorsal corner (Figure 2A, B). Part of the gonocoxite behind the suture, on posterior part, short (Figure 2B). Interior surface of gonocoxite membranous, but with a uniformly sclerotised and relatively flat structure in the middle part. Outer gonostylus widens gradually to tip, ending obliquely at dorsal margin (Figure 3E). Lower anterior part of inner gonostylus with concentration of long setae (Figure 3A–C). Anterior end of anterior arm of inner gonostylus with a long beak-like elongation (Figure 3A–C). Posterior arm of inner gonostylus with posterior half of the dorsal margin bearing a concentration of strong thorn-like setae directed anteriorly, anterior corner ending in thorn-like process (Figure 3A–C). Posterior part of inner gonostylus with a small triangular posterolateral extension medially (Figure 3D).

sperm pump with posterior apodemes fused in the horizontal plane (Figure 3F–H). Parameres small and triangular (Figure 2B).

Female terminalia (Figure 4A). Cercus slightly curved downward and terminating in a rounded apex (Figure 4A). Hypogynal valves only moderately sclerotised and fused for approx. two thirds of their length. End of membranous area of sternite VIII at base of hypogynal valves distinctly acute. Base of hypogynal valves bulbous. Ventral wall of genital chamber, near opening of gonopore is distinctly sclerotised. Vestigial sternite IX present as a slender, but well-sclerotised structure.

Etymology. The species epithet *gjipeensis* translates to “from the Gjipe Gorge” and was formed by appending the Latin suffix *-ensis* to the name of the gorge where the new species was collected.

Ecological notes and distribution. During our investigation in the south-western part of Albania, the new species described here was only detected in the highly-isolated humid habitat in the Gjipe Gorge, near the shore of the Adriatic Sea and very close to Gjipe Beach. The gorge is cut by a small stenotherm brook, fed by a spring ca. 2–3 km upstream. The river bed is filled with large limestone boulders and rocks, and has abundant mossy cover. The brook spring is surrounded by dense riparian vegetation, where the adults flew during daytime or were sometimes seen to rest on trees near the river. The microclimate of the river valley was roughly 10 °C cooler than in the surrounding macchia (L Keresztes pers. obs.). Specimens were collected in early May. The river was completely dry in June and no additional flying adults were collected, suggesting a short phenology between April and May (LP Kolcsár pers. obs).

Discussion

Systematic position and affinities of *M. gjipeensis* sp. n.

The new species belongs to the subgenus *Mediotipula*, a crane fly group restricted to the western Palearctic area, with the majority of taxa (eight out of twelve) having a range-restricted distribution in the Mediterranean area and the Caucasus. *Mediotipula* has a rather isolated phylogenetic position among the western Palearctic Tipulidae, sharing a combination of synapomorphies that is unique for this subgenus (De Jong 1995), and present also in *T. (M.) gjippensis*, such as the relatively small discoidal cell, the entirely fused, plate-like posterior apodemes of the sperm pump and a laterally compressed projection on the posterolateral corner of the gonocoxite in males. Additionally, females have the hypogynal valves fused for approx. one-half to two thirds of the length, in comparison with the totally separated (up to their bases) hypogynal valves in females of other *Tipula* (for more details see De Jong 1995).

The new species is most similar to *T. (M.) stigmatella*, having the inner gonostylus of the male terminalia approx. two times as high as inner gonostyli of other species of *Mediotipula* (Figs 3D, 6B, G). However, the new species can be easily distinguished from the latter species, because in the males the posterior margin of tergite IX–X has a medial spiny

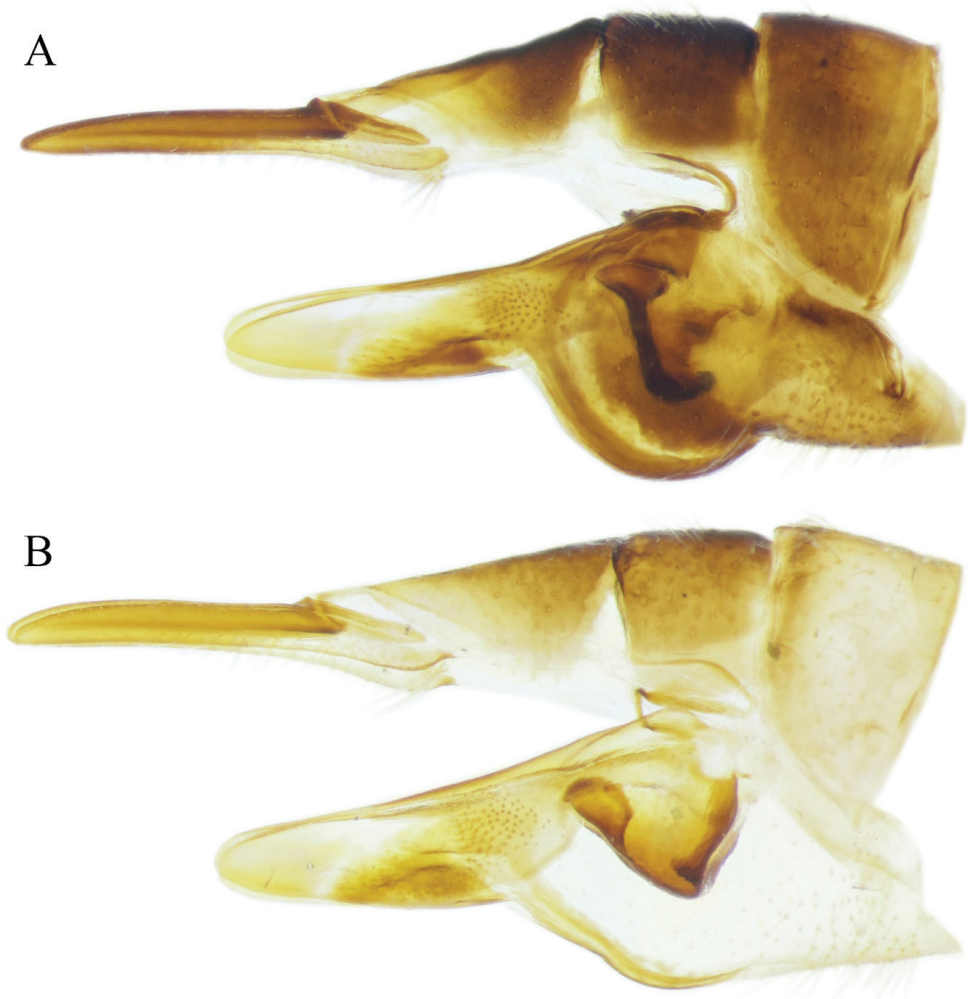


Figure 4. Photographs of the female terminalia, lateral view. **A** *Tipula (Mediotipula) gjipeensis* and **B** *T. (M.) stigmatella*.

extension with a wide base that gradually narrows towards the tip (Figure 2C), instead of the narrowed and rounded medial spinous extensions seen in *T. (M.) stigmatella* (Figure 5A, C). The medial spiny extension is relatively small (Figure 2E) in comparison with the similar structure in *T. (M.) stigmatella* (Figure 5B). In *T. (M.) gjipeensis* the lateral corner of the posterior margin of tergite IX–X is mostly rounded (Figure 2C) instead of pointed, as in *T. (M.) stigmatella* (Figure 5A, C) and the ventral surface of the posterior margin of tergite IX–X is flat (Figure 2E), while *T. (M.) stigmatella* has two triangular protuberances (Figure 5B). In *T. (M.) gjipeensis* males a narrow medial longitudinal suture is present on the medial part of the disk of tergite IX–X (Figure 2C), with a reduced whitish area close to the posterior margin, instead of the long light stripe in the middle part found in *T. (M.) stigmatella* (Figure 5A, C). In *T. (M.) gjipeensis* males, the posterior margin of ster-

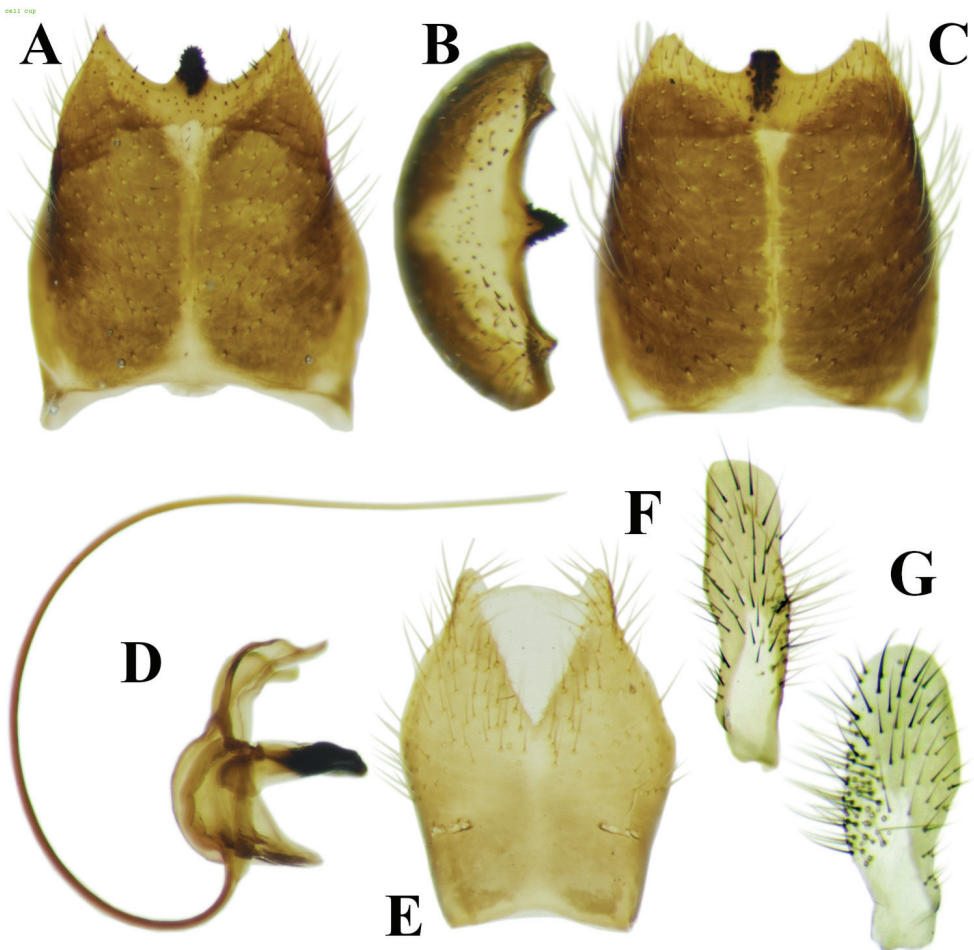


Figure 5. Photographs of the morphological structures of the male genital structures of individuals of *Tipula (Mediotipula) stigmatella* Schummel, 1833. Specimen from Kavala (Greece) **A, B, D, E, F** Specimen from Kulata (Bulgaria) **G**; Specimen from Lunca Bradului (Romania) **(C)** **A, C** tergite IX dorsal view **B** tergite IX distal view **D** aedeagus complex lateral view **E** sternite VIII ventral view **F, G** outer gonostylus, lateral view.

nite VIII ends straight (Figure 2D), instead of having two lateral projections as in *T. (M.) stigmatella* (Figure 5E). The outer gonostylus widens gradually to tip, ending obliquely towards the dorsal margin (Figure 2E), while in *T. (M.) stigmatella*, the anterior and posterior edges of the outer gonostylus run more or less parallel, ending straight or rounded toward dorsal margin (Figure 5F, G). The posterior arm of the inner gonostylus has its dorsal margin in the posterior half with a concentration of strong thorn-like setae directed anteriorly, anterior part bare, ending with a thorn-like process (Figure 3A–C). while in *T. (M.) stigmatella* a concentration of strong setae covers the entire dorsal margin of the posterior arm of the inner gonostylus, with the anterior corner rounded, but a conspicuous subterminal acute process directed ventrally is present (Figure 6A, C–E, F, H). In *M.*

gjipeensis, the posterior part of the inner gonostylus has a small triangular posterolateral extension present in the middle (Figure 3D), differing from the long thorn-like process displayed in *T. (M.) stigmatella* (Figure 6B, G) and *T. (M.) sarajevensis*, while in all other members of *Mediotipula* such processes are absent. Parameres in the new species are small and triangular (Figure 2B), similar to *T. (M.) stigmatella*, but not lobe-like and spiny, as in *T. (M.) siebkei* (De Jong 1995). The females of the new species are clearly distinct from all other *Mediotipula* in having a bulbous base of the hypogynal valve (Figure 4A), rather than the gradually narrowed base found in all other species except *T. (M.) stigmatella*. However, *T. (M.) gjipeensis* is also distinct from *T. (M.) stigmatella* in having the bulbous base of the hypogynal valve rounded, instead of angular (Figure 4B).

Morphological variability of *M. stigmatella* in the Carpathian-Balkan area

During our investigation, morphological differences were detected between allopatric populations of *T. (M.) stigmatella* in the Carpathian-Balkan area. Most important divergences were detected in the shape of the posterior margin of the tergite IX–X between populations from the Carpathians (Figure 5C) and the Balkans (Figure 5A), but no important differences in the general shape of the outer and inner gonostylus were found between populations from Lunca Bradului (the Carpathians) (Figure 6D, E) and Kavala (Greece) (Figs 5F, 6A–C). However, a series of important structures were detected between more proximal populations from Kavala (Greece) together with individuals from Vevchani (FY of Macedonia) and Kulata (Bulgaria), mostly on the width of the outer gonostylus (Figure 5F, G), and on the apex of the posterior arm of the inner gonostylus (Figure 6A–C, F–H). The triangular-like apex of the posterior side of the posterior arm of the inner gonostylus of the specimens from Kavala (Greece) and Vevchani (FY of Macedonia) is shorter, with a broader base (Figure 6B), while in specimens collected from Kulata (Bulgaria) such similar structure is longer, with a narrowed base (Figure 6G). Without having a clear geographic pattern of the detected morphological divergences in the studied population, and with only a limited number of individuals, more data is required, covering the whole of the species distribution area, in order to evaluate the taxonomic importance of the detected differences.

The eastern Mediterranean area as a diversity hotspot

Current systematic and phylogeographical studies of the Mediterranean terrestrial fauna (Oosterbroek and Arntzen 1992, De Jong 1998, Sloan et al. 2014) reveals complex origins and evolutionary histories of temperate taxa in relation with the complex paleoecological history of the area. High levels of species diversity are related to ancient events (Paleocene-Miocene) and also to more recent events (Pliocene-Pleistocene) followed by active speciation and even explosive radiations, leading finally to the emergence of the so-called “Mediterranean Sanctuary” of diversity, the second largest hotspot in the world and

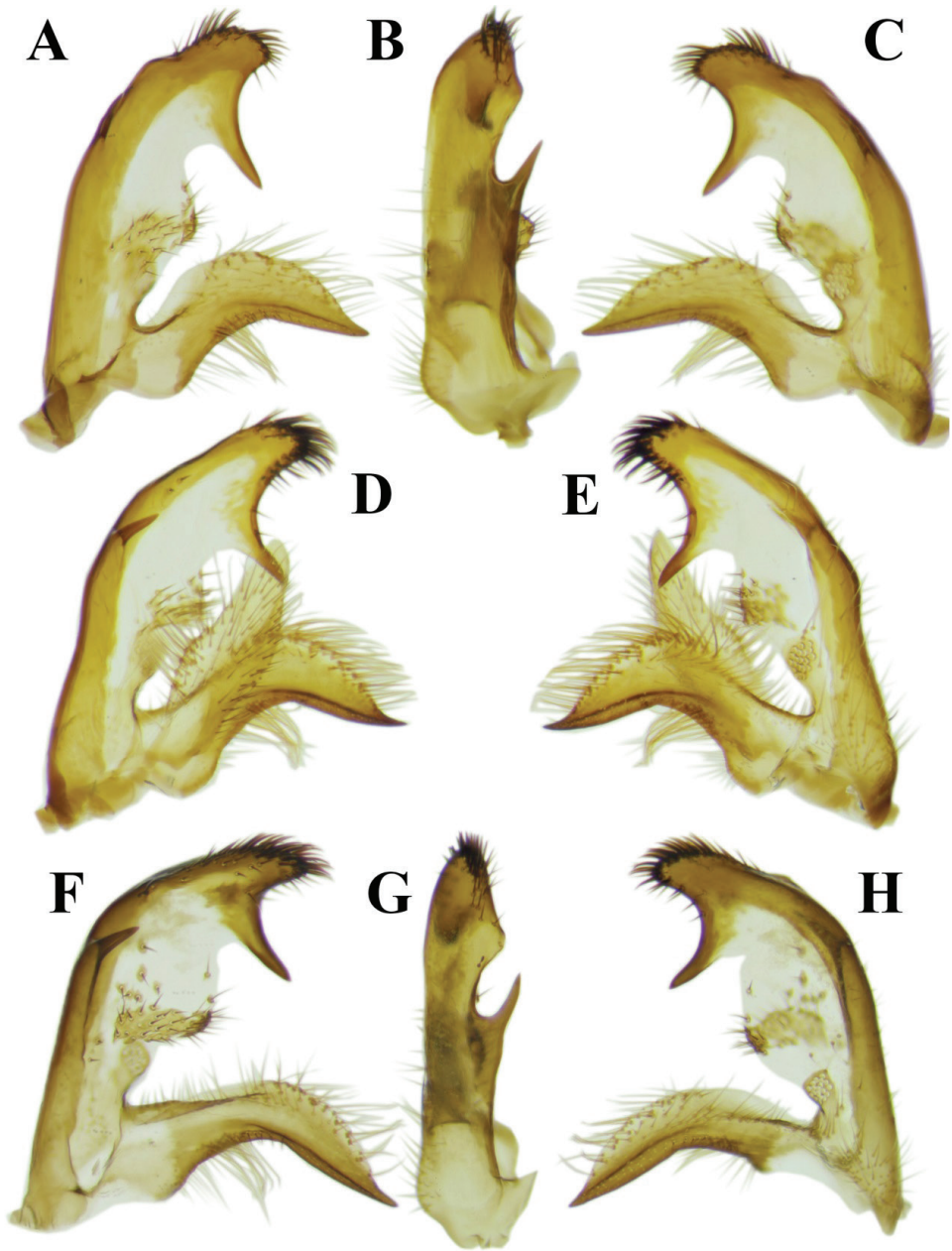


Figure 6. Photographs of the morphological structures of the male genital structures of individuals of *Tipula (Mediotipula) stigmatella* Schummel, 1833. Specimen from Kavala (Greece) **A, B, C** Specimen from Lunca Bradului (Romania) **D, E**; Specimen from Kulata (Bulgaria) (**F, G, H**) **A, F** inner gonostylus outer lateral view **B, G** inner gonostylus ventral view **C, H** inner gonostylus inner lateral view **D** gonostyli outer lateral view **E** gonostyli inner lateral view.

the largest of the world's five Mediterranean-climatic regions (Grabowski et al. 2017, Vargas et al. 2018). Albania belongs to the Eastern Mediterranean chorotype of the fauna, as proposed by Taglianti et al. (1999) including the NE-Mediterranean, Palestino-Cyprioto-Taurian, Palestino-Taurian, and Aegean distribution patterns of different animal species.

The eastern Mediterranean area, where the new member of the subgenus *Mediotipula* was collected, is recognised as an important centre of endemism, but no range-restricted *Mediotipula* species were detected in the area to date. *Tipula* (*M.*) *gjipeensis* sp. n. was identified by us only in a small, humid limestone gorge in Albania. We hypothesised a restricted distribution of the species, most probably as a result of the presently isolated distribution of humid ecosystems in the Mediterranean area. Several aquatic and semi-aquatic organisms have similarly restricted or fragmented distributions in the Mediterranean area, which most probably followed the general decline of humid ecosystems during the late Cainozoic and simultaneous retreat in highly-fragmented local populations (sometimes highly-divergent evolutionary significant units, or in many cases distinct species) (Fernandez-Mazuecos et al. 2014, Godunko et al. 2017, Neubauer et al. 2016).

However, a number of case studies on plant species (Allegrucci et al. 2017, Crowl et al. 2015) hypothesise an evolutionary process in lineages that are adapted to pre-Mediterranean (pre-Pliocene) conditions in relatively small, xeric areas. Later, they became strongly competitive and expanded as the Mediterranean climate became dominant (Pliocene-Quaternary) across the Mediterranean Basin, and most probably also began to penetrate into the northern parts of Europe. Similar patterns were detected in the case of the *Lacerta viridis* complex (Cassel-Lundhagen 2010), with leading edge populations that colonised large parts of Europe, but several fringe populations became genetically divergent or morphologically different in highly isolated populations in the Balkan area. This pattern is also most likely true for the sibling pairs *T.* (*M.*) *stigmatella* / *T.* (*M.*) *gjipeensis*, with a larger distribution in the south-central part of Europe to Caucasus, but with morphologically deeply divergent *T.* (*M.*) *gjipeensis* from Albania, and less, but notable morphological differences between populations of *T.* (*M.*) *stigmatella* in the Balkan area, identified for example in Kavala (Greece) and Kulata (Bulgaria) (Figure 6B, G). The presence of morphologically divergent allopatric populations of *T.* (*M.*) *stigmatella* (possibly cryptic species) is likely a result of more recent isolation, followed by repeated dispersions and area fragmentations during the Pleistocene climate change. This needs to be subjected to a more comprehensive analyses of the species over its whole range.

Faunistic and ecological notes

Albania is located in the western part of the Balkan Peninsula and is one of the most important Mediterranean biodiversity hotspots (Caković et al. 2018, Szabolcs et al. 2017), but is still considered to be the last “terra incognita” for European biodiversity. A series of recent studies, which focused on different groups of plants and animals,

brings major contributions to the diversity and distribution of a number of organisms from Albania (Barina et al. 2013, Graf et al. 2018, Kaltsas et al. 2008, Stevanović et al. 2007). The description of *T. Mediotipula gjipeensis* sp. n. is an important addition to the faunal list of the Albanian Tipulidae and highlights the importance of similarly isolated pristine ecosystems to local and regional diversity of the Mediterranean Area.

Ecological demands of the majority of *Mediotipula* species are largely overlooked because of a high number of undescribed larvae. Based on adult distributions, species inhabiting open woods and hedges exposed to the sun seem to have generally larger distributions (e.g., *T. (M.) stigmatella*, *T. (M.) sarajevensis* etc.) in comparison with species that are restricted to steep river valleys (e.g., *T. (M.) brolemani*, *T. (M.) mikiana*, *T. (M.) gjipeensis* sp. n.) (Oosterbroek 2018). Such humid and sheltered “ecological islands” set in larger xeric areas could act as refuges for a number of range-restricted or endemic species. For example, within the steep Gjipe Gorge (only a few kilometres in length), other than *T. (M.) gjipeensis*, the Mediterranean cranefly species *Dolichopeza (D.) furiscipes* Bergroth, 1889 was also detected (L Keresztes unpublished data), having a fragmented distribution in similar habitats in the southern part of continental Europe, but also on some Mediterranean islands (Mederos Lopez 2012, Oosterbroek 2018). The mayfly *Electrogena hellenica* Zurwerra & Tomka, 1986 has an even more restricted distribution in the Mediterranean area which is limited to western Greece, along rivulets in steep valleys at 300 m a.s.l. (Bauernfeind and Soldan 2012), but which was also collected by the first author of this paper from the Gjipe Gorge (L Keresztes unpublished data). Similar ecosystems in the Mediterranean area are rare and isolated but they are seriously affected by human activity (limestone and rock quarries, water extraction, habitat deterioration, discharge of sewage effluents, etc.) enforced by ongoing global climate change and therefore needing special attention and perhaps protection.

Acknowledgements

We thank Pete Boardman and Matthey Coupley for linguistic revisions and comments. We thank Herman de Jong, Pjotr Oosterbroek, and Jukka Salmela for their valuable comments on an earlier version of the manuscript, improving considerably the final form, as well as a number of anonymous reviewers for their help. Special thanks go to the subject editor Christopher Borkent for careful review and supporting the publication of the paper. During the preparation of the manuscript, LP Kolcsár and E Török received financial support from the Eötvös Loránd University, Hungary.

References

Allegrucci G, Ketmaier V, Di Russo C, Rampini M, Sbordon V, Cobolli M (2017) Molecular phylogeography of *Troglophilus* cave crickets (Orthoptera, Rhabdophoridae): A com-

- bination of vicariance and dispersal drove diversification in the Eastern Mediterranean region. *Journal of Zoological Systematics and Evolutionary Research* 57: 1–16. <https://doi.org/10.1111/jzs.12172>
- Barina Z, Rakaj M, Pifkó D (2013) Contributions to the fauna of Albania, 4. *Willdenowia* 43: 165–184. <https://doi.org/10.3372/wi.43.43119>
- Bauernfeind E, Soldán T (2012) *The Mayflies of Europe (Ephemeroptera)*. Apollo Books, New York, 783 pp.
- Caković D, Stešević D, Schönswetter P, Frajman B (2018) Long neglected diversity in the Accursed Mountains of northern Albania: *Cerastium hekuravense* is genetically and morphologically divergent from *C. dinaricum*. *Plant Systematics and Evolution* 304: 57. <https://doi.org/10.1007/s00606-017-1448-1>
- Cassel-Lundhagen A (2010) Peripheral Relict Populations of Widespread species: Evolutionary Hotspots or just more of the same? In: Habel JC, Assmann T (Eds) *Relict Species – Phylogeography and Conservation Biology*. Springer-Verlag, Berlin-Heidelberg, 1–451. https://doi.org/10.1007/978-3-540-92160-8_15
- Crowl AA, Visger CJ, Mansion G, Hand R, Wu HH, Kamari G, Phitos D, Cellinese N (2015) Evolution and biogeography of the endemic Roucela complex (Campanulaceae: Campanula) in the Eastern Mediterranean. *Ecology and Evolution* 5(22): 5329–5343. <https://doi.org/10.1002/ece3.1791>
- Dufour C (1986) *Lest Tipulidae de Suisse (Diptera, Nematocera)*. *Documenta Faunistica Helvetica* 2: 1–187.
- Fernandez-Mazuecos M, Jimenez-Mejias P, Rotllan-Puig X, Vargas P (2014) Narrow endemics to Mediterranean islands: moderate genetic diversity but narrow climatic niche of the ancient, critically endangered *Naufraga* (Apiaceae). *Perspectives in Plant Ecology, Evolution and Systematics* 16: 190–202. <https://doi.org/10.1016/j.ppees.2014.05.003>
- Godunko RJ, Soldán T, Staniczek AH (2017) *Baetis (Baetis) cypronix* sp. n., a new species of the *Baetis alpinus* species group (Insecta, Ephemeroptera, Baetidae) from Cyprus, with annotated checklist of Baetidae in the Mediterranean islands. *ZooKeys* 644: 1–32. <https://doi.org/10.3897/zookeys.644.10413>
- Graf W, Pauls SU, Vitecek S (2018) *Isoperla vjosae* sp. n., a new species of the *Isoperla tripartita* group from Albania (Plecoptera: Perlodidae). *Zootaxa* 4370(2): 171–179. <https://doi.org/10.11646/zootaxa.4370.2.5>
- Grabowski M, Mamos T, Bącela-Spychalska K, Rewicz T, Wattier R (2017) Neogene paleogeography provides context for understanding the origin and spatial distribution of cryptic diversity in a widespread Balkan freshwater amphipod. *PeerJ* 5: e3016. <https://doi.org/10.7717/peerj.3016>
- Hewitt GM (2011) Chapter 7. Mediterranean Peninsulas: The Evolution of Hotspots. In: Zachos FE, Habel JC (Eds) *Biodiversity Hotspots. Distribution and Protection of Conservation Priority Areas*. Springer-Verlag, Berlin-Heidelberg, 123–147. https://doi.org/10.1007/978-3-642-20992-5_7
- Höchstetter L (1963) Beiträge zur Biologie, Oekologie und Systematik der Tipuliden-Larven (Diptera). *Sitzungsberichten der Physikalisch-Medizinischen Societat zu Erlangen* 82: 33–112.
- Jong de H (1995) The phylogeny of the subgenus *Tipula (Mediotipula)* (Diptera, Tipulidae). *Tijdschrift voor Entomologie* 138: 269–282.

- Jong de H (1998) In search of the historical biogeographic patterns in the western Mediterranean terrestrial fauna. *Biological Journal of the Linnean Society* 65: 99–164. <https://doi.org/10.1006/bijl.1998.0239>
- Kaltsas D, Stathi I, Fet V (2008) Scorpions of the Eastern Mediterranean – Advances in Arachnology and Developmental Biology. In: Makarov SE, Dimitrijević RN (Eds) Papers dedicated to Prof. Dr. Božidar Ćurčić. Inst. Zool., Belgrade; BAS, Sofa; Fac. Life Sci., Vienna; SASA, Belgrade & UNESCO MAB Serbia. Vienna, Belgrade, Sofa, Monographs 12: 209–246.
- Kolcsár LP, Veres R, Keresztes L (2018) The TransDiptera Online Database. <https://doi.org/10.18426/OBM.5sskml13ip0> [Accessed on: 01.03.2018]
- Kraitsek S, Klossa-Kilia E, Papisotiropoulos V, Alahiotis SN, Kiliass G (2008) Genetic Divergence Among Marine and Lagoon *Atherina boyeri* Populations in Greece Using mtDNA Analysis. *Biochemical Genetics* 46(11–12): 781–798. <https://doi.org/10.1007/s10528-008-9193-3>
- Markova S, Sanda R, Crivelli A, Shumka S, Wilson IF, Vukic J, Berrebi P, Kotlik P (2010) Nuclear and mitochondrial DNA sequence data reveal the evolutionary history of *Barbus* (Cyprinidae) in the ancient lake systems of the Balkans. *Molecular Phylogenetics and Evolution* 55: 488–500. <https://doi.org/10.1016/j.ympev.2010.01.030>
- Mederoz López J (2012) First record of *Dolichozeza* (*Dolichozeza*) *fuscipes* Bergroth, 1889 (Diptera: Tipulidae) from Minorca, Balearic Islands (Spain). *Boletín de la Sociedad Entomológica Aragonesa* 50: 567–568.
- Neubauer TA, Georgopoulou E, Harzhauser E, Mandic MO, Kroh A (2016) Measurements of gastropods shell sizes from 23 fossil and extant long-lived lakes. *PANGAEA*. <https://doi.org/10.1594/PANGAEA.858575>
- Oosterbroek P (2018) Catalogue of the Crane flies of the World (Insecta, Diptera, Nematocera, Tipuloidea). <http://ccw.naturalis.nl/> [Accessed on: 07.02.2018]
- Oosterbroek P, Arntzen JW (1992) Area cladograms of Circum-Mediterranean taxa in relation to Mediterranean paleogeography. *Journal of Biogeography* 19: 3–20. <https://doi.org/10.2307/2845616>
- Pinkert S, Dijkstra KD, Zeuss D, Reudenbach C, Brandl R, Hof C (2017) Evolutionary processes, dispersal limitations and climatic history shape current diversity patterns of European dragonflies. *Ecography* 40: 1–10. <https://doi.org/10.1111/ecog.03137>
- Previšić A, Graf W, Vitecek S, Kučinić M, Bálint M, Keresztes L, Pauls SU Waringer J (2014) Cryptic diversity of caddisflies in the Balkans: the curious case of *Ecclisopteryx* species (Trichoptera: Limnephilidae). *Arthropod Systematics and Phylogeny* 72: 309–329.
- Rodriguez-Ramirez J, Santonja M, Baldi V, Ballini C, Montez N (2017) Shrub species richness decreases negative impacts of drought in a Mediterranean ecosystem *Journal of Vegetation Science*. <https://doi.org/10.1111/jvs.12558>
- Savchenko EN (1966) On the distribution, ecology and preimaginal phases of the crane fly *Tipula* (*Mediotipula*) *bidens* Bergr. (Diptera, Tipulidae). *Entomologicheskoe Obozrenie* 45: 286–293.
- Savchenko EN (1979) Phylogenie und Systematik der Tipulidae. Translated and revised by Br. Theowald and G. Theischinger. *Tijdschrift voor Entomologie* 122: 91–126.
- Savchenko EN (1983) Crane-flies (Fam. Tipulidae), Introduction, Subfam. Dolichozezinae, subfam. Tipulinae (start). *Fauna USSR, N.S.* 127, Nasekomye Dvukrylye [Diptera] 2(1–2): 1–585.

- Sloan S, Jenkins CI, Joppa LN, Gaveau DLA, Laurance WF (2014) Remaining natural vegetation in the global biodiversity hotspots. *Biological Conservation* 177: 12–24. <https://doi.org/10.1016/j.biocon.2014.05.027>
- Stevanović V, Kit T, Petrova A (2007) Mapping the endemic fora of the Balkans – a progress report. *Bocconea* 21: 131–137.
- Szabolcs M, Mizsei E, Jablonski D, Vági B, Mester B, Végvári Zs, Lengyel Sz (2017) Distribution and diversity of amphibians in Albania: new data and foundations of a comprehensive database. *Amphibia-Reptilia* 38: 435–448. <https://doi.org/10.1163/15685381-00003126>
- Taglianti V, Audisio A, Biondi PA, Bologna M, Carpaneto MA, Biase A, Fattorini AD, Piattella S, Sindaco E, Venchi R, Zapparoli AM (1999) A proposal for a chorotype classification of the Near East fauna, in the framework of the Western Palearctic Region. *Biogeographia* 20: 31–59. <https://doi.org/10.21426/B6110172>
- Theowald B (1967) Familie Tipulidae (Diptera, Nematocera). Larven und Puppen. *Bestimmungsbucher zur Bodenfauna Europas* 7: 1–100.
- Theowald B (1978) 15. Tipulidae. In: Lindner E (Ed.) *Die Fliegen der palaearktischen Region* 3(5)1, Lief. 318: 405–436.
- Triantis KA, Mylonas M, Weiser MD, Lika K, Verdinoyannis K (2005) Species richness, environmental heterogeneity and area: a case study based on land snails in Skyros archipelago (Aegean Sea, Greece). *Journal of Biogeography* 32: 1727–1735. <https://doi.org/10.1111/j.1365-2699.2005.01322.x>
- Vargas P, Fernández-Mazuecos M, Heleno R (2018) Phylogenetic evidence for a Miocene origin of Mediterranean lineages: species diversity, reproductive traits and geographical isolation. *Plant Biology* 20(1): 157–165. <https://doi.org/10.1111/plb.12626>
- Zachos FE, Habel JC (2011) *Biodiversity of Hotspots. Distribution and Protection of Conservation Priority Areas*. Springer-Verlag, Berlin-Heidelberg, 546 pp.

Low genetic diversity in broodstocks of endangered Chinese sucker, *Myxocyprinus asiaticus*: implications for artificial propagation and conservation

Dongqi Liu^{1,2}, Yu Zhou¹, Kun Yang¹, Xiuyue Zhang¹, Yongbai Chen³, Chong Li³, Hua Li⁴, Zhaobin Song^{1,5}

1 Sichuan Key Laboratory of Conservation Biology on Endangered Wildlife, College of Life Sciences, Sichuan University, Chengdu 610065, PR China **2** School of Biological and Chemical Engineering, Panzhuhua University, Panzhuhua 617000, PR China **3** China Three Gorges Corporation, Beijing 100038, PR China **4** Fisheries Research Institute, Sichuan Academy of Agricultural Sciences, Chengdu 611731, PR China **5** Key Laboratory of Bio-Resources and Eco-Environment of Ministry of Education, College of Life Sciences, Sichuan University, Chengdu 610065, PR China

Corresponding author: Zhaobin Song (zbsong@scu.edu.cn)

Academic editor: M.E. Bichuette | Received 31 January 2018 | Accepted 21 September 2018 | Published 23 October 2018

<http://zoobank.org/14FC8819-4ABA-4C2D-B713-35C825B8390F>

Citation: Liu D, Zhou Y, Yang K, Zhang X, Chen Y, Li C, Li H, Song Z (2018) Low genetic diversity in broodstocks of endangered Chinese sucker, *Myxocyprinus asiaticus*: implications for artificial propagation and conservation. ZooKeys 792: 117–132. <https://doi.org/10.3897/zookeys.792.23785>

Abstract

The releasing program of Chinese sucker (*Myxocyprinus asiaticus*) has been conducted for years in China. To prevent loss of genetic variation in wild populations, it is important to assess and monitor genetic diversity of broodstocks before release of offspring. Three broodstocks (Pixian Base of Sichuan Fisheries Research Institute, China (PBS), Yibin Base of Sichuan Fisheries Research Institute, China (YBS) and Yibin Rare Aquatic Animal Research Institute, China (YRA)) were investigated using mitochondrial control region and 12 microsatellites. The relatively low genetic diversities of these broodstocks were detected (PBS, haplotype diversity (h) = 0.877, observed heterozygosity (H_o) = 0.416; YBS, h = 0.812, H_o = 0.392; YRA, h = 0.818, H_o = 0.365). PBS showed higher H_o than YBS and YRA ($P < 0.05$). Genetic divergence (F_{ST}) based on microsatellites between PBS and YRA was significant ($F_{ST} = 0.1270$, $P < 0.05$), the same situation happened between YBS and YRA ($F_{ST} = 0.1319$, $P < 0.05$). However, divergence between PBS and YBS was not significant ($F_{ST} = 0.0029$, $P > 0.05$). Structure analysis revealed that YRA were distinct from PBS and YBS. Based on these results, it is important to propose some suggestions of genetic management for artificial propagation of Chinese sucker, such as broodstock exchange among hatcheries and broodstock supplement from wild.

Keywords

genetic management, genetic varieties, *Myxocyprinus asiaticus*, parent fish, resources protection

Introduction

Myxocyprinus asiaticus (Nelson, 1976), an endangered freshwater fish in China and the only representative of the family Catostomidae in Asia (Nelson 1976; Wang 1998), is distributed mainly in the Yangtze River drainage (Ding 1994). It used to be an important part of fish catches in its distribution areas (Zhang et al. 2000; Zhu et al. 2009). But since 1970s, natural reproduction and resources of *M. asiaticus* have dramatically declined due to some anthropogenic factors, such as habitat destruction, water pollution, and over fishing (Zhang et al. 1999, 2000; Zhang and Zhao 2000; Jiang and Yu 2003; Gan et al. 2011). Therefore, *M. asiaticus* was listed as second class national protected animal in China (Wang 1998; Wang and Xie 2004).

In order to restore the wild resources in the Yangtze River drainage, artificial propagation of *M. asiaticus* has been carried out since the 1970s, and a releasing program on a large scale was conducted first in 1996 (Zhang et al. 2000; Zhu et al. 2009). Release of hatchery reared individuals may increase the productivity of fishery, accelerate recovery of depleted stocks, and ensure the survival of stocks threatened with extinction (Ireland et al. 2002). But without genetic management, genetic variation of the hatchery juveniles will be reduced, which may have negative impacts on wild populations after releasing (Gow et al. 2011; Ortega-Villaizan et al. 2011). An effective restocking program for endangered fish populations requires not only the increase of quantity, but also a broad recovery of their genetic diversities (Vrijenhoek et al. 1985). For example, studies on genetic management of *Hucho hucho* and *Salvelinus alpinus* have been launched in Europe or North America (Blackie et al. 2011; Kucinski et al. 2015). However, compared to nearly 20-year history (since 1996) of artificial breeding and releasing of *M. asiaticus*, genetic management studies on broodstocks are very limited. The genetic investigation has only been carried out in a few broodstocks of *M. asiaticus* (Xu et al. 2013), and the genetic management has so far almost not been considered.

Because wild individuals were difficult to obtain in recent years and the qualified parental fish used in propagation were limited, some of first generation offspring of *M. asiaticus* were supplemented as broodstocks for artificial propagation (Wu 2014). Besides, there were almost no detailed archives of each individual in those broodstocks, so effective management could not be executed and genetic variation of the hatchery stock may be reduced. The situation would be more serious after several generations of artificial propagation.

Wu (2014) reported the genetic diversity of three wild populations (Wanzhou, Mudong, and Luzhou; Figure 1) based on mtDNA control region and microsatellites. The genetic diversity of broodstocks needs to be compared with that of wild populations, which is very important for artificial propagation and wild conservation of the species. Previous studies based on microsatellite markers reported low genetic diversity and weak differentiation in broodstocks of *M. asiaticus*, which were mainly collected from

middle Yangtze River (Xu et al. 2013). However, as the major participator of releasing program in upper Yangtze River, broodstocks in Sichuan Province have not been investigated and managed systematically yet. It was far from enough for genetic analysis of Chinese sucker broodstocks. In this study, by means of mitochondrial control region and 12 microsatellite markers, we present a genetic study of three broodstocks of *M. asiaticus* from different local hatcheries in Sichuan. Our objectives are (i) to assess the genetic diversity and relationship of the broodstocks; (ii) to propose suggestions of genetic management for artificial propagation, and (iii) to provide necessary information for genetic conservation for implementation hatchery release program in the future.

Materials and methods

Sample collection

A total of 134 individuals of *M. asiaticus* were used in this study, including 53 (15 males and 38 females) sampled from the Yibin Base of Sichuan Fisheries Research Institute, China (**YBS**), 60 (22 males and 38 females) from the Pixian Base of Sichuan Fisheries Research Institute, China (**PBS**) and 21 (7 males and 14 females) from the Yibin Rare Aquatic Animal Research Institute, China (**YRA**) (Fig. 1). Fin clips of each individual were sampled and stored in 95% ethanol during 2013 – 2015. Some individuals of YBS are wild ones captured from the Yibin range of the Jinsha River, and from Yibin and Nanxi range of Yangtze River in middle of 1990s (Figure 1) and most are first generation offspring of wild *M. asiaticus* that were artificially propagated and reared in YBS for more than ten years. Some individuals of PBS are first generation offspring of wild *M. asiaticus* artificially propagated in YBS and reared for more than ten years as well. The rest individuals of PBS are wild, but their sources are unclear. All individuals of YRA are wild ones captured from Nanxi and Jiang'an range of the Yangtze River (Figure 1) in middle of 1990s.

In addition, the artificially propagated Chinese suckers were firstly released into the Yangtze River in 1996. The released juveniles were much smaller than the wild originated individuals when they were captured from the rivers. Therefore, it is not likely that wild collected broodstocks included some artificially released ones or hybridized ones of artificially breeding broodstock and wild populations.

DNA extraction and PCR amplification

Total genomic DNA was extracted from the fin clips of *M. asiaticus* using TIANamp marine animals DNA Kit (TIANGEN, China). Polymerase chain reaction (PCR) was used to amplify the mitochondrial control region with the primers DL1 (ACCCCTG-GCTCCCAAAGC, Ta: 61°C) and DH2 (ATCTTAGCATCTTTCAGTG, Ta: 61°C) (Liu et al. 2002). The PCR protocol followed Wu et al. (2016). PCR products were purified using E.Z.N.A. Gel Extraction Kit (OMEGA, USA) and then directly sequenced on an ABI 3730 Genetic Analyzer (Applied Biosystems, China).

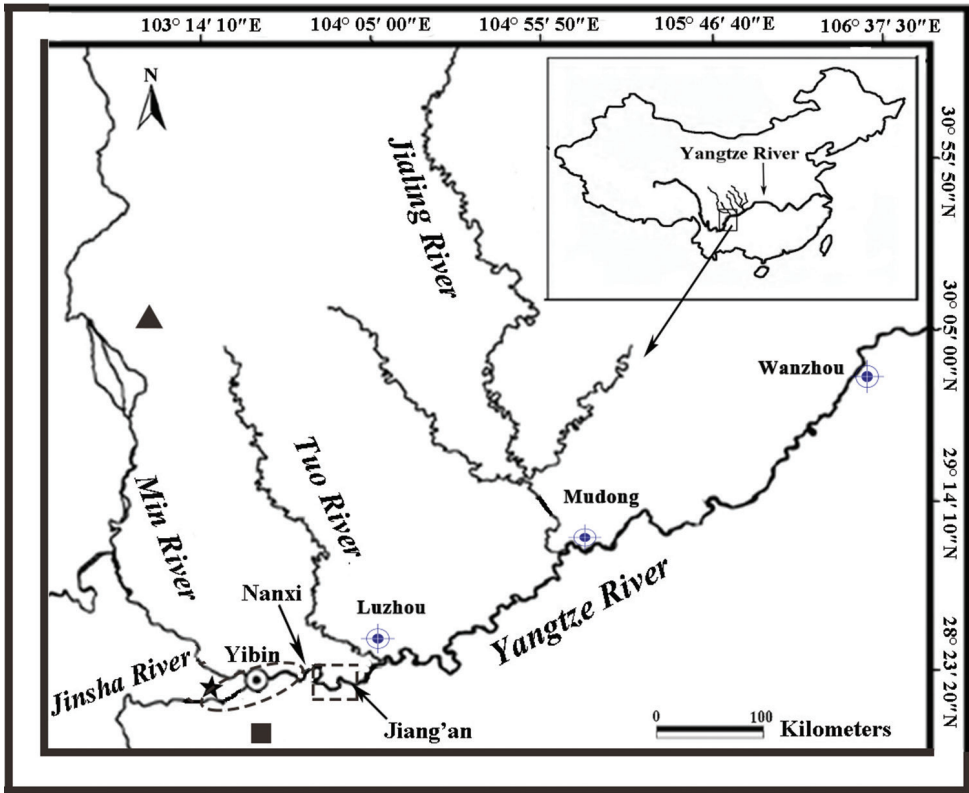


Figure 1. Map of sampling sites for the three *Myxocyprinus asiaticus* broodstocks. Key: black triangle Pixian Base of Sichuan Fisheries Research Institute, China (PBS); black star Yinbin Base of Sichuan Fisheries Research Institute, China (YBS); black square Yibin Rare Aquatic Animal Research Institute, China (YRA); broken circle river range where the wild broodstocks source of YBS; broken rectangle river range where the wild broodstocks source of YRA.

Twelve microsatellite loci (Yang et al 2009; Chen et al 2010) were used for analyses. The total PCR reaction volume was 25 μL contained 1 μL genomic DNA (50 ng/ μL), 3 μL 10 \times PCR buffer (plus Mg^{2+}), 1 μL dNTPs (10 mmol/L each), 0.5 μL for each primer (10 $\mu\text{mol/L}$), 0.5 U Taq DNA polymerase (TaKaRa, Japan), and 18.7 μL ddH₂O. PCR was programmed as follows: 94 $^{\circ}\text{C}$ for 5 min, followed by 35 cycles at 94 $^{\circ}\text{C}$ for 30 s, 54–63 $^{\circ}\text{C}$ for 40 s, 72 $^{\circ}\text{C}$ for 30 s, and a final extension at 72 $^{\circ}\text{C}$ for 10 min. Electrophoresis, fluorescent microsatellite detection and determination of genotypes were as described in Chen et al. (2010).

Data analysis

All mitochondrial control region sequences were aligned using Mega version 5.0 (Kumar et al. 2004) and refined manually. Nucleotide composition, number of polymor-

phic sites (v), haplotype diversity (h) and nucleotide diversity (π) (Nei 1987) were used to evaluate the genetic diversity of samples, and were estimated by DNASP version 4.10.7 (Rozas et al. 2003). We used two methods to construct the phylogenetic trees of the haplotypes: maximum likelihood method (ML) by PAUP version 3.1.1 (Swofford 2002) and Bayesian inferences (BI) by MRBAYES version 3.1.2 (Huelsenbeck and Ronquist 2001). Control region sequences of *Catostomus commersonii* (GenBank No. AB127394) and *Cycleptus elongates* (GenBank No. EF062437) were obtained from GenBank and used as outgroups. The relationships among the haplotypes were evaluated by NETWORK version 4.2.0.6 (Bandelt et al. 1999). Genetic distances among broodstocks were calculated by MEGA version 5.0 (Kumar et al. 2004).

To estimate genetic diversity of the three broodstocks and genetic differentiation among them, numbers of alleles (**A**), allelic richness within individuals (**Ai**), expected and observed heterozygosities (**Ho** and **He**) were calculated using the software AUTOTET which is especially developed for autotetraploid species (Thrall and Yong 2000; Seeber et al. 2014; Hopley et al. 2015; Liu et al. 2015; Qiang et al. 2015). The genetic diversities of the broodstocks were compared with that of the wild populations investigated by Wu (2014) and the broodstocks investigated by Xu et al. (2013). Paired *t*-test was used to evaluate whether significant differences of diversity indices occurred among populations (Jansson et al. 2012). The number of rare alleles and private alleles were calculated by Convert version 1.31 (Glaubitz 2004). Exact tests for Hardy–Weinberg equilibrium and tests for linkage disequilibrium were conducted using GENEPOP version 4.0 (Raymond and Rousset 1995). Null alleles were tested in MICROCHRCHEER version 2.2 (Oosterhout et al. 2004). To evaluate the amount of genetic variation among and within broodstocks, an analysis of molecular variance (AMOVA) was conducted in ARLEQUIN version 3.11 (Excoffier et al. 2005). Pairwise F_{ST} were also calculated in ARLEQUIN version 3.11. F_{IS} were calculated for polymorphic loci using FSTAT version 2.932 (Goudet 2002). A test for bottleneck assessment was conducted using the BOTTLENECK version 1.9 (Piry et al. 1999). Neighbor-joining tree of broodstocks and relationship of individuals was constructed in MEGA version 5.0. Clustering procedure was performed to infer the relationship of broodstocks in STRUCTURE version 2.3 (Pritchard et al. 2000). We set the number of clusters (K) to vary initially from 1 to 8 (ten replicates for each K). Each run started with a burn-in period of 100,000 steps followed by 1,000,000 Markov Chain Monte Carlo (MCMC) steps. Finally, the Delta K method in STRUCTURE HARVESTER (Earl et al. 2012) was used to infer the optimal K value.

Results

Genetic diversity

Control region sequences for 134 individuals of *M. asiaticus* were acquired and the aligned sequences were 947 base pairs (bp) in length. The number of variable sites was

Table 1. Information of the three *Myxocyprinus asiaticus* broodstocks and genetic diversity.

Broodstock	N	n	h	π	Ra	Pa	F _{IS}	P
PBS	60	19	0.877	0.0260	8	4	0.055	0.421
YBS	53	13	0.819	0.0238	10	2	0.067	0.390
YRA	21	11	0.818	0.0278	11	13	0.088	0.085
Total	134	30	0.864	0.0287	29	19		

N: sample number, n: number of haplotypes, h: haplotype diversity, π : nucleotide diversity, Ra: rare alleles for microsatellites, Pa: private alleles for microsatellites, FIS: mean inbreeding coefficients for microsatellites, P: the p value of FIS

82 (71, 68, 65 in PBS, YBS, YRA, respectively). Most polymorphic sites were transitional mutations, and only a few were transversions or inserts/deletions. The average nucleotide difference was 24.1%. The average base composition was A = 28.5 %, T = 31.4 %, C = 22.4 % and G = 17.7 %. The haplotype diversity and nucleotide diversity was 0.864 and 0.028 across all samples, respectively (Table 1). PBS showed higher haplotype diversity (h = 0.877) than that of YBS and YRA (h = 0.812 and 0.818, respectively) (Table 1). However, YRA possessed higher nucleotide diversity (0.0278) than that of PBS and YBS (Table 1).

Among the 12 microsatellites, one locus (MA61) was monomorphic in all broodstocks, two (MA53, MA39) were monomorphic in PBS and YBS, and one (MA21) was monomorphic in YRA. The number of amplified alleles per locus ranged from 1 (MA61) to 16 (MA27) with an average of 8.1, and allele richness per locus varied from 1.00 at locus MA61 in PBS to 2.00 at locus MA64 in YBS (Table 2). Average observed heterozygosity (Ho) ranged from 0.365 in YRA to 0.416 in PBS. Under both chromosome segregation and chromatid segregation, average values of Ho were lower than those of expected heterozygosities (He) in all broodstocks (Table 2), and average values of the fixation index estimated over all loci were positive in all broodstocks analyzed, suggesting a deficit of heterozygotes in all broodstocks. Total 29 rare alleles and 19 private alleles were identified in the three broodstocks. The number of rare alleles ranged from 8 to 11, and the number of private alleles ranged from 2 to 13 (Table 1). YRA possesses most private alleles (13) and almost half rare alleles (11) (Table 1).

The broodstocks from middle Yangtze River were investigated based on same microsatellites, and Average He ranged from 0.443 to 0.523 (Xu et al. 2013), which were higher than that of the three broodstocks in the present study (paired *t*-test, $P < 0.05$). Wu (2014) reported the genetic diversity of three wild populations (Wanzhou, Mudong, and Luzhou) based on mtDNA control region and same microsatellites. Wanzhou showed higher haplotype diversity (h = 0.975) than that of Mudong and Luzhou (h = 0.905 and 0.899, respectively). Average PIC ranged from 0.779 in Luzhou to 0.816 in Wanzhou. Compared to wild populations of *M. asiaticus* (Wu 2014; Wu et al. 2016), lower genetic diversities (Ai, G, Ho, He, PIC) in the broodstocks were found in present study (paired *t*-test, $P < 0.05$).

Table 2. Genetic diversity of the *Myxocyprinus asiaticus* broodstocks based on twelve microsatellite loci.

Broodstock	Locus	A	Ai	G	Ho	He(Ce)	He(Cd)	PIC
PBS	MA21	5	1.933	13	0.622	0.732	0.683	0.684
	MA10	6	1.650	11	0.433	0.623	0.582	0.575
	MA61	1	1.000	1	0.000	0.000	0.000	0.000
	MA06	2	1.567	3	0.378	0.420	0.392	0.331
	MA19	7	1.867	17	0.578	0.818	0.764	0.793
	MA53	1	1.000	1	0.000	0.000	0.000	0.000
	MA39	1	1.000	1	0.000	0.000	0.000	0.000
	MA64	3	1.983	3	0.656	0.516	0.481	0.398
	MA04	9	1.717	20	0.478	0.816	0.762	0.791
	MA38	3	1.600	5	0.400	0.584	0.545	0.519
	MA27	16	2.683	35	0.758	0.902	0.842	0.894
	MA13	10	2.333	19	0.683	0.824	0.769	0.805
Means	5	1.694	11	0.416	0.520	0.485	0.483	
YBS	MA21	4	1.900	8	0.600	0.726	0.678	0.676
	MA10	5	1.833	7	0.556	0.664	0.620	0.602
	MA61	1	1.000	1	0.000	0.000	0.000	0.000
	MA06	2	1.367	3	0.244	0.406	0.379	0.323
	MA19	7	1.733	9	0.489	0.699	0.652	0.646
	MA53	1	1.000	1	0.000	0.000	0.000	0.000
	MA39	1	1.000	1	0.000	0.000	0.000	0.000
	MA64	2	2.000	1	0.667	0.500	0.467	0.398
	MA04	7	1.833	9	0.556	0.681	0.636	0.375
	MA38	3	1.633	5	0.422	0.531	0.496	0.519
	MA27	13	2.733	15	0.761	0.888	0.829	0.877
	MA13	5	1.633	9	0.406	0.676	0.631	0.609
Means	4	1.639	6	0.392	0.481	0.449	0.419	
YRA	MA21	1	1.000	1	0.000	0.000	0.000	0.000
	MA10	6	1.710	10	0.476	0.718	0.670	0.386
	MA61	1	1.000	1	0.000	0.000	0.000	0.000
	MA06	6	1.760	10	0.508	0.782	0.730	0.431
	MA19	3	1.140	4	0.095	0.534	0.498	0.384
	MA53	2	1.710	2	0.476	0.459	0.429	0.321
	MA39	8	1.810	10	0.540	0.756	0.706	0.598
	MA64	3	1.950	4	0.635	0.618	0.577	0.378
	MA04	3	1.000	3	0.000	0.594	0.554	0.711
	MA38	6	1.760	10	0.508	0.724	0.676	0.739
	MA27	7	2.000	6	0.667	0.811	0.757	0.788
	MA13	3	1.710	4	0.476	0.582	0.543	0.711
Mean	4	1.550	5	0.365	0.548	0.512	0.454	

A: number of alleles per locus, Ai: allelic richness within individuals, G: genotype richness, Ho: observed heterozygosity, He (Ce): expected heterozygosity under chromosome segregation, He (Cd): expected heterozygosity under chromatid segregation, PIC: polymorphism information content

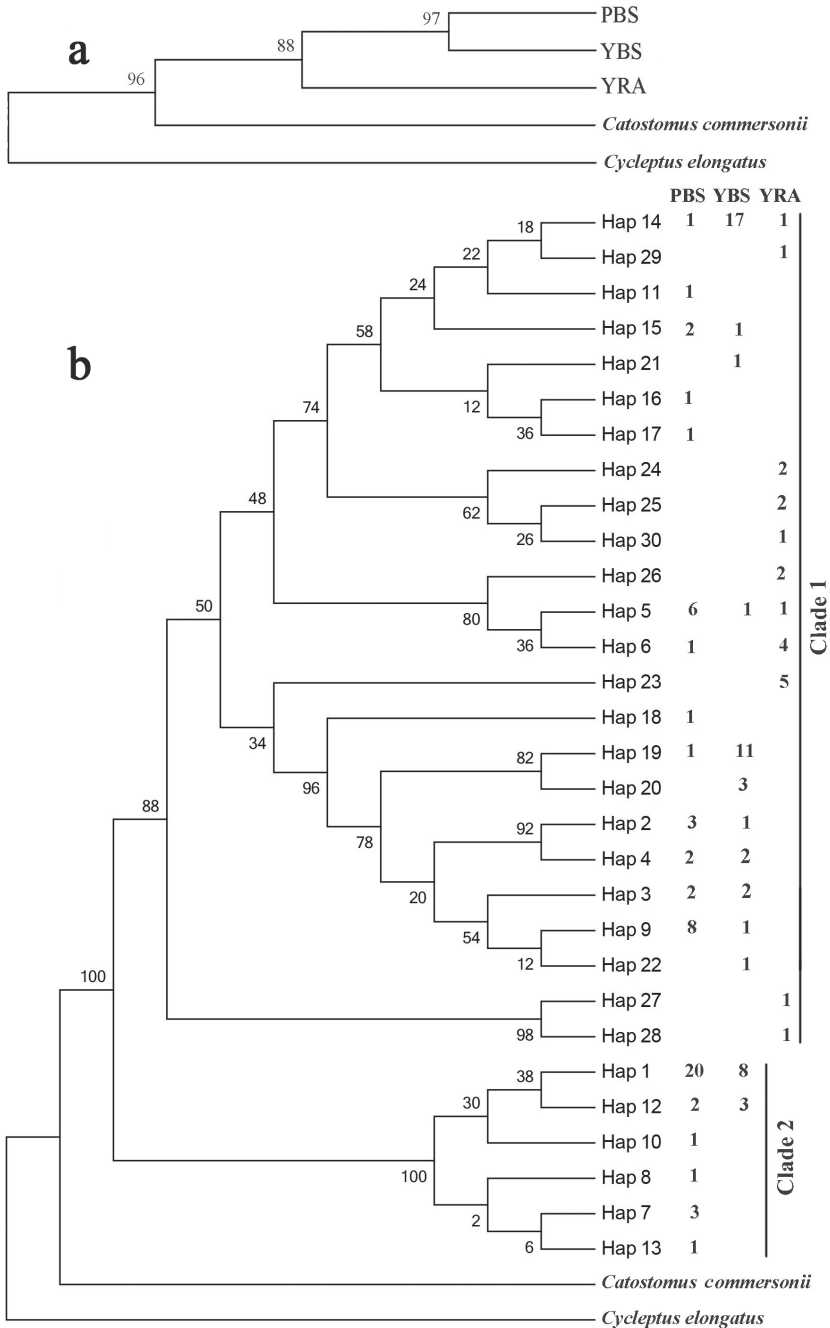


Figure 2. Neighbor-joining tree based on F_{ST} values of the mtDNA control region (a) and phylogenetic tree of mtDNA control region haplotypes in *Myxocyprinus asiaticus* reconstructed with Bayesian inference (b). Bayesian posterior probabilities and bootstrap values are shown at nodes of neighbor-joining tree and BI tree, respectively. The number behind each haplotype represents the number of individuals from different sampling locations.

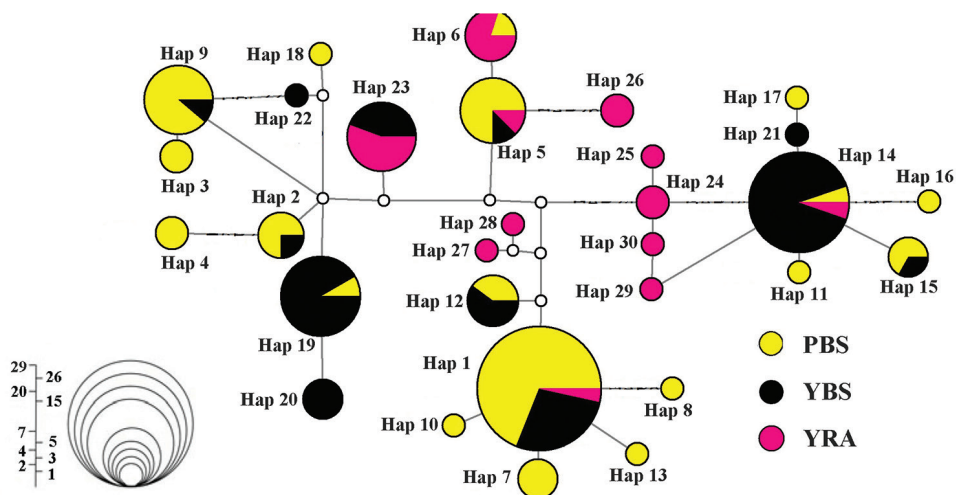


Figure 3. Median-joining network of the mtDNA control region haplotypes of *Myxocyprinus asiaticus*. The size of each circle indicates the frequency of the corresponding haplotype in the whole data set.

Genetic relationship

An AMOVA performed based on microsatellite markers showed insignificant molecular variance among broodstocks (6.45%, $P > 0.05$) and significant variance among individuals within hatcheries (93.55 %, $P < 0.01$). Significant divergence was observed between PBS and YRA ($F_{ST} = 0.1270$, $P < 0.05$), and the same situation occurred between YBS and YRA ($F_{ST} = 0.1319$, $P < 0.05$). But no significant divergence was observed between PBS and YBS ($F_{ST} = 0.0029$, $P > 0.05$). The analysis based on mtDNA control region showed congruent results derived from microsatellites. The genetic distances between PBS and YRA, YBS and YRA were larger than that between PBS and YBS. Furthermore, PBS and YBS broodstocks were clustered together in neighbor-joining tree based on F_{ST} values (Figure 2a).

The topologies of the phylogenetic trees produced by ML and BI were nearly identical (Bayesian tree was presented in Figure 2b). All mtDNA haplotypes were clustered into two distinct clades that were well supported by high bootstrap values. Clade 1 was composed of the haplotypes from all three broodstocks, while clade 2 was composed of the haplotypes only from PBS and YBS. Only two of the 30 haplotypes (Hap14, Hap5) were shared among all three samples while 8 haplotypes were shared between PBS and YBS, and most haplotypes in YRA were clustered together. Hap1 was most widespread, and included 28 individuals (Figure 2b). The median-joining network of all haplotypes showed that distribution of haplotypes from PBS and YBS were widespread, but the YRA haplotypes were more concentrated. Hap1, hap14, hap19, and hap9 were the most common haplotypes. PBS and YRA possessed ten and seven specific haplotypes, respectively and YBS had only three (Figure 3).

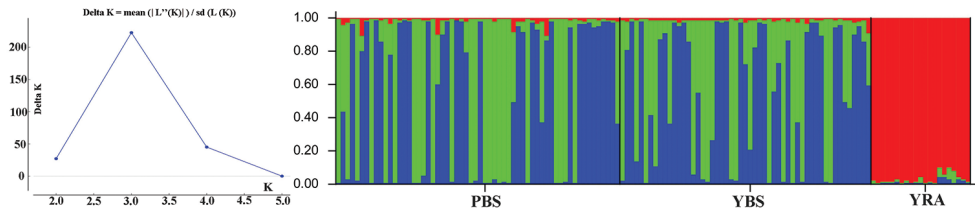


Figure 4. Results of STRUCTURE of *Myxocyprinus asiaticus* broodstocks based on K = 3. Each column represents one individual and the colors represent the probability membership coefficient of that individual for each genetic cluster.

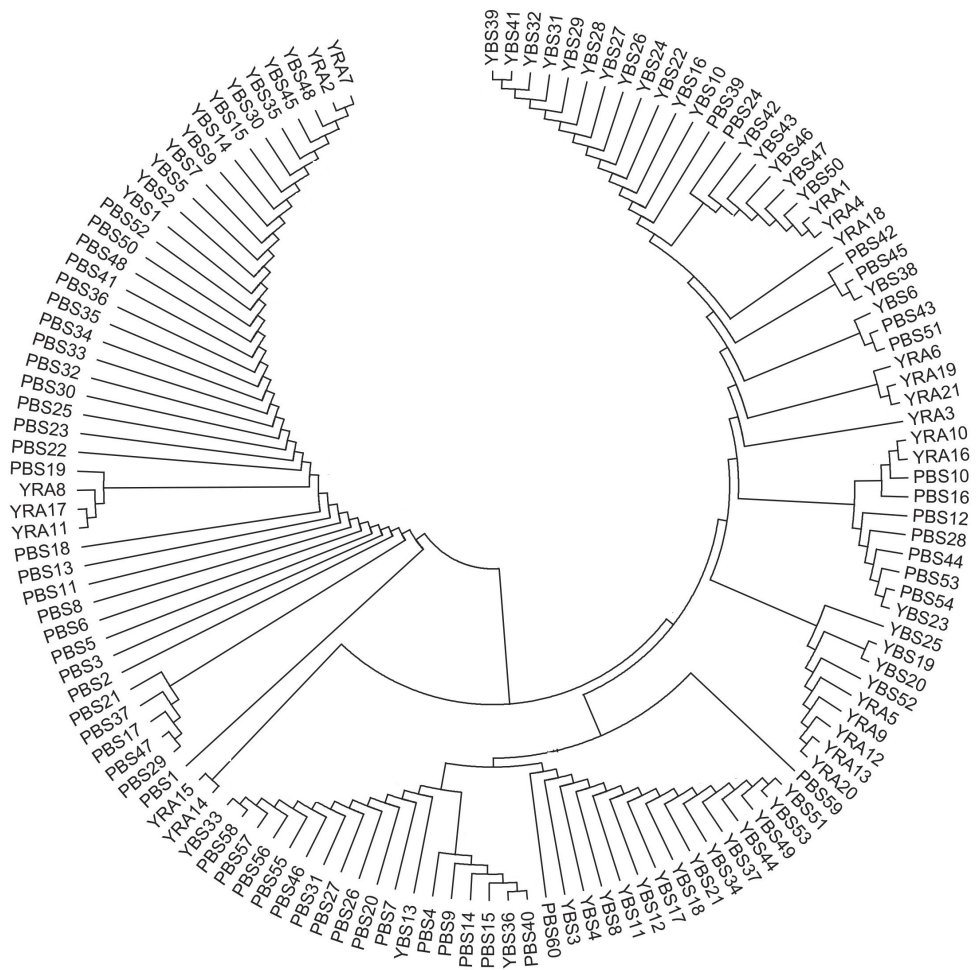


Figure 5. Neighbor-joining trees of individuals in three *Myxocyprinus asiaticus* broodstocks based on mtDNA control region.

Table 3. Probabilities from tests (Wilconxon's) for mutation drift equilibrium (bottlenecks) in the three *Myxocyprinus asiaticus* broodstocks under three mutation models (IAM, TPM and SMM).

Broodstocks	Mutation-drift test			Model shift
	I.A.M	S.M.M	T.P.M	L-shaped
PBS	0.1243	0.5431	0.3330	normal
YBS	0.0465*	0.6772	0.7870	normal
YRA	0.0374*	0.3448	0.0625	normal

* $p < 0.05$ (rejection of mutation drift equilibrium)

Structure Harvester online showed the highest peak of Delta K (222.58) when $K = 3$ (Figure 4), which indicated that the genetic structure of the broodstocks had three genetic clusters. The majority of YRA broodstock belonged to one cluster, and most of individuals from PBS and YBS broodstocks were promiscuously assigned to the other two clusters, which suggested that YRA were distinct from PBS and YBS (Figure 4).

On the basis of individual genetic distance, individual neighbor-joining tree was divided into two main branches, with one of them further divided into two branches. Individual distributions were widespread in neighbor-joining tree and did not cluster together based on broodstocks (Figure 5).

Demography of broodstocks

The F_{IS} was calculated using 12 microsatellite loci. Insignificant F_{IS} was found in all broodstocks ($P > 0.05$). Under the infinite allele model (IAM) heterozygosity excesses were detected in YBS and YRA. However, under stepwise mutation model (SMM) and the two-phase model (TPM), all broodstocks showed insignificant heterozygosity excess, and did not suffer from bottleneck or founder effects in the past (normal situation in Wilcoxon sign rank test) (Table 3).

Discussion

Through surveys and interviews of the three hatcheries before, we knew that the hatcheries reared a limited number of parental fish. Furthermore, those parental fish which could be qualified for artificial propagation were fewer. Besides, some individuals of first generation of artificially propagated *M. asiaticus* have been used as parental fishes and usually, one male was used for propagation with five or more females. These contributed to the lower genetic diversities in the broodstocks than that in wild populations of *M. asiaticus* (Wu 2014; Wu et al. 2016) and broodstocks investigated by Xu (2013) which used the different set of microsatellites and consequently might resulted in inbreeding and thus reduced the genetic quality of the offspring easily.

Both microsatellites and mtDNA markers revealed that the genetic diversity of YRA was lower than that of YBS and PBS, which might be attributed to the relative small sample size of YRA, and there were not enough wild ones to supplement broodstocks for a long time. In addition, both Pixian Base and Yibin Base hatcheries belong to the Sichuan Fisheries Research Institute, and thus frequently exchange the parental fish each other. This should contribute the relatively higher genetic variations in these two stocks as well.

Private alleles were results of lengthy evolution, which may have some special adaptation function or chain with some special properties (Zhang 2008). Both private and rare alleles have important values in propagation and may be lost from gene pool in domestic environment due to the role of genetic drift (Zhang 2008). Therefore, it is important to preserve these rare and private alleles of *M. asiaticus* broodstocks during artificially propagating, especially for YRA. YRA possesses most private alleles and almost half rare alleles. Nevertheless, the numbers of rare and private alleles might be affected by the number of parental fish in each hatchery, and should be further investigated through relatively large samples of broodstocks in the hatcheries in order to provide more accurate data for propagation in the future.

A previous study revealed that there was insignificant genetic differentiation in most broodstocks of *M. asiaticus* (Xu et al. 2013). The present study also showed insignificant genetic differentiation between YBS and PBS. The genetic distance was very low (0.002) between them. However, the genetic differentiations between PBS and YRA, and between YBS and YRA were significant. The genetic distances between YRA and PBS or YBS were larger than that between PBS and YBS. Great genetic differences between YRA and PBS or YBS might be attributed to that they originated from different cohorts in upper Yangtze River. Also, it was probably caused by a small number of wild founders which possessed limited gene pool and easily resulted in genetic drift (Xu et al. 2013). According to our investigation, some individuals we sampled from the PBS came from the first generation of offspring of YBS, which therefore weakened the genetic differentiation between them. There are more haplotypes shared between PBS and YBS than between one of them and YRA. Structure analysis indicated that some individuals from PBS and YBS belonged to one cluster. Therefore, PBS and YBS of *M. asiaticus* have a very close genetic relationship, and YRA was a separated broodstock.

According to the analysis of genetic diversity and relationship of the three broodstocks, we can propose some implications for artificial propagation and releasing program of *M. asiaticus*. First, although hatchery-release program has not much affected the genetic diversity (Wu 2014; Wu et al. 2016) and inbreeding coefficient and bottleneck of the three broodstocks were not significant, potential inbreeding problems are likely in the future. So the hatcheries should pay attention to the individual genetic relationship during artificial propagating and improve aquaculture conditions to increase the number of qualified individuals. The fish should be fed with more animal foods rather than ordinary pellet fodder, flowing water should be provided to stimulate broodstocks before propagation rather than still water environment, sufficient light and dissolved oxygen, and optimum temperature should be kept during over-winter-

ing stage to avoid death and accelerate development, and disease prevention and control, especially for saprolegniasis and parasite infection, should be paid more attention to as well. In order to increase size of qualified broodstocks and replenish the genetic pool, hatcheries should make efforts to collect more wild mature individuals. Second, breeding without genetic management will exacerbate decreasing genetic diversity and may increase genetic divergence among cultured broodstocks of different hatcheries, which may finally affect the wild populations (Gow et al. 2011; Ortega-Villaizan et al. 2011). Unfortunately, according to the results of the present study, genetic diversity and relationship of the broodstocks seemed to have been artificially influenced. Restocking efforts should strive to maintain genetic connectivity and exchange among local broodstocks in the hatcheries to avoid inbreeding and increase genetic variation. Especially, many rare and private alleles in YRA might have important values in propagation or adaptation, so it is necessary to do genetic exchange between YRA and PBS or YBS. Because the broodstocks of three hatcheries originated from neighboring ranges of the Yangtze River, genetic exchange does not mean mixing different genetic populations and would not affect the genetic characteristics of the wild populations through hatchery-release program. Hatcheries also need to record all details of each individual including body weight and length, gender, ID and genetic information. This precise information of existing broodstocks will be helpful for effective management (Kucinski et al. 2015). Third, in order to make sure that individuals are better adapted to live in natural environment, the juveniles of each batch should be randomly sampled for examining. Only when the samples are strong and healthy, can they be qualified for releasing. In addition, the continuous genetic monitoring of hatchery stocks is essential and baseline genetic data including archives and exchange records need to be renewed timely in the future, which are crucial to guide future population specific conservation programs and research efforts on *M. asiaticus* in China.

Acknowledgements

The work was supported by China Three Gorges Corporation (No. 0799531), the China Sinohydro Corpora on Shengda Sinohydro Co. Ltd. (No. AG2012/S-46-B) and China Scholarship Council. We are grateful to Steven Gaines and Dan Ovando for correcting the grammar mistakes. We would like to thank Jian Zhou, Qiang Li, Xianjun Chen, Bo Zhou, Liang Zhou, and Pengfei Yan for their help in sample collection.

References

- Bandelt HJ, Forster P, Rohlf A (1999) Median-joining network for inferring intraspecific phylogenies. *Molecular Biology and Evolution* 16: 37–48. <https://doi.org/10.1093/oxford-journals.molbev.a026036>

- Beamesderfer R, Paragamian V, Wakkinen V, Siple J (2002) Success of hatchery-reared juvenile white sturgeon (*Acipenser transmontanus*) following release in the Kootenai River, Idaho, USA. *Journal of Applied Ichthyology* 18: 642–650. <https://doi.org/10.1046/j.1439-0426.2002.00364.x>
- Blackie CT, Morrissey MB, Danzmann RG, Ferguson MM (2011) Genetic divergence among broodstocks of Arctic charr *Salvelinus alpinus* in eastern Canada derived from the same founding populations. *Aquaculture Research* 42: 1440–1452. <https://doi.org/10.1111/j.1365-2109.2010.02736.x>
- Chen N, Wang HL, Wang WM, Simonsen V (2010) Isolation of polymorphic microsatellite loci from an endangered freshwater species Chinese sucker, *Myxocyprinus asiaticus*. *Conservation Genetics Resources* 2: 73–75. <https://doi.org/10.1007/s12686-010-9177-6>
- Ding R, (1994) The fishes of Sichuan, China. Sichuan Publishing House of Science and Technology, Chengdu, China, 45 pp. (in Chinese)
- Earl DA, von Holdt BM (2012) STRUCTURE HARVESTER: a website and program for visualizing STRUCTURE output and implementing the Evanno method. *Conservation Genetics Resources* 4: 359–361. <https://doi.org/10.1007/s12686-011-9548-7>
- Excoffier L, Laval LG, Schneider S (2005) Arlequin ver. 3.0: An integrated software package for population genetics data analysis. *Evolutionary Bioinformatics* 1: 47–50 <https://doi.org/10.1177/117693430500100003>
- Gan X, Xiong J, Wang Z (2011) Resources and Conservation Status of *Myxocyprinus asiaticus* in Chongqing City. *Journal of Anhui Agricultural Science* 39: 5909–5911. (in Chinese)
- Glaubitz JC (2004) CONVERT: a user friendly program to reformat diploid genotypic data for commonly used population genetic software packages. *Molecular Ecology Notes* 4: 309–310. <https://doi.org/10.1111/j.1471-8286.2004.00597.x>
- Goudet J (1995) FSTAT, a computer program to calculate F-statistics. *The Journal of Heredity* 8: 485–486 <https://doi.org/10.1093/oxfordjournals.jhered.a111627>
- Gow JL, Tamkee P, Heggenes J, Wilson GA, Taylor EB (2011) Little impact of hatchery supplementation that uses native broodstock on the genetic structure and diversity of steelhead trout revealed by a large-scale spatio-temporal microsatellite survey. *Evolutionary Applications* 4: 1752–1757. <https://doi.org/10.1111/j.1752-4571.2011.00198.x>
- Hopley T, Zwart A, Yong A (2015) Among-population pollen movement and skewed male fitness in a dioecious weed. *Biological Invasions* 17: 2147–2161. <https://doi.org/10.1007/s10530-015-0867-6>
- Huelsenbeck JP, Ronquist F (2001) Mr Bayes: Bayesian inference of phylogenetic trees. *Bioinformatics* 17: 754–755 <https://doi.org/10.1093/bioinformatics/17.8.754>
- Jansson E, Ruokonen M, Kojola I, Aspi J (2012) Rise and fall of a wolf population: genetic diversity and structure during recovery, rapid expansion and drastic decline. *Molecular Ecology* 21: 5178–5193. <https://doi.org/10.1111/mec.12010>
- Jiang W, Yu D (2003) The present situation and resources restore of *Myxocyprinus asiaticus* in Tongling range of Yangtze River. *Special Wild Economic Animal and Plant Research* 3(3): 31–34 (in Chinese)
- Kumar S, Tamura K, Nei M (2004) MEGA3: Integrated software for molecular evolutionary genetics analysis and sequence alignment. *Briefings Bioinformatics* 5: 150–63. <https://doi.org/10.1093/bib/5.2.150>

- Kucinski M, Fopp-Bayat D, Liszewski T, Svinger VW, Lebeda I, Kolman R (2015) Genetic analysis of four European huchen (*Hucho hucho* Linnaeus, 1758) broodstocks from Poland, Germany, Slovakia, and Ukraine: implication for conservation. *Journal of Applied Genetics* 56: 469–480. <https://doi.org/10.1007/s13353-015-0274-9>
- Liu D, Hou F, Liu Q, Zhang X, Yan T, Song Z (2015) Strong population structure of *Schizopygopsis chengi* and the origin of *S. chengi baoxingensis* revealed by mtDNA and microsatellite markers. *Genetica* 143: 73–84. <https://doi.org/10.1007/s10709-015-9815-8>
- Liu HZ, Tzeng CS, Teng HY (2002) Sequence variations in the mitochondrial DNA control region and their implications for the phylogeny of the Cypriniformes. *Canadian Journal Zoology* 80:569–81 <https://doi.org/10.1139/z02-035>
- Nelson EM (1976) Some notes on the Chinese sucker. *Copeia* 3:594–595 <https://doi.org/10.2307/1443385>
- Oosterhout CV, Hutchinson WF, Wills DP, Shipley P (2004) Micro-checker: software for identifying and correcting genotyping errors in microsatellite data. *Molecular Ecology Notes* 4: 535–538. <https://doi.org/10.1111/j.1471-8286.2004.00684.x>
- Ortega-Villaizan MM, Noguchi D, Taniguchi N (2011) Minimization of genetic diversity loss of endangered fish species captive broodstocks by means of minimal kinship selective crossbreeding. *Aquaculture* 318: 239–243. <https://doi.org/10.1016/j.aquaculture.2011.04.047>
- Piry S, Luikart G, Cornuet JM (1999) Bottleneck: a computer program for detecting recent reduction in the effective population size using allele frequency data. *Journal of Heredity* 95: 53–539. <https://doi.org/10.1093/jhered/90.4.502>
- Pritchard JK, Stephens M, Donnelly P (2000) Inference of population structure using multilocus genotype data. *Genetics* 155: 945–959
- Qiang H, Chen Z, Zhang Z, Wang X, Gao H, Wang Z, (2015) Molecular diversity and population structure of a worldwide collection of cultivated tetraploid Alfalfa (*Medicago sativa* subsp. *sativa* L.) germplasm as revealed by microsatellite markers. *PLoS ONE* 97: 348–349 <https://doi.org/10.1371/journal.pone.0124592>
- Raymond M, Rousset F (1995) GENEPOP (version 1.2): population genetics software for exact tests and ecumenicism. *Journal of Heredity* 86: 248–249. <https://doi.org/10.1093/oxfordjournals.jhered.a111573>
- Rozas J, San D, Barrio JC, Messeguer X, Rozas R (2003) DnaSP, DNA polymorphism analyses by the coalescent and other methods. *Bioinformatics* 19: 2496–2497. <https://doi.org/10.1093/bioinformatics/btg359>
- Seeber E, Winterfeld G, Hensen I, Sharbel T, Durka W, Liu J, Yang Y, Wesche K (2014) Ploidy in the alpine sedge *Kobresia pygmaea* (Cyperaceae) and related species: combined application of chromosome counts, new microsatellite markers and flow cytometry. *Botanical Journal of the Linnean Society* 176: 22–35. <https://doi.org/10.1111/boj.12189>
- Swofford DL (2002) PAUP: Phylogenetic analysis using parsimony (and other methods). Sinauer Associates, Sunderland.
- Thrall PH, Yong A (2000) AUTOTET: a program for analysis of autotetraploid genotypic data. *Journal of Heredity* 91: 348–349. <https://doi.org/10.1093/jhered/91.4.348>
- Wang S (1998) China red data book of endangered animals. Science Press, Beijing, 84 pp. [in Chinese]
- Wang S, Xie Y (2004) China species red list. Higher Education Press, Beijing, 85 pp. [in Chinese]

- Wu J (2014) The morphological difference, genetic diversity and population structure of wild-caught and artificially propagated Chinese sucker (*Myxocyprinus asiaticus*). Sichuan University, Chengdu, China, 26 pp. [in Chinese with English]
- Wu J, Wu B, Hou F, Chen Y, Li C, Song Z (2016) Assessing genetic diversity of wild and hatchery samples of the Chinese sucker (*Myxocyprinus asiaticus*) by the mitochondrial DNA control region. *Mitochondrial DNA* 27: 1411–1418 <https://doi.org/10.3109/19401736.2014.953072>
- Xu N, Yang Z, Que Y, Shi F, Zhu B, Xiong M (2013) Genetic diversity and differentiation in broodstocks of the endangered Chinese sucker, *Myxocyprinus asiaticus*, using microsatellite markers. *Journal of World Aquaculture Society* 44: 520–527. <https://doi.org/10.1111/jwas.12053>
- Yang Z, Shi F, Que Y, Xiong M, Xu N, Zhu B (2009) Construction of microsatellite library enriched and its application prospect in Chinese sucker (*Myxocyprinus asiaticus*). *Journal of Hydroecology* 2(2): 73–75. [in Chinese with English]
- Yuan Y, Gong S, Yang H, Lin Y, Yu D, Luo Z (2010) Apparent digestibility of selected feed ingredients for Chinese sucker, *Myxocyprinus asiaticus*. *Aquaculture* 306: 238–243. <https://doi.org/10.1016/j.aquaculture.2010.05.017>
- Yue P, Chen Y (1998) China red data book of endangered animals. Science Press, Beijing, 42 pp. [in Chinese]
- Zhang X (2008) Isolation of microsatellite markers and genetic diversity analysis of rock carp (*Procypris rabaudi*). Sichuan University, Chengdu, China, 8 pp. (in Chinese with English)
- Zhang C, Zhao Y, Kang J (2000) A discussion on resources status of *Myxocyprinus asiaticus* (Bleeker) and their conservation and the recovery. *Journal of Natural Resources* 15(2): 155–9. [in Chinese with English]
- Zhu B, Zheng HT, Qiao Y, Que YF, Chang JB (2009) Fish stocking program in the Yangtze River. *Chinese Fisheries Economy* 27(2): 74–87. [in Chinese with English]

Conservation priorities for terrestrial mammals in Dobrogea Region, Romania

Iulia V. Miu¹, Gabriel B. Chisamera², Viorel D. Popescu^{1,3}, Ruben Iosif⁴,
Andreea Nita¹, Steluta Manolache¹, Viorel D. Gavril^{5,6},
Ioana Cobzaru⁶, Laurentiu Rozyłowicz¹

1 University of Bucharest, Center for Environmental Research and Impact Studies, 1 N. Balcescu, 010041, Bucharest, Romania **2** National Museum of Natural History Grigore Antipa, 1 Kiseleff Blvd., 011341, Bucharest, Romania **3** Department of Biological Sciences, Ohio University, Athens, OH, USA **4** University Ovidius Constanța, Faculty of Natural Sciences and Agricultural Sciences, 1 Al. Universității, corp B, 900470, Constanța, Romania **5** University of Bucharest, Faculty of Biology, 91–95 Splaiul Independenței, 050095, Bucharest, Romania **6** Romanian Academy, Institute of Biology, 296 Splaiul Independenței, 060031 Bucharest, Romania

Corresponding author: Iulia V. Miu (iulia.miu@drd.unibuc.ro)

Academic editor: J. Maldonado | Received 27 March 2018 | Accepted 30 August 2018 | Published 23 October 2018

<http://zoobank.org/8F7EBA17-46D6-4236-B91B-A3B2DE8CC950>

Citation: Miu IV, Chisamera GB, Popescu VD, Iosif R, Nita A, Manolache S, Gavril VD, Cobzaru I, Rozyłowicz L (2018) Conservation priorities for terrestrial mammals in Dobrogea Region, Romania. ZooKeys 792: 133–158. <https://doi.org/10.3897/zookeys.792.25314>

Abstract

Based on species occurrence records of museum collections, published literature, and unpublished records shared by mammalian experts, we compiled a distribution database for 59 terrestrial mammals populating the extensively protected Dobrogea Region of Romania. The spatial patterns of mammal distribution and diversity was evaluated and systematic conservation planning applied to identify priority areas for their conservation. The spatial analyses revealed that intensive sampling was not directly correlated to mammal diversity but rather to accessibility for inventory. The spatial prioritisation analysis indicated a relatively aggregated pattern of areas with a high or low conservation value with virtually no connecting corridors between them. The significant overlap between Natura 2000 sites and national protected areas induced an over-optimistic vision of the effectiveness and representativeness of existing Natura 2000 network for species found in Annexes II and IV of the Habitats Directive. These results represent a key step in identifying core areas for the protection of mammal diversity and dispersal corridors for improved connectivity, and to guide future conservation efforts in increasing the effectiveness of the existing protected areas in the context of environmental changes.

Keywords

Dobrogea, Natura 2000, species distribution, species richness, systematic conservation planning, terrestrial mammals

Introduction

Terrestrial mammals are well-studied taxa, yet their distribution and conservation status are not fully understood (Crooks et al. 2011). Mammalian population decline accelerates the loss of ecosystem services and poses a substantial threat to species diversity at the community level (Ceballos 2002, Rodrigues et al. 2004). Since mammals display diverse traits and can exploit a wide range of ecological niches, they are also effective focal species for conservation, and their population status might be a proxy for both fragmentation and connectivity across landscapes (Crooks et al. 2011).

A common conservation strategy to prevent the loss of biodiversity is the creation of protected areas (Margules and Pressey 2000, Williams et al. 2002). Protected areas must ensure the long-term persistence and viability of species and should ideally support many rare, threatened, or endemic taxa, particularly those with low mobility and high sensitivity to environmental alterations (Rodrigues et al. 2004, Possingham et al. 2006). However, typically, the effectiveness of protected areas is undermined by poor governance (Eklund et al. 2011, Manolache et al. 2018, Nita et al. 2018) and lack of funding and relevant resources (Sánchez-Fernández et al. 2017).

The Natura 2000 network of protected areas of European importance represents one of the most extensive networks of conservation areas worldwide (Nita et al. 2017). Scientists and policymakers often question the effectiveness of this network due to the Member States allocating fewer funds than needed to implement conservation programs (Nita et al. 2017, Sánchez-Fernández et al. 2017). Natura 2000 is more effective in protecting species listed in Birds Directive because of a better overlap between ancillary conservation investments such as Common Agricultural Policy and biodiversity value (Lung et al. 2014, Maiorano et al. 2015), and because birds are more intensely studied than other vertebrate groups. To be more effective, Natura 2000 network must incorporate potential changes in species distributions (Popescu et al. 2013, Kukkala et al. 2016). Failure to acknowledge changes in species ranges may lead to gaps in protecting species that are sensitive to climate change and other anthropogenic pressures (Araújo et al. 2011).

One of Romania's legal obligations since joining the European Union in 2007 was to designate Natura 2000 sites in a short time (Ioja et al. 2010). Due to the lack of adequate species and habitat distribution data, regions that already benefited from protection under national laws were preferred for the first phase of the designation process. Consequently, the EU conservation goals were not met, which resulted in the designation of additional protected areas (Ioja et al. 2010, Popescu et al. 2013) and a disproportionate increase of land protected in some regions such as it is the case of Dobrogea (now 63% under protection, 9700 km²). The Natura 2000 network from Dobrogea includes 67 sites (35 Sites of Community Importance - SCI and 32 Special

Protection Areas – SPA, most of the SCIs and SPAs spatially overlap). Within Dobrogea, highlands and floodplains gained extensive protection while lowlands occupied by arable lands remained largely unprotected. However, the latter areas are inhabited by endangered species such as the marbled polecat (*Vormela peregusna*) and the steppe polecat (*Mustela eversmanii*) (Murariu et al. 2009, 2010).

Due to the diverse landforms, climatic influences, and habitats, Dobrogea harbours a large number of mammal species (Murariu 1996, Murariu et al. 2010). To date, 59 mammal species have been documented in this region, three of which reach the outer limit of their geographic range (the marbled polecat *Vormela peregusna*, the stoat *Mustela erminea*, and the common hamster *Cricetus cricetus*), and two other species have their core range in Dobrogea (the Romanian hamster *Mesocricetus newtoni* and the Southern birch mouse *Sicista nordmanni*) (Bunescu 1959, 1961, Popescu and Murariu 2001, Murariu and Munteanu 2005). Of the 59 mammal species, 14 are protected by Habitats Directive. Despite the focus of many Natura 2000 sites within Dobrogea on protecting mammal species, limited and outdated distributional databases are available for individual species, e.g., the Romanian hamster *Mesocricetus newtoni* (Hamar and Schutowa 1966), the Eurasian beaver *Castor fiber* (Kiss et al. 2012, Kiss et al. 2014), the European mink *Mustela lutreola* (Cuzic and Marinov 2004), and the Southern birch mouse *Sicista nordmanni* (Ausländer and Hellwing 1957). Moreover, with few exceptions, (e.g., Murariu 1996, 2006, Murariu et al. 2009, Murariu et al. 2010) the Dobrogea Region lacks actual regional species distribution data.

One tool supporting management decisions and for investigating species population coverage within protected areas is spatial conservation prioritisation (Pouzols et al. 2014). As part of systematic conservation planning (Margules and Pressey 2000) and accounting for complementarity, spatial prioritisation can be an efficient instrument in identifying spatial priorities and in achieving conservation goals (Pressey et al. 2007) even in broadly protected and underfunded regions such as Dobrogea (Rozyłowicz et al. 2017). In this study, we evaluate priority areas for mammal conservation in Dobrogea, Romania and assess the spatial patterns of distribution and diversity of terrestrial mammals by: (1) compiling mammal distribution records from published papers, museum records, and unpublished data, (2) analyzing spatial patterns of distribution data, and (3) using systematic conservation planning in identifying high priority areas for conservation of terrestrial mammal listed in Annexes II and IV of Habitats Directive within the regional Natura 2000 network.

Materials and methods

Mammal species occurrences

To map the distribution of mammals in Dobrogea, we extracted species occurrence records from three primary sources: museum collections, published data, and unpublished field data. Occurrences that could not be georeferenced to a location (e.g., as-

signed to a large watershed or geographical province), or associated with unspecified taxa within genera, were not included in this geodatabase. The species taxonomy considered in this paper is based on Wilson and Reeder (2005) and Arslan et al. (2016). Sibling species which are difficult to discriminate in the field, such as the yellow-necked mouse *Apodemus flavicollis*, the wood mouse *Apodemus sylvaticus* (Bartolommei et al. 2016), the common vole *Microtus arvalis*, and the East European vole *Microtus levis* (Jaarola et al. 2004), were included as individual species, as their occurrences were acquired through museum collections and published data. Red list status was based on Temple and Terry (2009).

The dataset used to map the species distribution includes 6724 occurrence records for 59 mammal species. For spatial pattern analyses, we excluded species found exclusively in fenced areas (the European mouflon *Ovis aries musimon*), the vagrant species (elk *Alces alces*), and synanthropic species (the rats *Rattus rattus*, *Rattus norvegicus* and the house mouse *Mus musculus* (Table 2)), resulting in 5593 occurrence records for 54 species. For creating species distribution maps, we aggregated the occurrence records at a Universal Traverse Mercator spatial resolution of 25 km² (UTM 5 × 5 km). Following Cogalniceanu et al. (2013), the occurrence records were classified based on the year of observation into *old records*, if recorded before 1990, and *recent records*, if recorded after 1990. For spatial pattern analyses, we increased the cell size to UTM 10 × 10 km, allowing us to highlight regional patterns in richness, rarity, and dissimilarity, and to reduce the potential bias in sampling (Graham and Hijmans 2006). For spatial prioritisation of mammal conservation within Natura 2000 sites, we used the UTM 5 × 5 km occurrences maps of 14 native species listed in Annexes II and IV of Habitats Directive (Figure 1).

Spatial bias in species occurrence

Potential bias at the scale of the study area was assessed using the overall spatial autocorrelation in mammal records per 5 × 5 km grid cell. We used Global Moran's I test (Fortin and Dale 2005) to evaluate spatial pattern of sampling per grid cell being significantly clustered ($Z > 0$) or dispersed ($Z < 0$) across Dobrogea. To assess the local patterns of sampling bias we used the Getis Ord G_i^* spatial statistic. This analysis identifies clusters of records with values numerically higher than expected by random chance within a specified searching distance (Ord and Getis 1995). The distance threshold for the aggregation patterns was set up to 7100 m to include the neighbouring eight grid cells for each UTM grid of interest. The Getis Ord G_i^* test returns a Z-score for every cell, which, depending on the level of aggregation describes spatial clusters of high or low sampling effort. We identified clusters of UTM 5 × 5 km cells where the sampling effort was significantly higher (hotspots of occurrence, $G_iZScore > 1.87$) or lower (cold spots of occurrence, $G_iZScore < 1.87$). All spatial analyses were performed using ARCMAP 10.3 (ESRI, CA) (Figure 1).

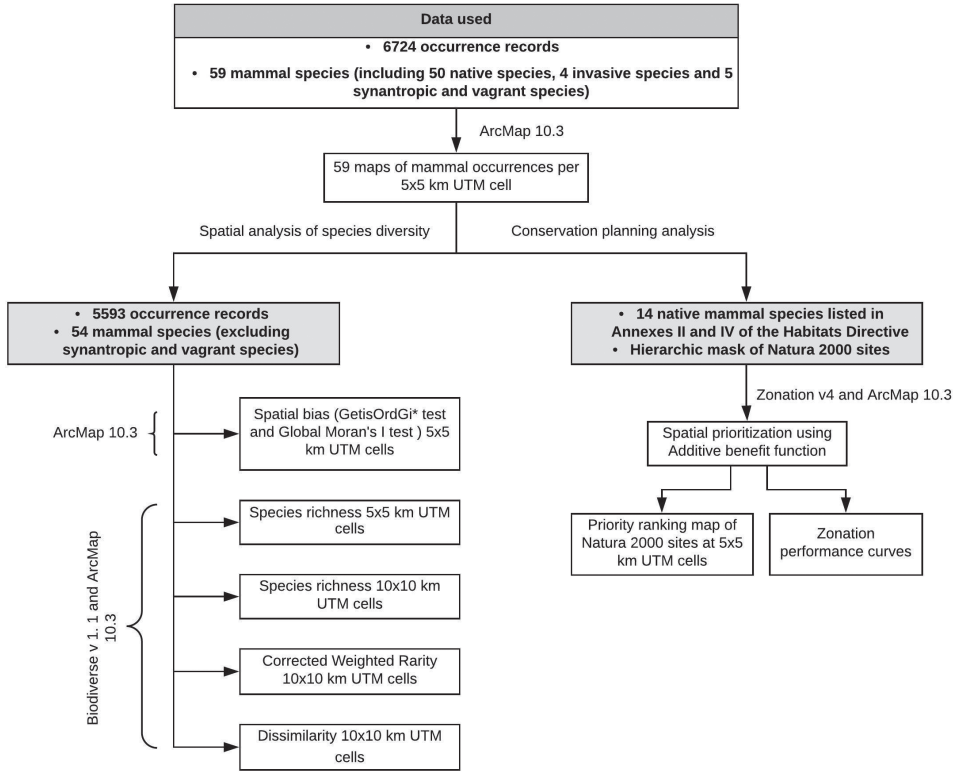


Figure 1. Flowchart of diversity analyses and spatial prioritisation of conservation of terrestrial mammals within Dobrogea Region, Romania.

Estimating species richness, rarity, and dissimilarity

To emphasise regional patterns of richness, rarity, and dissimilarity of mammals of Dobrogea, we aggregated the occurrence records at 5×5 km and 10×10 km and imported them into BIODIVERSE software (v. 1.1) (Laffan et al. 2010), a tool for spatial analysis of biodiversity (Figure 1).

Richness index was measured as the number of species in each grid cell. Species rarity was assessed by dividing the corrected weighted rarity (CWE) by the total number of species in the respective cell, where CWE is (Equation 1).

$$CWE = WE / Richness \tag{1}$$

Weighted rarity (WE) of a species represents the occurrence records of sample counts of the respective species divided by the number of occurrence records of all species in the dataset (Equation 2).

$$WE = \sum_{t \in T} \frac{S_t}{S_t} \tag{2}$$

where t is a taxon in the set of taxa T across neighbourhood set 1, s_t is the sum of the sample counts for t across the elements in neighbouring sets 1 and 2, and S_t represents the total number of samples across the data set for t (Laffan et al. 2010). In our case, only one neighbouring set is specified.

To calculate the differences in species composition across Dobrogea, we used the turnover index (S_2), which refers to changes in species composition from one community to another along a gradient and across different sites (Whittaker 1972). S_2 calculates the dissimilarity between two sets of species. We compared a focal quadrat with one of its eight neighbours (Equation 3).

where a is the total number of species found in both neighbour sets, b is the number of species unique to the neighbour set 1, and c is the number of species unique to the neighbour set 2 (Laffan et al. 2010).

$$S_2 = 1 - \frac{a}{a + \min(b, c)} \quad (3)$$

Selecting the smallest values of b or c in the S_2 equation denominator reduces the impact of imbalances of species richness on neighbour dissimilarity. The highest value that S_2 can result is the value of one (1), which indicates the focal quadrat has no species in common with any neighbour and the lowest possible value is zero (0), indicating that all quadrats have an identical set of species (Lennon et al. 2001).

Identifying high-priority areas for Natura 2000 mammal species conservation

To identify high-priority areas for mammal species conservation across Natura 2000 sites within Dobrogea Region, we used systematic conservation planning software ZONATION v4 (Lehtomäki and Moilanen 2013, Moilanen et al. 2014). This software uses a complementarity-based algorithm including connectivity, with the result that landscapes can be zoned according to their conservation potential. Using a deterministic iterative process, ZONATION creates a hierarchical ranking of the landscape from the highest to the lowest conservation value (Moilanen et al. 2014).

For priority analysis, we used 5×5 km raster layers for presence/absence data for 14 mammal species listed in Annexes II and IV of the Habitats Directive and a hierarchic mask of the Natura 2000 Sites of Community Importance within Dobrogea Region (Figure 1). A hierarchic mask represents a mask layer specifying priority land uses, in our case the Natura 2000 network. This planning design forces the prioritisation algorithm to undertake ranking cells outside the Natura 2000 network, followed by ranking those in the Natura 2000 network, allowing the application to analyse an optimal conservation area network. We sequenced the prioritisation model using an additive benefit function with exponent $z = 0.25$, which is a default value representing the exponent of the species-area curve (Moilanen et al. 2014). In this prioritisation model, the function sums the loss across features, converted

via feature-specific benefit functions, giving high importance to the cells containing many species (Arponen et al. 2005).

The outputs of the analysis are conservation priority ranking of the landscape, derived from the order of iterative cell ranking whereby each grid cell has a value between 0 and 1, indicating that ranking close to 0 are removed first (low priority), while ranking close to 1 are retained until the end of the iteration. The outputs show the most important areas for mammal species conservation across Natura 2000 sites and a set of curves describing the absolute performance levels of species conservation. We considered as high-priority areas for conservation, all grid cells falling in the top 20% of the predicted priority ranks, a proportion that maximises mammal species representation at the regional level (Arponen et al. 2005). Suppl. material 3 presents the methodology used to identify high-priority Natura 2000 sites with Zonation v4.

The data underpinning the analysis reported in this paper are deposited at GBIF, the Global Biodiversity Information Facility, <http://ipt.pensoft.net/resource?r=mammalsdobrogea>.

Results

Mammal species occurrences in Dobrogea

We collected 4451 records from published museum collections data (66%), 1326 personal records shared by experts (20%), and 947 records from other papers reporting the results of fauna inventories (14%). Of all the accessible papers (published museum collections and fauna inventories) 67% were published before the year 1990 and 33% after 1990 (Suppl. material 1). Over 54% of all the records were reported before 1990, and 46% are records collected after 1990. Occurrences maps for 59 mammal species aggregated at 5 × 5 km resolution are presented in Suppl. material 2.

The rate of accumulation of mammal occurrences increased in 1956 by 688 records, due to the rediscovery of the Southern birch mouse (*Sicista nordmanni*) at Valu lui Traian in 1955. That report attracted additional fieldwork by mammalogists the following year, consequently, an increase in the number of records for other rodent species. After 1990, and up to 2017, the peak number of records per year took place in 2007 with 456 new records (Figure 2, Table 1).

Spatial patterns in mammal species occurrences in Dobrogea

Of 757 UTM 5 × 5 km grid cells encompassing the Dobrogea Region, only 335 grid cells (i.e., 44%) include reported mammal sightings (Figure 3). At the regional scale, Global Moran's I test indicated a random pattern in the number of mammal occurrences per UTM 5 × 5 grid cell ($Z = 1.87$, $p = 0.06$). However, the local Getis Ord G_i^*

Table I. Checklist of mammals of Dobrogea Region, Romania.

Order	Family	Species	Total number of records	New records (after 1990)	Total number of UTM 5 × 5 occupied cells	Habitats Directive Annexes	European Red List status
Rodentia	Sciuridae	<i>Sciurus vulgaris</i> (Linnaeus, 1758)	6	3	4	–	Least concern
		<i>Spermophilus citellus</i> (Linnaeus, 1766)	214	92	95	II/IV	Vulnerable
	Gliridae	<i>Dryomys nitedula</i> (Pallas, 1778)	35	22	20	IV	Least concern
		<i>Muscardinus avellanarius</i> (Linnaeus, 1758)	1	1	1	–	Least concern
		<i>Glis glis</i> (Linnaeus, 1766)	3	3	3	–	Least concern
	Castoridae	<i>Castor fiber</i> (Linnaeus, 1758)	12	12	5	II/IV	Least concern
	Dipodidae	<i>Sicista nordmanni</i> (Keyserling & Blasius, 1840)	76	0	2	II/IV	Vulnerable
	Spalacidae	<i>Nannospalax leucodon</i> (Nordmann, 1840)	163	82	57	–	Least concern
	Cricetidae	<i>Cricetus cricetus</i> (Linnaeus, 1758)	2	0	1	IV	Least concern
		<i>Mesocricetus newtoni</i> (Nehring, 1898)	98	13	31	II/IV	Near threatened
		<i>Ondatra zibethicus</i> (Linnaeus, 1766)	87	37	57	–	Invasive
		<i>Arvicola amphibius</i> (Linnaeus, 1758)	29	12	22	–	Least concern
		<i>Microtus agrestis</i> (Linnaeus, 1761)	28	11	18	–	Least concern
		<i>Microtus arvalis</i> (Pallas, 1779)	187	40	44	–	Least concern
		<i>Microtus levis</i> (Miller, 1908)	29	9	13	–	Least concern
		<i>Microtus subterraneus</i> (Selys-Longchamps, 1836)	16	7	9	–	Least concern
		<i>Myodes glareolus</i> (Schreber, 1780)	1	0	1	–	Least concern
		Muridae	<i>Micromys minutus</i> (Pallas, 1771)	36	15	24	–
	<i>Apodemus agrarius</i> (Pallas, 1771)		451	96	50	–	Least concern
	<i>Apodemus flavicollis</i> (Melchior, 1834)		134	80	34	–	Least concern
	<i>Apodemus sylvaticus</i> (Linnaeus, 1758)		1327	330	65	–	Least concern
	<i>Apodemus uvalensis</i> (Pallas, 1811)		16	6	8	–	Least concern
	<i>Mus spicilegus</i> (Petényi, 1882)		20	20	19	–	Least concern
Myocastoridae	<i>Myocastor coypus</i> (Molina, 1782)	5	2	5	–	Invasive	
Lagomorpha	Leporidae	<i>Lepus europaeus</i> (Pallas, 1778)	262	255	102	–	Least concern
Erinaceomorpha	Erinaceidae	<i>Erinaceus roumanicus</i> (Barrett-Hamilton, 1900)	52	40	39	–	Least concern

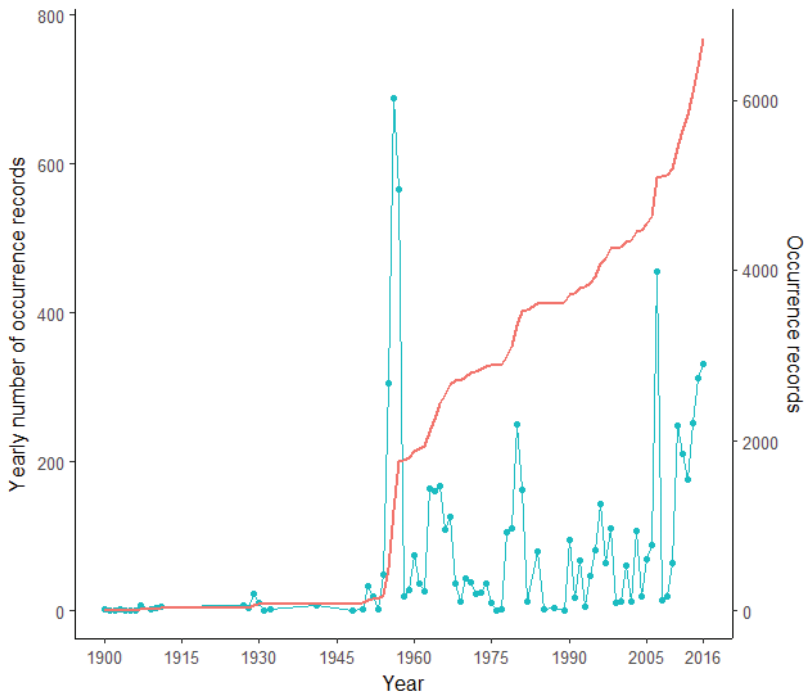
Order	Family	Species	Total number of records	New records (after 1990)	Total number of UTM 5 × 5 occupied cells	Habitats Directive Annexes	European Red List status
Soricomorpha	Soricidae	<i>Crociodura leucodon</i> (Hermann, 1780)	85	14	18	–	Least concern
		<i>Crociodura suaveolens</i> (Pallas, 1811)	131	40	36	–	Least concern
		<i>Neomys anomalus</i> (Cabrer, 1907)	12	4	8	–	Least concern
		<i>Neomys fodiens</i> (Pennant, 1771)	5	1	4	–	Least concern
		<i>Sorex araneus</i> (Linnaeus, 1758)	63	14	25	–	Least concern
		<i>Sorex minutus</i> (Linnaeus, 1766)	15	9	10	–	Least concern
	Talpidae	<i>Talpa europaea</i> (Linnaeus, 1758)	65	53	55	–	Least concern
	Carnivora	Felidae	<i>Felis silvestris</i> (Schreber, 1777)	101	94	52	IV
Felidae		<i>Lynx lynx</i> (Linnaeus, 1758)	2	1	2	II/IV	Least concern
Canidae		<i>Canis aureus</i> (Linnaeus, 1758)	214	198	94	–	Least concern
		<i>Canis lupus</i> (Linnaeus, 1758)	27	22	14	II/IV	Least concern
		<i>Nyctereutes procyonoides</i> (Gray, 1834)	87	35	41	–	Invasive
		<i>Vulpes vulpes</i> (Linnaeus, 1758)	230	223	122	–	Least concern
Mustelidae		<i>Mustela erminea</i> (Linnaeus, 1758)	25	7	23	IV	Vulnerable
		<i>Mustela eversmannii</i> (Lesson, 1827)	31	24	25	II/IV	Vulnerable
		<i>Mustela lutreola</i> (Linnaeus, 1761)	119	109	50	II/IV	Endangered
		<i>Mustela nivalis</i> (Linnaeus, 1766)	67	54	50	–	Least concern
		<i>Mustela putorius</i> (Linnaeus, 1758)	89	74	61	–	Least concern
		<i>Vormela peregusna</i> (Güldenstädt, 1770)	70	16	39	II/IV	Vulnerable
		<i>Martes foina</i> (Erxleben, 1777)	98	97	58	–	Least concern
		<i>Martes martes</i> (Linnaeus, 1758)	36	36	20	–	Least concern
		<i>Meles meles</i> (Linnaeus, 1758)	102	92	60	–	Least concern
	<i>Neovison vison</i> (Schreber, 1777)	2	2	1	–	Invasive	
	<i>Lutra lutra</i> (Linnaeus, 1758)	55	49	35	II/IV	Near threatened	
Artiodactyla	Suidae	<i>Sus scrofa</i> (Linnaeus, 1758)	221	204	105	–	Least concern
	Cervidae	<i>Dama dama</i> (Linnaeus, 1758)	46	29	21	–	Least concern
		<i>Cervus elaphus</i> (Linnaeus, 1758)	38	32	25	–	Least concern
		<i>Capreolus capreolus</i> (Linnaeus, 1758)	262	190	119	–	Least concern

Table 2. Checklist of synanthropic and vagrant mammals of Dobrogea Region, Romania.

Order	Family	Species	Total number of records	New records (after 1990)	Total number of UTM 5 × 5 occupied cells
Rodentia	Muridae	<i>Rattus norvegicus</i> (Berkenhout, 1769)	114	49	64
Rodentia	Muridae	<i>Rattus rattus</i> (Linnaeus, 1758)	3	2	3
Rodentia	Muridae	<i>Mus musculus</i> (Linnaeus, 1758)	1001	139	78
Artiodactyla	Cervidae	<i>Alces alces</i> (Linnaeus, 1758)	4	0	3
Artiodactyla	Bovidae	<i>Ovis aries musimon</i> (Pallas, 1881)	9	5	4

spatial statistic indicates 3 hotspots for mammal sightings: Valu lui Traian Biological Research Station (mean $Z = 7.73$), North Dobrogea Plateau Natura 2000 site (mean $Z = 3.26$), and Letea Forest, a natural reserve within Danube Delta (mean $Z = 2.75$). Additionally, there are few moderately sampled regions such as Măcin Mountains National Park in the northwest, Dumbrăveni-Urului Valley-Vederoasa Lake Natura 2000 site and Canaraua-Fetii Iortmac Natura 2000 site in the southwest, and Hagieni – Cotul Văii Forest Natura 2000 site in the southeast (Figure 4).

The mammal occurrences at 5 × 5 km resolution ranged between 1 and 35 reported species per quadrat (Figure 5). The map highlights a lower sampling effort in southern and central Dobrogea, areas with intensive agriculture, and the highest diversity in the northern and southwest parts of Dobrogea, comprising mostly forested habitat.

**Figure 2.** Accumulation of mammals' occurrence records (blue) and the number of records per year (red) within Dobrogea Region, Romania.

Species richness, rarity, and dissimilarity

When aggregating species records at 10×10 km, the number of reported species ranged from 2 to 45 per cell grid, with the highest species diversity located in the northern part of Dobrogea Region overlapping the following Natura 2000 sites: North Dobrogea Plateau with a maximum richness of 45 species, western part of Danube Delta with 39 species and Agighiolului Hills with 38 species. Most of the grid cells with species richness are concentrated in the northern region reflecting an optimal sampling of mammal species (number of species from 29 to 37) (Figure 6), while grid

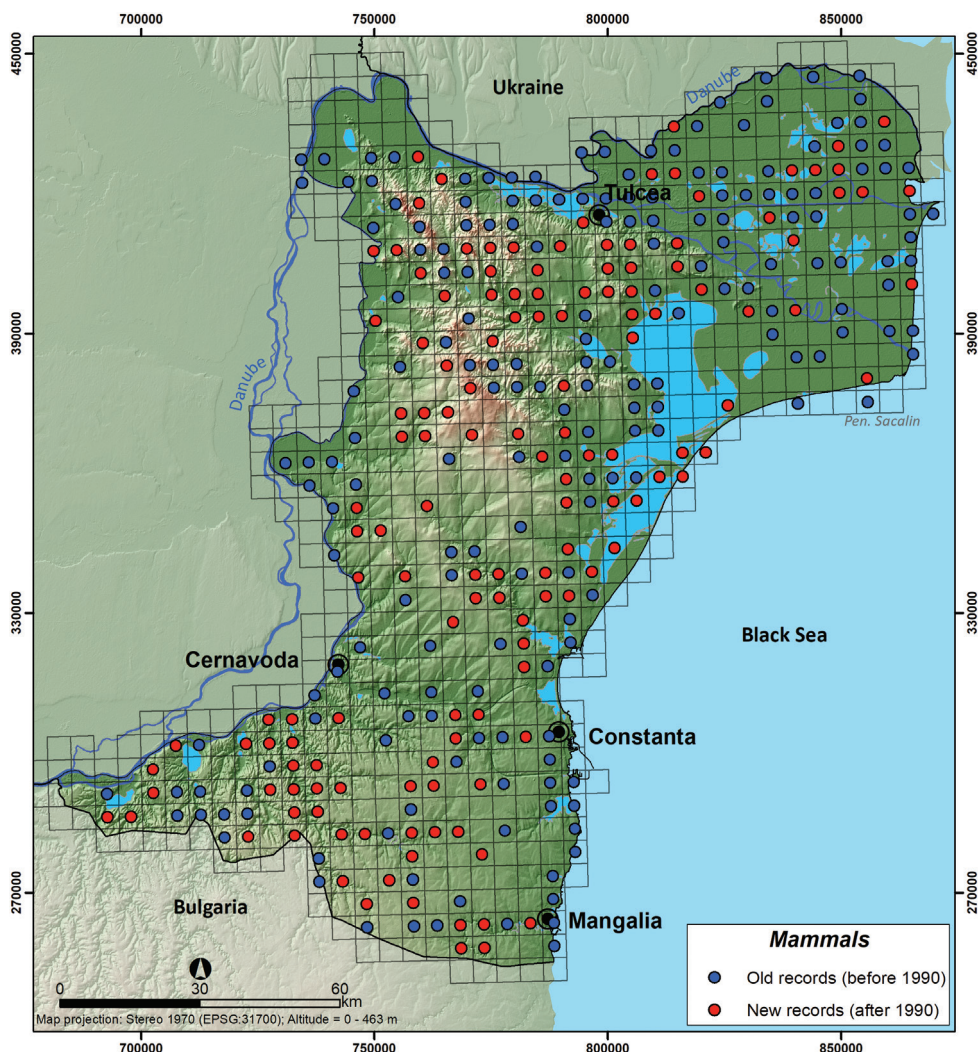


Figure 3. Mammals reported occurrences in Dobrogea Region, Romania at 5×5 km resolution. Grids with reported occurrences before 1990 were plotted as old records whereas those with reported occurrences after 1990 were considered new records (reports of synanthropic and vagrant mammals were excluded).

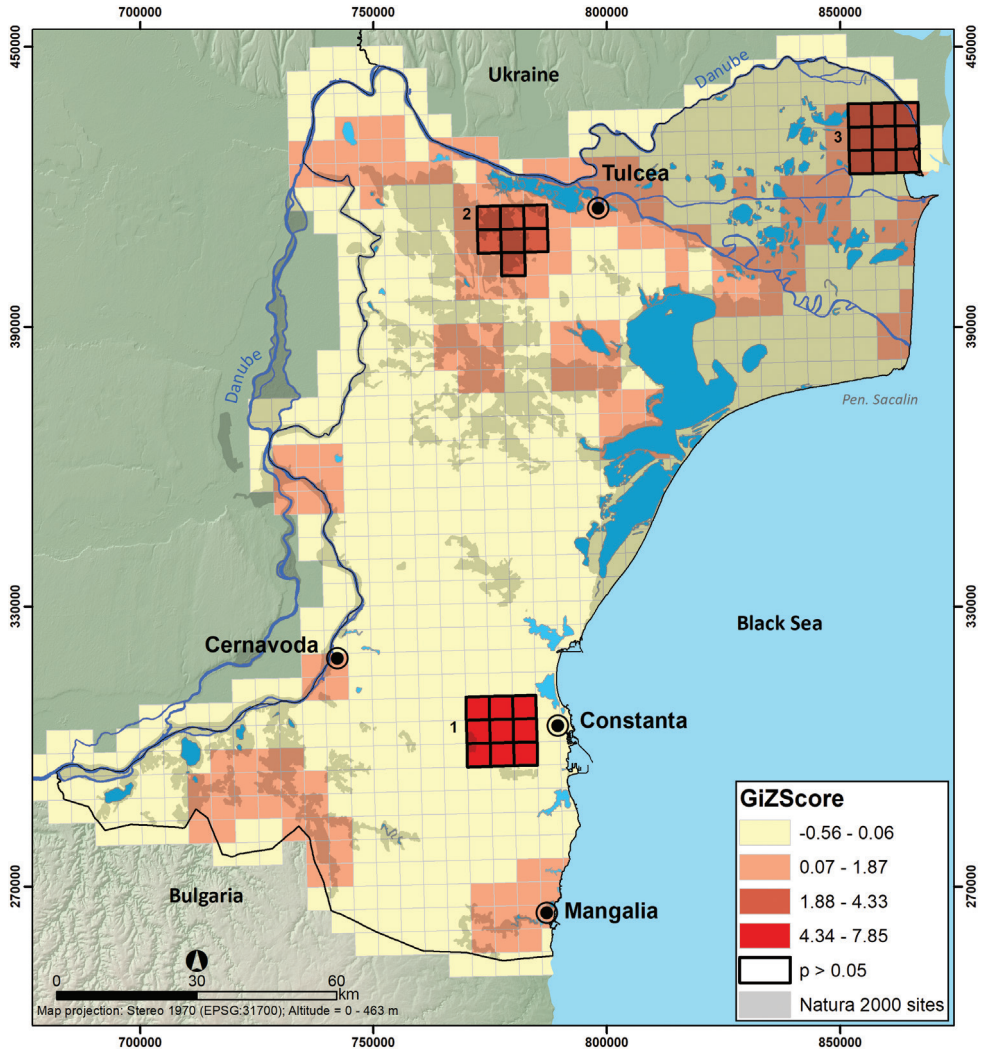


Figure 4. Hotspots of sampling efforts within Dobrogea. The numbered statistically significant hot-spots are **1** Valu lui Traian Biological Research Station and Fântânița-Murfatlar **2** North Dobrogea Plateau **3** Letea Forest Natural Reserve in the Danube Delta.

cells with the lowest richness values are distributed in the southern and central part of Dobrogea Region.

Corrected weighted rarity (CWE) varied across Dobrogea from 0.0087 for cell grids with widespread species to 0.62 grid cells with species of restricted distribution. The highest value of corrected weighted rarity can be found in the Danube Delta, specifically in the levee complex of Puiu – Roșu – Lumina, with a value up to 0.62 (Figure 7).

The values of dissimilarity index S_2 ranged from 0 to 1 with the highest turnover quadrats in the southern area of Dobrogea where there are low richness zones. The

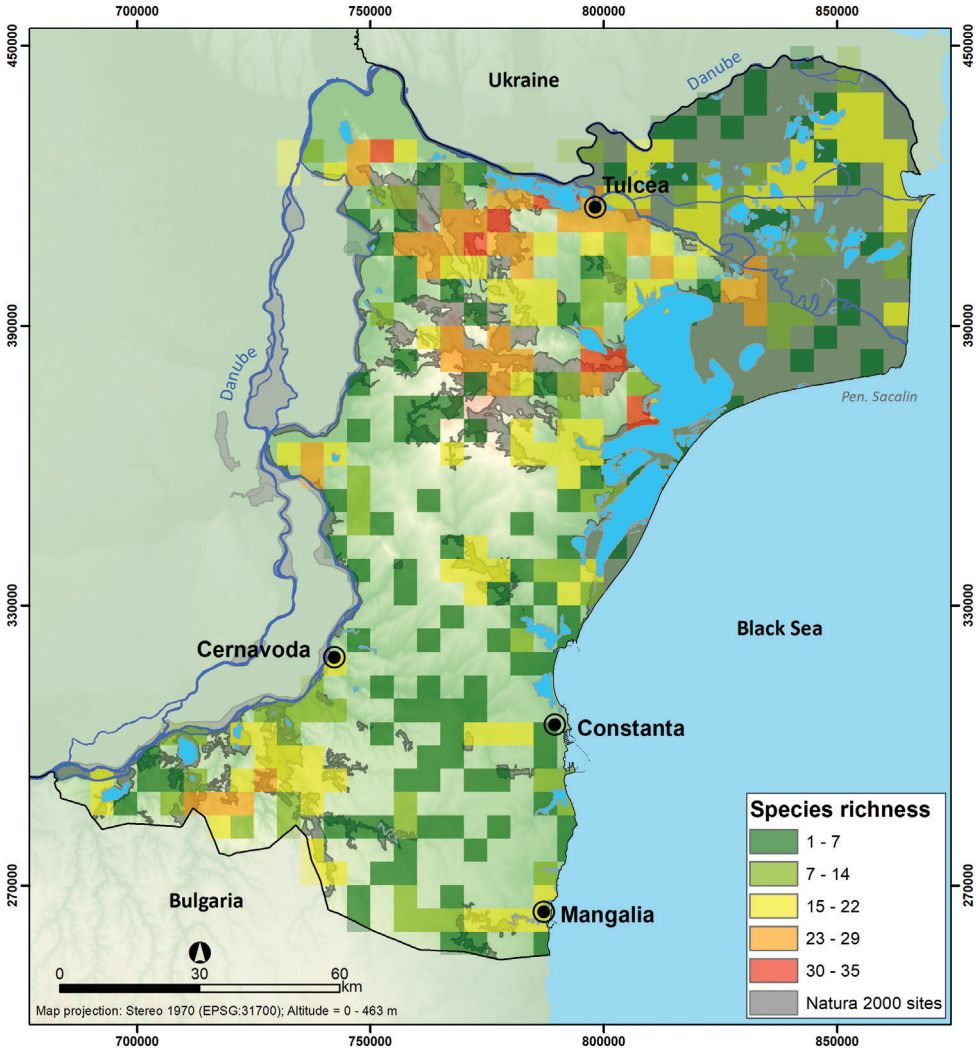


Figure 5. The mammal species richness at 5×5 km grid resolution within Dobrogea.

value of 1 implies that the quadrat has no species in common with any neighbour (Figure 8). We found that areas with the higher richness of species have more species in common with their neighbours.

High-priority areas for conservation within Natura 2000 sites

Based on the Zonation analysis results, the top spatial conservation priorities overlap Danube Delta, North Dobrogea Plateau, and the Măcin Mountains in the northern part of Dobrogea region, where a relatively aggregated pattern of top conservation value areas appear due to their extensive wetland area and forested

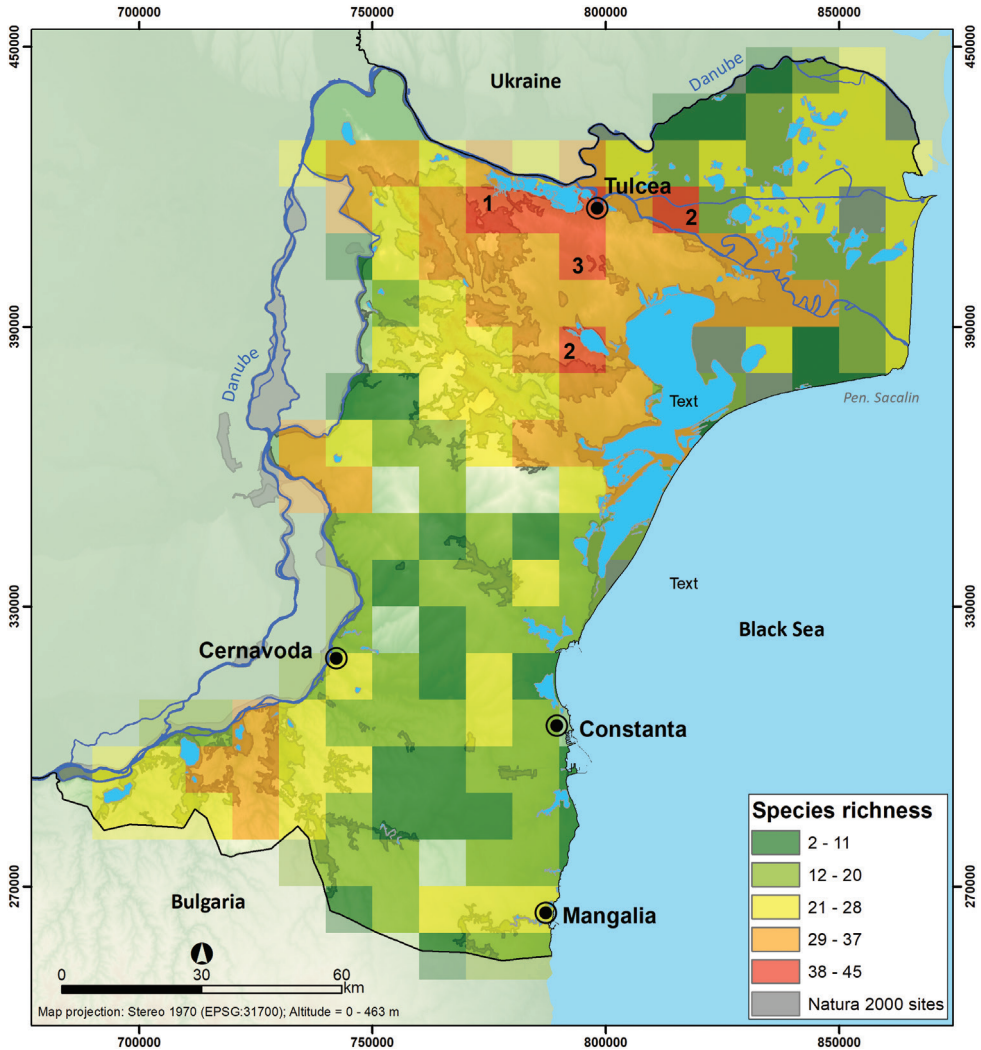


Figure 6. Mammal species richness of Dobrogea at 10 × 10 km. Grids with high richness partially overlap. **1** North Dobrogea Plateau **2** Danube Delta, and **3** Agighiolului Hills.

habitats. Isolated hotspots are represented by Dumbrăveni-Urliua Valley-Vederoasa Lake in the southwest, Hagieni – Cotul Văii Forest in the southeast, and Cheia Jurassic Reefs in Central Dobrogea. Grid cells with the lowest ranking are located in the central and southern part of Dobrogea Region, where the majority of the regions' agricultural lands are clustered (Figure 9). Nevertheless, the Natura 2000 network encompasses 45% of mammal species distribution listed in Annexes II and IV of the Habitats Directive when top 20% of the landscape is protected by Natura 2000 sites (Figure 10).

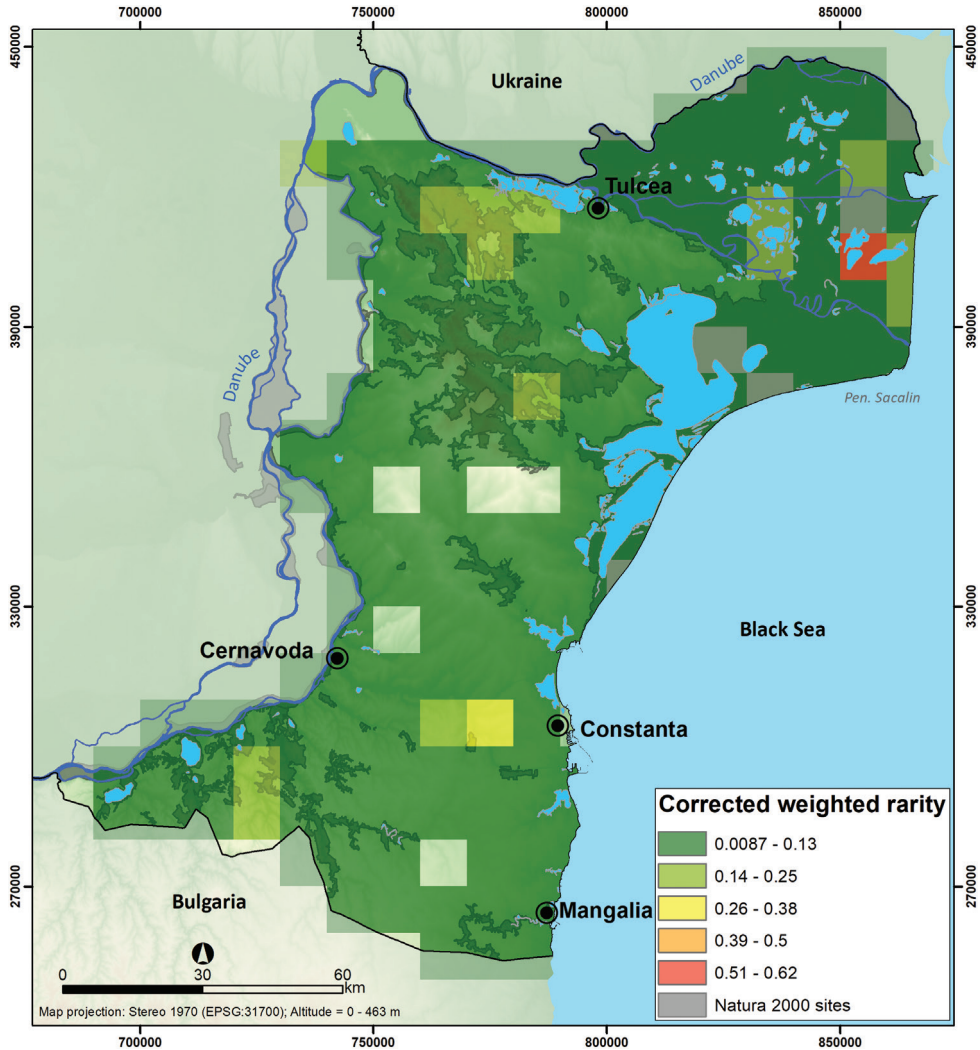


Figure 7. Corrected weighted rarity map of Dobrogea mammal species.

Discussion

By using an updated distribution of terrestrial mammals, we identified high priority areas for protecting mammal diversity to guide future conservation efforts in an extensively protected Romanian region. In the broader context of systematic conservation planning, the prioritisation analysis is a useful tool to identify key areas for biodiversity conservation, e.g., where species are more likely to survive (Ferrier and Wintle 2009, Wilson et al. 2009, Kukkala and Moilanen 2013).

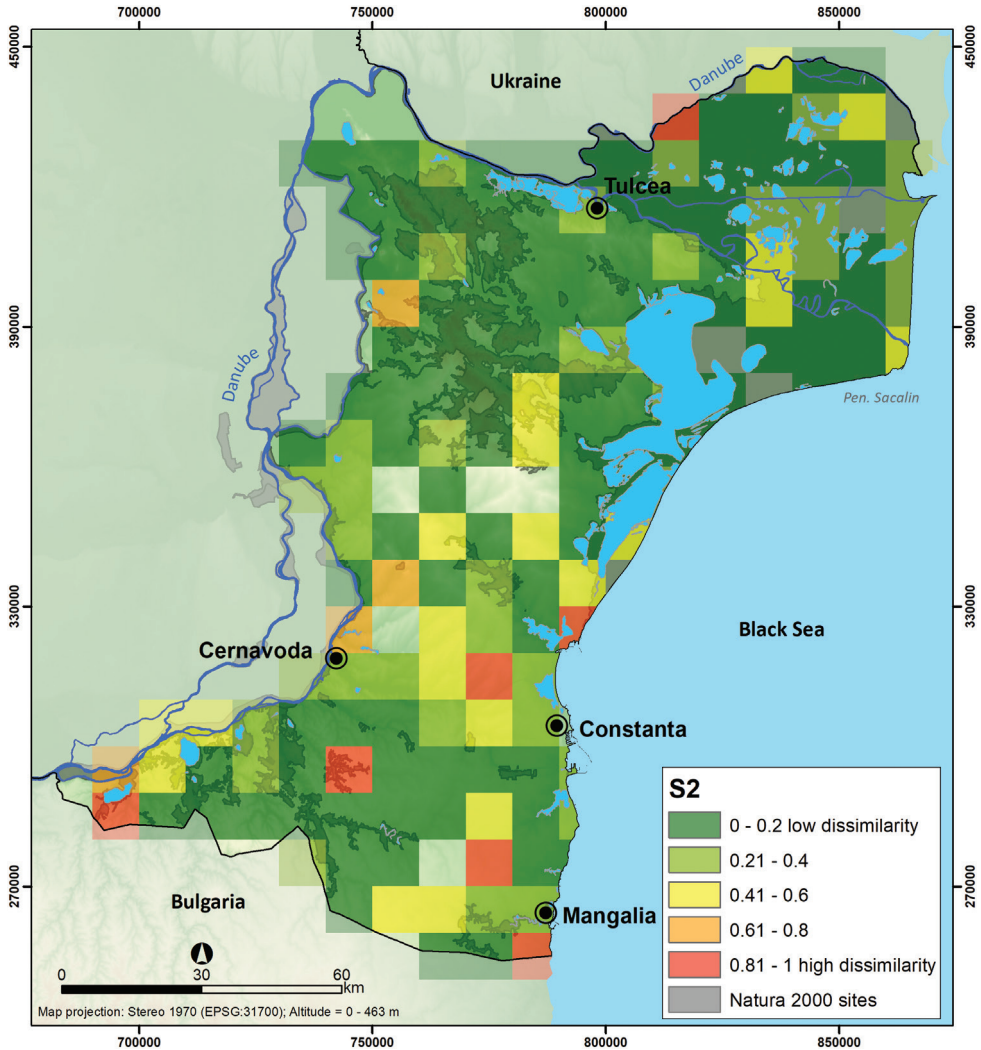


Figure 8. Dissimilarity map of Dobrogea mammal species, Romania (S2 index).

The number of reported occurrences in Dobrogea varied among species. The largest number of records (20%) are for the wood mouse (*Apodemus sylvaticus*), mostly because they are widespread within the region, have a higher population abundance, and are evidently. The wood mouse may be easily misidentified as a yellow-necked mouse (*Apodemus flavicollis*) (Bartolommei et al. 2016), but it still retains the first rank because of their higher population in Dobrogea (Popescu and Murariu 2001).

The lowest number of records in Dobrogea is recorded for the hazel dormouse (*Muscardinus avellanarius*) and the bank vole (*Myodes glareolus*), with only one record per each species. Two other widespread species, but with an uncharacteristically low number of reported presences are the red fox (*Vulpes vulpes*) and the roe deer (*Capreolus capreolus*),

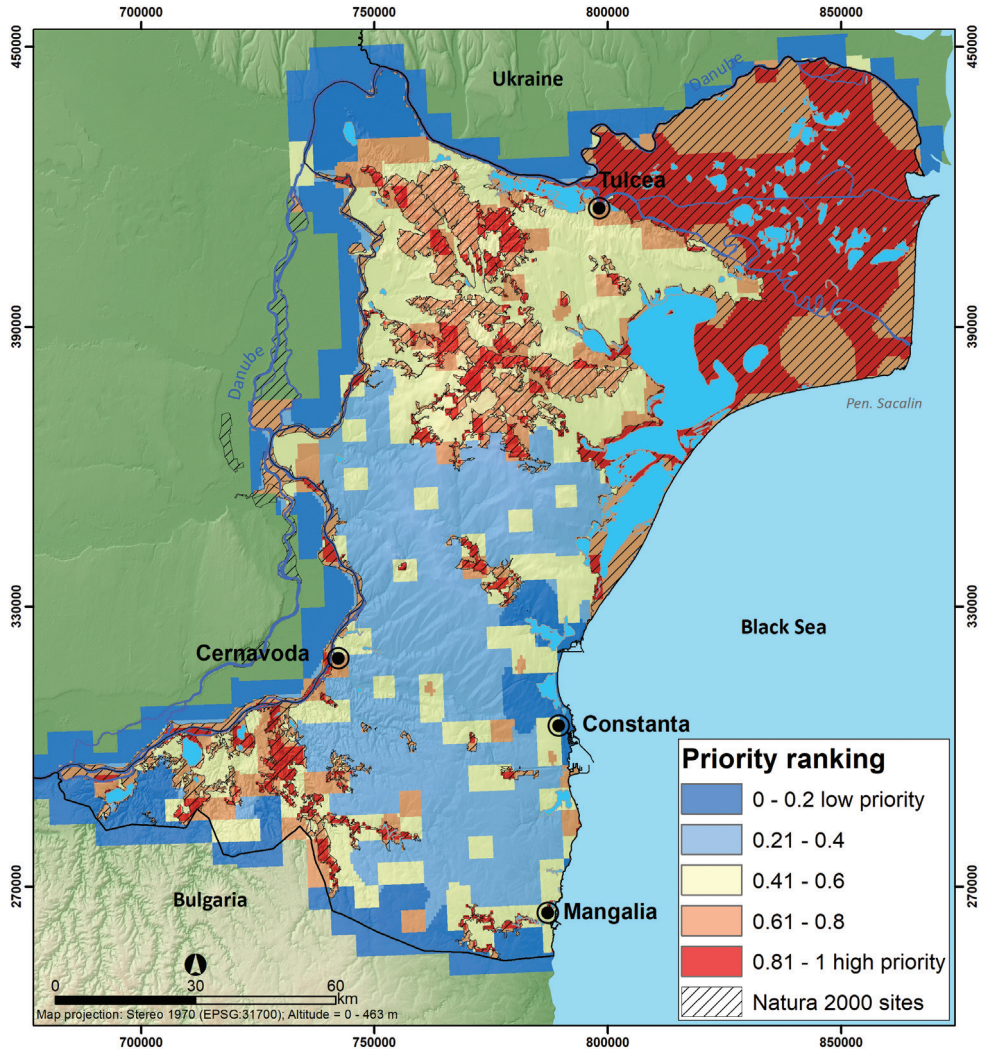


Figure 9. Priority conservation areas for mammal species listed in Annexes II and IV of the Habitats Directive within Natura 2000 sites of Dobrogea. Areas have been graded according to their priority rank, with highest priorities (top 20%) shown in red.

possibly because they are common species, with minor interest for biologists. The research effort for species sampling was focused on selected areas: Măcin Mountains National Park, Danube Delta Biosphere Reserve, and the North Dobrogea Plateau. Here, we recorded a higher than expected number of species occurrences per grid cell, mostly because the long-term protection status attracted faunistic inventory projects over time. Typically, the sampling bias is higher in protected areas because they attract more conservation funds leading to greater efforts for biodiversity research (e.g., Botts et al. 2011). This process describes most of the biodiversity spatial databases (Lobo et al. 2007). A

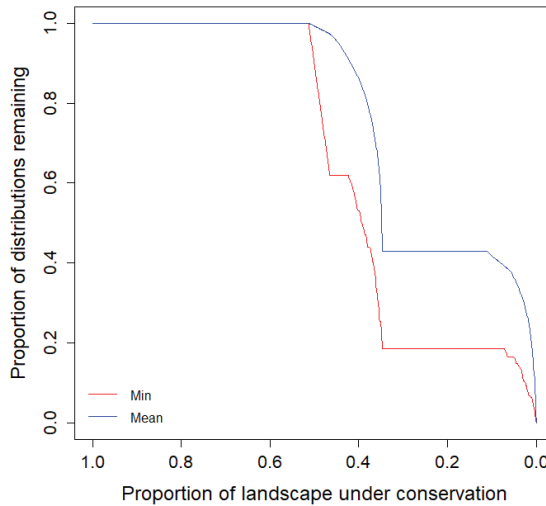


Figure 10. Zonation performance curves quantifying the proportion of remaining species occurrences covered by Natura 2000 sites in Dobrogea. When considering 20% of landscape within Natura 2000 sites as protected (e.g., conservation measures are enforced), 45% of Natura 2000 mammal occurrences are protected.

higher than expected sampling effort also was evident near cities, major roads, and research facilities, which are easily accessible to researchers (e.g., Valu lui Traian Biological Research Station - see Figure 4). We noted a lack of research interest in central and southern Dobrogea, where most of the agricultural landscape is located, and only small patches of natural habitats remain as wildlife refuges (Rey et al. 2007). However, agricultural landscapes are essential for many species protected by Habitats Directive, such as *Vormela peregusna*, *Mustela eversmanii*, *Spermophilus citellus*, *Mesocricetus newtoni*, and *Cricetus cricetus* (Popescu and Murariu 2001, Murariu and Munteanu 2005, Murariu et al. 2009, 2010). Those identified species have restrictive ecological requirements, and hence, the researchers should focus on increasing sampling effort in these neglected areas to draft appropriate conservation plans.

We found that high species richness did not match all the hotspots of sampling efforts, such as in Valu lui Traian Biological Research Station and Fântânița-Murfatlar (location 1 in Figure 4) and Letea Forest Natural Reserve in the Danube Delta (location 3 in Figure 4). This validates the finding that intensive sampling was not directly correlated with mammal diversity, but rather ease of access to the regions (Santos et al. 2017). To better understand the patterns of species richness at the regional level, we expanded the resolution to 10 × 10 km, but the spatial pattern did not change between the two mapping resolutions. In both cases, the highest diversity (35 species at 5 × 5 km resolution, see Figure 5); 45 mammal species at 10 × 10 km resolution, see Figure 6), is found in the northern part of Dobrogea, overlapping North Dobrogea Plateau Natura 2000 site, where habitat heterogeneity is high (Rey et al. 2007).

The spatial turnover index (S_2) suggests that areas with lower species richness are dissimilar compared to their neighbours. Notably, we observed some affinities of par-

ticular species towards low species richness areas (Lennon et al. 2001), e.g., species dependent on steppe or agricultural landscape (Popescu and Murariu 2001, Murariu and Munteanu 2005). Typically, the spatial turnover tends to be correlated with species richness (Gaston et al. 2007), but in our study, the variation in turnover is determined by the rarity of the species which then tend to have narrower habitat niches and drive turnover patterns more than widespread species. By analysing species richness and turnover index maps, we found low congruency between the Natura 2000 sites and areas with high species richness and areas occupied by species with a narrower range. Species with narrow ranges (e.g. *Lutra lutra*, Memedemin et al. 2017) are often underrepresented in protected areas, potentially resulting in suboptimal effectiveness of the Natura 2000 network in protecting such species in Dobrogea, despite the large area protected under conservation.

Our results regarding the identification of high-priority areas in Dobrogea for mammal species listed in Annexes II and IV of the Habitats Directive highlight a relatively aggregated pattern of the grid cells with high conservation value in the north-eastern and northern Dobrogea Region, where there are extensive wetlands and forests (i.e., Danube Delta, Măcin Mountains National Park, and North Dobrogea Plateau) (Rey et al. 2007). Additionally, we identified small isolated high-priority areas in agricultural landscapes of southern and central Dobrogea, where biodiversity-friendly agricultural practices should be considered as a conservation method. Distribution of top spatial conservation priorities demonstrated a lack of connectivity between Natura 2000 sites with high conservation values from the northern part of Dobrogea, isolated priority areas in the center of the region, as well as those in the southern part of the region. The distribution of high-priority areas for conservation suggests the necessity of addressing the lack of connectivity, as non-priority areas are essential for the dispersal of species (Christie and Knowles 2015).

The significant overlap between Natura 2000 sites and the other protected areas statutes leads to misunderstandings in law enforcement and an over-optimistic vision of their effectiveness (Ioja et al. 2010). As an example, species whose distributions are limited to the EU Steppic Biogeographic Region or reach the boundaries of their geographic range in Dobrogea tend to be under-represented (Popescu and Murariu 2001, Murariu and Munteanu 2005) as in the case of reptiles and amphibians (Popescu et al. 2013). In Dobrogea, isolation of protected areas leads to low connectivity between habitat patches, which then need to be addressed in future conservation planning and protected area management plans. The lack of research in agricultural landscapes may potentially lead to the populational decline of certain species by not being aware of their distribution and by using flawed species range data (Grant et al. 2007).

The absence of buffer zones and corridors between Natura 2000 sites and small isolated protected areas (the area of the smallest Natura 2000 site in Dobrogea is 0.11 km²), are not beneficial in maintaining viable populations, causing the isolation of species with low mobility and specific habitat requirements (Christie and Knowles 2015). Establishing corridors between Natura 2000 sites, especially in the central and southern part of Dobrogea increases connectivity and promotes species dispersal.

Our study is limited by the lack of viable and current distribution data. Most records do not identify geographical coordinates, but localities or toponymies. This makes the niche modelling at a fine scale a challenge. Furthermore, elusive species such as *Mesocricetus newtoni*, *Sicista nordmanni*, and *Vormela peregusna*, are data deficient, and the lack of records (false absences) may influence the results of the analysis. Similarly, misidentification of sibling species may lead to over- or under- estimation of their range. Notably, a study analysing the distribution of amphibians in Dobrogea (Székely et al. 2009) indicates similar issues regarding biased and incomplete distribution data due to the lack of comprehensive surveys of areas with difficult accesses. Another similarity is that some amphibians (e.g., *Bombina bombina*, *Bufo viridis*, *Hyla arborea*), as well as some mammals (e.g., *Capreolus capreolus*, *Apodemus sylvaticus*) are considered widespread and highly detectable, while amphibians such as *Pelobates fuscus* and *Pelobates syriacus*, are cryptic and elusive species and therefore, have low detectability and incomplete distributions (Székely et al. 2013), and that includes species such as *Vormela peregusna*, *Sicista nordmanni* or *Mesocricetus newtoni*. However, biased data lead to more priority areas to protect fewer species (Grant et al. 2007), which is not a shortcoming. Furthermore, Rodrigues et al. (2011) concluded that decision-based on incomplete taxonomic and/or phylogenetic data (such as misidentified sibling species) are robust, and the researcher can safely make use of the best available systematic data.

Future research may focus on identifying buffer zones around Natura 2000 sites to minimise potential negative impacts, particularly in Natura 2000 sites that are adjacent to agricultural areas. From this assessment, we envisage further mapping of corridor networks between small isolated protected areas in southern and central Dobrogea. New research should focus on systematic surveys of agricultural landscapes in central and southern Dobrogea, where vegetation patches remain as refuges for some species listed in Annexes II and IV of the Habitats Directive (*Vormela peregusna*, *Mustela eversmannii*, *Spermophilus citellus*, *Mesocricetus newtoni*, *Cricetus cricetus*, and *Sicista nordmanni*).

Acknowledgments

IVM, VDP, AN, SM, and LR were supported by a grant from the Romanian National Authority for Scientific Research, PN-III-P4-ID-PCE-2016-0483. Editing and proof-reading by Edward F. Rozyłowicz streamlined the flow of the manuscript. We thank Maria Patroescu, Tiberiu Sahlean, and an anonymous reviewer for their comments that improved the manuscript. We are grateful to Dumitru Murariu, Nastase Radulet, Bogdan Bejenariu, Catalin Stanciu, Dragos Mantoiu, Ionut Stefan Iorgu, Daniyar Memedemin, Razvan Popescu Mirceni, Silviu Petrovan, Marius Skolka, Razvan Zaharia, Alexandra Telea, Dragos Balasoiu, Mihaela Stanescu, and Elena Buhaciuc-Ionita for sharing their data on species occurrences.

References

- Araújo MB, Alagador D, Cabeza M, Nogués-Bravo D, Thuiller W (2011) Climate change threatens European conservation areas. *Ecology Letters* 14: 484–492. <https://doi.org/10.1111/j.1461-0248.2011.01610.x>
- Arponen A, Heikkinen RK, Thomas CD, Moilanen A (2005) The value of biodiversity in reserve selection: Representation, species weighting, and benefit functions. *Conservation Biology* 19: 2009–2014. <https://doi.org/10.1111/j.1523-1739.2005.00218.x>
- Arslan A, Kryštufek B, Matur F, Zima J (2016) Review of chromosome races in blind mole rats (*Spalax* and *Nannospalax*). *Folia Zoologica* 65: 249–301. <https://doi.org/10.25225/fozo.v65.i4.a1.2016>
- Ausländer D, Hellwing S (1957) Beiträge zur variabilität und biologie der streifenmaus (*Sicista subtilis nordmanni* Keys. et Blas, 1840). *Travaux du Muséum d'Histoire naturelle Grigore Antipa* 1: 255–274.
- Bartolommei P, Sozio G, Bencini C, Cinque C, Gasperini S, Manzo E, Petre S, Solano E, Cozzolino R, Mortelletti A (2016) Field identification of *Apodemus flavicollis* and *Apodemus sylvaticus*: a quantitative comparison of different biometric measurements. *Mammalia* 80: 541–547. <https://doi.org/10.1515/mammalia-2014-0051>
- Botts EA, Erasmus BFN, Alexander GJ (2011) Geographic sampling bias in the South African Frog Atlas Project: Implications for conservation planning. *Biodiversity and Conservation* 20: 119–139. <https://doi.org/10.1007/s10531-010-9950-6>
- Bunescu A (1959) Contribution à l'étude de la répartition géographique de quelques mammifères méditerranéens en Roumanie. *Säugerierkundliche Mitteilungen* 1: 1–4.
- Bunescu A (1961) Contribuții la studiul răspândirii geografice a unor animale mediteraneene din R. P. Română, Nota II – Vertebrate. *Probleme de Geografie* 8: 123–144.
- Christie MR, Knowles LL (2015) Habitat corridors facilitate genetic resilience irrespective of species dispersal abilities or population sizes. *Evolutionary Applications* 8: 454–463. <https://doi.org/10.1111/eva.12255>
- Cogalniceanu D, Rozyłowicz L, Székely P, Samoilă C, Stanescu F, Tudor M, Székely D, Iosif R (2013) Diversity and distribution of reptiles in Romania. *ZooKeys* 341: 49–76. <https://doi.org/10.3897/zookeys.341.5502>
- Crooks KR, Burdett CL, Theobald DM, Rondinini C, Boitani L (2011) Global patterns of fragmentation and connectivity of mammalian carnivore habitat. *Philosophical transactions of the Royal Society of London: Series B, Biological sciences* 366: 2642–2651. <https://doi.org/10.1098/rstb.2011.0120>
- Cuzic M, Marinov M (2004) Date privind situația populației de nură europeană (*Mustela lutreola* L, 1761) (Mammalia, Carnivora, Mustelidae) în câteva zone din Rezervația Biosferei Delta Dunării. *Muzeul Brukenthal. Studii și Comunicări Științele Naturii* 29: 231–239.
- Eklund J, Arponen A, Visconti P, Cabeza M (2011) Governance factors in the identification of global conservation priorities for mammals. *Philosophical transactions of the Royal Society of London: Series B, Biological sciences* 366: 2661–2669. <https://doi.org/10.1098/rstb.2011.0114>

- Ferrier S, Wintle BA (2009) Quantitative approaches to spatial conservation prioritization: matching the solution to the need. In: Moilanen KA, Wilson HPP (Eds) Spatial Conservation Prioritization: Quantitative Methods & Computational Tools. Oxford University Press, Oxford, 1–13.
- Fortin M, Dale M (2005) Spatial Analysis – A Guide for Ecologists. Cambridge University Press, Cambridge, 365 pp.
- Gaston KJ, Davies RG, Orme CDL, Olson VA, Thomas GH, Ding TS, Rasmussen PC, Lennon JJ, Bennett PM, Owens IP, Blackburn TM (2007) Spatial turnover in the global avifauna. *Proceedings of the Royal Society B: Biological Sciences* 274: 1567–1574. <https://doi.org/10.1098/rspb.2007.0236>
- Grand J, Cummings MP, Rebelo TG, Ricketts TH, Neel MC (2007) Biased data reduce efficiency and effectiveness of conservation reserve networks. *Ecology Letters* 10: 364–374. <https://doi.org/10.1111/j.1461-0248.2007.01025.x>
- Hamar M, Schutowa M (1966) Neue daten über die geographische veränderlichkeit und die entwicklung der gattung *Mesocricetus* Nehring, 1898 (Gires, Mammalia). *Zeitschrift-Saeugetierkunde* 31: 237–251.
- Ioja CI, Patroescu M, Rozyłowicz L, Popescu VD, Vergheș M, Zotta M, Felciuc M (2010) The efficacy of Romania's protected areas network in conserving biodiversity. *Biological Conservation* 143: 2468–2476. <https://doi.org/10.1016/j.biocon.2010.06.013>
- Jaarola M, Martínková N, Gündüz İ, Brunhoff C, Zima J, Nadachowski A, Amori G, Bulatova NS, Chondropoulos B, Fragedakis-Tsolis S, González-Esteban J, José López-Fuster M, Kandaurov AS, Kefelioglu H, da Luz Mathias M, Villate I, Searle JB (2004) Molecular phylogeny of the speciose vole genus *Microtus* (Arvicolinae, Rodentia) inferred from mitochondrial DNA sequences. *Molecular Phylogenetics and Evolution* 33: 647–663. <https://doi.org/10.1016/j.ympev.2004.07.015>
- Kiss JB, Doroșencu A, Marinov ME, Alexe V, Bozagiievici R (2012) Considerations regarding the occurrence of the Eurasian Beaver (*Castor fiber* Linnaeus 1758) in the Danube Delta (Romania). *Scientific Annals of the Danube Delta Institute* 18: 49–56. <https://doi.org/10.7427/DDI.18.05>
- Kiss JB, Marinov M, Alexe V, Doroșenco A (2014) Eurasian Beaver (*Castor fiber* L. 1758), Pine Marten (*Martes martes* L. 1758) and Stone Marten (*Martes foina* Erxleben, 1777) in the Danube Delta (Romania). *Beiträge zur Jagd-und Wildforschung* 39: 347–355.
- Kiss JB, Marinov M, Alexe V, Doroșenco A, Sandor A (2013) Pătrunderea jderului de copac (*Martes martes*, Linnaeus 1758) în Delta Dunării (România) și considerații privind urmările ecologice scontate al acestui fenomen. *Revista Pădurilor* 128(3): 38–47.
- Kiss JB, Marinov M, Alexe V, Sandor A (2012) First record of the Pine Marten (*Martes martes*) in the Danube Delta. *North-Western Journal of Zoology* 8: 195–197.
- Kukkala AS, Moilanen A (2013) Core concepts of spatial prioritisation in systematic conservation planning. *Biological Reviews* 88: 443–464. <https://doi.org/10.1111/brv.12008>
- Kukkala AS, Santangeli A, Butchart SHM, Maiorano L, Ramirez I, Burfield IJ, Moilanen A (2016) Coverage of vertebrate species distributions by Important Bird and Biodiversity Areas and Special Protection Areas in the European Union. *Biological Conservation* 202: 1–9. <https://doi.org/10.1016/j.biocon.2016.08.010>

- Laffan SW, Lubarsky E, Rosauer DF (2010) Biodiverse, a tool for the spatial analysis of biological and related diversity. *Ecography* 33: 643–647. <https://doi.org/10.1111/j.1600-0587.2010.06237.x>
- Lehtomäki J, Moilanen A (2013) Methods and workflow for spatial conservation prioritization using Zonation. *Environmental Modelling and Software* 47: 128–137. <https://doi.org/10.1016/j.envsoft.2013.05.001>
- Lennon JJ, Koleff P, Greenwood JJD, Gaston KJ (2001) The geographical structure of British bird distributions: Diversity, spatial turnover and scale. *Journal of Animal Ecology* 70: 966–979. <https://doi.org/10.1046/j.0021-8790.2001.00563.x>
- Lung T, Meller L, van Teeffelen AJA, Thuiller W, Cabeza M (2014) Biodiversity Funds and Conservation Needs in the EU Under Climate Change. *Conservation Letters* 7: 390–400. <https://doi.org/10.1111/conl.12096>
- Maiorano L, Amori G, Montemaggiori A, Rondinini C, Santini L, Saura S, Boitani L (2015) On how much biodiversity is covered in Europe by national protected areas and by the Natura 2000 network: Insights from terrestrial vertebrates. *Conservation Biology* 29: 986–995. <https://doi.org/10.1111/cobi.12535>
- Manolache S, Nita A, Ciocanea CM, Popescu VD, Rozyłowicz L (2018) Power, influence and structure in Natura 2000 governance networks. A comparative analysis of two protected areas in Romania. *Journal of Environmental Management* 212: 54–64. <https://doi.org/10.1016/j.jenvman.2018.01.076>
- Margules CR, Pressey RL (2000) Systematic conservation planning. *Nature* 405: 243–253. <https://doi.org/10.1038/35012251>
- Memedemin D, Tudor M, Cogalniceanu D, Skolka M, Banica G, Rozyłowicz L (2017) Update on the Geographic Distribution of *Lutra lutra* at the Romanian Black Sea Coast. *Travaux du Muséum National d'Histoire Naturelle Grigore Antipa* 60: 413–417. <https://doi.org/10.1515/travmu-2017-0004>
- Moilanen A, Veach V, Meller L, Arponen A, Kujala H (2014) Spatial conservation planning methods and software. Version 4. User Manual. University of Helsinki, Helsinki, Finland, 290 pp. <https://doi.org/10.1017/CBO9781107415324.004>
- Murariu D (1996) Mammals of the Danube Delta (Romania). *Travaux du Muséum National d'Histoire Naturelle* 36: 361–371
- Murariu D (2006) Mammal ecology and distribution from North Dobrogea (Romania). *Travaux du Muséum national d'Histoire naturelle* 49: 387–399.
- Murariu D, Atanasova I, Raykov I, Chișamera G (2009) Results on mammal (Mammalia) survey from Bulgarian and Romanian Dobrogea. *Travaux du Muséum national d'Histoire naturelle* 52: 371–386.
- Murariu D, Chișamera G, Petrescu A, Atanasova I, Raykov I (2010) Terrestrial vertebrates of Dobrogea – Romania and Bulgaria. *Travaux du Muséum national d'Histoire naturelle Grigore Antipa* 53: 357–375. <https://doi.org/10.2478/v10191-010-0027-2>
- Murariu D, Munteanu D (2005) Fauna României – Mammalia – Carnivora. Editura Academiei Române, Bucharest, 224 pp

- Nita A, Rozyłowicz L, Manolache S, Ciocanea CM, Miu IV, Popescu VD (2016) Collaboration Networks in Applied Conservation Projects across Europe. PLoS ONE 11(10): e0164503. <https://doi.org/10.1371/journal.pone.0164503>
- Nita A, Ciocanea CM, Manolache S, Rozyłowicz L (2018) A network approach for understanding opportunities and barriers to effective public participation in the management of protected areas. Social Network Analysis and Mining 8. <https://doi.org/10.1007/s13278-018-0509-y>
- Ord JK, Getis A (1995) Local spatial autocorrelation statistics: distributional issues and an application. Geographical Analysis 27: 286–306. <https://doi.org/10.1111/j.1538-4632.1995.tb00912.x>
- Popescu A, Murariu D (2001) Fauna României. Mammalia. Rodentia. Editura Academiei Române, Bucharest, 214 pp.
- Popescu VD, Rozyłowicz L, Cogalniceanu D, Niculae IM, Cucu AL (2013) Moving into protected areas? Setting conservation priorities for Romanian reptiles and amphibians at risk from climate change. PLoS ONE 8: e79330. <https://doi.org/10.1371/journal.pone.0079330>
- Possingham HP, Wilson KA, Andelman SJ, Vynne CH (2006) Protected areas: Goals, limitations, and design. In: Groom MJ, Meffe GK, Carroll CR (Eds) Principles of Conservation Biology. Sinauer Associates, Sunderland, 509–533.
- Pouzols F, Toivonen T, Di Minin E, Kukkala AS, Kullberg P, Kuusterä J, Lehtomäki J, Tenkanen H, Verburg PH, Moilanen A (2014) Global protected area expansion is compromised by projected land-use and parochialism. Nature 516: 383–386. <https://doi.org/10.1038/nature14032>
- Pressey RL, Cabeza M, Watts ME, Cowling RM, Wilson K (2007) Conservation planning in a changing world. Trends in Ecology & Evolution 22: 583–92. <https://doi.org/10.1016/j.tree.2007.10.001>
- Rey V, Ianos I, Groza O, Patroescu M (2007) Atlas de la Roumanie Nouvelle edition. Reclus, Montpellier, 208 pp.
- Santos BPA, Bitencourt C, Rapini A (2017) Distribution patterns of *Kielmeyera* (Calophyllaceae): the Rio Doce basin emerges as a confluent area between the northern and southern Atlantic Forest. Neotropical Biodiversity 3: 1–9. <https://doi.org/10.1080/23766808.2016.1266730>
- Rodrigues ASL, Andelman SJ, Bakarr MI, Boitani L, Brooks TM, Cowling RM, Fishpool LDC, Da Fonseca GAB, Gaston KJ, Hoffmann M, Long JS, Marquet PA, Pilgrim JD, Pressey RL, Schipper J, Sechrest W, Stuart SN, Underhill LG, Waller RW, Watts MEJ, Yan X (2004) Effectiveness of the global protected area network in representing species diversity. Nature 428: 640–3. <https://doi.org/10.1038/nature02422>
- Rodrigues ASL, Grenyer R, Baillie JEM, Bininda-Emonds ORP, Gittlemann JL, Hoffmann M, Safi K, Schipper J, Stuart SN, Brooks T (2011) Complete, accurate, mammalian phylogenies aid conservation planning, but not much. Philosophical Transactions of the Royal Society B: Biological Sciences 366: 2652–2660. <https://doi.org/10.1098/rstb.2011.0104>

- Rozyłowicz L, Nita A, Manolache S, Ciocanea CM, Popescu VD (2017) Recipe for success: A network perspective of partnership in nature conservation. *Journal for Nature Conservation* 38: 21–29. <https://doi.org/10.1016/j.jnc.2017.05.005>
- Sánchez-Fernández D, Abellán P, Aragón P, Varela S, Cabeza M (2017) Matches and mismatches between conservation investments and biodiversity values in the European Union. *Conservation Biology* 32: 109–115. <https://doi.org/10.1111/cobi.12977>
- Székely P, Iosif R, Székely D, Stanescu F, Cogalniceanu D (2013) Range extension for the Eastern spadefoot toad *Pelobates syriacus* (Boettger, 1889) (Anura: Pelobatidae). *Herpetology Notes* 6: 481–484.
- Székely P, Plaiasu R, Tudor M, Cogalniceanu D (2009) The distribution and conservation status of amphibians in Dobrudja (Romania). *Turkish Journal of Zoology* 33: 147–156. <https://doi.org/10.3906/zoo-0805-12>
- Temple HJ, Terry A (2009) European mammals: Red List status, trends, and conservation priorities. *Folia zoologica* 58: 248
- Whittaker RH (1972) Evolution and measurement of species diversity. *Taxon* 21: 213–251. <https://doi.org/10.2307/1218190>
- Williams PH, Margules CR, Hilbert DW (2002) Data requirements and data sources for biodiversity priority area selection. *Journal of Biosciences* 27: 327–338. <https://doi.org/10.1007/BF02704963>
- Wilson DE, Reeder DM (2005) *Mammal Species of the World. A Taxonomic and Geographic Reference* (3rd edn). Johns Hopkins University Press, 2142 pp.
- Wilson KA, Cabeza M, Klein CJ (2009) Fundamental concepts of spatial conservation prioritization. In: Moilanen A, Wilson KA, Possingham HP (Eds) *Spatial Conservation Prioritization: Quantitative Methods and Computational Tools*. Oxford University Press, New York, 16–27.

Supplementary material I

Publications used to compile distribution of terrestrial mammal species from Dobrogea Region, Romania (field reports and data from museum collections)

Authors: Iulia V. Miu, Gabriel B. Chisamera, Viorel D. Popescu, Ruben Iosif, Andreea Nita, Steluta Manolache, Viorel D. Gavril, Ioana Cobzaru, Laurentiu Rozyłowicz

Data type: reference

Copyright notice: This dataset is made available under the Open Database License (<http://opendatacommons.org/licenses/odbl/1.0/>). The Open Database License (ODbL) is a license agreement intended to allow users to freely share, modify, and use this Dataset while maintaining this same freedom for others, provided that the original source and author(s) are credited.

Link: <https://doi.org/10.3897/zookeys.792.25314.suppl1>

Supplementary material 2

Occurrences maps for 59 mammal species

Authors: Iulia V. Miu, Gabriel B. Chisamera, Viorel D. Popescu, Ruben Iosif, Andreea Nita, Steluta Manolache, Viorel D. Gavril, Ioana Cobzaru, Laurentiu Rozyłowicz

Data type: occurrence

Explanation note: The mammal species old (before 1990) and new (after 1990) occurrence records at a 5 × 5 km grid resolution within Dobrogea, Romania.

Copyright notice: This dataset is made available under the Open Database License (<http://opendatacommons.org/licenses/odbl/1.0/>). The Open Database License (ODbL) is a license agreement intended to allow users to freely share, modify, and use this Dataset while maintaining this same freedom for others, provided that the original source and author(s) are credited.

Link: <https://doi.org/10.3897/zookeys.792.25314.suppl2>

Supplementary material 3

Methodology used to identify high-priority Natura 2000 sites with Zonation v4

Authors: Iulia V. Miu, Gabriel B. Chisamera, Viorel D. Popescu, Ruben Iosif, Andreea Nita, Steluta Manolache, Viorel D. Gavril, Ioana Cobzaru, Laurentiu Rozyłowicz

Data type: methodology

Copyright notice: This dataset is made available under the Open Database License (<http://opendatacommons.org/licenses/odbl/1.0/>). The Open Database License (ODbL) is a license agreement intended to allow users to freely share, modify, and use this Dataset while maintaining this same freedom for others, provided that the original source and author(s) are credited.

Link: <https://doi.org/10.3897/zookeys.792.25314.suppl3>

